





Universitat Autònoma de Barcelona

**ADVERTIMENT.** L'accés als continguts d'aquesta tesi queda condicionat a l'acceptació de les condicions d'ús establertes per la següent llicència Creative Commons:  [http://cat.creativecommons.org/?page\\_id=184](http://cat.creativecommons.org/?page_id=184)

**ADVERTENCIA.** El acceso a los contenidos de esta tesis queda condicionado a la aceptación de las condiciones de uso establecidas por la siguiente licencia Creative Commons:  <http://es.creativecommons.org/blog/licencias/>

**WARNING.** The access to the contents of this doctoral thesis it is limited to the acceptance of the use conditions set by the following Creative Commons license:  <https://creativecommons.org/licenses/?lang=en>

**UAB**

Universitat Autònoma  
de Barcelona

PhD Thesis

**Updating the current dichotomic “I”  
classification of metallothioneins to a  
new “Y” setting: Differentiation  
between genuine Zn- and Cd-thioneins**

Mario García-Risco Aguado

Chemistry PhD program

Supervised by

Mercè Capdevila Vidal & Òscar Palacios Bonilla

Chemistry Department

Faculty of Science

**2022**



Manuscript presented to obtain the PhD Degree by Mario García-Risco Aguado

**Mario García-Risco Aguado**

With the approval of the supervisors of the Doctoral Thesis, Mercè Capdevila Vidal, full professor of Universitat Autònoma de Barcelona and Òscar Palacios Bonilla, associate professor of Universitat Autònoma de Barcelona

**Dr. Mercè Capdevila Vidal**

**Dr. Òscar Palacios Bonilla**



# FINANCIAL SUPPORT

The work described in this PhD Thesis has been possible to perform thanks to the financial support of the following projects:

- *“COMPRESION DE LAS INTERACCIONES MOLECULARES ENTRE METALES Y SISTEMAS BIOLÓGICOS PARA EL DISEÑO DE APLICACIONES BIOMÉDICAS Y BIOTECNOLÓGICAS. SP2- APROXIMACION QUÍMICA”;* BIO2015-67358-C2-2-P; PI: Mercè Capdevila Vidal. Granted by Spanish Ministerio de Ciencia e Innovación and FEDER. This project has also permitted to perform a research stay at Warwick’s University under the supervision of Professor Claudia Blindauer.
- *PIF scholarship of 4 years granted by Universitat Autònoma de Barcelona to develop this PhD thesis in the Metal·lotioneïnes: relació estructura/funció i aplicacions research grup.*







[REDACTED]

# ABSTRACT

Protein classification is a handy tool to characterise freshly discovered proteins. By comparing their three-dimensional structure with other well-known proteins, their function may be proposed. However, the function of metallothioneins (MTs), which are a group of cysteine-rich proteins with high coordinating capacity, is quite challenging to determine. This is mainly consequence of their labile 3D-structure, which is modulated by the metal cluster associated to the protein. These proteins are physiologically found wrapping clusters of several metal ions and each metal-MT association has a variable stability, which means that each polypeptide sequence has specific affinities for each kind of metal. By characterising the biochemical properties of these metal-MT complexes, it is possible to make assumptions about MTs' biological functions. Besides, it is straightforward to assume that if an MT builds a stable metal cluster with a certain metal ion, its function will relate to a biological function involving that metal ion. Based on that, our group designed a method to aid in the prediction of MTs' function by classifying them by their metal-binding abilities, separating those that show high affinity when rendering complexes of divalent metal ions (Zn-thioneins) and those that display high stability in association with monovalent metal clusters (Cu-thioneins), considering all the intermediate steps between them. Then, this criterion perfectly differentiates between these two extreme behaviours, however, due to the chemical similarities of Zn and Cd, their interaction with MTs in most of the cases barely differ between them and, thus, it has never been contemplated the existence of two different metal-binding behaviours specific for each metal ion. It is the research performed over decades that permitted to gather some cases of MTs with differential selectivity towards Cd(II) ions and lead us to consider the possibility to separate the current Zn-thioneins group into Zn- and Cd-thioneins. To demonstrate that, this PhD thesis has been devoted to characterising several examples of MTs, revealing that each of the two metal-binding behaviours hypothesised display differential traits. Thanks to the data and discussion presented here it has been possible to update the dichotomic MT classification (Zn- to Cu-thioneins) into a three-band classification (Zn-, Cd- and Cu-thioneins). We anticipate that this work will allow to advance into the research of MTs and the pursuit of the finding of their functions.



# SYMBOLS AND ABBREVIATIONS

<b>aa</b>	Amino acid/s
<b>CD</b>	Circular dichroism
<b>Cys</b>	Cysteine
<b>XRD</b>	X-Ray diffraction
<b><i>E. coli</i></b>	<i>Escherichia coli</i>
<b>EDTA</b>	Ethylenediaminetetraacetic acid
<b>ESI-MS-TOF</b>	Electrospray Ionisation Mass Spectrometry Time of Flight
<b>Eq.</b>	Molar equivalent/s
<b>FPLC</b>	Fast Protein Liquid Chromatography
<b>His</b>	Histidine
<b>ICP-AES</b>	Inductively Coupled Plasma Absorption Emission Spectroscopy
<b>i.d.</b>	Inner diameter
<b>LMCT</b>	Ligand Metal Charge Transfer
<b>NMR</b>	Nuclear Magnetic Resonance
<b>M(II)</b>	Divalent metal
<b>MTs</b>	Metallothioneins
<b>MW</b>	Molecular Weight
<b>Q<sup>+</sup></b>	Charge state of the species shown by ESI-MS
<b>SAQ</b>	Servei d'anàlisis Químiques (UAB Services of chemical analyses)
<b>SCys</b>	Cysteine's sulphur
<b>Tris</b>	Tris(hydroxymethyl)aminomethane
<b>UV-vis</b>	Ultraviolet-visible absorption spectrometry



# INDEX

<b>1. Introduction</b> .....	1
1.1. Metallothioneins.....	1
1.1.1. Synthesis and Purification: Obtention of MTs.....	3
1.1.2. Structural properties: Characterisation of MTs.....	6
1.1.3. Metallothioneins' chemistry: Reactivity and functionality of MTs.....	11
1.1.4. Classes and classification of MTs.....	15
1.2. State-of-art of the MT systems.....	19
<b>2. Objectives</b> .....	29
<b>3. Results and discussion</b> .....	33
3.1. In depth characterisation of the MT systems.....	34
3.1.1. Mollusc MT systems.....	35
3.1.2. Urochordate MT system.....	40
3.1.3. <i>Candida albicans</i> MT system.....	44
3.1.4. Final remarks on the characterisation of the MT systems.....	45
3.2. Characterisation of the metal-binding abilities of non-specific MTs.....	46
3.2.1. Study of <i>Arion vulgaris</i> MT2.....	46
3.2.2. Study of <i>Pomacea bridgesii</i> MT1 and MT2.....	49
3.2.3. General traits of non-specific MTs.....	54
3.3. Characterisation of the metal-binding abilities of genuine Zn-thioneins.....	55
3.3.1. Study of <i>Arion vulgaris</i> MT1.....	55
3.3.2. Study of <i>Nerita peloronta</i> MT1.....	60
3.3.3. Study of <i>Falciidens caudatus</i> MT1 and its $\alpha$ fragment.....	63
3.3.4. Study of <i>Candida albicans</i> MT: CaCUP1.....	67
3.3.5. General observations of Zn-thioneins.....	70
3.4. Characterisation of the metal-binding abilities of putative Cd-thioneins.....	71
3.4.1. Study of <i>Lottia gigantea</i> MTs.....	71
3.4.2. Study of <i>Nautilus pompilius</i> MT.....	76
3.4.3. Study of <i>Nerita peloronta</i> MT2.....	80
3.4.4. Study of <i>Oikopleura dioica</i> MT system.....	84
3.4.5. Study of some ascidian MTs: <i>Ciona robusta</i> , <i>Hallocynthia roretzi</i> and <i>Botryllus schlosseri</i> MT systems.....	90

3.4.6.	Study of <i>Salpa thompsoni</i> MT system.....	92
3.4.7.	Common traits in the described Cd-thioneins .....	94
3.5.	Glycosylation: The Zn <sub>2</sub> S enigma.....	94
3.5.1.	Surveying an intriguing additional mass of 162 Da .....	95
3.5.2.	Proposing glycosylation as a justification of the extra mass .....	97
3.5.3.	Demonstrating that the MTs are glycosylated.....	97
3.5.4.	Characterisation of <i>Escherichia coli</i> glycosylation .....	98
3.5.5.	Cadmium inhibits glycosylation.....	101
3.5.6.	Glycosylation relies on MTs flexibility .....	103
3.5.7.	Glycosylation affects metal-binding of MTs.....	104
3.5.8.	Final remarks of glycosylation.....	106
3.6.	A new MT classification proposal .....	106
3.6.1.	Comparison of Zn- and Cd-thioneins metal-binding abilities towards Zn(II) ions	107
3.6.2.	Comparison of Zn- and Cd-thioneins metal-binding abilities towards Cd(II) ions	109
3.6.3.	Comparison of Zn- and Cd-thioneins metal-binding abilities towards Cu(I) ions.	109
3.6.4.	Final remarks on the proposal of a new scheme of MT classification.....	110
4.	<b>Conclusions</b> .....	115
5.	<b>Experimental procedures</b> .....	121
5.1.	Protein synthesis and purification.....	121
5.2.	Protein characterisation .....	122
5.2.1.	Proteins' nomenclature .....	123
5.2.2.	Inductively coupled plasma atomic emission spectroscopy (ICP-AES).....	123
5.2.3.	Electrospray Ionisation Mass Spectrometry Time-of-Flight (ESI-MS-TOF).....	124
5.2.4.	Ultraviolet-Visible absorption spectroscopy (UV-Vis) .....	125
5.2.5.	Circular Dichroism (CD) .....	126
5.2.6.	Protein digestion.....	127
5.3.	Cd(II) and Cu(I) titrating agents .....	128
5.3.1.	Cd(II) solution.....	128
5.3.2.	Cu(I) solution .....	128
6.	<b>Bibliography</b> .....	131
7.	<b>Annex</b> .....	153
7.1.	Data sheets of the parameters measured from the recombinant productions.....	155
7.2.	Experimental characterisation of the studied MTs.....	180
7.3.	Published and submitted articles.....	199

“Since its detection in 1957 metallothionein and its possible function have provided a splendid source of frustration for the many who have been attracted to this Sphinx and tempted to solve its riddle.”

(Metallothionein co-discoverer Bert L. Vallee)

"Discovery consists of seeing what everybody has seen and thinking what nobody has thought."

(Nobel-Prize winner Albert von Szent-Györgyi)

“Journey before Destination”

(Brandon Sanderson)





# 1. INTRODUCTION

---



# 1. Introduction

---

## 1.1. Metallothioneins

When one enters the world of metallothioneins (MTs), it is impossible to avoid getting more and more involved. This peculiar family of metalloproteins still hide lots of enigmas, especially due to their biochemical features, for their research is covered by numerous scientific disciplines. The key amino acid (aa) by which all this system is sustained is cysteine (Cys). These usually low-weight proteins (<10 kDa) contain a significant percentage of Cys residues (~30%) that provide MTs with their principal feature: binding transition metal ions, especially those with  $d^{10}$  configuration [1]. This is of great importance, because their free-metal form (apo) lacks secondary structural motifs while their three-dimensional structure is dictated by the metal ions bound to the protein [2, 3]. Of course, each one of the existing sequences presents specific traits, showing high variation in their length and Cys distribution (**Figure 1.1**). In fact, if we consider all the sequences known, MTs form a highly diverse group of “not-so-much” homologous proteins. This means that, in general, MT sequences possess specific number and content of amino acids in a unique arrangement that is only conserved between closely related organisms. Still, the high number of Cys residues confer to all of them the capacity of building metal-clusters and, most likely, share similar functions. The diversity of their sequences and, yet the similarity of their functions, make the classification of MTs a challenging task.

Ubiquitous MTs have been found in most of the organisms studied to date, ranging from humans and closely related vertebrates to prokaryote unicellular bacteria [4]. MTs were first reported in 1957 by Margoshes and Vallee [5], who isolated a protein associated to Cd(II) from horse kidney cortex. Later, this protein was termed by Kägi and Vallee as Metallothionein, in view of the high number of metals and thiols present in that biological molecule [1]. Kägi and Vallee's first

approximation of Metallothionein included a protein of low molecular weight and high amount of Cys, which was able to bind transition metal ions, and possessed a very low content of aromatic amino acids (due to its low absorbance at 280 nm). After that, many more properties have allowed to complete the definition of Metallothionein and more MTs have been described for a collection of organisms over the years.

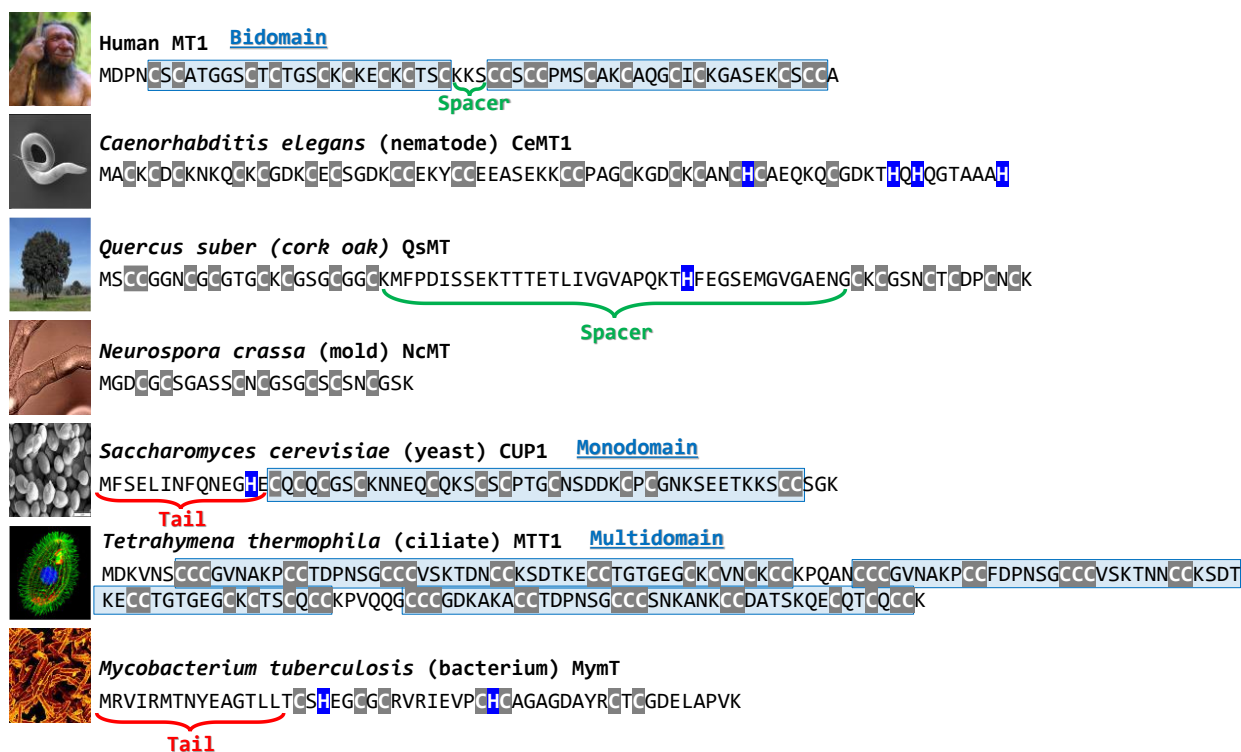


**Figure 1.1** MT sequences of different organisms of varied evolutionary origin in which highly diverse Cys-motifs, peptide lengths and domain structures are observed. Some sequences are structured in one, two or multiple domains (blue boxes), some display short or long spacers (green highlighters) and some show non-coordinating bits of sequence, called tails (red highlighters).

This initial period, since MTs were first described until the 70s, involved the publication of fewer than 10 scientific articles [6]. Today, at the time this PhD thesis is being written, this number has increased to approximately 30,400 entries in SciFinder. Its growing interest lies in MTs' particular characteristics, the study of which involves advances in elemental biology (and all connected disciplines) and the improvement of experimental procedures in metalloprotein research. Elucidating all the biochemical processes in which MTs are implicated promotes a better understanding of the biological functions of all metalloproteins and their biological roles. In turn, this research results in numerous applications, ranging from medicine and pathological processes [7, 8, 9] to ecology and detection of toxicity in ecosystems [10, 11, 12].

Nowadays, our group itself has already studied more than 100 MT sequences of many distinct organisms, from the more of the 6500 MT entries reported in UniProt. It would be excessive to collect here all the paramount volume of information achieved during the last 30 years, which in fact has been reviewed recently in the literature [6, 13, 14, 15]. For this reason, the introduction to this PhD thesis is centred in those aspects that are closer to the research presented here and it is structured in a way that the basic concepts around MTs' research are explained as they would be encountered along the experimental process followed in the study of MTs. This means, for instance, that while the synthesis and purification procedures are explained, the recombinant theory is also defined; when the structural and spectroscopic features of MTs are described, their characterisation it is portrayed as well, and this criterion is continued for the following steps of the research.

### *1.1.1. Synthesis and Purification: Obtention of MTs*

As logical as it may seem, protein samples are needed to study MTs. These samples must be pure and concentrated, and proteins should retain their physiological characteristics, that is, their native form, for a good analytical characterisation. Obtaining valid samples of MTs has been a struggling task over the years, exhibiting some drawbacks due to the main characteristics of these complex proteins: high polymorphism within the same organism, complex genetical expression pattern and induction, and extremely high coordinative abilities [6].

As explained before, the first MT ever characterised was isolated from animal organs [5]. After that first extraction, this procedure was established and the MTs were recovered from the original organism tissues in which the biosynthesis of the protein in its native form was induced [16]. This induction could be triggered by the exposition to a surplus of metal ions, stress conditions, radiation, or hormones [17, 18]. Afterwards, the MT was isolated and purified from the tissue where it was overexpressed. During this process, MTs had to be separated from other proteins and debris, and more importantly, other MT isoforms with high homology that might coexist in the same tissue, which hindered the obtention of a homogenous preparation [19]. Moreover, other inconveniences of using this procedure were the need of large amounts of tissue, a tedious purification process, the recovery of preparations with poor concentration and protein purity, the obvious limitation on the obtention of MT samples for all the organisms (specially from the smallest) and, very importantly, the extraction and purification conditions could affect the

metal stoichiometry of the metal-MT complexes and, thus, lead to the obtention of inaccurate results.

Overall, an especially relevant drawback of this methodology was the over-manipulation of the sample when a full characterization of the sample was required. When an MT is induced with a certain metal ion (*e.g.*, Cd(II)), the purified sample and, therefore, the recovered metalloprotein, will contain this inductor. Consequently, the metal-MT species obtained by this methodology will possibly differ from the physiological ones and could not be representative of the biological role of the native protein. In order to characterise the MT of interest with the physiological metal ions (*i.e.*, Zn(II) and Cu(I)), the purified Cd-MT must be demetallated by acidification (apo-MT form), isolated from the metallated medium with Cd(II), and be reconstituted with the desired metal ions. The main disadvantage of this procedure is that the *in vitro* conditions in which this metal exchange occurs might lead to the obtention of non-physiological Zn- or Cu-MT complexes (*i.e.*, other metal-MT species which are non-isostructural with the native species) [20].

To overcome some of the difficulties encountered in obtaining native MTs from the original tissues, the alternative used was the synthetic production of small proteins and peptides by chemical synthesis of the polypeptide chain on a solid support [21]. This method was used to synthesise apo-MTs from short isoforms such as fungal MTs [21, 22] or MT fragments such as those of the mammalian MT domains [23, 24, 25, 26]. A handy application of this procedure is that it is possible to direct specific mutations to proteins, meaning that some modifications can be designed in the MTs of interest to evaluate the biochemical properties of the protein when certain amino acids are substituted. However, the synthetical production of MT samples showed some drawbacks as well. These include the fact of having to deal with the easiness by which thiol groups get oxidised (Cys residues of the primary structure of the protein) during the chemical synthesis, the limitations in the longitude of the polypeptide chain to be synthesised, or the *in vitro*, and possibly inaccurate, reconstitution of the metal clusters from an apo-MT, as well as the low purity of the samples [27].

Eventually, these methodologies were substituted in the 90s with the development of the recombinant DNA technology (**Figure 1.2**). This technique consists of manipulating the genes of a host organism (commonly the bacterium *Escherichia coli*) to produce the desired heterologous proteins (proteins that do not belong to *E. coli* itself), in our case, by inoculating any MT gene of any organism of interest into *E. coli* [28]. However, introducing eukaryotic gene systems into a

prokaryote environment also brings some difficulties, since bacteria require familiar conditions to render decent production yields. Therefore, it was necessary to design adequate experimental conditions, *e.g.*, appropriate vectors (DNA fragment that contains the gene of interest) easily recognisable for *E. coli* or the use of chimeric proteins (fused proteins composed by a bacterial protein and the protein of interest) to improve the recovery yield [29, 30, 31]. The vector (or plasmid) should comply important requisites: (1) to contain the sequence that codify the protein of interest, (2) to trigger the appropriate transcription and translation signals, (3) to contain a selective advantage (*i.e.*, antibiotic resistance) to separate those bacteria that included the plasmid from those that did not, and (4) to bring enough relevance to the cell to maintain the plasmid and transmit it to their progeny. In 1997, our group proposed a methodology that involved the use of a bacterial pGEX-based expression system and complied all the above-mentioned requirements, achieving relevant yielding scores [32, 33]. To date, this methodology has allowed us to obtain more than one hundred of highly concentrated and pure metal-MT preparations of a number of distinct organisms covering all the tree of life [13].

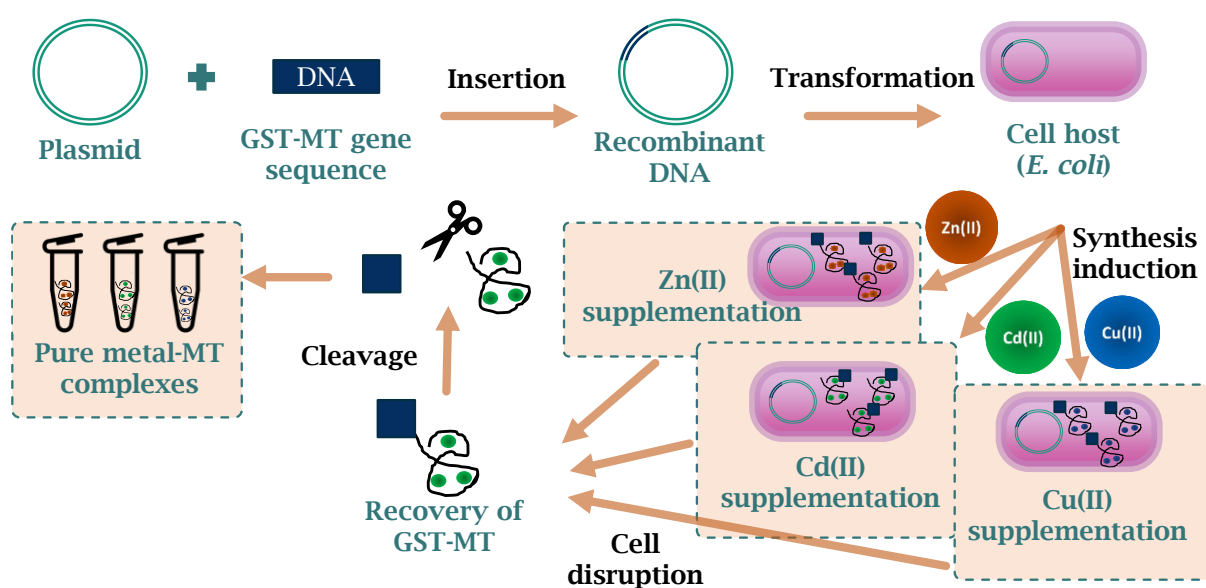


**Figure 1.2.** General scheme of recombinant proteins obtention and purification.

It additionally permitted reproducing the *in vivo* conditions that provide the original cells and, therefore, rendering physiologically interesting species, and improving the disadvantages of the previously used techniques that had to deal with harsh purification processes from the organism tissues. Importantly, recombinant DNA technology also permits to synthesise separate domains and to perform site-directed mutagenesis, which allows to characterise complex



biochemical features of MTs, adding precious value to this technique. Moreover, by supplementing the bacterial culture medium with different transition metal ions, it is possible to recover metal-MT complexes with these desired metal ions already coordinated (**Figure 1.2**).

All the advantages provided by this technique make it the preferred procedure for obtaining and purifying MTs for their subsequent characterisation. Consequently, all the proteins studied in this PhD thesis have been produced by means of the recombinant DNA technology.

### 1.1.2. Structural properties: Characterisation of MTs

Considering the experimental process followed in the research of this PhD thesis, once the MTs are biosynthetically produced, their biochemical properties are characterised. MTs three-dimensional structure and thus, their biochemical properties, cannot be understood without considering Cys residues and their interaction with metal ions. Due to this characteristic composition of MTs, inorganic metal-thiolate complexes have been used to achieve a better understanding of the metal sites rendered by cysteines in biological systems [34]. As mentioned, Cys represent about the 30% of these metalloproteins, which confer them the ability to bind  $d^{10}$  configuration transition metal ions [6, 13, 14]. The generation of the metal-MT complexes relies on the coordination of the metal ion to the thiolate groups of Cys residues (and/or, occasionally, to the imidazolate groups of His), satisfying the specific coordination geometries of each bound metal ion: in this environment, Zn(II) and Cd(II) only present a tetrahedral coordination, while Cu(I) can show either tetrahedral, trigonal or diagonal coordination geometry [35]. Besides, Cys residues can be found linked to one ion (terminal thiolates) or to two metal ions (bridging thiolates), being the former more reactive than the latter [36]. Despite histidine (His) residues can also coordinate metal ions in some MTs [37, 38, 39, 40], cysteine is the main coordinating agent in these proteins. Cysteine thiolates, acting as soft Lewis bases, tend to bind soft Lewis acids such as Cd(II) and Cu(I), as well as intermediate acids like Zn(II) [41]. Moreover, MT thiolate moieties are extremely reactive towards electrophiles and free radical species. As thiolates are (reversibly) oxidised to thioethers, disulphides, or other noncoordinating sulphur species, MTs' metal-binding capability is nullified [42]. Some studies showed that the apo form reacts easier to oxidants than metal-charged MT [43]. Thus, coordinating metals are protecting those redox-active thiolate ligands [44]. In either way, all metallothioneins are characterised for forming metal clusters involving their high number of Cys residues, wrapping

around this metal cluster, and giving a tertiary structure to the peptide chain. This association ranges from the simplest  $\text{Zn}_2(\text{SCys})_6$  metal cluster of MMT1 of *Magnaporthe grisea* [45] to the most complex organization of metal clusters that generate an enormous  $\text{Cd}_{17}$ -MTT1 metal cluster of the multidomain MT of *Tetrahymena thermophila* [46].

In spite of the massive variation in the primary structure of the known MT sequences (**Figure 1.1**), all of them reveal a high proportion of Cys residues that, if examined closely, display conserved patterns shared among different MTs (*e.g.*, CC, CxC, CCC, etc.). These arrangements of Cys are distributed in a specific position and number defining different Cys motifs [47]. Consequently, there are multiple MT structures such as vertebrate bidomain MTs that render two independent metal clusters linked by a short spacer sequence of few aa [48]; monodomain yeast MTs, which invest most of the aa sequence to perform a unique metal cluster but a short bit of the terminal sequence is mobile (free tail) [49]; or plant MTs that commonly render a single metal cluster coordinated by the two terminal Cys-rich regions separated by a quite long spacer sequence of several aa, displaying a hairpin-like structure [50] (**Figure 1.3**). Regardless of such varied structures, all aa sequences equivalently build metal clusters, though their metal-binding preferences and three-dimensional structures are determined by the specific biochemical traits of each MT sequence [51]. The combination of both metal-binding preferences and three-dimensional structure provides MTs with their biological function.

Therefore, each domain builds different metal clusters, generating the so-called functional domains. This concept was firstly specified and characterised for mammalian MTs [52], and later, for other animal MTs [53, 54, 55, 56]. All these structures build  $\alpha$  and/or  $\beta$  domains, which are motifs of 11/12 Cys residues coordinating four divalent metal ions in the case of the  $\alpha$  domains and 9 Cys residues binding three divalent metal ions in  $\beta$  domains. Additionally, both modules are joined with a linker sequence usually constituted by few amino acids. However, there are some MTs that display variations of this structure, such is the case of plant MTs, which are constituted by two Cys-rich terminal domains separated by a long spacer sequence [57, 58]. In both cases, the number of amino acids of the linker might affect interdomain contacts but not the stability of the metal clusters of those domains [55, 59]. When first discovered, mammalian  $\alpha$  and  $\beta$  domains were also called C- and N-terminal domains, respectively, due to their position in the amino acid sequence (**Figure 1.3A**). However, this nomenclature has changed after characterising and finding more MTs such as that of sea urchin that



Moreover, physiological metal ions such as Zn(II) and Cu(I) do not have any active isotope in NMR, impeding the determination of the metal-cysteine bonds and forcing to use other metal ions active to NMR as a probe, such as Cd(II) for Zn(II) and Ag(I) for Cu(I), which not always render isostructural complexes [63, 64]. All these difficulties led to a low productivity in terms of solving MT three-dimensional structures and only a few are available nowadays (**Table 1.1**).

Alternatively, other spectroscopic techniques such as circular dichroism (CD), UV-vis absorption or inductively coupled plasma optical emission spectroscopy (ICP-AES) have been widely implemented in the characterisation of MTs [6, 13, 14]. These techniques allow to determine some structural properties of the protein and of their metal-protein bonds, providing information on the stoichiometry of the metal-MT complexes [65]. One of the main advantages of using UV-vis and CD is that MTs normally lack of aromatic residues that might interfere in the results. Therefore, the ligand-to-metal charge transfer (LMCT) bands of the spectra, only rendered by the metal-MT (holo form), range from 230-400 nm, while the chromophores detected for the apo-MT will be below 220 nm, corresponding to the peptide bond [66].

**Table 1.1.** State-of-art of the currently available MT 3D structures in PDB solved by X-ray diffraction (XRD) or solution NMR (NMR).

Organism	Metal-MT complex	PDB ID	Method	Reference
<i>R. rattus</i> (Rat)	Cd <sub>5</sub> Zn <sub>2</sub> -MT2	4MT2	XRD	[61, 67, 68]
	Cd <sub>7</sub> -MT2	1MRT, 2MRT	NMR	[69, 70, 71]
<i>H. sapiens</i> (Human)	Cd <sub>7</sub> -MT2	1MHU, 2MHU	NMR	[72, 73]
	Cd <sub>7</sub> -MT3	2F5H, 2FJ4, 2FJ5	NMR	[74]
<i>M. musculus</i> (Mouse)	Cd <sub>7</sub> -MT2	1DFS 1DFT	NMR	[74]
	Cd <sub>7</sub> -MT3	1JI9	NMR	[75]
<i>O. cuniculus</i> (Rabbit)	Cd <sub>7</sub> -MT2A	1MRB, 2MRB	NMR	[76]
<i>N. coriiceps</i> (Fish)	Cd <sub>7</sub> -MT	1M0J, 1M0G	NMR	[77]
<i>C. sapidus</i> (Crab)	Cd <sub>6</sub> -MT1	1DME, 1DMF, 1DMC, 1DMD	NMR	[78]
<i>H. americanus</i> (Lobster)	Cd <sub>6</sub> -MT1	1J5M, 1J5L	NMR	[54]
<i>H. pomatia</i> (Snail)	Cd <sub>6</sub> -HpCdMT	6QK6	NMR	[56]
	Zn <sub>6</sub> -HpCdMT	6QK5	NMR	[56]
<i>L. littorea</i> (Periwinkle)	Cd <sub>9</sub> -LLMT	5ML1	NMR	[55]
	Zn <sub>9</sub> -LLMT	5MN3	NMR	[55]
<i>S. purpuratus</i> (Sea urchin)	Cd <sub>7</sub> -MTA	1QJK, 1QJL	NMR	[53]
<i>S. cerevisiae</i> (Yeast)	Cu <sub>8</sub> -CUP1	1RJU	XRD	[62]
	Cu <sub>7</sub> -CUP1	1AQR, 1AQS, 1FMY	NMR	[49, 79]
	Ag <sub>7</sub> -CUP1	1A00, 1AQQ	NMR	[49]
<i>N. crassa</i> (Mould)	Cu <sub>6</sub> -NcMT	1T2Y	NMR	[80]
<i>T. aestivum</i> (Wheat)	Zn <sub>4</sub> -β <sub>E</sub> -E <sub>c</sub> -1	2KAK	NMR	[50]
	Cd <sub>2</sub> -γ-E <sub>c</sub> -1	2MFP, 2L61	NMR	[81, 82]
	Zn <sub>2</sub> -γ-E <sub>c</sub> -1	2L62	NMR	[81]
<i>P. fluorescens</i> (Bacteria)	Cd <sub>4</sub> -PflQ2 MT	6GV6, 6GV7, 6GRV	NMR	[83]
	Zn <sub>4</sub> -PflQ2 MT	6GW8	NMR	[83]
<i>S. elongatus</i> (Cyanobacteria)	Zn <sub>4</sub> -SmtA	1JJD	NMR	[84]

### 1.1.3. Metallothioneins' chemistry: Reactivity and functionality of MTs

The characterisation of MTs permits to hypothesise about their function and biological use. The great variety of functions associated to MTs and the difficulties to relate some biological functions to these proteins cause researchers to be cautious about MTs' ultimate functions, for this topic is still a matter of debate [85, 86]. However, it is a fact that MTs develop an important role in the biological functions of the organisms, since they are present in all kingdoms of life, from the ancient prokaryotes to the most complex eukaryotes, and have been pervasive over the years [4]. MTs function is dominated, once again, by their intrinsic biochemical properties, provided mainly by their high content in Cys. The high coordinative capacity of Cys residues and the great kinetic lability of metal-thiolate bonds permit a rapid metal exchange with other proteins [87, 88]. Likewise, the high redox activity of Cys residues confer to MTs the capacity to react with other electrophilic species and free radicals, easily and reversibly oxidising the thiol groups [89, 90]. All these facts relate MTs to metal metabolism activities and oxidative stress reduction [91]. Therefore, MTs reactivity is characterised by:

- **High capacity of coordinating transition metal ions:** the polydentate ligand's nature of MTs affords great affinity for soft metal ions. In fact, some studies revealed that MTs are found both in extracellular and cytosolic media in their demetallated (apo-MT) or semi-demetallated form, suggesting that this status favours the metal ions uptake [92, 93].
- **Ease of exchanging metal ions:** the great lability of the metal-thiol bonds facilitates a quick exchange of ions in the metallated MTs. This exchange is based on the affinity of metal ions towards thiolate ligands as described by the series of Irvin-Williams [94]:  $\text{Fe(II)} \approx \text{Zn(II)} \approx \text{Co(II)} < \text{Pb(II)} < \text{Cd(II)} < \text{Cu(I)} < \text{Au(I)} \approx \text{Ag(I)} < \text{Hg(II)} < \text{Bi(III)}$ . According to these series, a Zn(II) loaded MT is more reactive than a Cu(I) loaded one, meaning that Zn(II)-MT's tendency to exchange its metal ions is higher than that of Cu(I)-MT's. Therefore, in case of exposure to toxic Cd(II), Pb(II) or Hg(II), Zn(II)-MTs will easily exchange their initial ions by the toxic ones, which show more affinity towards thiolate ligands.
- **Metal transfer between MTs and other proteins or biomolecules:** the interaction between MTs, which interchange their metals it is well-known [95], but also the metal transfer between MTs and other intra or/and extracellular biomolecules [88, 96, 97]. This property of MTs expands the view of a simple molecule with high capacity of binding metal ions of the medium and

exchanging them with other metal ions in solution, to a molecule capable of interact with other proteins, suggesting that MTs perform a biological function.

- **Redox activity:** at a physiological level, MTs are found in three different conditions: oxidised (thionins, TOs), reduced without metals as apo-MT form (thioneins, Ts), and associated to metals as holoproteins (metallothioneins, MTs) [90]. TOs are barely reactive, since all the Cys residues are oxidised as disulphide bonds, while Ts and MTs are reactive species to oxidant agents such as reactive metal species, reactive oxygen species (ROS) or reactive nitrogen species (RNS). The equilibrium and coexistence of these three species inside the cell depend on the cellular type and its metabolic activity (*i.e.*, MTs synthesis/degradation rate and cell redox conditions) [98]. Therefore, the interaction of oxidising agents with MTs gradually triggers the metal release from the protein and the formation of Ts that, in turn, becomes TOs after being oxidised. This process is reversible and reducing agents such as glutathione (an asset closely linked to MTs) can reverse this oxidation returning TOs to Ts [90]. In fact, glutathione acts either reducing TOs to Ts and oxidising MTs, regulating the metal levels of the MTs [99].

These properties have been experimentally demonstrated and, as they are diverse and very specific, MTs have been proposed to be involved in a multitude of biological processes:

- **Essential metals' homeostasis:** physiological metal ions such as Zn(II) and Cu(I) are essential for the proper development of the organisms and are in association with plenty of metalloproteins [100]. However, a destabilisation on the concentrations of this intricate equilibrium might lead to a toxic environment. Consequently, living organisms have developed mechanisms to maintain this fine balance, for instance by using MTs and other chelating agents. MTs have been proposed as a key factor in the regulation of Zn(II) and Cu(I) ions levels because of their great coordinating capacity and the labile nature of their thiolate-metal bonds. These properties are ideal for capturing metal ions in solution at high concentrations but disposing them at low concentrations. Besides, these properties not only are of use to regulate the metal levels in solution but also to facilitate the transfer of metals from MTs to other proteins [101]. For that reason some studies involve MTs with the regulation and absorption of Zn(II) and Cu(I) ions in the cytosol [102], but

also in their distribution, reservoir and supplying at different physiological conditions [85, 98, 103, 104]

- **Toxic metals detoxification:** toxic metal ions such as Cd(II), Hg(II) or Pb(II), due to their high affinity for thiolate ligands, compete with essential metal ions in the active site of some metalloproteins, which cause a malfunctioning of those proteins. Specially in the case of Cd(II), with similar chemical properties to Zn(II), there is a great interaction with Zn-dependent metalloproteins [105]. The high sensibility to a metal exposure of organisms genetically modified unable to produce MTs [85, 106, 107] and the fact that some *MT* genes are overexpressed or induced under Cd(II) stimulus has led to hypothesise that some MTs could be involved in heavy metals handling and detoxification [108, 109, 110]. The Cd-selectivity shown by some MTs is another important feature that supports this detoxification putative function. Some MTs are not only induced by Cd(II) but also their three-dimensional structure and their metal clusters are more stable when Cd(II) is involved [56, 111, 112].
- **Antioxidant agents:** some studies show that mammalian and snail *MT* genes are upregulated after an oxidative stress stimulus [113, 114], others show their indirect involvement in oxidative stress by modulating the activation of Cu/Zn superoxide dismutase [115]. These specific situations and their high content in reactive thiolate moieties suggest that MTs might be involved in antioxidative stress activities. Moreover, MTs are detected along with ROS and RNS in events of cellular stress conditions caused by different factors (*i.e.*, external radiation or redox reactions from internal processes) [116, 117, 118]. In fact, the cellular damage originated by ROS is more destructive in those cells whose *MT* genes have been suppressed than in control cells, suggesting that MTs neutralise free radicals such as hydroxyl, peroxide, or superoxide [119, 120, 121].
- **Molecular chaperones:** chaperones form a protein family that assist other proteins in building their conformational folding or in assembling macromolecular complexes. MTs have been suggested to be involved in the formation and activation of several allosteric enzymes, providing the necessary metals to activate them [122, 123, 124]. Therefore, MTs could



be directly or indirectly involved in metalloproteins folding through metals supplying [125].

- **Antiapoptotic role:** related with their role in aiding protein folding, MTs, specifically MT2A, have been involved in multiple types of tumour proliferation due to their interaction with transcription factors [126, 127]. The downregulation of human MT2A have demonstrated to inhibit cancer cell growth, suggesting a tight relationship of this MT with cell proliferation and chemoresistance [128, 129]. In fact, *MT2A* gene is suggested to be a great biomarker to detect cancer risk, as a deregulation of this gene might develop an uncontrolled proliferation of the cell [130]. Related to this, MT1H has been reported to suppress cancer cell proliferation and invasion by inhibiting Wnt/ $\beta$ -catenin pathway [131].
- **Protective agent in cellular senescence:** the antioxidant properties of MTs are highly important preventing DNA damage [132]. These properties, as well as their heavy metal scavenging role, relate MTs with functions in cellular homeostasis and immunity, lowering the levels of metals and free radicals. In turn, this triggers a modulation of the effect of inflammation and stress response in tissues that prevents an early senescence of the cells [133, 134].
- **Metabolic control:** it has been described the effect of high-fat diet on MT-knockout mice, which become obese [135]. MTs regulate the energetic cellular balance through the formation of adipose tissue. These metalloproteins neutralise superoxide radicals and endoplasmic reticulum stress that induce obesity-related diseases [136]. Moreover, MTs are involved in the signalling pathway of insulin, whose interference provokes an elevated lipid accumulation, inducing the development of obesity [137].

Clearly, all these examples put on the table a family of proteins with very complex interactions with other proteins, which hinders the quest of finding a specific function for MTs. Somehow, MTs have been pervasive along the evolution and have been maintained by the organisms, confirming their utility within the biological system, but their special biochemical features have not restricted them to a single biological function.

#### 1.1.4. Classes and classification of MTs

On the search of a function for MTs, their classification is essential. Proteins are typically sorted into protein families, which group proteins that share a common evolutionary origin and display similar structural and functional properties [138]. Duplications and other genetic mechanisms permit that one protein evolves into two different proteins, leading to developing new functions [139]. These are termed homologous proteins and their “homology” allows to score the resemblance between them [140]. Taking this homology into account, structural and functional properties can be proposed for a novel unknown protein that display similar amino acid sequence with another described protein. By relating homologous protein sequences, it is possible to generate phylogenetic trees that permit to better understand the function and evolution of these proteins. Besides, protein classification allows to evaluate and hypothesise about other proteins whose structures or functions are difficult to solve.

In the MTs field, protein classification embodies a multitude of opinions as various sorting criterions have been used ever since they were first discovered [141]. The first attempt of MT classification was the one established at the Second International Meeting on Metallothionein in 1985 [142]. The committee proposed the division into three classes, based on the similarity of the primary structure of the known MTs with that of the first mammalian MT described:

- \* Class I included closely related MTs with conserved Cys alignment with the mammalian MT;
- \* Class II comprised non-homologous MT sequences whose cysteines were not distributed as the first reported MT and;
- \* Class III considered polypeptides enzymatically synthesised (without using ribosomes) that displayed Cys in their sequence and were able to bind metal ions [143].

Class I included a great variety of MTs, from mammal to invertebrates through other vertebrate families, all of them governed by a bidomain structure. In class II yeast, plant, invertebrate, and some bacteria MTs were described. Most of them are monodomain proteins with poor alignment with mammalian MTs. Finally, the origin of class III MTs is not from mRNA but from the enzymatic synthesis. These special MTs are found in plants, algae, and some fungi and some are known as phytochelatins or cadystins [144, 145, 146]. They were considered a class of

metallothioneins despite their distinct primary structure because they could coordinate a high amount of transition metal ions.

This classification became outdated when new class II members (highly distant to each other) were incorporated over the years. The sequences' length, amino acid composition and number and distribution of Cys residues were appreciably varied for a group of proteins belonging to a same class. For that reason, Binz and Kägi proposed a new classification method based on sequence similarity and phylogenetic relationships [141]. This criterion drove to as many MT families as taxonomic groups were known. However, although the alignment of amino acid sequences is a good tool to perform evolutive studies, one should be careful to relate similar sequences to a determined biological function. It is not always fulfilled that two similar MTs with identical Cys motifs always render equal metal-binding preference and, thus, similar biological function. As an example, the same Cys motifs are found in the Cd-, Cu- and Cd/Cu-MT isoforms of the *Helix pomatia* and *Cantareus aspersus* snails, with clearly distinct metal preferences and biological functions [51, 147]. For that reason, this method is considered incomplete to relate functions and reactivity among MTs and it should be considered as complementary to the following classification.

In view of efficiently gather MTs for their structure and function, our group devised in 2001 a functional classification that unifies MTs by their metal-binding preferences [148]. This classification has been in constant improvement and more and more features have been included along the years to generate a handy tool to compare MTs by their biochemical properties, so that the biological function of novel MTs could be inferred. Since the 3D structure of a biomolecule determines its function [149] and considering that the structure of each MT is governed by the metal ion associated to this protein [150, 151], it is straightforward to assume that the metal ion coordinated to each metal-MT species is related with a physiological function. Based on that supposition and that Zn(II) and Cu(I) are two of the most common essential metals in organisms, and that the coordinative preferences of these two metal ions are clearly different (see **Section 1.1.2**) our group proposed an MT classification separating two marked metal-binding preferences and therefore two metal-binding "behaviours": Zn-thioneins and Cu-thioneins [148]. The former group is associated to MTs with high preference for divalent metal ions. These proteins have been demonstrated to perform biological functions related to Zn(II) homeostasis and trafficking or Cd(II) detoxification [6, 14]. In contrast, Cu-thioneins render very stable Cu-MT complexes, for which are

connected with biological processes involving this metal ion: Cu(I) ions reservoir or supplier, ion sequestering, etc. [6, 152, 153].

This proposed classification of MTs into two extreme metal-binding behaviours covered all research and classification purposes by the time it was released. However, as new “class II” MTs were discovered, more and more different metal-binding features were described, so the initial proposal was updated to a more precise one [154]. This new model demonstrated that not all known MTs displayed “extreme” metal-binding preferences towards divalent or monovalent metal ions, rather there was a stepwise gradation of metal-binding preferences between what were denominated “genuine” Zn- and Cu-thioneins (**Figure 1.4**).

More interestingly, the continued research made in our group also allowed to propose key factors that established the metal-preferences of MTs in order to classify them. Among others, the discovery of labile sulphide ligands ( $S^2$ ) as a third component of the metal-MT clusters in some recombinant MT productions [155] and the realisation that the oxygenation degree of the *E. coli* cultures had an influence on the homo- or heterometallic nature of the Cu-MT preparations [156] were determinant factors to design this fine-tuning classification of MTs [13].



**Figure 1.4.** Schematic representation of the gradual MT classification in function of their Zn- or Cu-thionein behaviour.

This final classification was based in the following bullet points to evaluate the metal-binding features of each MT:

- Presence or absence of Zn(II) ions in the Cu-MT complexes biosynthesised in Cu(II)-enriched *E. coli* cultures under different oxygenation degrees.
- Presence or absence of sulphide ligands in the *in vivo* Cd-MT complexes.
- Presence or absence of Zn(II) ions in the biosynthesised Cd-MT species.

- Reluctance of the *in vivo* Zn-MT species to total metal-exchange of Zn(II) by Cd(II)
- Number of Cu(I) equivalents needed *in vitro* to reproduce the *in vivo* Cu-MT ones

The metal-binding properties observed for genuine Zn- and Cu-thioneins are shown in **Table 1.2** [13]:

**Table 1.2.** Comparison of the features of the products rendered by genuine Zn-thioneins and genuine Cu-thioneins.

Genuine Zn-thioneins	Genuine Cu-thioneins
Render unique M(II)-MT species when synthesised in Zn(II)- or Cd(II)-enriched medium	Render mixtures of Zn(II)- or Cd(II)-MT species when produced in M(II)-supplemented media
Might yield heterometallic Zn,Cd-MT complexes when produced in Cd(II)-supplemented <i>E. coli</i> cultures	The products of the biosynthesis in Cd(II)-enriched <i>E. coli</i> cultures contain labile sulphide ligands (S <sup>2-</sup> )
Are reluctant to <i>in vitro</i> exchange Zn(II) by Cd(II)	No resistance to fully exchange Zn(II) by Cd(II) <i>in vitro</i>
Formation of heterometallic Zn,Cu-MT species when recombinantly synthesised in Cu(II) supplemented media (process dependent on the oxygenation degree of the culture)	Yield homometallic Cu-MT species when biosynthesised in Cu(II)-enriched media (independently of the oxygenation degree of the culture)

The main feature of Zn-thioneins is that they render unique well-structured M(II)-MT complexes when synthesised in culture media supplemented with divalent metal ions. This means that this group of proteins displays high affinity for divalent, Zn(II) and Cd(II), ions. However, it should be clarified that genuine Zn-thioneins show more preference for Zn(II) than for Cd(II). For that reason, in some cases, there is a reluctance of Zn(II) ions to be displaced by Cd(II). This occurs either *in vivo* in the Cd(II)-MT productions, rendering heterometallic Zn,Cd-MT complexes, or *in vitro* during the Zn(II)/Cd(II) exchange experiments, in which the initial Zn(II)-MT complex does not fully exchange its metal ions by Cd(II). It is important to clarify that, in this PhD thesis, the *in vivo* complexes are those species obtained from the biosynthesis in *E. coli* cultures, while the *in vitro* species are those formed during a metal exchange experiment, or as consequence of any

manipulations performed out of the living cell. With regards to why Zn(II) ions should be displaced in the *in vivo* formation of Cd(II)-MT complexes, there is a hypothesis that states that probably all MTs are initially produced in the cytoplasm in association with Zn(II) ions and, that afterwards, they exchange these Zn(II) ions depending on their necessities [157]. For that reason, it is possible to observe Cd(II)-productions which render heterometallic Zn,Cd-MT complexes *in vivo*. Related to this very phenomenon, another main feature of genuine Zn-thioneins is that they render heterometallic Zn,Cu-MT complexes when biosynthesised in Cu(II)-supplemented cultures. Following the same reasoning, the high preference of these MTs for Zn(II) makes them reluctant to totally exchange Zn(II) by the high concentration of Cu(I) ions present in the cell. The Zn(II) metal ions already present in the cluster stabilise the complex, so they can be considered structural ions.

As a counterpart, Cu-thioneins include all the MTs with high preference for Cu(I) ions. They render unique well-structured homometallic Cu(I)-MT complexes when are bioproduced in Cu(II)-enriched *E. coli* cultures. Additionally, the discovery of the presence of labile sulphide ligands in some preparations was determinant for this classification proposal, since it was possible to relate the quantity of these ligands with the Cu-thionein behaviour of the considered MT. These ligands are only found in the preparations of MTs which show a poor Zn-thionein features, and especially during the *in vivo* biosynthesis of Cd-MT preparations, facilitating therefore, the detection of genuine Cu-thioneins. Cu-thioneins do not efficiently render Zn(II)-MT complexes, and for that reason, they yield a mixture of Zn(II)-MT species when synthesised in Zn(II) supplemented media. The situation is even worse when this Cu-thionein is synthesized in a Cd(II)-enriched media, as the bigger size of the Cd(II) ions in comparison to those of Zn(II), requires the participation of “external” ligands such as  $S^{2-}$  to stabilize the “artefactual” Cd-MT species that are recovered under these conditions.

So far, this has been the most complete functional classification to evaluate the metal-binding features of MTs. However, the exploration of new phylogenetic groups is continuously providing new data of novel MT sequences with distinct biochemical and metal-binding features.

## 1.2. State-of-art of the MT systems

Ubiquitous MTs have been reported from most of living beings, involving a massive number of biological processes, asserting the importance of these proteins to the organisms. Their high versatility has connected them to many research projects of a vast number of different science branches, from ecology [158, 159,

160] to medicine [161, 162, 163] through genetics and evolution [164, 165]. Since they have been found in all kingdoms of life (**Figure 1.5**), several research groups have focused their efforts to specialise on MTs' biochemical features of a specific group of organisms. These groups range from Vasák and Kägi advancing on the knowledge of vertebrate MTs [48, 52, 70, 166, 167], Calderone and Meloni focusing on Cu-specific MTs such the fungi MTs [62, 168], and Freisinger and Blindauer contributing into the insights of plant MTs [50, 58, 82, 169, 170]. Blindauer also greatly expanded the understanding of bacteria MTs' biochemical features [37, 84]. Although MTs' research covers most of the phylogenetic groups, mammalian MTs are the most studied, due to their anthropocentric and medical implications [reviewed in 6]. Mammalian MT was the first to be discovered [5] and, after that, many different isoforms and their variants were reported [171], displaying a complex system in which MTs are expressed under distinct physiological situations, tissues, or life stages [reviewed in 14]. There are four mammalian MT isoforms, named from MT-1 to MT-4. MT-1 and MT-2 are expressed in all the tissues of the organism, while MT-3 and MT-4 are tissue specific MTs [172]. The two first MTs have been widely reported because they are easily induced upon metal exposure [44]. In fact, they are physiologically isolated in association with Zn(II) and/or Cd(II) metal ions. For that reason, they are linked to roles of detoxification and homeostasis of heavy metal ions [173, 174]. Regarding MT-3, it has been natively recovered from brain tissue [175], displaying a monodomain Cu(I)<sub>4</sub>Zn(II)<sub>4</sub>-MT-3 structure and considering it the mammalian MT with more Cu-thionein behaviour [166, 176, 177]. Finally, MT-4 is found in epithelial tissue, showing some resemblances to MT-3 metal-binding features [167]. In general, their three-dimensional structure is that of a dumbbell, in which two functional domains build independent metal clusters connected by a flexible hinge region [178]. This topology is found when MTs are bound to divalent metal ions, containing two types of clusters: a M(II)<sub>3</sub>(SCys)<sub>9</sub> at N-terminal  $\beta$  domain and a M(II)<sub>4</sub>(SCys)<sub>11</sub> at C-terminal  $\alpha$  domain [48]. However, this bidomain structure is distorted when the protein is forced to fully bind monovalent Cu(I) ions [179].

From all this research, our group widely contributed to extend the knowledge of the metal-binding abilities of human MTs and both  $\alpha$  and  $\beta$  domains towards many metal ions (*e.g.*, Cd(II), Zn(II) and Cu(I) but also Ag(I), Pb(II) and Hg(II)) with more than 23 studies [6, 32, 33, 176, 180, 181, 182, 183]. During this research, the use of mutants has been a generous support to understand the systems [57, 184, 185]. Besides mammalian MTs' characterisation, our group has been involved in

the analysis of other vertebrate MTs such as chicken MT [186], and several invertebrate MTs.

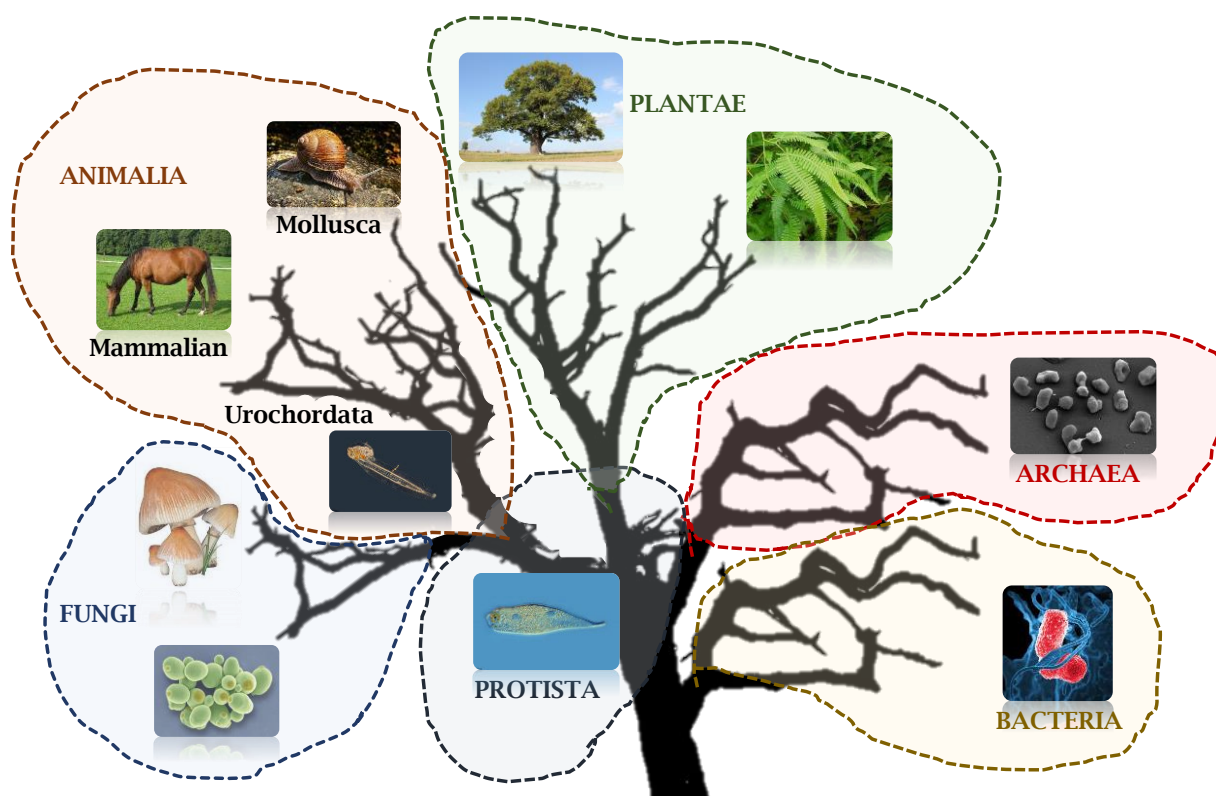


**Figure 1.5.** Tree of life representing all six currently accepted kingdoms.

Despite invertebrate MTs have been relatively less studied than mammalian MTs, their investigation has provided valuable information about animal organisms development (*e.g.*, in the study of *Drosophila melanogaster*) [187, 188], or the ecological implications of contaminants to the habitats of certain organisms [189, 190]. Our group, always devoted to better understanding MTs' metal-binding abilities, characterised the *D. melanogaster* MT system, finding in these MTs an exceptionally general preference towards Cu(I) ions [191, 192, 193, 194, 195]. In addition to *Drosophila* system, our group got involved in the characterisation of other invertebrate MTs, such as sea urchin MTs (SpMTA and SpMTB) [196], lobster MT (HMT) [148], and lancelet MTs (BfMT1 and BfMT2) [197]. However, most of the invertebrate MT systems characterised by our group belong to molluscs (16 publications and a few more in publishing stages).

Mollusc phylum represents a vast collection of species that have been proved of great importance from an economical, medical, and ecological point of view [198]. This phylum includes some relevant phylogenetic groups in the study of MTs, such as the case of gastropods. This group of molluscs have adapted their lifestyles to practically all habitats on Earth [199], denoting high genetical



heterogeneity and constituting an interesting group to perform evolutionary studies, especially from an ecological point of view [158, 159, 160]. In fact, the genetic mechanisms around MTs such as *MT* gene duplications [200, 201], *MT* domain multiplications [165, 202, 203], modulation of the *MT* gene expression [204, 205, 206], and changes in the metal-binding preference [51, 207, 208], have been crucial not only for molluscs, but for all the organisms' adaptation to different environments. Yet, it is important to consider that in order to preserve MTs' structure and their metal cluster, hence, their function, MTs' special features such as the Cys residues positions are to be conserved [209]. For that reason, the amino acid sequences of the MTs within the same phylogenetic group have a good alignment and their comparison provides straightforward evolutive information [210]. Therefore, the conserved modularity of mollusc MTs (consequence of these genetical processes) have permitted to trace all these lineage-specific evolutionary events occurred along all mollusc phylogenetic groups, connecting them with the conditions of their habitats and the metal-binding preferences of their MTs.

It is of relevant interest the case of Cd(II)-selective MTs found in some snail and slug species, which have been connected with Cd(II) detoxification functions [51, 55, 111, 112, 147, 185, 211, 212]. In fact, these MTs are genetically activated after Cd(II) exposure [17, 114], meaning that Cd(II) ions activate physiological pathways to synthesise these MTs. This type of MTs was included in the sack of Zn-thioneins, following our stepwise gradation classification of MTs. The physicochemical similarities between Zn(II) and Cd(II) provoke that an important amount of MTs show equivalent metal-binding behaviours for these two metal ions. This is the main reason why only a dichotomic Zn- to Cu-thionein scale was initially proposed. Thus, the intriguingly tight relationship between these MTs and Cd(II) ions led to perform an exhaustive evolutive study to seek the origin of the Cd-selectivity [210]. This work comprised a massive number of MT sequences of mollusc species from either marine, terrestrial and freshwater habitats to cover all the environments with considerably distinct Cd(II) concentrations. Moreover, the coordinating abilities of some of these MTs were already characterised, so an evolutive study allowed the construction of a phylogenetic tree that related their evolutive origin and their metal-binding preferences. The lineage-specific metal-binding properties of mollusc MTs and the correlation of the habitats with that metal-specificity reported in this work suggests that Cd-selectivity has been modulated by the Cd(II) concentration levels present in the molluscs habitats during their evolution. In many species this Cd-selectivity has been maintained due to the Cd-levels of their environment, however, some freshwater snails lost this metal-selectivity, probably,

because the levels of Cd(II) ions are, at least, a couple of magnitudes lower than those of the rest of habitats and they did not suffer an evolutionary pressure to maintain that feature [210, 213].

This complete study comprising most of the reported gastropod MT sequences, along with the NMR studies, supported the hypothesis that the prototypical gastropod MT is a bidomain structure [56]. This structure contains two equivalent domains of 9 conserved Cys residues and each one binds three divalent (mainly Zn(II) or Cd(II)) or six monovalent (mainly Cu(I)) metal ions (**Figure 1.6**). From this conserved topology, some snail MTs have been modified at their N-terminal domain such in Patellogastropoda MTs, which show 10 Cys residues instead of 9 [210]; or duplicated their domains once or more times as in the case of *Littorina littorea* MT [55], *Pomatias elegans* MT [212], or the multidomain *Alinda biplicata* MT [203].

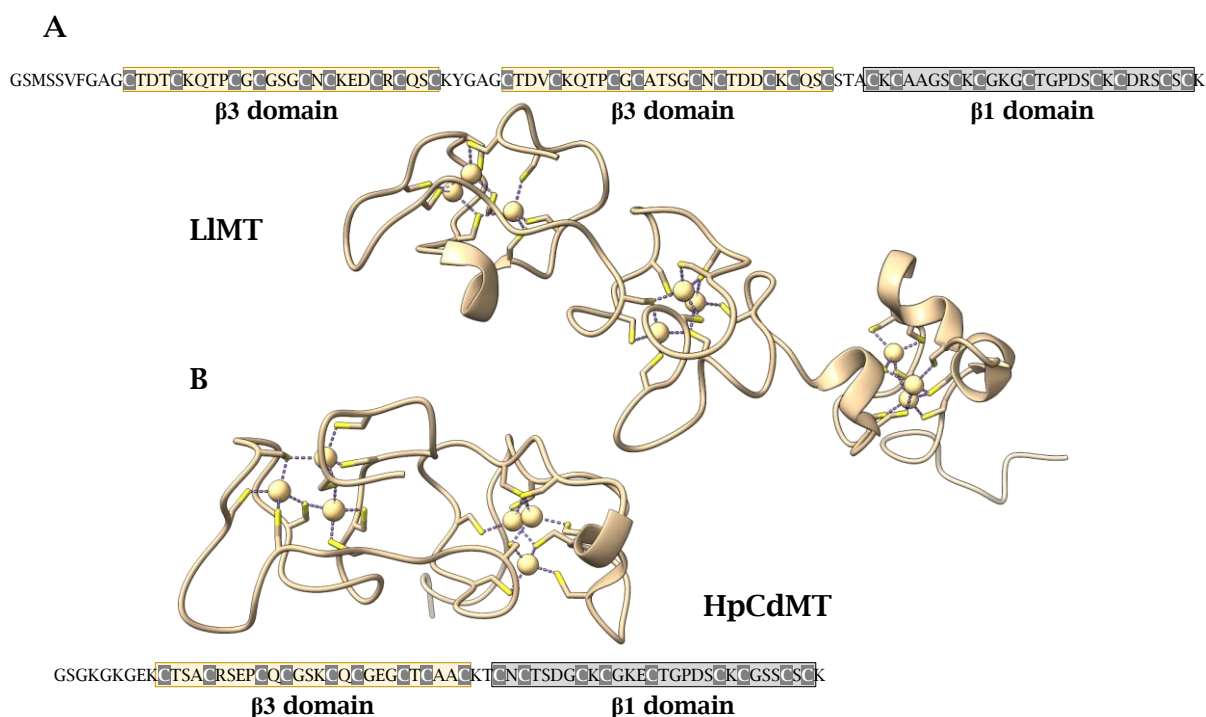


**Figure 1.6.** Amino acid sequences and 3D structures of (A) *Littorina littorea* MT [55] and (B) *Helix pomatia* CdMT [56] solved by solution NMR (PDB entries 5MN3 and 6QK6, respectively). Cd(II) ions are represented as yellow spheres, Cys residues as yellow sticks and coordination bonds as purple dotted lines. Coloured boxes contain Cys-rich regions that represent distinct  $\beta$  domains.

Overall, the study of gastropod MTs has provided useful information about MTs' evolution but also about metal-binding specificities in MTs. A research line performed by our group and collaborators was devoted to the biochemical mechanisms that rule the metal-binding specificity of the MTs. This prolific research demonstrated, by studying terrestrial snails' MTs, that the ratio of lysine

(K) and asparagine (N) residues drives the metal-binding preference of these organisms [112, 211]. All the MT sequences of both *Helix pomatia* and *Cantareus aspersus* conserved their Cys residues positions, being the non-coordinating residues the unique changing factor between them. Thus, these studies observed that while the K:N ratio was higher, the preference towards divalent metal ions also raised, otherwise, if the K:N ratio was lower in the sequences, their preference towards Cu(I) ions increased. This phenomenon helped to understand better the metal-binding preferences of terrestrial gastropod MTs. In addition to these experiments, the extraordinary Cd-selectivity found in some snail MTs contrast with the concept of the current functional MT classification. Considering the above demonstrated importance of Cd(II) ions during the evolution of the MTs of this phylogenetic group and the paradigmatic metal-binding behaviour displayed by some “extreme” Cd-selective MTs, it is straightforward to hypothesise whether it exists a “genuine” Cd-thionein metal-binding behaviour, independent from the current Zn-thionein one, that display particular coordinating features not shared with the other groups of the present dichotomic Zn(II)/Cu(I)-thionein MT classification. A holistic study which comprised MT sequences from all classes of mollusc would provide essential information to the evolutive origins and metal-binding features of mollusc MTs and, with all this new information, the structure of the current MT classification could be assessed. It could be updated to a three-band classification involving genuine Zn(II)-, Cu(I)- and Cd(II)-thioneins. Following this motivation, this PhD thesis is devoted to elucidating this hypothesis.

The MT system of urochordates is also quite unknown. In this phylogenetic group are included filter-feeding species, whose dynamic gene evolution [214, 215] and their close genetical relationship with vertebrates set an ideal scenario to learn about the origin and evolution of chordate MTs. Urochordates, or tunicates, form the sister clade of vertebrates and, together with the standalone group of cephalochordates, constitute the phylum Chordata. In turn, urochordates are divided in three classes: Larvacea, Thaliacea, and Ascidiacea. The filtering lifestyle of these organisms entails a considerable exposure to the elements present in the seawater habitats (*e.g.*, heavy metals) and, thus, a great tendency to accumulate them. Consequently, urochordate species rely on molecular mechanisms to palliate these troubled waters. Obviously, MTs are one of these mechanisms used for this matter. As mentioned in mollusc MTs, the presence (and quantity) of Cd(II) ions in these organisms' habitats was of great relevance to the evolution of the metal-specificity of their MTs [210]. Gaining metal-selective MTs for the inactivation of the Cd(II) ions present in the seawaters where urochordates dwell would represent

an advantage for these species. However, the current insights into the MTs of this group of organisms are scarce. In fact, there is only one work that openly describes and characterises a tunicate MT [216], and another publication insinuates the existence of a metallothionein in the tunicate species *Pyura stolonifera* [217]. For that reason, a biochemical characterisation of urochordate MTs would provide information of the evolutive origin of chordate MTs and the metal-binding features of a new group of MTs.

Finally, it is important to mention the contribution of our group to the characterisation of MTs outside the animal kingdom. Part of the research performed in this group is dedicated to both *Saccharomyces cerevisiae* MTs [20, 156] and fungal pathogenicity. Fungal pathogenicity has been associated to the dispute between the host organism and these pathogens for the metal handling [218]. This conflict may be given by the sequestration of host essential metal ions by the pathogen or by an excessive Cu-overload at the hand of the host immune system to kill the pathogen [219, 220]. In either case, a protein designed to bind metal ions would be an advantage for the pathogen against these drawbacks. Once again, MTs arise as a plausible option to control a metal-related metabolism function and to understand better how fungal pathogenicity works [221]. Therefore, our group developed a research line studying a collection of fungal MTs and their mutants to determine a relationship between pathogenicity and MTs. This relationship was clearly established in *Cryptococcus neoformans* MTs and their high affinity towards Cu(I) ions [152, 153, 221]. This pathogen is able to counteract against the toxic response of macrophages, sequestering high concentrations of Cu(I) ions from the medium. Similarly, *Tremella mesenterica* MT is a long modular protein with high metal-binding capacity [222]. Although the Cu(I)-selectivity of the full protein is not as good as *C. neoformans* MTs', the results obtained from the cytotoxicity experiments performed on the living organism showed elevated tolerance to high concentrations of copper, suggesting a biological function related with Cu(I) homeostasis and Cu-enzymes synthesis.

Therefore, it is not negligible the importance of obtaining the biochemical properties of fungal MTs, as they are generally considered Cu-thioneins and, altogether with the Cd-selective mollusc and the novel urochordate MTs, fungi MTs may provide a wide perspective in the search of a new MT classification.



## 2. OBJECTIVES

---



## 2. Objectives

---

As a main objective of this PhD thesis, we question ourselves if the current dichotomic classification of metallothioneins (MTs) in Zn/Cd-thioneins (divalent metal ions specificity) and Cu-thioneins (monovalent metal ions specificity) is still valid. Therefore, we intend to elucidate whether genuine Cd-selective metallothioneins do exist and, if this is the case, to ascertain if they display differential metal-binding features in comparison with the existing so-called genuine Zn-thioneins to update the present functional MT classification. The strategy devised to confirm this hypothesis consisted in characterising until nowadays unknown MTs, which complete the current scenario with more data about their metal-binding features. Among these MTs we have chosen several mollusc and primitive urochordate MTs. The partial objectives that will aid into the global objective achievement are:

1. *The study of the coordinating capabilities of different mollusc MTs, completing the missing data of all gastropod MTs.*
2. *Characterisation of the metal-binding features of all domains that compose mollusc MTs.*
3. *To describe the metal-binding abilities of the MTs of the three tunicate classes: Ascidiacea, Thaliacea, and Appendicularia, expanding our current knowledge about chordate MTs' origins.*
4. *Sorting all the characterised MTs into three different groups by their metal-binding features: the two existing Zn(II)- and Cu(I)-thioneins and the putative Cd(II)-thioneins.*
5. *To evaluate whether the three types of MTs are sufficiently different to belong to distinct classes and to prove the methodology with already reported data.*





# 3. RESULTS AND DISCUSSION

---



## 3. Results and discussion

---

The characterisation of the MTs exposed in this PhD thesis was motivated by the possibility to evaluate the biochemical features of a great collection of sequences from three phyla that display specific interesting features. Our collaborators at the UB surveyed all the mollusc and urochordate MTs characterised (at that moment there were 15 gastropod MTs whose metal-binding behaviour was described) and proposed the synthesis of the MTs of those groups that were uncovered. They performed the phylogenetical studies of the proposed MTs, while we, at the UAB, characterised them and their metal-binding features. In addition, our collaborators from UB identified new MTs, collecting (known and unknown MTs) up to 272 new mollusc MT sequences from 189 different species and categorising them by classes, elaborating the most comprehensive phylogenetic tree made on mollusc MTs and permitting the identification of specific Cys patterns for each class (**Annex 7.3.4: Article 4**). Likewise, they obtained 160 new urochordate MT sequences from 44 different species, performing similar evolutionary studies about the origin of chordate MTs' evolution (**Annex 7.3.6: Article 6**).

This section aims to present and to discuss the principal results obtained from this extensive project, starting by a genetical contextualisation of the MT systems described in this PhD thesis (**Section 3.1**). Fortunately, this project provided a valuable opportunity to characterise a considerable number of MTs of extremely varied origins and with distinctly marked biochemical features, which constructed an ideal scenario to expand our insights into MTs' metal-binding properties and to polish the dichotomic MT classification postulated by our group 10 years ago [13]. To expose all the results gathered for all organisms' MTs and yet maintaining a "reading-friendly" text, the results are presented grouping them by families of proteins that show similar metal-binding features. Additionally, bearing in mind

that the current dichotomic classification already considers a gradation between extreme Zn-thioneins and extreme Cu-thioneins and that one of the hypotheses postulates the existence of an independent Cd-thionein behaviour distinct from the current defined Zn-thionein one, we considered convenient to stress the separation between genuine Zn- and putative Cd-thioneins. Thus, this section contains three subsections that report the different metal-binding properties found in this thesis. The first one describes those MTs without any specific preference for any of the studied metals (**Section 3.2**), the second one gathers those MTs that comply with the current definition of Zn-thioneins based on the description made by our group (**Section 3.3**), and the latter block groups those proteins, with high specificity for Cd(II) ions, that show distinct metal-binding features from those understood nowadays as Zn-thioneins (**Section 3.4**). To evaluate the coordinating properties of all the MTs at physiological conditions, the proteins have been recombinantly synthesised in *E. coli* cultures supplemented with Zn(II), Cd(II) or Cu(II) salts (**Section 5.1**), purified and characterised by means of spectroscopic (CD, UV-Vis and ICP-AES) and spectrometric (ESI-MS) methods (**Section 5.2**). These same techniques have also allowed to characterise *in vitro* the MTs' metal-binding abilities by adding solutions of distinct metal ions to the *in vivo* obtained preparations (**Section 5.3**).

Besides, **Section 3.5** introduces an intriguing phenomenon found in some of the studied samples that has been crucial to characterise the metal-binding features of the MTs. Finally, **Section 3.6** exposes all the facts that support the main hypothesis and partial objectives of this thesis: the proposal of a new functional classification that groups MTs by their metal-binding behaviour: Zn-, Cd- and Cu-thioneins. Another point to mention is that the discussion will reference the functional classification already proposed by our group [13], as the new classification postulated in the hypothesis of the current work is an update of that previous one.

### 3.1. In depth characterisation of the MT systems

The necessity of an extended population of MT sequences to achieve the main objective of this PhD thesis with significance and coherence led us to work with a wide collection of organisms with specific MT systems. The species reported here are representative organisms of their phylogenetic group as none or only few MTs are described in that group. In general terms, we have explored MTs from animal and fungi kingdoms. From the former, we focused on chordate and mollusc species. From one side, mollusc MT evolution provides an opportunity to learn

more about metal-binding preference, since this model system have several works reported that provide background on that matter, easing the design of future experimental procedures [51, 112]. From the other side, the chordate MTs reported here correspond to the sister branch of vertebrate organisms. This phylogenetic group, named urochordates, will provide prime information about the origins of the evolution of vertebrate MTs and, thus, being their study of great relevance. Hence, this section is divided in three subsections, including information of the MT systems of mollusc, urochordate, and fungi species.

### 3.1.1. Mollusc MT systems

Taking advantage of these insights into mollusc MTs model, we found convenient to complete the global view of mollusc MT evolution by characterising some of their representative MTs from unexplored phylogenetic groups. Molluscs are commonly divided in seven or eight taxonomic classes, depending on whether Aplacophora subgroups (Solenogastres and Caudofoveata) are considered classes or not [199] (**Figure 3.1**). From these classes, three are reported in this PhD thesis.

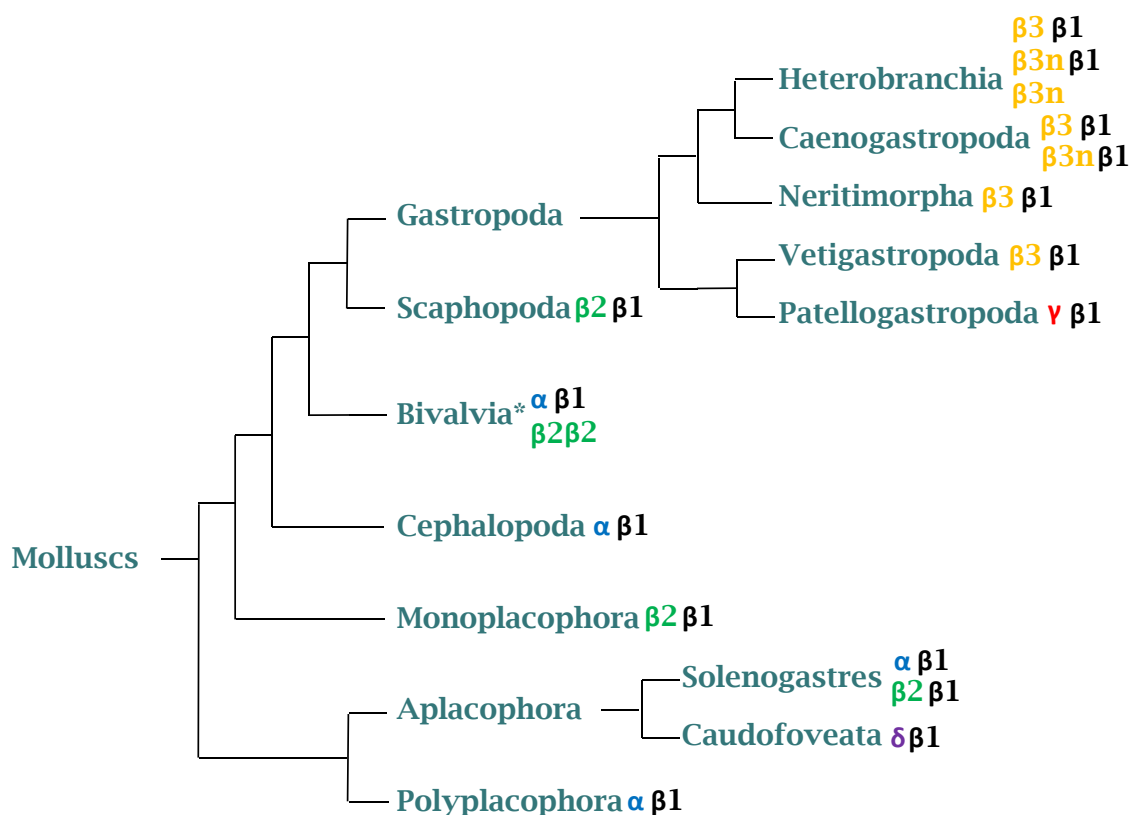


**Figure 3.1.** Scheme of the phylogenetic relationships between mollusc species based on [223]. For each class there is specified the prototypical domain structure of the representative MTs. \*Bivalvia display more combinations of domain structures not shown in the scheme. Gastropoda includes multi-modular MTs with more than two domains ( $\beta 3 n \beta 1$ ).

Mollusc MTs are homogenously spread among the phylogenetic groups. Their modular structure display equivalences between taxonomic groups, denoting a common evolutive origin [210]. From all the proteins characterised, four mollusc MT domains have been observed, considering the distribution and number of Cys residues:  $\alpha$ ,  $\beta$ ,  $\gamma$ ,  $\delta$ . In the case of  $\beta$  domains, three conserved Cys distributions are regarded:  $\beta 1$  ([Cx<sub>3</sub>C]<sub>x<sub>3</sub></sub>[Cx<sub>3</sub>C]<sub>x<sub>3</sub></sub>Cx<sub>3</sub>[Cx<sub>3</sub>C]<sub>x<sub>3</sub></sub>[Cx<sub>3</sub>C]),  $\beta 2$  ([Cx<sub>3</sub>C]<sub>x<sub>5</sub></sub>[Cx<sub>3</sub>C]<sub>x<sub>3</sub></sub>[Cx<sub>3</sub>C]<sub>x<sub>4</sub></sub>[Cx<sub>3</sub>C]<sub>x<sub>2</sub></sub>C) and  $\beta 3$  (Cx<sub>3</sub>Cx<sub>4</sub>[Cx<sub>3</sub>C]<sub>x<sub>3</sub></sub>[Cx<sub>3</sub>C]<sub>x<sub>4</sub></sub>[Cx<sub>3</sub>C]<sub>x<sub>2</sub></sub>C). Except in some Bivalvia species, mollusc MTs' C-terminal domain is a nine conserved Cys residues  $\beta 1$  domain, while the N-terminal end is variable from group to group. Thus, all mollusc MTs have lineage-specific N-terminal domains that have allowed to report genetic changes along mollusc evolution (**Annex 7.3.4: Article 4**). Interestingly, some of the MTs even display special traits such as multiple domains before C-terminal  $\beta 1$  domain [55, 203], or newly reported Cys motifs. One of those novel Cys motifs is found in *Falcidens caudatus*, which belongs to Aplacophora/Caudofoveata class (**Figure 3.1**). The members of this class have a lineage-specific 14 Cys domain ( $\delta$ ) at the N-terminal region that is not shared with any of the other mollusc species. This domain showed independency forming metal clusters (**Section 3.3.3**) and, together with the C-terminal  $\beta 1$  domain, it results a 23 Cys MT (**Figure 3.2**). The *de novo* introduction of this domain and the fact that this MT reveals an uncommon combination in the MTs field, makes of it a special case to closely follow up.

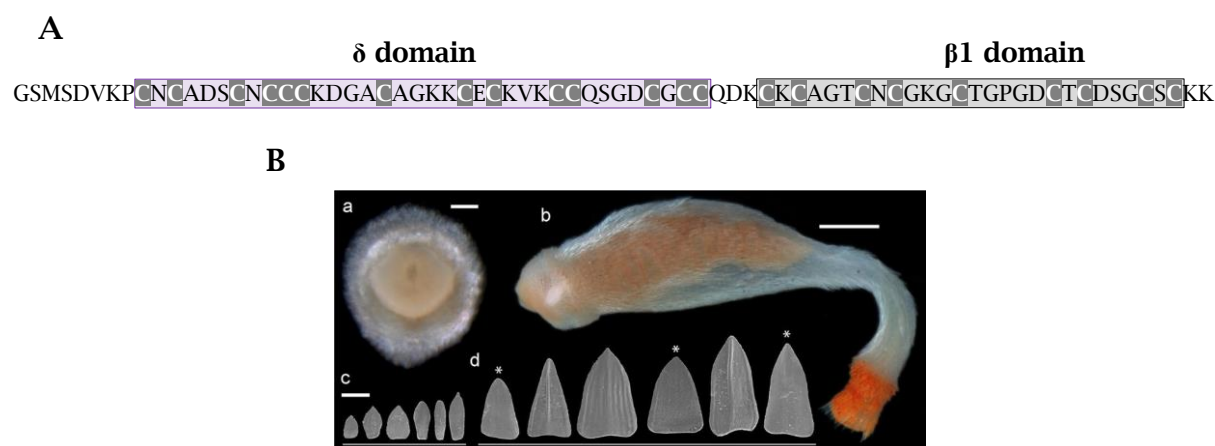


**Figure 3.2.** (A) *Falcidens caudatus* MT (FcaMT1) amino acid sequence. Cys residues are highlighted and  $\delta$  and  $\beta 1$  domains are contained within a clear violet and grey boxes, respectively. (B) *F. caudatus* micrograph obtained from [224] picturing the frontal and lateral side of the specimen, as well as the isolated sclerites that cover its body.

Another unique case found in this PhD thesis is the one of *Lottia gigantea* MT system. This species from the subclass Patellogastropoda contains two MTs that differ in structure with the rest of gastropod MTs. LgiMT1 and LgiMT2 show identical amino acid composition and arrangement except in three positions, which may lead to think that these MTs are encoded in the same gene and the identification of two isoforms is an artefact of the genome sequencing. However, both isoforms were detected after PCR amplification of the genetic material extracted from *Lottia* tissue, corroborating that both MTs are present in this organism. Their Cys arrangement follows a new distribution at the N-terminal region. This new domain is called  $\gamma$  and contains ten Cys residues organized in five CC duplets (**Figure 3.3**). This novel composition has not been reported before and stands between the 11/12 Cys  $\alpha$  domains and the nine Cys  $\beta$  ones, for it is also a case to observe closely.

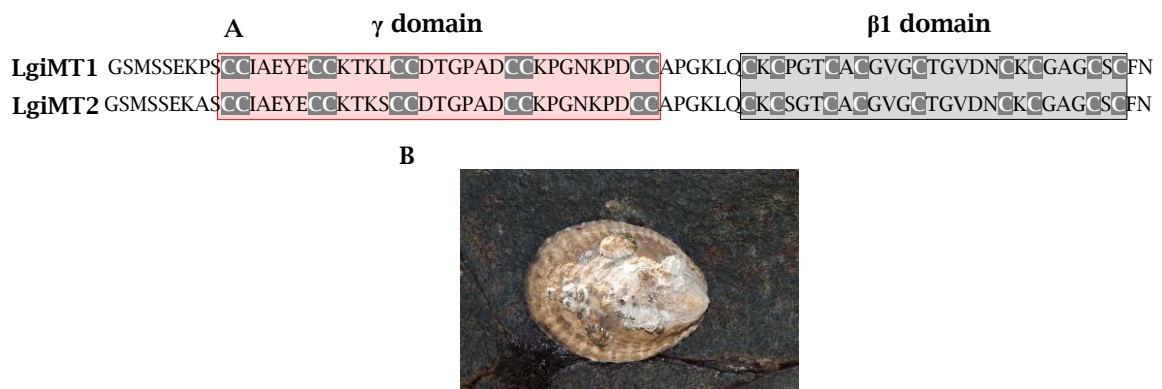


**Figure 3.3.** (A) *Lottia gigantea* MTs (LgiMT1 and LgiMT2) amino acid sequences. Cys residues are highlighted and  $\gamma$  and  $\beta$ 1 domains are contained within a red and grey boxes, respectively. (B) Picture of a *L. gigantea* specimen.

Continuing with other mollusc classes, here it is described the MT of *Nautilus pompilius*, the living-fossil mollusc with a notorious spiral shell. This cephalopod only possesses one MT reported so far. *N. pompilius* MT1 (NpoMT1) has a conserved domain structure within its taxonomical group, constituted by a 12 Cys  $\alpha$  domain and the common 9 Cys  $\beta$ 1 domain (**Figure 3.4**). This distribution resembles to that of the mammal MTs [225].





**Figure 3.4.** (A) *Nautilus pompilius* MT (NpoMT1) amino acid sequence. Cys residues are highlighted and  $\alpha$  and  $\beta$ 1 domains are contained within a blue and grey boxes, respectively. (B) Picture of a *N. pompilius* specimen.

Taking advantage of the information already available for gastropod MTs, we considered convenient to explore the rest of the groups of this subclass. Thus, four MT sequences of four distinct gastropod subclasses out of the existing five have been biochemically characterised. Gastropod species, as the rest of mollusc species, also present a lineage-specific N-terminal motif, probably derived from the archetypal  $\beta$ 2 domain. This module, called  $\beta$ 3 domain, contains nine Cys residues as well, but with a different distribution with respect to  $\beta$ 1 and  $\beta$ 2 domains. *Arion vulgaris*, with two  $\beta$ 3/ $\beta$ 1 MT isoforms, covers the data of Heterobranchia subclass (Figure 3.5). This slug expands our knowledge about what it is already known of terrestrial snails (e.g., *Helix pomatia* and *Cantareus aspersus*).

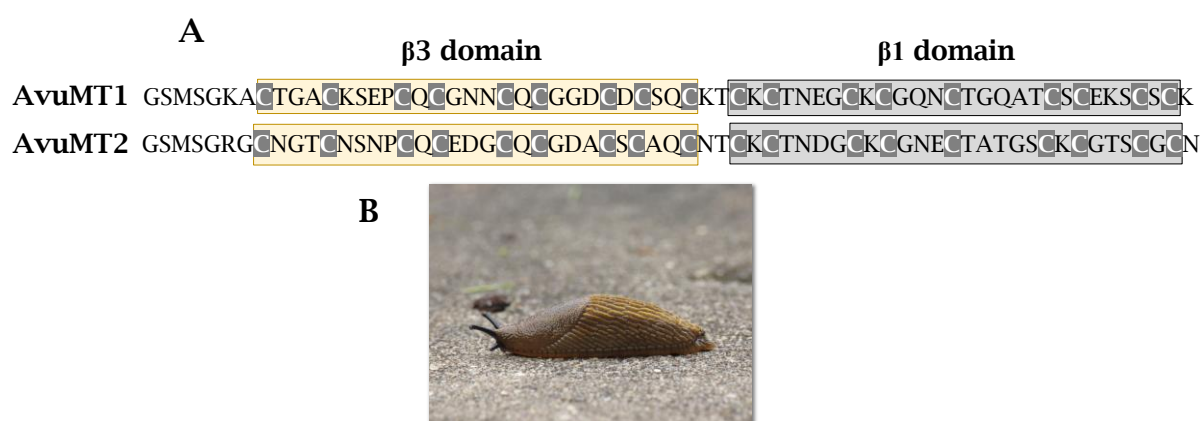


**Figure 3.5.** (A) *Arion vulgaris* MTs (AvuMT1 and AvuMT2) amino acid sequences. Cys residues are highlighted and  $\beta$ 3 and  $\beta$ 1 domains are contained within a yellow and grey boxes, respectively. (B) Picture of an *A. vulgaris* specimen.

Another case of  $\beta$ 3/ $\beta$ 1 MT arrangement is in the marine snail *Nerita peloronta*, which possesses two MT isoforms with these gastropod-specific domain composition. *N. peloronta* forms part of the Neritimorpha clade, one of the main

mollusc phylogenetic groups and represents the first species to be reported from its taxon. These MTs show some peculiarities, for instance, NpeMT1 contains an extra Cys residue, while NpeMT2 possesses one His residue in each terminal end of the sequence (**Figure 3.6**).

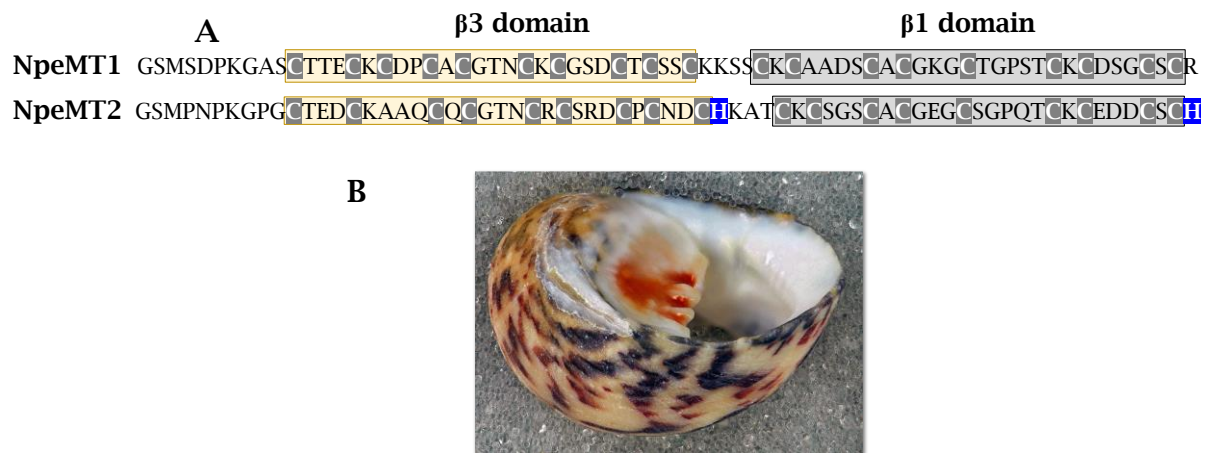


**Figure 3.6.** (A) *Nerita peloronta* MTs (NpeMT1 and NpeMT2) amino acid sequences. Cys and His residues are highlighted and  $\beta 3$  and  $\beta 1$  domains are contained within a yellow and grey boxes, respectively. (B) Picture of a *N. peloronta* specimen.

Finally, the last gastropod species studied is *Pomacea bridgesii*. This freshwater gastropod dwells in ponds and rivers, where the concentration of Cd is lower than in marine habitats. This fact led to hypothesise that the strong Cd-selective properties found in the evolutive origin of mollusc MTs might have been lost during the adaptation to freshwater habitats [210]. This species from Caenogastropoda subclass possesses two MT isoforms (PbrMT1 and PbrMT2) that are longer than the rest of gastropod MTs reported in this PhD thesis due to genetical modifications suffered during evolution. From one side, PbrMT1 acquired a novel module with four His and four Cys residues ( $H_4C_4$  motif) that adds up to the conserved  $\beta 3\beta 1$  domain architecture. On the other side, PbrMT2 lost its terminal  $\beta 1$  domain and duplicated its  $\beta 3$  domain twice, one entirely and a second time partially, resulting in a  $\beta 3/\beta 3/\beta 3_{1/2}$  domain structure (**Figure 3.7**). *Pomacea* species are considered a pest [226, 227], which may also be reflected by their metal-binding capacity, increased by the extra number of coordinating ligands. In this case, PbrMT1 gained a  $H_4C_4$  motif and PbrMT2 duplicated its domains.

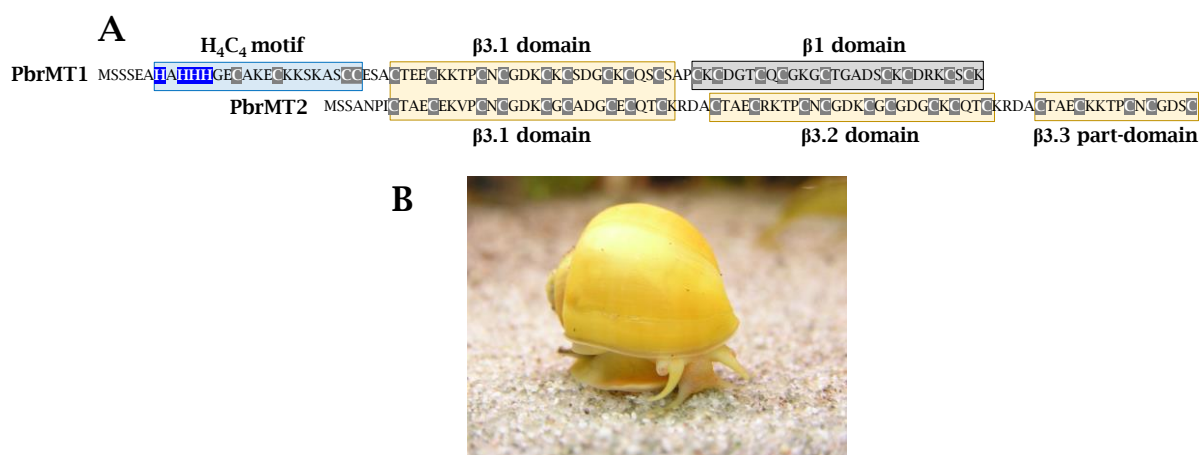


**Figure 3.7. (A)** *Pomacea bridgesii* MTs (PbrMT1 and PbrMT2) amino acid sequences. Cys and His residues are highlighted, and H<sub>4</sub>C<sub>4</sub> motif, β3 and β1 domains are contained within a blue, yellow, and grey boxes, respectively. **(B)** Picture of a *P. bridgesii* specimen.

Overall, this extensive collection of MTs covers most of the taxon groups in Gastropoda class and some unexplored classes of mollusc species. The results obtained from this study will permit to take conclusions about the origins of mollusc evolution and the metal-binding features of the different MT domains. It should be noticed, though, that the number of Cys residues present in the domains only informs about the metal-binding capacity or the possible metal cluster structure, but not about the metal-binding specificity. This fact was demonstrated by the study made on *Helix pomatia* MT isoforms, which all of them present an equal number of perfectly aligned Cys residues but different metal-binding specificity [211].

### 3.1.2. Urochordate MT system

Urochordata (Animalia kingdom) is the sister phylogenetic group of vertebrates and include three classes: Ascidiacea, Thaliacea and Appendicularia (**Figure 3.8**). The relevance of the species forming these classes in the ecology of marine habitats is well-known for representing an important component of food for fish and other zooplankton, as well as for their contribution on the vertical transport of carbon [228, 229]. The representative species selected for Appendicularia (or Larvacea) class was *Oikopleura dioica*. This species displays the highest evolutionary rates of all animal kingdom, and this is evident when their genetics are closely investigated [230, 231, 232, 233]. For that reason, it is not unlikely to find peculiar evolutionary events in the MTs of this species.

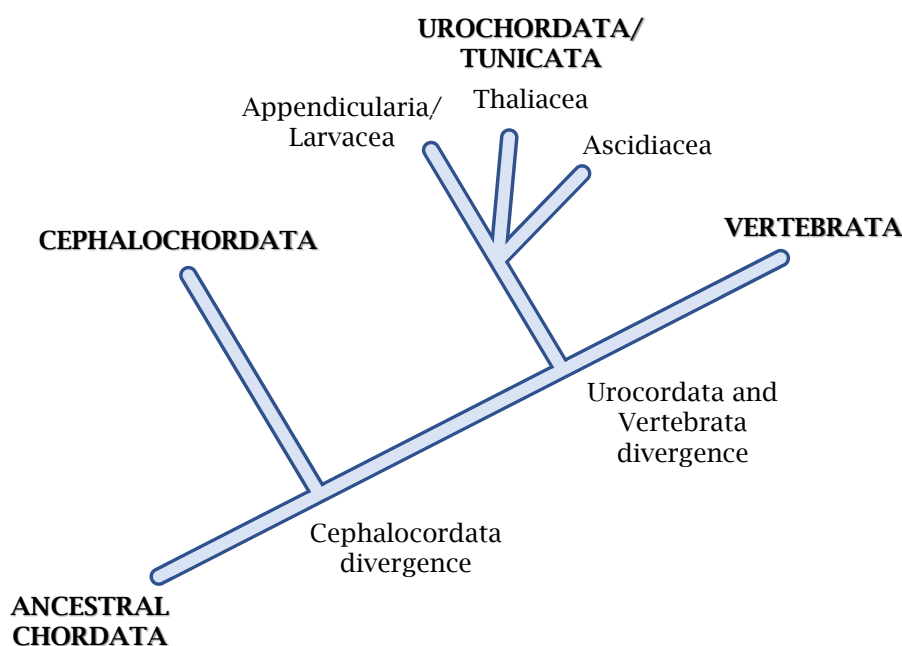


**Figure 3.8.** Phylogenetic tree of Chordata filum representing the most probable relationship between the three phylogenetic groups contained within this filum [234].

*O. dioica* possesses two MT isoforms, a prototypical 20 Cys residues MT (OdiMT1) and a multi-modular MT (OdiMT2). The interest of these MTs lies on their structure. At first, we exposed that OdiMT1 had two 7-Cys motifs (C7 motifs) whose arrangement were conserved along other *Oikopleura* species' MTs and OdiMT2 (**Annex 7.3.2: Article 2**). In fact, OdiMT2 is composed by the repetition of six OdiMT1-like-units (**Figure 3.9B**). These repeated units (RU) have a good alignment between themselves, meaning that are equivalent but not equal. However, after a deeper phylogenetic study of OdiMTs comprising more sequences of *Oikopleura*, we determined that OdiMT1 is actually arranged in two domains: a 12-Cys motif (12C) and a trimmed 12C domain of 9 Cys (t12C) (**Annex 7.3.5: Article 5**). Therefore, OdiMT1 displays a particular domain structure that differs from the ancestral chordate  $\alpha/\beta$  domains. After aligning the amino acid sequences of a number of tunicate MTs, it was postulated that Larvacea MT genes suffered a series of parallel evolutionary events (**Annex 7.3.6: Article 6**). Initially, a loss and gain of their MT genes provoked that the Cys motifs in larvacean MT sequences diverged from those found in the rest of tunicate MTs. After that, it followed a domain duplication, for which the archetypal MT became bidomain, and a domain modification, leading to the actual structure of larvacean MTs. Finally, this gene was duplicated, obtaining two isoforms. The second isoform suffered additional domain duplications that led to the current multi-modular larvacean MTs (**Figure 3.9A**).

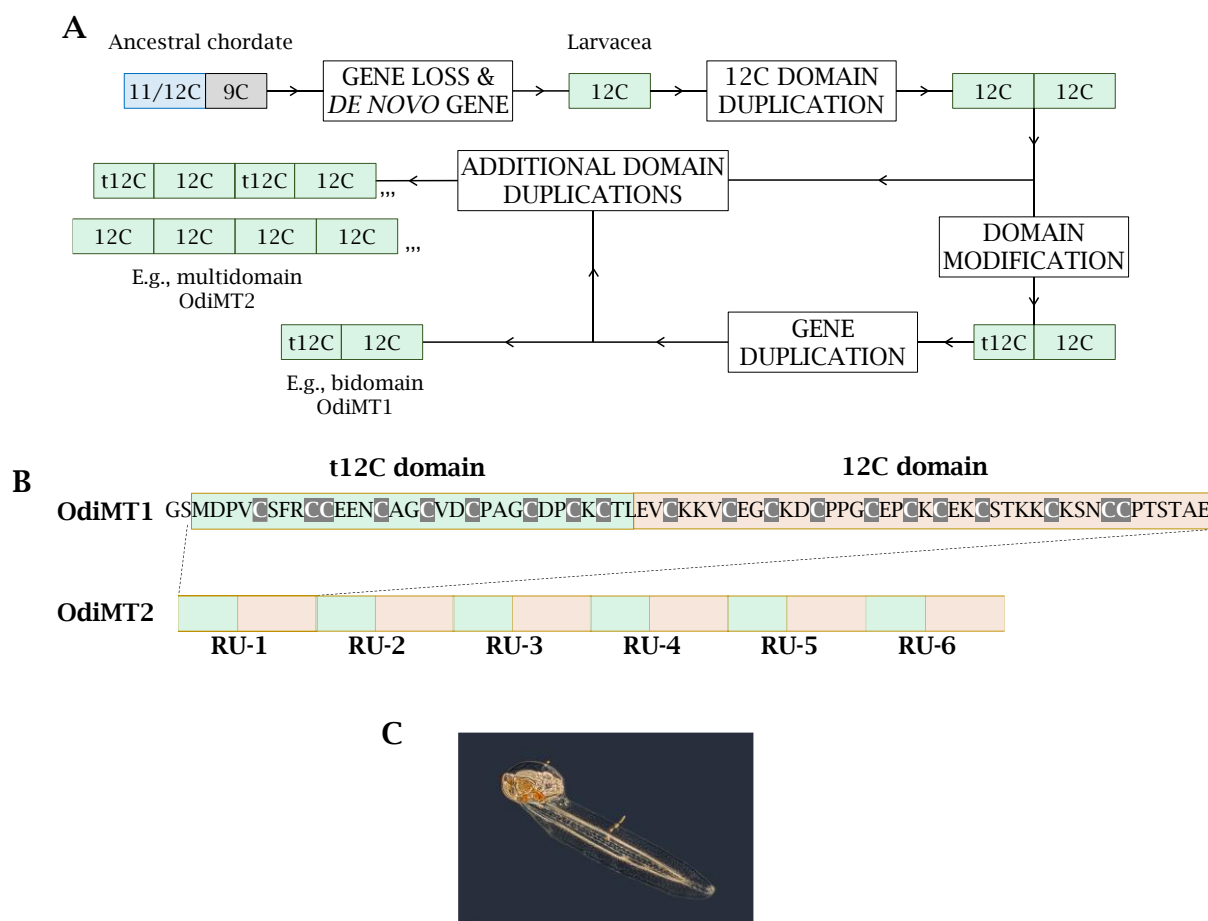


**Figure 3.9.** (A) Scheme of the postulated MT evolution in Larvacea clade. (B) *Oikopleura dioica* MT1 (OdiMT1) amino acid sequence, showing a 9 and 11 Cys residues domains: the t12C (green box) and the 12C (red box), respectively. OdiMT2 is schematically represented as multiple RUs equivalent to OdiMT1. (C) Picture of *O. dioica* specimen.

After all the evolutionary events, larvacean MTs can be considered bidomain MTs constituted by a 12 Cys residues domain (12C) at C-terminal and a trimmed 12C domain of 7 conserved Cys residues (t12C) at N-terminal. It should be noticed that OdiMT1 displays variations in three amino acid positions with respect to other larvacean MT sequences (and even OdiMT2), resulting in an MT of 9 Cys residues in t12C domain and 11 Cys residues in 12C (Figure 3.9B). Despite these variations, OdiMT1 sequence has a good alignment with other larvacean MT sequences, and therefore, the t12C/12C domain arrangement is considered for OdiMT1 as well. Regarding OdiMT2, the tandem gene multiplication events suffered by OdiMT1's paralog (the gene resulting of OdiMT1 duplication) led to an MT composed by 6 repeated units (RU) resembling to OdiMT1 (Figure 3.9B). The Cys residues are well conserved in all OdiMT2's RU and with OdiMT1, meaning that the Cys residues positions are coincident when the sequences are aligned. OdiMT2 is one of the longest MTs reported to date (399 aa), overcoming the massive *Tremella mesenterica* MT [13, 222] and, with 123 Cys residues, it represents an extreme

mechanism for heavy metal sequestration. With all this data on the table, the characterisation of *O. dioica* MT system is of great interest for MTs' field.

The next group investigated is ascidians, a well-studied group of tunicates that are also known as sea squirts. These animals are sessile at their adult stage and are usually dwelling in the shallow waters of all the world. Ascidian MTs are characterised for being monodomain and containing 12 conserved Cys residues. These species are also filtering-feeding animals, thus, their mechanisms for Cd(II) detoxification should be advanced, being metal-selective MTs an ideal option. The species reported in this PhD thesis are *Ciona robusta*, that possesses one isoform (CroMT1), *Halocynthia roretzi*, with two MT isoforms (HroMT1 and HroMT2), and *Botryllus schlosseri* that contains one constitutive MT (BscMT1). The two first systems include monodomain 12C MTs, however, BscMT1 is a long multi-modular MT of 365 amino acids and 105 Cys residues (**Figure 3.10**). Similar to OdiMT2, BscMT1 is composed by nine RU, each repetition contains 12 Cys and resembles to the prototypical ascidian MT, suggesting that BscMT1 is product of a domain multiplication event, just as OdiMT2. Once more, this enormous MT seems an extreme mechanism for heavy metal sequestration.

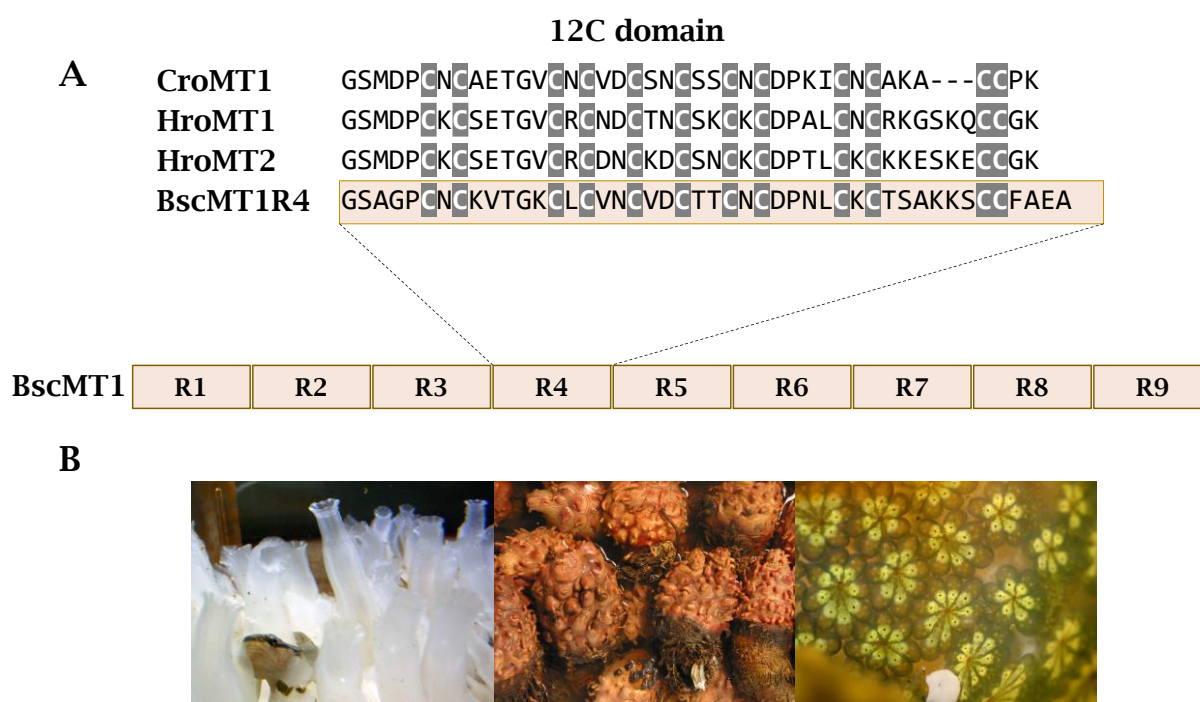


**Figure 3.10.** (A) *Ciona robusta* (CroMT1), *Halocynthia roretzi* (HroMT1 and HroMT2) and *Botryllus schlosseri* (BscMT1) MT amino acid sequences. (B) Pictures from left to right of *C. robusta*, *H. roretzi*, and *B. schlosseri* colonies.

Finally, thaliacean species complete the tunicate classes of the MTs studied. These marine animals are also filter feeders and rely on molecular mechanisms to

protect themselves from contaminants present in the environment. *Salpa thompsoni* has been selected to represent thaliacean MTs due to the quality of the sequence found in the databases. *S. thompsoni* possess four potentially putative MTs: SthMT1, SthMT2, SthMT3, and SthMT4, being, the latter, only partially sequenced, and all of them contain about 40 aa and 12 Cys residues organised in a single functional domain (**Figure 3.11**). The Cys arrangement of these MTs is identical to that of the prototypical ascidian MTs, confirming the hypothesis that supported their common origin [234]. Additionally, the thaliacean MTs surveyed do not show multi-modular structures.

**A**

### 12C-domain

**SthMT1** GSMDPCNCNTSDMCHCDSCKDCSKCNCARKTCKCSTKGCCCSPK

**SthMT2** GSMDPCNCKVTGACHCDQCTDCGKCSCNPANCKCSKP-CCPK

**SthMT3** GSMDPCNCQDTQSCYCNSCTDCSKCACAKTTCKCSAKGCCCSPI

**SthMT4** GSMDPCNCNTSVMCHCDTCESCSESNCAKQTCKSSTKRCCSPQ

**B**



**Figure 3.11.** (A) Amino acid sequences of the four *Salpa thompsoni* MT isoforms. (B) Picture of *S. thompsoni* specimen.

The information extracted from the tunicate MT systems will definitely be of use to solve many questions about vertebrates MTs' evolutionary origins and their metal-specificity. Moreover, it is noticeable that domain and gene multiplicity is a frequent genetical mechanism in tunicate species in comparison with the more "conservative" vertebrate species [214], for its intricate genetical mechanisms specific from this subphylum are revealed.

#### 3.1.3. *Candida albicans* MT system

Continuing our group's research on the fungal pathogenicity field, we have characterised *Candida albicans* MT (CaCUP1). The yeast *C. albicans* is an opportunistic parasite that dwells in the human gut and that has been used as a

model organism for fungal pathogens [235]. Interestingly, CaCUP1 is characterised for being the shortest MT reported in this PhD thesis with only 35 aa and six Cys residues. Its sequence also contains aromatic residues, which are rarely present in MTs (**Figure 3.12**).

**A**

GSMSKFELVNYASGCSGADCKCASETECKASKK

**B**



**Figure 3.12.** (A) *Candida albicans* MT (CaCUP1) amino acid sequence. (B) Micrograph of *C. albicans* colony.

Thus, the characterisation of CaCUP1 will provide useful information to battle this pathogen and to understand other fungal pathogens. Besides, fungal MTs are tightly related with Cu(I) sequestration [219, 220]. A Cu-thionein will contrast with the expected metal-selectivity of the MTs studied in this PhD thesis, more likely to be related with Cd(II) detoxification or Zn(II) homeostasis. This uncommon MT will give contrast to the rest of MTs reported in this study.

#### 3.1.4. Final remarks on the characterisation of the MT systems

The study of the different MT systems has revealed common traits within the two major phylogenetic groups reported in this PhD thesis. First, it can be stated that mollusc MTs are mostly structured in two domains. A C-terminal domain, which in most of the cases is a conserved 9 Cys  $\beta$ 1 domain, and an N-terminal domain that is variable and lineage-specific. Four variable domains have been reported:  $\alpha$  (11/12 Cys),  $\beta$  (9 Cys),  $\gamma$  (10 Cys),  $\delta$  (14 Cys). Second, the archetype MT stated for urochordates is a 12C domain of 12 conserved Cys residues. This 12C domain has suffered variations between sister phylogenetic groups, such is the case of *Oikopleura* MTs, whose MT is structured in two domains and one of them is truncated (12C/t12C). Interestingly, some urochordates display multi-modular MTs that can reach up to 399 Cys residues, as OdiMT2, which show high coordinating capacity potential.



## 3.2. Characterisation of the metal-binding abilities of non-specific MTs

Here we introduce those MTs with metal-binding abilities that are not shared in any of the currently accepted genuine Zn- or Cu-thionein behaviours. The proteins exposed next are mollusc MTs that do not show an acute selectivity for any of the metals studied. It is important to remember that not all situations are black or white and that there is a graduality with regards metal-binding abilities in MTs. During the text, **Section 7.1**, which contains the data sheet information about the analytical and spectroscopic data (ICP-AES and FPLC) for each MT isoform studied in this work, is used as supporting information. Additionally, **Section 7.2** will be referenced to show additional data of the MTs reported in this section.

### 3.2.1. Study of *Arion vulgaris* MT2

The European slug *Arion vulgaris* is a species of terrestrial gastropod mollusc that synthesises two isoforms of MTs (AvuMT1 and AvuMT2) with distinct metal-binding preferences (**Section 3.1.1**). Only AvuMT2's coordinating abilities are detailed in this section. AvuMT2 (**Annex 7.1.1**) has a 60% of identity with respect to AvuMT1, which proves the high similarity between both isoforms. However, they differ in their metal-binding behaviour, probably because they perform different functions, as suggests their gene expression levels (**Annex 7.3.1: Article 1**).

The synthesis of AvuMT2 in Zn(II)-supplemented *E. coli* cultures renders a mixture of Zn-AvuMT2 complexes (**Figure 3.13B**). This mixture of species reveals a poor preference towards Zn(II) ions from AvuMT2, which contrasts with the metal-binding behaviour of a genuine Zn-thionein that always render unique Zn-MT complexes in these conditions [13]. However, that Zn<sub>6</sub>-AvuMT2 is the most abundant species in the sample (**Figure 3.13B**) is concordant with the results obtained from other gastropod MTs with 18 Cys residues and, thus,  $\beta/\beta$  conformation (**Figure 3.13A**) [56]. The most probable structure is a dumbbell-like bidomain MT that holds two  $M(II)_3(S_{Cys})_9$  clusters. Certainly, this is not the unique conformation but the most energetically favourable, as seen by ESI-MS (**Figure 3.13B**). The heterogeneous stoichiometries found in the sample suggest that this is a highly labile metal cluster. In fact, the Zn-AvuMT2 complexes possessed a low optical activity, showing a faint CD envelope (**Figure 3.13F**), which confirms the poor robustness of the metal-cluster. Thus, AvuMT2 does not share its biochemical traits with those of genuine Zn-thionein.



by ESI-MS, coping with three extra Cd(II) ions than the number expected for an 18 Cys MT. The presence of sulphide ions explains this increase on the coordinating capacity of the protein. These ligands do not belong to the amino acid composition and are found in certain metal aggregates, enlarging the coordinating capacity of the MTs, and allowing the formation of metal clusters with certain stability [155]. At any rate, it is demonstrated that AvuMT2 does not show Cd-selectivity, as denoted by the mixture of species yielded and the presence of sulphide labile ions.

Finally, the metal-binding behaviour of AvuMT2 towards Cu is neither that expected for a genuine Cu-thionein, though it shares some traits with this behaviour. From one side, we discard that AvuMT2 is a genuine Cu-thionein because its production in Cu-supplemented cultures rendered highly heterogenous samples, as observed by FPLC (**Annex 7.1.1**) and ESI-MS (**Figure 3.13D** and **E**). It should be clarified that, from the two samples collected by FPLC in the normal aeration production, only the second peak was characterised, since the first was impossible to detect by the commonly used techniques. From the other side, when synthesised under Cu(II) surplus, AvuMT2 renders a mixture of homometallic species, being  $\text{Cu}_{14}$ -AvuMT2 the most important species (**Figure 3.13D**). Moreover, the CD envelope of the Cu-species is more intense than the one rendered by the Zn-species (**Figure 3.13F**), suggesting a more compact structure in the former metal clusters and revealing some traits of the Cu-thionein character. From this data and considering that the expression of AvuMT2 (at *Arion*'s adult stage) is not regulated by metals as AvuMT1, this isoform could be functional at some point at the early stage of this animal's life, probably related with a biological role involving Cu (**Annex 7.3.1: Article 1**).

In conclusion, AvuMT2 is a protein that shows no similarities with a genuine Zn-thionein, since its productions in Zn(II)- and Cd(II)-supplemented cultures render a mixture of species whose M(II)-MT complexes exhibit poor robustness. Although it does not yield a unique Cu-MT complex when synthesised in Cu(II)-enriched media, confirming that this is not the case of a genuine Cu-thionein, it shows some traits of this metal-binding behaviour such is the homometallic nature of its Cu-AvuMT2 species and the presence of sulphide labile ligands in the Cd(II)-enriched productions. Therefore, AvuMT2 is a non-specific MT that exhibits none of the extreme metal-selective behaviours observed in either genuine Zn- or Cu-thioneins, but that shares features with the latter.

### 3.2.2. Study of *Pomacea bridgesii* MT1 and MT2

The MT system expressed by *Pomacea bridgesii*, PbrMT1 and PbrMT2, have some interesting features in their sequences (**Figure 3.14A**). Both isoforms show divergences from the archetypal  $\beta 3/\beta 1$  domain structure of most of the mollusc MTs. From one side, PbrMT1 possesses a  $H_4C_4$  motif ( $HxHHHx_2Cx_3Cx_6CC$ ) in its N-terminal end that is described in other species of the same genus such as *Pomacea diffusa* MT1, indicating that this might be an evolutive event of a specific lineage (**Annex 7.3.4: Article 4**). With these additional residues, PbrMT1 contains 22 Cys, arranged in a  $H_4C_4$  motif/ $\beta 3/\beta 1$  structure. On the other side, PbrMT2 displays a variation of the  $\beta 3/\beta 1$  domain structure, it lost its C-terminal  $\beta 1$  motif and duplicated its  $\beta 3$  motif twice, one full-length and the other partially. This means that PbrMT2 structure is  $\beta 3.1/\beta 3.2/\beta 3.3$  (**Figure 3.14A**) and contains 23 Cys residues.

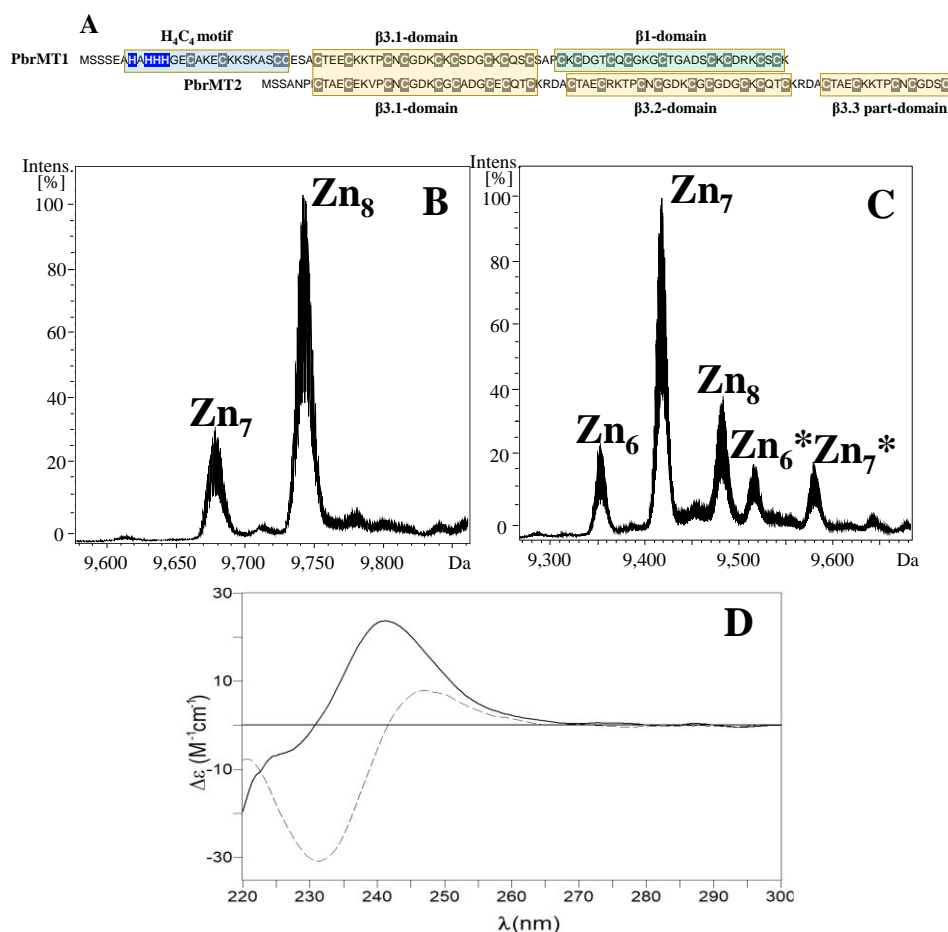


**Figure 3.14.** (A) Architecture of PbrMT1 and PbrMT2 amino acid sequences, Cys residues are shadowed, yellow boxes highlight the 9-Cys ( $\beta 3$  domain) motifs, the green box highlight the 9-Cys ( $\beta 1$  domain) motif, and the blue box highlight the  $H_4C_4$  motif of the sequences. Deconvoluted ESI-MS spectrum at pH 7.0 of (B) Zn-PbrMT1 and (C) Zn-PbrMT2 productions. Glycosylated species are signalled with an asterisk (\*). (D) CD envelopes of Zn-PbrMT1 (solid line) and Zn-PbrMT2 (dashed line) productions.

The samples obtained from the PbrMTs' productions (**Annex 7.1.2** and **7.1.3**) carried out in Zn-supplemented media rendered a mixture of species with different stoichiometries (**Figure 3.14B**). In PbrMT1 samples, Zn<sub>8</sub>-PbrMT1 has been found as the major species, along with Zn<sub>7</sub>-PbrMT1 as minor species. While in the PbrMT2 bioproduction, the most intense ESI-MS peak corresponds to the Zn<sub>7</sub>-PbrMT2 species, although Zn<sub>8</sub>- and Zn<sub>6</sub>-PbrMT2 have been detected as well. Additionally, it is worth to mention the presence of glycosylated species in the PbrMT2 samples, which denote high flexibility of the polypeptide sequence (See **Section 3.5**). The complexes obtained from both isoforms' productions display different CD envelopes: a Gaussian band centred at *ca.* 240 nm corresponding to the labile clusters of the Zn-PbrMT1 production and an *exciton coupling* centred at *ca.* 240 nm that suggests more stability and compactness of the Zn<sub>7</sub> cluster build by PbrMT2 (**Figure 3.14D**). Considering these results, none of the PbrMTs show a genuine Zn-thionein behaviour.

Similarly, the bio-produced samples of PbrMTs in Cd(II)-supplemented *E. coli* cultures rendered a mixture of species. While PbrMT1 rendered monomers of Cd<sub>7</sub>-, Cd<sub>7</sub>S<sub>2</sub>- and Cd<sub>8</sub>-PbrMT1 complexes (being the latter the major species), PbrMT2 yielded both dimers and monomers (**Figure 3.15**).

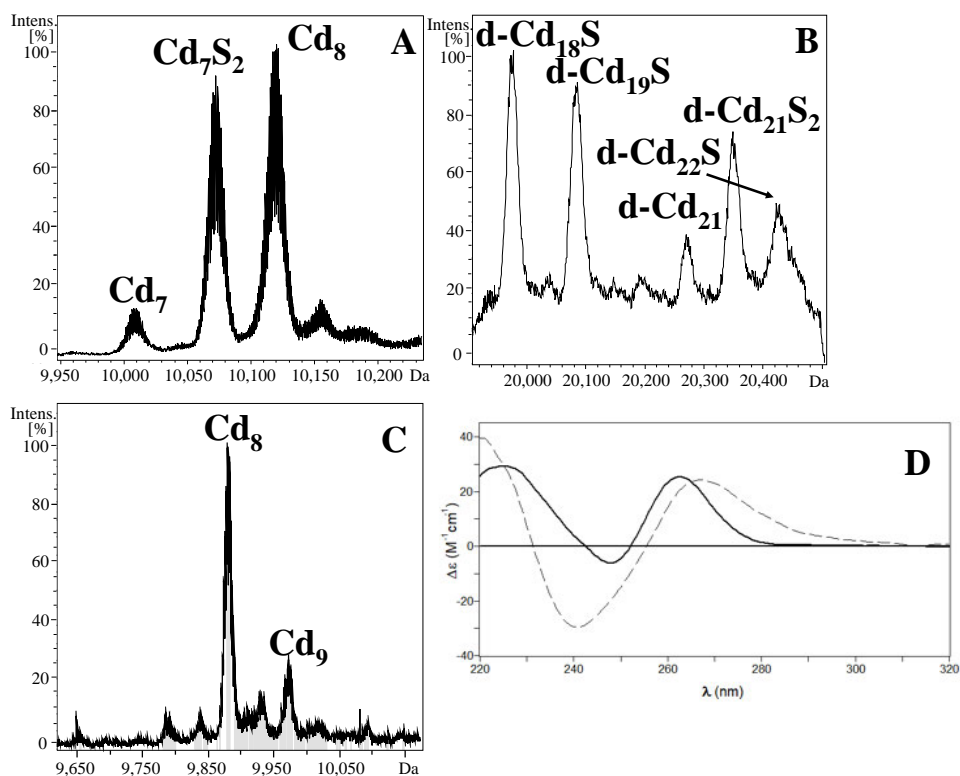


**Figure 3.15.** Deconvoluted ESI-MS spectrum at pH 7.0 of (A) Cd-PbrMT1, (B) Cd-PbrMT2 (dimeric species) and (C) Cd-PbrMT2 (monomeric species) productions. (d-) stands for dimeric species. (D) CD envelopes of Cd-PbrMT1 (solid line) and Cd-PbrMT2 (dashed line) productions.

The monomeric forms of PbrMT2 are Cd<sub>8</sub>- (major), and Cd<sub>9</sub>-PbrMT2, while the dimeric forms range from Cd<sub>18</sub>S- to Cd<sub>22</sub>S-PbrMT2. Both isoforms coincide in that eight Cd(II) ions is the predominant stoichiometry for the complexes formed. Considering that other 20 Cys MTs structured as  $\alpha/\beta$  (11 + 9 Cys) bidomain MTs bind seven M(II) ions, the extra Cys of PbrMTs provide them with higher coordinating capacity, adding an extra divalent metal ion to the complex. This capability of binding extra Cd(II) ions may suppose an adaptative advantage of this organism to cope with higher heavy metal concentration over other organisms, and could explain the invasive ability of the *Pomacea* species [226, 226]. Despite the mixture of species found in the samples of both isoforms, the CD envelopes of the Cd-PbrMTs complexes render an *exciton coupling* centred at *ca.* 250 nm, suggesting a high level of structuration probably aided by the labile sulphide ligands, which, in turn, display a signal at 260-280 nm (**Figure 3.15D**).

Complementary, the metal exchange experiments show dissimilarities in the metal binding behaviour of both PbrMT isoforms. After 10 Cd(II) equivalents added to the *in vivo* Zn-PbrMT1 and Zn-PbrMT2 samples, the former renders a major Zn<sub>1</sub>Cd<sub>7</sub>-PbrMT1 complex (**Annex 7.2: Sheet 7.2.1.1**), while the latter exhibits a major Cd<sub>8</sub>-PbrMT2 complex along with certain species associated to 9 and 10 Cd(II) ions (**Annex 7.2: Sheet 7.2.1.2**). The CD envelope of PbrMT1 at the final stage of the experiment is quite close to the *in vivo* Cd-PbrMT1 sample (**Figure 3.16A**), suggesting that, probably, the characteristics of the chromophores are the same in both cases.

In PbrMT2, the homometallic Cd-PbrMT2 complexes found at the final stage of the Zn/Cd exchange experiment are reflected on the CD envelopes, where the final stage CD spectrum of the titration is blue shifted in comparison to that of the *in vivo* Cd-PbMT2 (**Figure 3.16B**). These differences in the CD absorption between both *in vivo* and *in vitro* Cd-PbrMT2 complexes was expected taking into account the lack of dimeric species detected in the *in vitro* experiment and the absence of S<sup>2-</sup> anions in the initial Zn-PbrMT2 sample. If PbrMT1, reluctant to fully exchange the Zn(II) by Cd(II) ions, and PbrMT2 are compared, it can be stated that PbrMT2 denotes higher capacity to bind Cd(II) than PbrMT1, while PbrMT1 shows more preference to Zn(II) than PbrMT2.

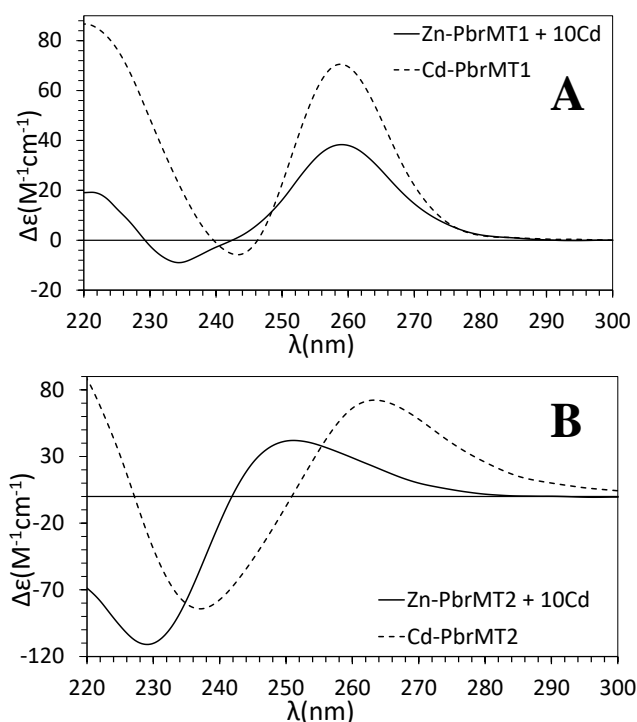


**Figure 3.16.** (A) Spectrum of the CD envelopes of the *in vivo* Cd-PbrMT1 product and the *in vivo* Zn-PbrMT1 after adding 10 equivalents of Cd(II) ions, *i.e.*, the *in vitro* Cd-PbrMT1. (B) Spectrum of the CD envelopes of the *in vivo* Cd-PbrMT2 product and the *in vivo* Zn-PbrMT2 after adding 10 equivalents of Cd(II) ions, *i.e.*, the *in vitro* Cd-PbrMT2.

When it comes to bind Cu, both PbrMT isoforms display divergent features. From one side, PbrMT1 renders a mixture of heterometallic Zn,Cu-MT complexes, while PbrMT2 yields a mixture of homometallic Cu-MT complexes (**Figure 3.17**). Both PbrMT1 and PbrMT2 productions were collected in two separated FPLC peaks (**Annex 7.1.2** and **7.1.3**). Both PbrMT1 peaks display equivalent species and only data from peak 2 is presented in this section. Peak 1 of PbrMT2 could not be detected by neither ESI-MS nor ICP-AES, thus, only peak 2 data is showed. Moreover, both PbrMTs were produced under low oxygenation conditions, supposedly favouring the yielding of homometallic Cu-species, but under these conditions the concentration of the samples was under the limit of detection of the commonly used techniques and there is no data to be shown. Thus, as detected by ESI-MS and supported by ICP-AES, PbrMT1 renders species of up to 12 Cu(I) ions, being  $M_{12}/Cu_{12}$  (neutral/acid pH) the major species yielded. In contraposition, PbrMT2 displays a major homometallic  $Cu_{15}$ -PbrMT2 complex, supported by the results of ICP-AES (15.60 Cu/MT). The Cu content of PbrMT2 is higher than that of PbrMT1 and also PbrMT2 does not require Zn(II) ions to stabilise its cluster as PbrMT1 does. This evidence indicate that PbrMT1 leans to a Zn-thionein metal-binding behaviour, while PbrMT2 does it to a Cu-thionein. However, despite there are differences in

the speciation and the elements that form Cu-PbrMTs' clusters, their samples present equivalent, low-intense CD envelopes (Figure 3.17C), denoting the poor folding degree of these proteins.

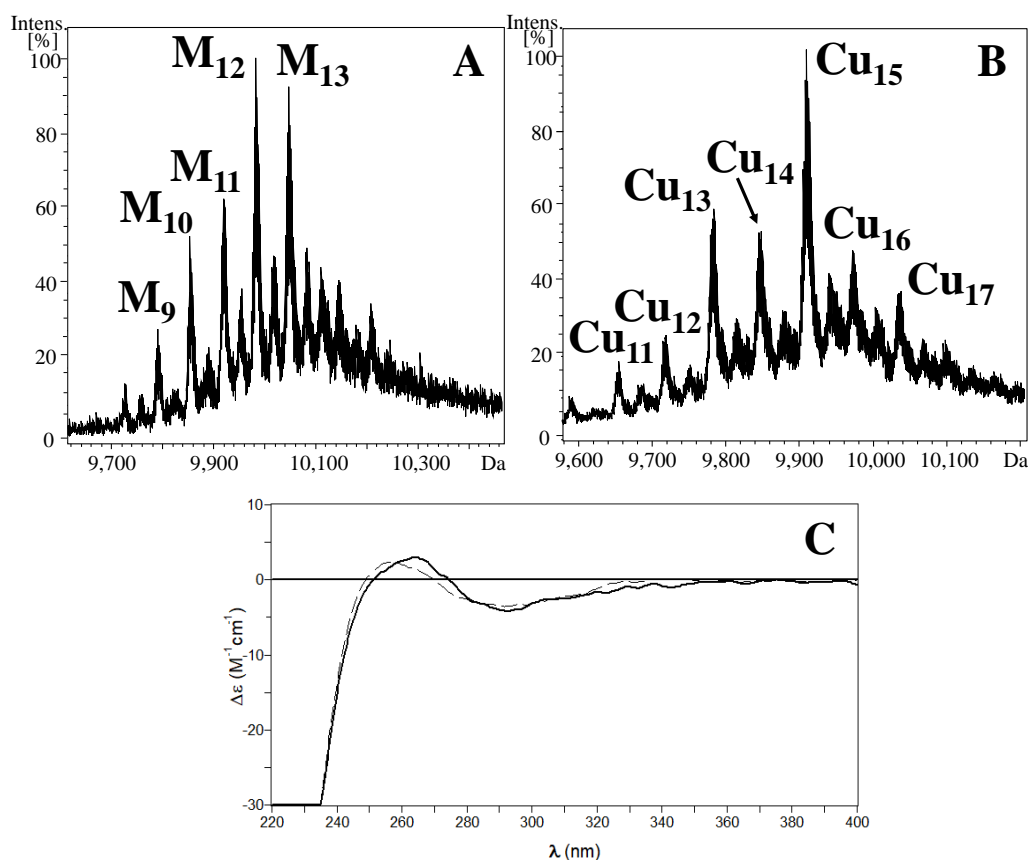


**Figure 3.17.** Deconvoluted ESI-MS spectrum at pH 7.0 of (A) Cu-PbrMT1, (B) Cu-PbrMT2 (C) CD envelopes of Cu-PbrMT1 (solid line) and Cu-PbrMT2 (dashed line) productions.

This low CD profile is also observed in the Zn/Cu exchange experiments, where the CD spectra of the final stage of the experiment reproduce similar envelopes with the *in vivo* samples (Figure 3.18). These experiments also showed that PbrMT1 and PbrMT2 are reluctant to completely exchange the Zn(II) of their cluster by Cu(I) ions, which denotes poor specificity towards Cu for both isoforms. Interestingly, PbrMT1 renders comparable *in vitro* species to those yielded *in vivo* (Annex 7.2: Sheet 7.2.1.3), however, the *in vitro* Cu-PbrMT2 complexes achieved at the final stage of the experiment contain less metal than the *in vivo* complexes (Annex 7.2: Sheet 7.2.1.4), denoting, again, poor specificity towards Cu(I). Overall, it can be concluded that despite PbrMT2 does not show a genuine Cu-thionein behaviour, this is higher than that shown by PbrMT1.



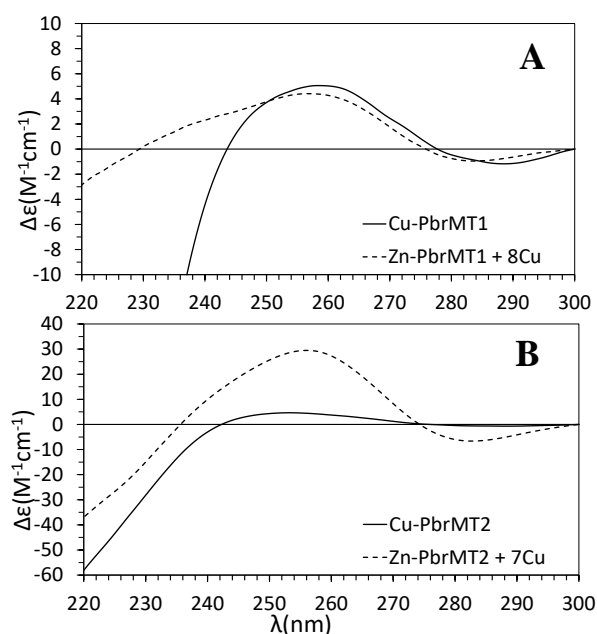


**Figure 3.18.** Spectra of the CD envelopes of the (A) *in vivo* Cu-PbrMT1 product and the *in vivo* Zn-PbrMT1 after adding 8 equivalents of Cu(I) ions, *i.e.*, the *in vitro* Cu-PbrMT1, and (B) the *in vivo* Cu-PbrMT2 product and the *in vivo* Zn-PbrMT2 after adding 7 equivalents of Cu(I) ions, *i.e.*, the *in vitro* Cu-PbrMT2.

In conclusion, the PbrMTs do not possess a strong preference for any of the metals studied. Despite they show similar biochemical features, PbrMT1 seems to display higher Zn-thionein features than PbrMT2 (higher content in Zn for the *in vivo* Zn-species and heterometallic Zn,Cu-complexes), while PbrMT2 exhibits more Cu-thionein behaviour than PbrMT1 (homometallic Cu-MT complexes). Besides, both isoforms render a mixture of Cd-species, some of which contain sulphide ions. These evidences confirm the loss of the metal-binding specificity towards Cd(II), which is still observed in other Caenogastropoda MTs [212]. This behaviour can be argued considering that the content of Cd(II) of the habitats of *P. bridgesii* is low and the pressure for maintaining their Cd-selective features has diminished, leading to a couple of unspecific MTs.

### 3.2.3. General traits of non-specific MTs

Overall, and more importantly, non-specific MTs do not yield unique species for any of the metals studied, which denotes no selectivity for any of them. These features harden the elucidation of these proteins' function. However, they exhibit interesting attributes that provide new insights into MTs biochemistry (*e.g.*, a very interesting  $H_4C_4$  motif in PbrMT1). Despite they do not show a marked extreme preference for any of the studied metals, they share some traits with Zn- or Cu-thioneins, which enlarge our knowledge about how these proteins bind metals. Some of them rendered glycosylated samples, some included sulphide labile ions

in their Cd(II) clusters and both hetero and homometallic Cu(I) complexes have been detected. All these features are useful to characterise these MTs' metal binding features, positioning them closer to an extreme behaviour or another in the current dichotomic classification.

### 3.3. Characterisation of the metal-binding abilities of genuine Zn-thioneins

The following section collects the characterisation of a number of MTs grouped by their similar metal-binding behaviour. These proteins fulfil all or most of the qualities that define a genuine Zn-thionein. This section exemplifies how the current dichotomic classification is used and supports, with more data, the existence of an extreme Zn-thionein behaviour.

#### 3.3.1. Study of *Arion vulgaris* MT1

This section completes what it is known about the MT system of *Arion vulgaris*. As mentioned in **Section 3.2.1**, *A. vulgaris* is a gastropod species that dwells in terrestrial habitats, and it is considered an important pest organism. Thus, by learning about its MT system, we can understand its degree of tolerance towards heavy metals.

One of the main aspects that this thesis will focus on is the distribution of the Cys residues along the MT sequences. After the resolution of the structure of *Littorina littorea* and *Helix pomatia* MTs [55, 56], specific Cys arrangements have been connected to certain metal cluster configurations, becoming an essential issue for seeking functional domains and perform phylogenetic studies [210]. AvuMT1 amino acid sequence displays a Cys arrangement, as widely seen in other mollusc MTs, structured in two  $\beta$  domains (**Figure 3.19A**). These domains contain nine Cys residues, which commonly bind three divalent metal ions, forming two  $M(II)_3(S_{Cys})_9$  ( $M(II) = Zn(II)$  or  $Cd(II)$ ) clusters. Thus, it is not strange that we find this distribution in other MTs of relatively close species such as the Roman snail (*Helix pomatia*) and the garden snail (*Cantareus aspersus*), whose metal-binding abilities will be of use to compare with those of AvuMT1.

The characterisation of this isoform (**Annex 7.1.4**) provides a strong evidence of the Zn-thionein behaviour of this protein detecting a unique  $M(II)_6$ -AvuMT1 species by ESI-MS from the samples synthesised under Zn(II) or Cd(II) surplus (**Figure 3.19B** and C). Additionally, this 6-to-1 (metal-to-protein) stoichiometry is confirmed by ICP-AES (Zn-sample:  $2.3 \cdot 10^{-4}$  M and 5.9 Zn/MT; Cd-sample:  $0.3 \cdot 10^{-4}$  and 6.8 Cd/MT) (**Annex 7.1.4**), which nicely coincides with other stoichiometries

found for MTs with the same Cys arrangement such as the case of *Helix pomatia* HpCdMT [56]. Considering this HpCdMT example, whose 3D-structure have been solved, and although there is no solved structure of AvuMT1, the experimental evidences strongly suggest that AvuMT1 possess a dumbbell-like bidomain structure holding two  $M(II)_3(S_{Cys})_9$  clusters. The *in vivo* samples of these metal clusters have high optical activity, showing intense CD envelopes at the expected absorbance wavelength of the Zn- and Cd-thiolate chromophores (**Figure 3.19E**). These CD signals denote the tetrahedral coordination geometry  $M(II)(S_{Cys})_4$  of the divalent metals, the former ( $M=Zn(II)$ ) depicting a gaussian band centred at *ca.* 240 nm and the latter ( $M=Cd(II)$ ) yielding an *exciton coupling* centred at *ca.* 250 nm.

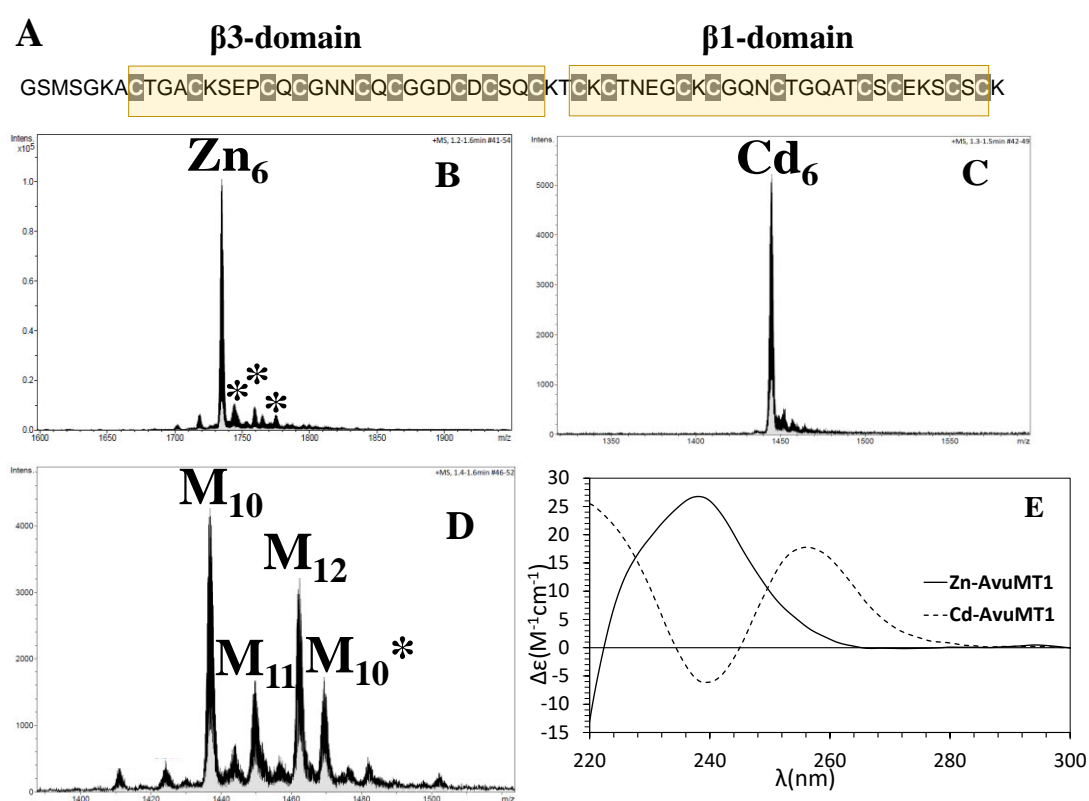


**Figure 3.19.** (A) Architecture of AvuMT1 amino acid sequence, Cys residues are shadowed, and yellow boxes highlight the two nine-Cys motifs of the sequence ( $\beta$ -domains). ESI-MS spectrum at pH 7.0 of (B) Zn-AvuMT1 ( $Q^+ = +4$ ), (C) Cd-AvuMT1 ( $Q^+ = +5$ ) and (D) Cu-AvuMT1 ( $Q^+ = +5$ ) productions. Heterometallic Zn,Cu-MT complexes are marked with M and glycosylated species are signalled with an asterisk (\*). (E) CD envelopes of Zn-AvuMT1 (solid line) and Cd-AvuMT1 (dashed line) productions.

In contrast, when AvuMT1 is purified from the Cu(II)-enriched cultures, it shows distinct (although informative) results. Clearly, AvuMT1 is a protein with selectivity for divalent metal ions, however, it is difficult to extract any conclusions of whether it is a genuine Zn- or a putative Cd-thionein just by considering the data exposed above. The characterisation of the Cu-AvuMT1 sample reveals interesting

features. First, AvuMT1 exhibits no capabilities to build a unique well-formed metal cluster with Cu(I) ions (**Figure 3.19D**), which confirms (following the criteria in ref. 13) that this isoform does not exhibit a Cu-thionein behaviour. Second, this protein yields heterometallic Cu,Zn-AvuMT1 species when synthesised in Cu-enriched *E. coli* cultures, which means that AvuMT1 uses Zn(II) as a structural ion [236], as observed in the rest of MTs presented in this section. Furthermore, and as discussed in **Section 3.6**, the chemical similarities of Zn(II) and Cd(II) cause some MTs displaying equivalent metal-binding features towards both metal ions. On the basis of all these considerations and the exposed results, we can state that AvuMT1 represents a clear Zn-thionein that displays high preference for Cd(II) ions, as well. Concordantly, these metal-binding features found on recombinant AvuMT1 support the metal exposure experiments made on the living organism (**Annex 7.3.1: Article 1**). This work shows that an exposure to Cd(II) triggers the overexpression of the *AvuMT1* gene, suggesting that AvuMT1 may play a detoxifying role in the organism, just as other mollusc CdMTs do [147, 237]. In fact, the phylogenetic studies made for this protein closely relate AvuMT1 to other stylummatophoran CdMTs.

Interestingly, despite that AvuMT1 shows a marked and clear Zn-thionein behaviour, this protein hides some peculiarities. The metal exposure experiments carried out on organisms showed that Cd(II) triggers the overexpression of the *AvuMT1* gene but a Cu(I) exposure also does it. To determine which is the real cognate metal, recombinant AvuMT1 was synthesised in *E. coli* cultures enriched with both Cd(II) and Cu(II) salts at different proportions (50%:50%, 25%:75% and 10%:90% Cd:Cu). These productions rendered really similar metallated species, as demonstrated by ESI-MS or CD spectra (**Figure 3.20**), with the exception of 10:90 Cd:Cu production, whose CD envelope denotes some differences in the chromophores of the sample with respect to the other two. As observed by ESI-MS (**Figure 3.20E and F**), this preparation contains a mixture of minor Cu-species, not present in the other spectra, which could explain the dissimilar optical features of the sample. However, it is remarkable that even the concentration of Cd(II) of the culture diminishes in detriment of the concentration of Cu(II), Cd<sub>6</sub>-AvuMT1 (major) and Cd<sub>6</sub>Cu<sub>1</sub>-AvuMT1 (minor) species are maintained for the three situations, confirming, once again, the metal-binding preference of this protein for divalent metal ions. However, it is motivating to observe that a genuine Zn/Cd-thionein, with a perfect Cys number and arrangement to build two stable M(II)<sub>3</sub>(S<sub>Cys</sub>)<sub>9</sub> clusters, can cope with an extra metal ion, Cu(I), and that, in addition, this ion is a non-cognate metal. This is a good example to understand that MTs cannot always be

considered as inflexible metal-complexes that comply with the same metal-binding behaviour characteristics. The special amino acid composition of MTs and the concrete conditions in which they are physiologically active, make of them very labile molecules adapted to respond very distinct scenarios. This example shows a clear Zn-thionein MT with high Cd-selectivity that has a detoxification function but that also may develop a Cu-related function in some cases.

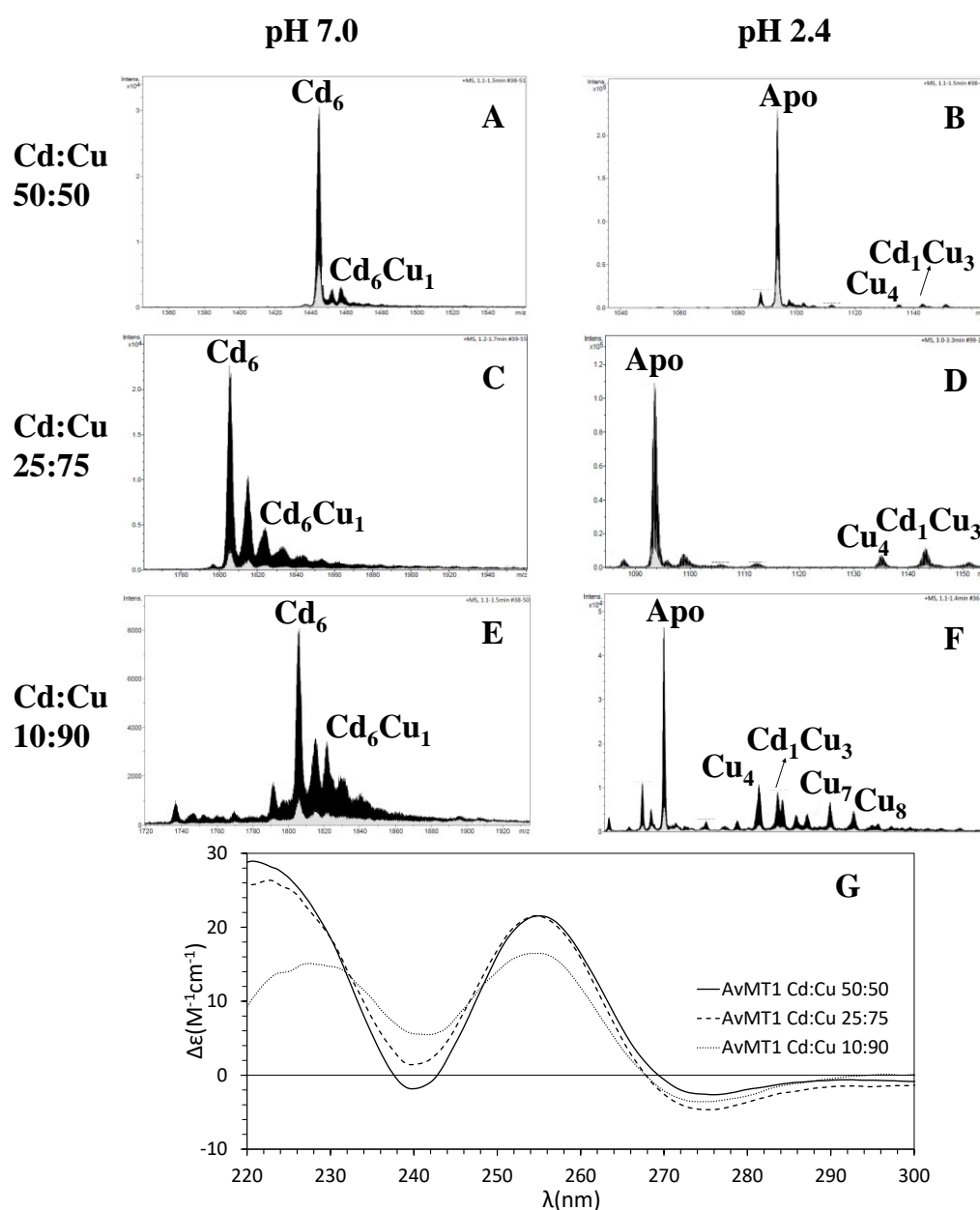


**Figure 3.20.** ESI-MS spectrum at pH 7.0 of AvuMT1 samples purified from the (A) 50:50 Cd:Cu ( $Q^+ = +5$ ), (C) 25:75 Cd:Cu ( $Q^+ = +4$ ) and (E) 10:90 Cd:Cu ( $Q^+ = +4$ ) productions. ESI-MS spectrum at pH 2.4 of the AvuMT1 metal-complexes recovered from the (B) 50:50 Cd:Cu ( $Q^+ = +6$ ), (D) 25:75 Cd:Cu ( $Q^+ = +6$ ) and (F) 10:90 Cd:Cu ( $Q^+ = +6$ ) productions. (G) CD envelopes of the AvuMT1 samples obtained from 50:50 Cd:Cu, 25:75 Cd:Cu and 10:90 Cd:Cu productions.

Additionally to all the features presented above, Zn(II)/Cd(II) and Zn(II)/Cu(I) metal exchange *in vitro* experiments were performed for Zn-AvuMT1 (ESI-MS and CD in **Annex 7.2.2: Sheets 7.2.2.1 and 7.2.2.2**). The Zn(II)/Cd(II) titration shows the formation of the Cd<sub>6</sub>-AvuMT1 complex by adding 6-7 equivalents of Cd(II) to Zn<sub>6</sub>-AvuMT1 (**Annex 7.2.2: Table 7.2.2.1**). This final species is maintained along the experiment, even in an excess of Cd(II), and exhibits equivalent spectroscopic features to those found in the *in vivo* samples purified from Cd(II)-enriched cultures (**Figure 3.21**). Once again, it is manifested the ability of this peptide to form stable clusters with divalent ions, as well as its Zn-thionein behaviour, due to its slight reluctance to fully exchange its Zn(II) ions, only totally replaced after seven Cd(II) equivalents added. ESI-MS spectra of the aliquots collected at some stages of the experiment display that all the intermediate species are formed by different Zn<sub>x</sub>Cd<sub>y</sub>-AvuMT1 complexes (where x+y=6), meaning that the coordination of one Cd(II) ion displaces one Zn(II) ion. This common metallic exchange has been described in the past in other MTs, such as mammal MT1 [33] and other mollusc MTs [211]. Additional equivalents of Cd(II) trigger slight variations on the CD envelopes but no extra Cd(II) is included in the cluster, as observed by ESI-MS.

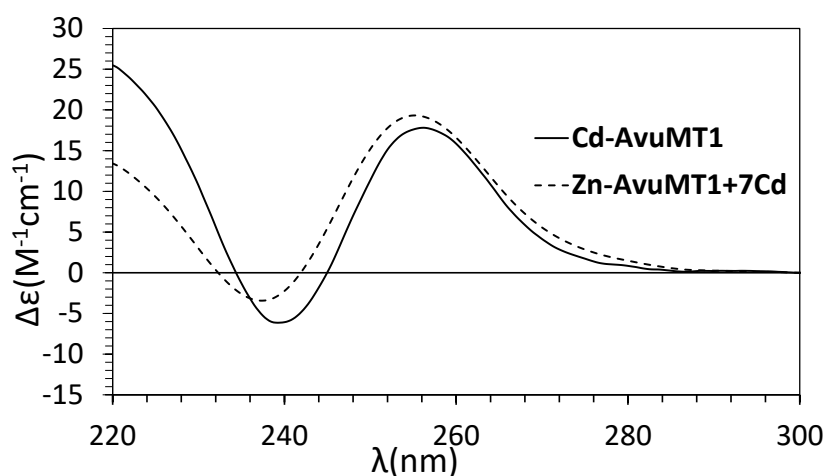


**Figure 3.21.** CD envelopes comparison of *in vivo* Cd-AvuMT1 (solid line) vs. *in vitro* Cd-AvuMT1 (dashed line) obtained after adding seven Cd(II) equivalents to *in vivo* Zn-AvuMT1.

Analogously, the Zn(II)/Cu(I) exchange experiment was performed to Zn<sub>6</sub>-AvuMT1 (**Annex 7.2.2: Sheet 7.2.2.2**). This experiment just allowed to confirm the incapability of AvuMT1 to form a unique energetically favoured metal complex with Cu(I) ions. The CD envelope of the *in vitro* sample obtained after adding eight equivalents of Cu(I) exhibit some analogy with the *in vivo* Cu-AvuMT1 CD envelope (**Figure 3.22**), which is not strange since both samples display a high degree of heterogeneity, according to the ESI-MS spectra (**Annex 7.2.2: Table 7.2.2.2 and Figure 3.19D**). Additionally, the ESI-MS spectra of the same aliquot registered at

pH 7.0 and pH 2.4 (**Annex 7.2.2**, **Table 7.2.2.2** and **7.2.2.3**) show that after 10 Cu(I) equivalents added all the metal-MT complexes present in the sample were exclusively Cu(I)-complexes, since the metal-to-protein stoichiometries at both pH values were analogous. Comparing these results to those of a close organism MT, such is HpCdMT, Zn/Cu-AvuMT1 metal exchange can be considered quite rapid, since HpCdMT only completely exchanges all its Zn(II) ions after adding 16 equivalents of Cu(I) [211]. These are reasonable circumstances if considering that solely AvuMT1 (and not AvuMT2, see **Section 3.2.1**) is expressed either after Cd(II) or Cu(II) exposure but HpCdMT is only produced when the organism experiences a Cd(II) insult, meaning that *Arion vulgaris* might normally synthesise AvuMT1 (expressing AvuMT2 in specific circumstances) but *Helix pomatia* has two distinct MTs (HpCdMT and HpCuMT) that have well-defined functions for determined situations. Therefore, AvuMT1 seems to have a multipurpose role that could explain the loose metal-binding behaviour of AvuMT1 with regards to Cu-binding.

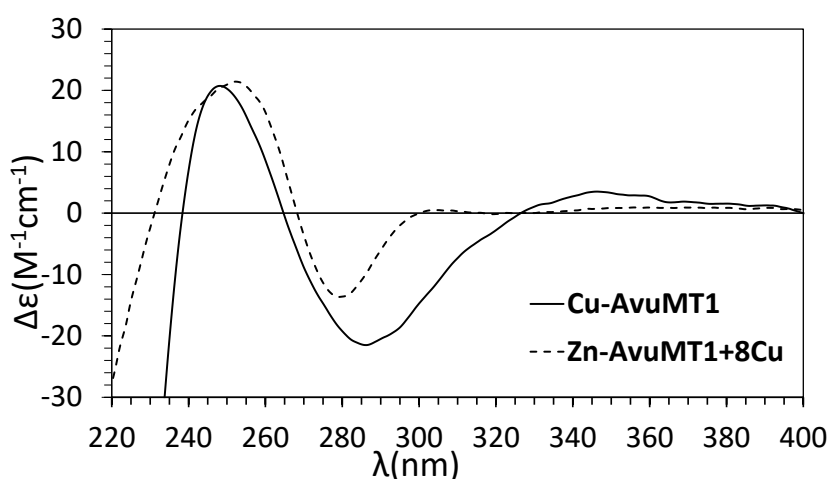


**Figure 3.22.** CD envelopes comparison of *in vivo* Cu-AvuMT1 (solid line) vs. *in vitro* Cu-AvuMT1 (dashed line) obtained after adding eight Cu(II) equivalents to *in vivo* Zn-AvuMT1.

In conclusion, AvuMT1 could be considered a multitask protein which most of its biochemical features are shared with the definition of a Zn-thionein that not only has a Cd-selective behaviour, but it also can cope with extra Cu(I) ions in certain conditions.

### 3.3.2. Study of *Nerita peloronta* MT1

*Nerita peloronta* is a species of marine snail also known as “bleeding tooth” that has two putative MTs (NpeMT1 and NpeMT2). However, in this section only NpeMT1 is described. NpeMT1 is structured as a  $\beta 3/\beta 1$  bidomain MT, which is found along all Neritimorpha clade (**Section 3.1**) but, in NpeMT1 case, it contains an additional Cys residue. Specifically, NpeMT1 possesses a  $\beta 3$  domain of 10 Cys

at the N-terminal and a  $\beta 1$  domain of nine Cys at the C-terminal. Despite the extra Cys residue, both domains are considered  $\beta$ -domains due to their common phylogenetic origin and genetic consistency within the group. Moreover, both domains render analogous metal clusters, since NpeMT1 (**Annex 7.1.5**) yields unique  $M(II)_6$ -NpeMT complexes (where  $M(II) = Zn(II)$  or  $Cd(II)$ ) (**Figure 3.23**), suggesting that, as AvuMT1 (**Section 3.3.1**), NpeMT1 folds into two  $M(II)_3(S_{Cys})_{9-10}$  clusters building a dumbbell-like bidomain structure.

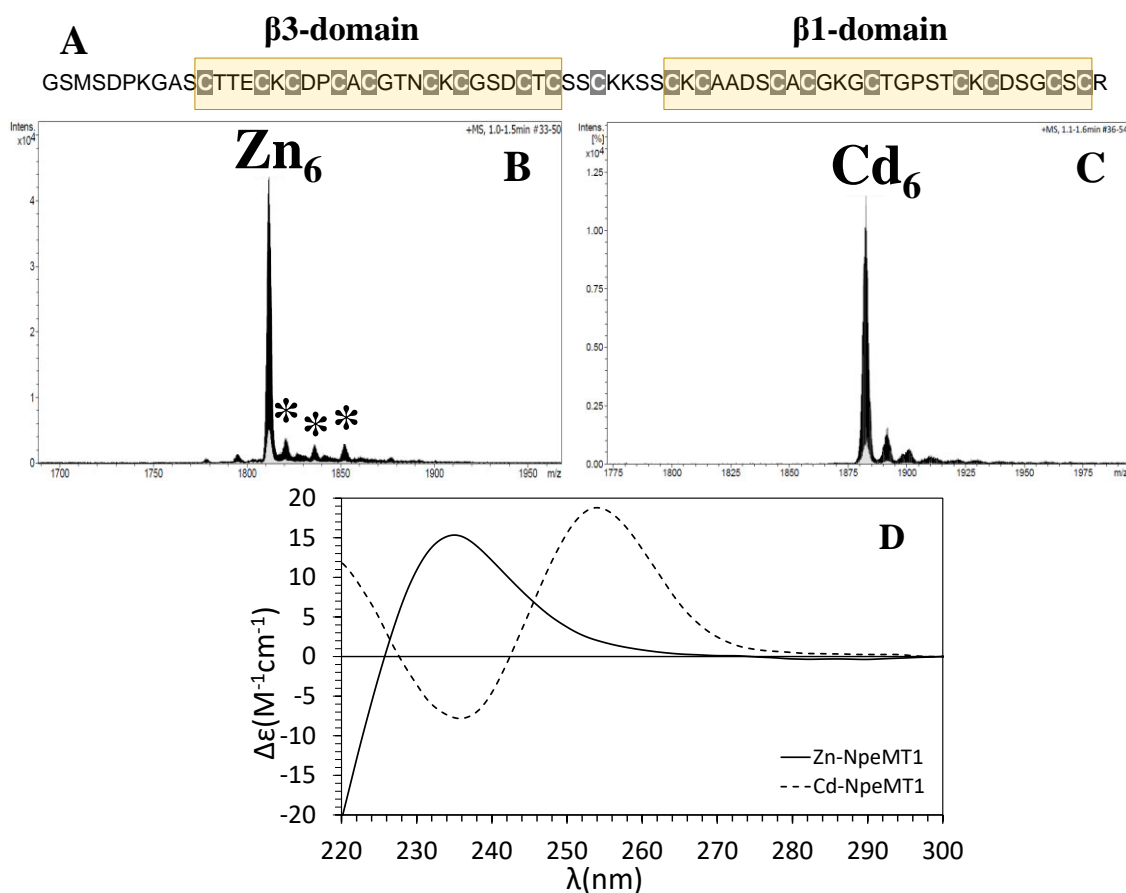


**Figure 3.23.** (A) Architecture of NpeMT1 amino acid sequence, Cys residues are shadowed, and yellow boxes highlight the two nine-Cys motifs of the sequence ( $\beta$ -domains). ESI-MS spectrum at pH 7.0 of (B) Zn-NpeMT1 ( $Q^+ = +4$ ) and (C) Cd-NpeMT1 ( $Q^+ = +4$ ). Glycosylated species are signalled with an asterisk (\*). (D) CD envelopes of Zn-NpeMT1 (solid line) and Cd-NpeMT1 (dashed line) productions.

This unique  $M(II)_6$ -NpeMT1 complexes rendered by NpeMT1 when synthesised in *E. coli* cultures enriched with Zn(II) or Cd(II) salts mark a clear preference of this MT for divalent metal ions and its 6-to-1 stoichiometry was corroborated by ICP-AES (Zn-sample:  $2.1 \cdot 10^{-4}$  M and 5.9 Zn/MT; Cd-sample:  $1.0 \cdot 10^{-4}$  M and 5.5 Cd/MT) (**Annex 7.1.5**). As mentioned previously, this protein probably is structured in two  $M(II)_3(S_{Cys})_{9-10}$  clusters, whose metals follow a tetrahedral coordination geometry, as



both CD spectra of Zn- and Cd-NpeMT1 samples suggest (Figure 3.23D). It should be marked, though, that despite Zn-NpeMT1 CD envelope displays a broad Gaussian band centred at *ca.* 235 nm, as usual for Zn-(S<sub>Cys</sub>)<sub>4</sub> chromophores, Cd-NpeMT1 exhibits an *exciton coupling* centred at *ca.* 240 nm, rather displaced from the habitual 250 nm. This displacement could be result from the formation of Cd clusters that, due to the extra Cys, adopt a variation (although compact) of the classical structure.

As regards with the biosynthesis of NpeMT1 in Cu(II)-supplemented culture medium, it rendered heterometallic Zn,Cu-NpeMT1 species (Figure 3.24). The two peaks obtained by FPLC (collected and characterised separately) (Annex 7.1.5) confirmed the variability of the sample produced. Nevertheless, both peaks exhibit equivalent ESI-MS spectra, showing species ranging from M<sub>8</sub> to M<sub>10</sub>-NpeMT1. These hybrid Zn(II) and Cu(I) clusters are found in the MT-complexes of genuine Zn-thioneins produced under Cu(II) surplus that, as mentioned before, use Zn(II) to build a more stable structure. Clearly, this protein is inefficiently binding Cu(I) ions, and this is evident when the ESI-MS spectrum measured at pH 7.0 is compared with that at pH 2.4 (Figure 3.24B and C).

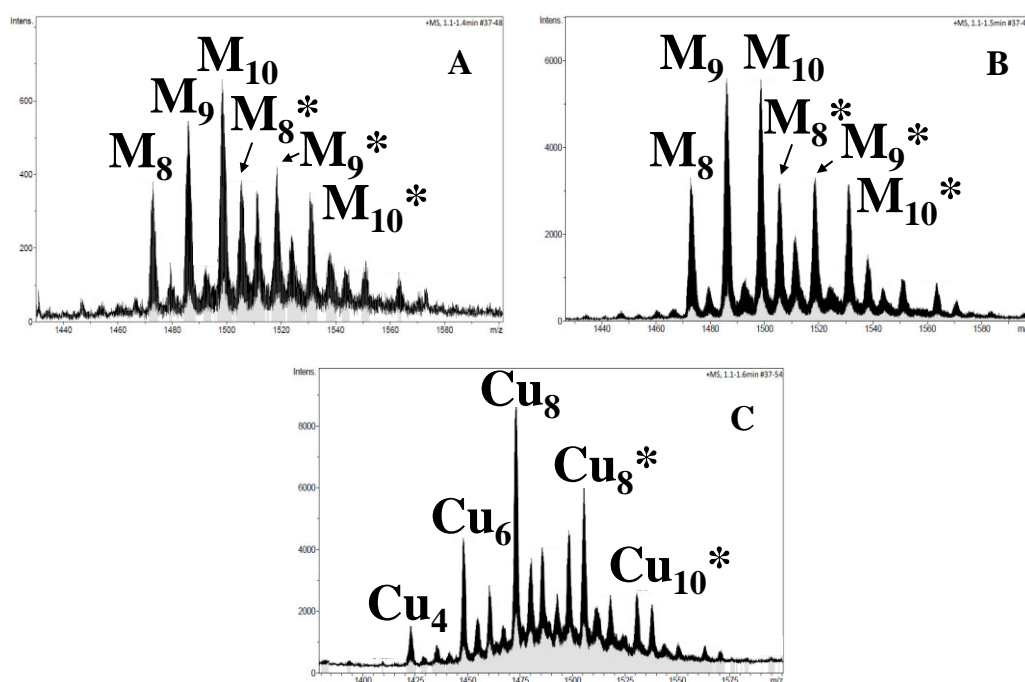


**Figure 3.24.** ESI-MS spectra at pH 7.0 of (A) the first FPLC peak collected ( $Q^+ = +5$ ) and (B) the second FPLC peak collected ( $Q^+ = +5$ ) of Cu-NpeMT1 production. (C) ESI-MS spectrum at pH 2.4 of the second FPLC peak collected ( $Q^+ = +5$ ) of the Cu-NpeMT1 production. Glycosylated species are marked with asterisk (\*).

The three major M-NpeMT1 species found at pH 7.0 contrast with the ones found at pH 2.4, denoting that the composition of the metal clusters is formed by

Zn(II) and Cu(I) ions, as revealed by ICP-AES (**Annex 7.1.5**). Finally, there is one feature worth to be mentioned. In contrast to the very few glycosylated species detected in the Zn(II)-productions, there is an important number of metal-MT complexes obtained from Cu-enriched cultures that exhibit glycosylation. These modified proteins have become an important phenomenon in this thesis, and the topic has its own section where it is widely described (**Section 3.5**), as well as a section that discusses the meaning of the appearance (or not) of these glycosylated metal-complexes (**Section 3.6**).

Overall, NpeMT1 displays features of an MT with high preference for divalent metal ions. The formation of unique species when it is synthesised in the presence of divalent metal ions denotes high affinity for these ions. In contrast, the mixture of heterometallic Zn,Cu-MT complexes obtained from the Cu(II)-supplemented cultures suggest poor Cu-thionein behaviour and show features of a genuine Zn-thionein. For this reason, and as concluded for AvuMT1, we can state that NpeMT1 is an MT that shows most of the traits of a genuine Zn-thionein.

### 3.3.3. Study of *Falciidens caudatus* MT1 and its $\alpha$ fragment

Following the set of MTs selected to enlarge the scope of the current reported mollusc MTs, *Falciidens caudatus* MT1 has been characterised. As mentioned in **section 3.1**, four distinct mollusc MT domains have been reported to date, two of them revealed in this PhD thesis ( $\alpha$ ,  $\beta$ ,  $\gamma$  and  $\delta$ ). Most mollusc MTs conserve their C-terminal  $\beta$ 1 domain, while the N-terminal domain suffered those evolutionary events, becoming the variable part of the protein. Our work aims to characterise all MTs containing each of the four kinds of domains or Cys arrangements. This section describes *Falciidens caudatus* MT1 (FcaMT1), which is organised in two modules, a C-terminal  $\beta$  domain (9 Cys) and a N-terminal  $\delta$  domain (14 Cys) (**Figure 3.25A**). It belongs to an unexplored group of MTs and, therefore, it is of valuable use to understand the metal-binding of this new arrangement of Cys. For that reason, both FcaMT1 and the independent fragment of its  $\delta$  domain have been characterised for the first time.

The unique Zn<sub>8</sub>- and Cd<sub>8</sub>-FcaMT1 species found by ESI-MS suggest that this MT (**Annex 7.1.6**) has preference for divalent metal ions (**Figure 3.25B** and **C**). Here, a very minor presence of Cd<sub>9</sub>-FcaMT1 has been highlighted to explain the behaviour of the  $\delta$  domain (*vide infra*). The most plausible scenario for FcaMT1 is that this protein also follows the same dumbbell-like bidomain structure as most of the mollusc MTs reported here. The C-terminal  $\beta$  motif is coordinating, as usual, three divalent metal ions and the new N-terminal  $\delta$  motif is binding the remaining five

divalent metal ions. The CD spectra of the Zn- and Cd-complexed proteins display the classical Gaussian band of Zn-(S<sub>Cys</sub>) chromophores centred at *ca.* 235 nm and an *exciton coupling* at *ca.* 245 nm of Cd-(S<sub>Cys</sub>) chromophores (Figure 3.25D).

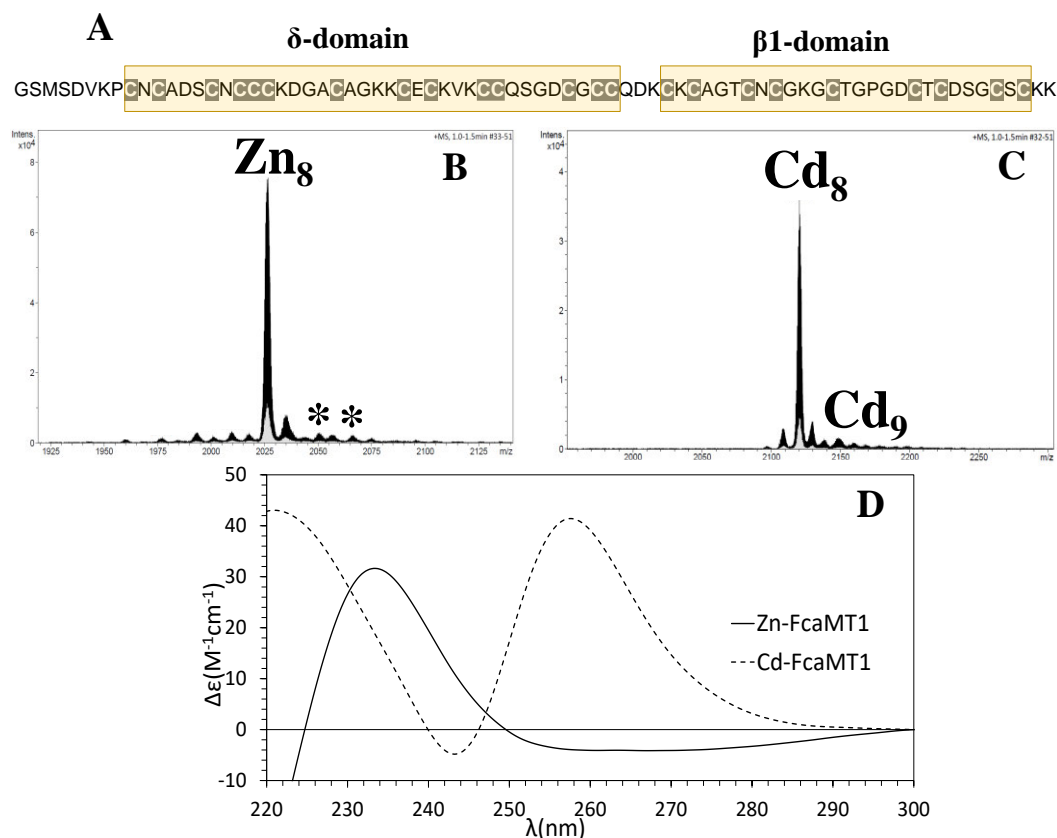


**Figure 3.25.** (A) Architecture of FcaMT1 amino acid sequence, Cys residues are shadowed, and yellow boxes highlight the 14-Cys ( $\delta$ -domain) and 9-Cys ( $\beta$ -domain) motifs of the sequence. ESI-MS spectrum at pH 7.0 of (B) Zn-FcaMT1 ( $Q^+ = +4$ ) and (C) Cd-FcaMT1 ( $Q^+ = +4$ ). Glycosylated species are signalled with an asterisk (\*). (D) CD envelopes of Zn-FcaMT1 (solid line) and Cd-FcaMT1 (dashed line) productions.

Therefore, FcaMT1 builds well-structured divalent metal clusters, confirming that the protein exhibits the features of a genuine Zn-thionein. The recently discovered Cys motif of the  $\delta$  domain confers to FcaMT1 a higher coordinating capacity (up to 8 M(II) ions) than the  $\beta/\beta$ -domain proteins described in earlier sections (up to 6 M(II) ions). The independency and high coordinating capacity of this  $\delta$  domain fragment were revealed by its biosynthesis in Zn(II)- and Cd(II)-enriched *E. coli* cultures, which produced unique M(II)<sub>5</sub>- $\delta$ FcaMT1 species (M(II) = Zn(II) or Cd(II)) (Figure 3.26A and B). The CD spectra of the Zn- and Cd- $\delta$ FcaMT1 complexes display, respectively, equivalent envelopes to those found in the whole protein (Figure 3.26C), denoting the same coordination geometry and suggesting two points: (1) the spectral signal of  $\delta$  domain is predominant over the one of  $\beta$  domain and (2)  $\delta$  domain is capable of independently form a functional metal

cluster. However, there is a slight exception in the samples obtained from the Cd-productions of both FcaMT1 and its  $\delta$  fragment. FcaMT1 shows a minor variability in its structure exhibiting an almost negligible  $\text{Cd}_5$ -FcaMT1 complex by ESI-MS (**Figure 3.25C**). This fact becomes more evident by the presence of the  $\text{Cd}_6$ - $\delta$ FcaMT1 species in the  $\delta$  fragment's Cd-productions (**Figure 3.26B**). These results denote that these peptides render more stable complexes with Zn(II) than with Cd(II), as more than one conformation can be found when associated with the latter metal ions. It is also remarkable that despite the presence of minor glycosylation,  $\text{Zn}_8$ -FcaMT1 is the main species found in the sample, confirming the high stability of this complex, as will be thoroughly explained in **Section 3.6**.

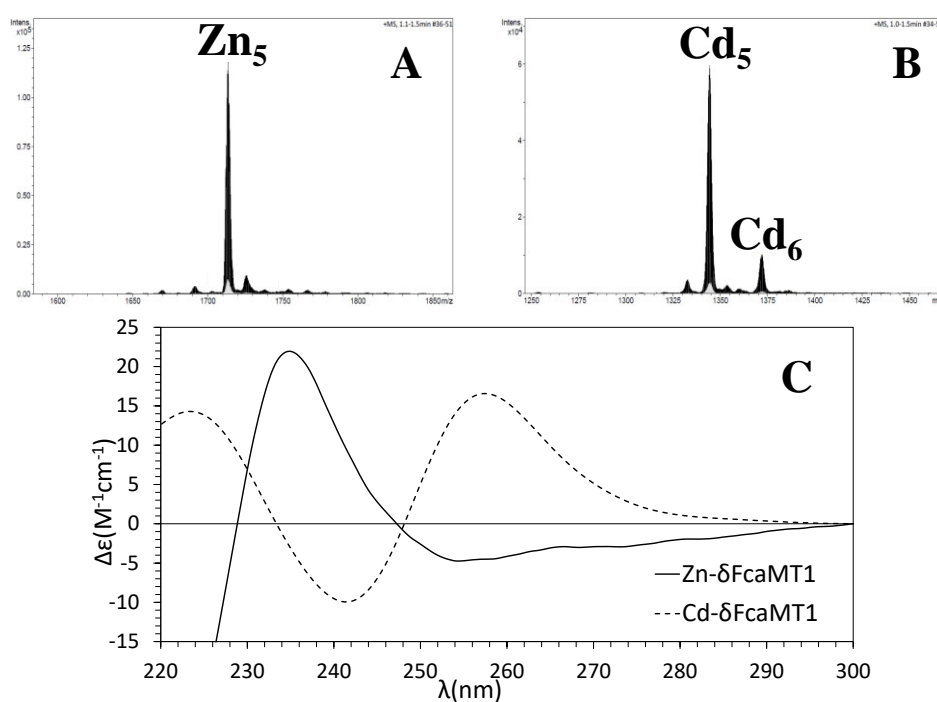


**Figure 3.26.** ESI-MS spectrum at pH 7.0 of (A) Zn- $\delta$ FcaMT1 ( $Q^+ = +3$ ) and (B) Cd- $\delta$ FcaMT1 ( $Q^+ = +4$ ). (C) CD envelopes of Zn- $\delta$ FcaMT1 (solid line) and Cd- $\delta$ FcaMT1 (dashed line) productions.

An additional evidence that supports that FcaMT1 displays Zn-thionein features is in the ICP-AES results obtained from the proteins produced in Cu(II)-supplemented cultures, displaying heterometallic Zn,Cu-FcaMT1 and Zn,Cu- $\delta$ FcaMT1 species. It should be noted that two FPLC peaks (**Annex 7.1.6**) were collected for both the whole protein and its fragment and that Zn(II) ions were detected in all those aliquots except in the first peak of  $\delta$ FcaMT1, whose concentration was so low that the small amount of Zn(II) contained in the protein was probably under the limit of detection. Both FPLC peaks in both FcaMT1 and  $\delta$ FcaMT1 productions showed the same speciation by ESI-MS. For that reason, and since the first peak of both peptides was less concentrated and their spectra

showed more background signal, only the second peak of both preparations is represented (**Figure 3.27**). The ESI-MS spectra of both peptides show a high degree of heterogeneity in the species present in the sample, corroborating their poor Cu-thionein behaviour. The instability of the cluster is confirmed by CD, that denotes a mixture of chromophores with highly variable bands (**Figure 3.27E**). Besides, the sole presence of Zn(II) ions in its metal cluster denote that FcaMT1 possesses high Zn-thionein behaviour. This behaviour is shared with its  $\delta$  fragment but, the speciation of  $\delta$ FcaMT1 is almost invariable from pH 7.0 to pH 2.4 (**Figure 3.27B** and **D**), suggesting that the presence of Zn(II) ions, as detected by ICP-AES, is residual. Interestingly, FcaMT1 and its  $\delta$  fragment show major  $\text{Cu}_8$ -MT species at pH 2.4 (**Figure 3.27C** and **D**). Maybe this data reveals that the  $\delta$  domain deals with most of the Cu(I) load, while the  $\beta$  domain copes with the Zn(II) ions. This is just a supposition and further studies should be performed in order to confirm it. In any case, both Cu-FcaMT1 and Cu- $\delta$ FcaMT1 samples display similar spectroscopical features at pH 7.0, as observed by CD (**Figure 3.27E**), denoting poor structuration of the metal clusters.

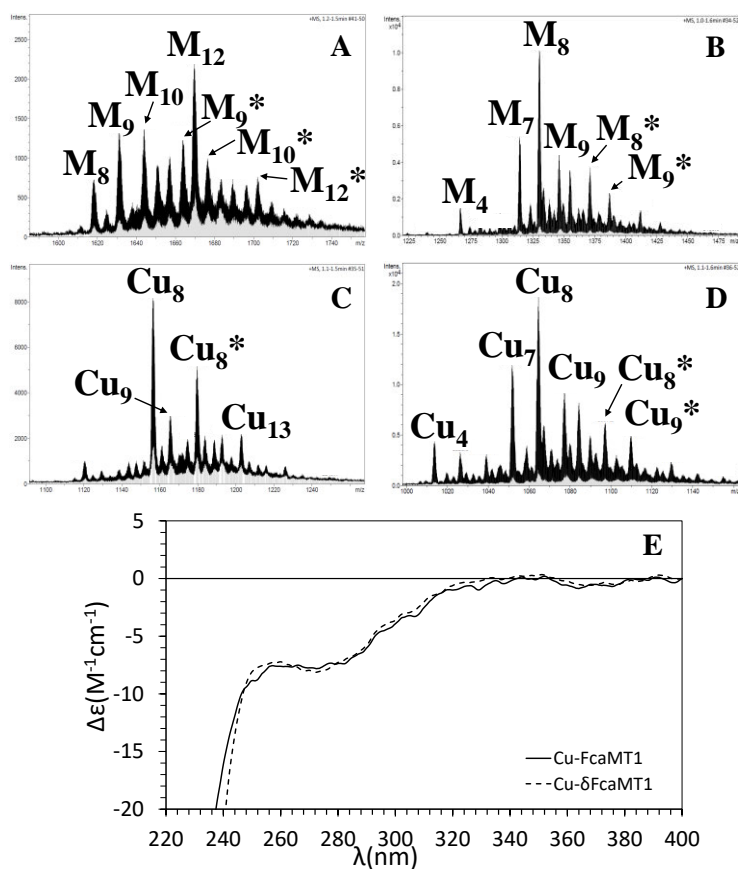


**Figure 3.27.** ESI-MS spectra at pH 7.0 of (A) Cu-FcaMT1 (peak 2) ( $Q^+ = +5$ ) and (B) Cu- $\delta$ FcaMT1 (peak 2) ( $Q^+ = +4$ ). ESI-MS spectra at pH 2.4 of (C) Cu-FcaMT1 (peak 2) ( $Q^+ = +7$ ) and (D) Cu- $\delta$ FcaMT1 (peak 2) ( $Q^+ = +5$ ). Glycosylated species are signalled with an asterisk (\*). (E) CD envelopes of Cu-FcaMT1 (—) and Cu- $\delta$ FcaMT1 (-----) productions at pH 7.0.

Another remarkable feature, once again, is that glycosylated proteins are detected in the Cu-FcaMT1 and Cu- $\delta$ FcaMT1 complexes. These species show higher ESI-MS intensities than the ones found in the MT productions enriched with Zn(II), revealing that the concentration of glycosylated species in relation with the non-glycosylated is higher in this case and, therefore, confirming that Cu-MT complexes are very flexible and low-structured (more information in **Section 3.5**).

In conclusion, FcaMT1 behaves as a genuine Zn-thionein in terms of metal-binding preferences since it yields Zn- and Cd-FcaMT1 complexes with a single energetically favourable form and it is incapable to perform a single well-structured Cu-FcaMT1 complex. This metal preference is shared with its  $\delta$ FcaMT1 fragment as well. This fragment renders Cd<sub>5</sub>-MT complexes as major species but also Cd<sub>6</sub>-MT complexes. That fact, added to the point that the productions supplemented with Cu(II) recovered samples with heterometallic Zn,Cu-FcaMT1 and Zn,Cu- $\delta$ FcaMT1 complexes, leads to consider this protein as a Zn-thionein.

#### 3.3.4. Study of *Candida albicans* MT: CaCUP1

CaCUP1 is a short MT (35 aa), in fact, it is the shortest MT presented in this thesis, that contains six Cys residues (**Figure 3.28A**). Additionally, CaCUP1 contains two aromatic residues (phenylalanine (Phe) and tyrosine (Tyr)), which, due to their biochemical properties, they should not interact with the metal ions. When CaCUP1 is synthesised in Zn(II)-enriched cultures, a unique Zn<sub>2</sub>-CaCUP1 species is rendered (**Figure 3.28A**) and this stoichiometry is corroborated by ICP-AES ( $2.1 \cdot 10^{-4}$  M and 2.2 Zn/MT) (**Annex 7.1.7**). Probably due to the aromatic residues, the optical traits of the polypeptide observed by CD show an uncommon negative Gaussian band centred at *ca.* 235 nm, near the absorbance wavelength of Zn-(S<sub>Cys</sub>)<sub>4</sub> chromophores (**Figure 3.28F**). This is, indeed, a rare CD envelope but the overall results suggest a genuine Zn-thionein behaviour for this MT and this is corresponded with the results obtained from the samples purified from the Cd(II)- and Cu(II)-enriched cultures.

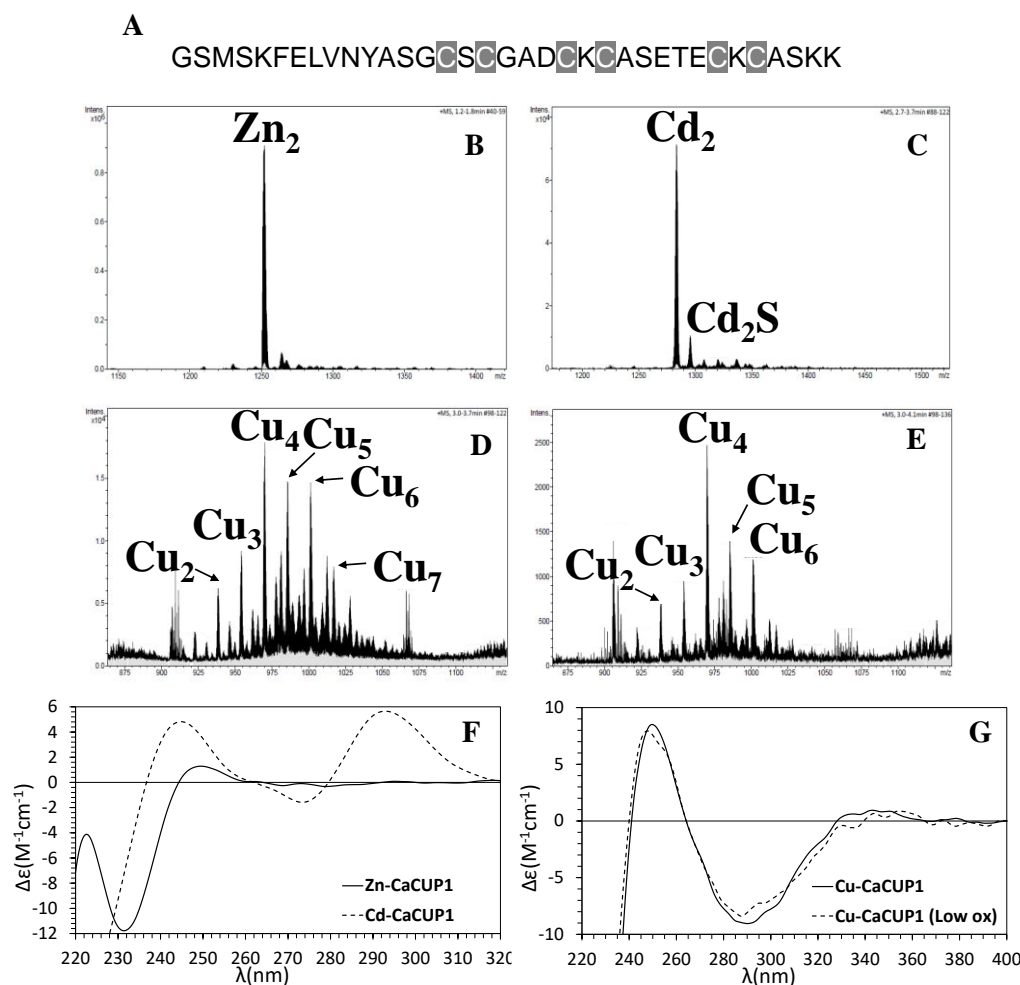


**Figure 3.28.** (A) Architecture of CaCUP1 amino acid sequence, Cys residues are shadowed. ESI-MS spectra at pH 7.0 of productions of (B) Zn-CaCUP1 ( $Q^+ = +3$ ), (C) Cd-CaCUP1 ( $Q^+ = +3$ ), (D) Cu-CaCUP1 from normal oxygenation cultures ( $Q^+ = +4$ ) and (E) Cu-CaCUP1 from low oxygenation cultures ( $Q^+ = +4$ ). (F) CD envelopes of Zn-CaCUP1 (solid line) and Cd-CaCUP1 (dashed line). (G) CD envelopes of Cu-CaCUP1 normal oxygenation (solid line) and Cu-CaCUP1 low oxygenation (dashed line).

The recombinant protein synthesised in the Cd(II)-supplemented culture yielded Cd<sub>2</sub>- (major) and Cd<sub>2</sub>S-CaCUP1 (minor) species, as by ESI-MS (Figure 3.28C). The presence of labile sulphide (S<sup>2-</sup>) ligands was confirmed by measuring the concentration of sulphur of the sample by ICP-AES before (1.6·10<sup>-4</sup> M and 2.8 Cd/MT) and after (0.8·10<sup>-4</sup> M and 3.7 Cd/MT) acidification with formic acid. The discrepancy between both measures denotes that the labile sulphur ligands were released as gaseous H<sub>2</sub>S after acidifying the sample (See Section 5.2.2). Additionally, the wide CD band detected at 300 nm (Figure 3.28F) can be related to the presence of chromophores of Cd-S<sup>2-</sup> [155].

As expected, this CD band is not present after Zn<sub>2</sub>-CaCUP1 complex, which lacks of these labile ions, exchanges its Zn(II) ions by Cd(II). This metal exchange experiment was followed by CD, measuring a spectrum at each equivalent addition (Annex 7.2.2: Sheet 7.2.2.3). The CD envelope at the final stage of the experiment

shows a Gaussian band centred at *ca.* 240 nm, displaced from the *in vivo* (and other Cd-MTs) characteristic band centred at *c.a.* 250 nm (**Figure 3.29A**).

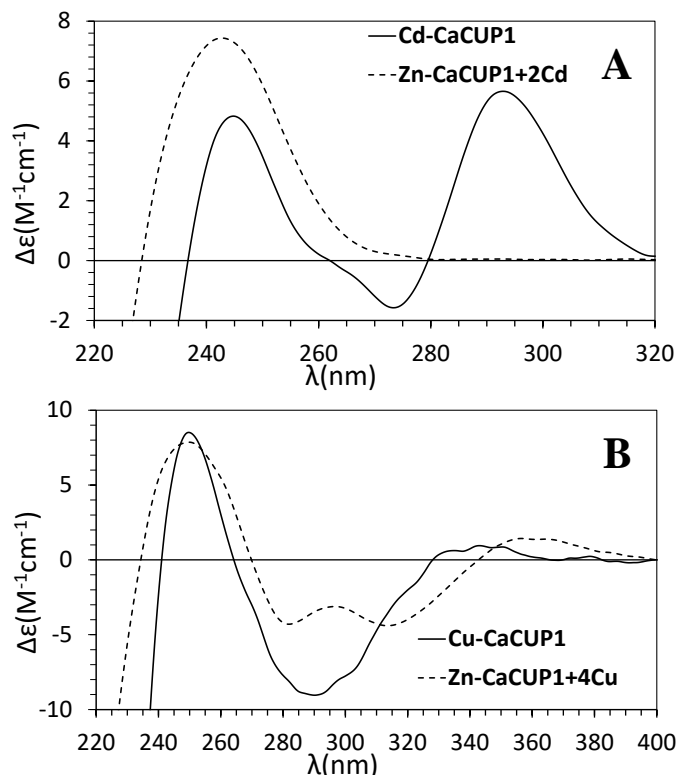


**Figure 3.29.** (A) CD envelopes of *in vivo* Cd-CaCUP1 (solid line) and *in vitro* Cd-CaCUP1 (dashed line) obtained from *in vivo* Zn-CaCUP1 after the addition of 2 Cd(II) equivalents. (B) CD envelopes of *in vivo* Cu-CaCUP1 (solid line) and *in vitro* Cu-CaCUP1 (dashed line) obtained from *in vivo* Zn-CaCUP1 after the addition of 4 Cu(I) equivalents.

The band associated to the sulphur chromophores is not detected since no labile  $S^{2-}$  ligands were present in the initial sample. Instead, a faded band at 280 nm is detected, most likely due to the presence of aromatic residues. The presence of labile  $S^{2-}$  ions in the CaCUP1 productions enriched with Cd(II) reveals poor preference for Cd(II) ions, a feature that has not been observed in the rest of the proteins of this section.

Additionally, the characterisation of the samples recovered from the Cu(II)-supplemented MT productions supports the hypothesis that CaCUP1 is a Zn-thionein. The most relevant characteristic found in the Cu(I)-loaded samples is the low concentration of the proteins recovered (**Annex 7.1.7**), denoting the difficulty of CaCUP1 to form stable metal clusters under these conditions (**Figure 3.28D** and **E**). Both conditions, normal and low aeration, rendered equivalent mixture of species, suggesting that maybe CaCUP1 do not render heterometallic Zn,Cu metal clusters as the genuine Zn-thioneins. Unfortunately, it was impossible to corroborate this through ICP-AES since neither S, Cu(I) nor Zn(II) concentrations



were sufficient to be clearly detected by the ICP-AES instrument. The CD spectrum of the highly heterogeneous Cu-CaCUP1 sample confirmed the lack of defined structures exhibiting a faint CD envelope (**Figure 3.28G**). Remarkably, despite of the fact that CaCUP1 shows none of the genuine Cu-thionein characteristics, the Zn/Cu exchange experiment revealed interesting data. Although unique Cu<sub>4</sub>-CaCUP1 complexes are not formed *in vivo* (**Figure 3.28D** and **E**), the *in vitro* experiments show the prevalence of this species. After 3-4 equivalent of Cu(I) added to the Zn-CaCUP1 sample, a unique Cu<sub>4</sub>-CaCUP1 species is detected by ESI-MS (**Annex 7.2.2: Sheet 7.2.2.4**). Moreover, this seems to be an almost cooperative process, since at the early stages of the metal exchange only Zn<sub>2</sub>-CaCUP1 and Cu<sub>4</sub>-CaCUP1 major species are observed. Again, as occurred with the metal exchange experiment with Cd(II), the *in vitro* and the *in vivo* CD spectra of the Cu-CaCUP1 complexes are different, suggesting a distinct overall arrangement of the metal cluster when the protein is *de novo* loaded with Cu(I) or when the initial Zn(II) ions are displaced by Cu(I). The homogeneous speciation makes the CD spectra measured after adding 4 Cu(I) equivalents to show the appearance of a band at *ca.* 300 nm (**Figure 3.29B**) with respect to the heterogeneous *in vivo* Cu-CaCUP1 sample. This band might not be shown before due to the complex speciation of the *in vivo* sample purified from the Cu-enriched cultures.

In conclusion, despite the unexpected results of the *in vitro* experiments, CaCUP1 shows a genuine Zn-thionein behaviour (unique Zn-CaCUP1 species, mixture of species recovered from the Cd(II)- and Cu(II)-supplemented MT productions), distinct from the Zn-thionein behaviour of the rest of the MTs presented in this section.

### 3.3.5. General observations of Zn-thioneins

The characterisation of the MTs presented in this section provided common features that will be considered to differentiate between genuine Zn-thioneins and putative Cd-thioneins. These features are: formation of unique Zn-MT complexes when they are synthesised in Zn-supplemented cultures, possible mixture of Cd-MT complexes recovered from Cd(II)-enriched cultures, and heterometallic Zn,Cu-MT complexes when produced in Cu(II)-enriched cultures. The proteins studied in this section comply with most of these features and are a good example to confirm that a metal-binding classification makes sense.

### 3.4. Characterisation of the metal-binding abilities of putative Cd-thioneins

The principal goal of this thesis is to elucidate whether the Zn,Cd-thionein (divalent metal-binding specificity) features might be split into two genuine Zn- and Cd-thionein independent behaviours. This hypothesis came up at the initial stages of this PhD thesis, after the evolutive study made on mollusc MTs that stated that Cd concentration levels in mollusc habitats drove the evolution of their MTs [210]. Most of the proteins presented in this thesis belong to mollusc organisms from very varied habitats and lifestyles. The following section groups MTs either from Mollusca clade, but also MTs from a close sister group of vertebrates called urochordates. All these proteins exhibit similar metal-binding traits, and these interesting results will be discussed along the text.

#### 3.4.1. Study of *Lottia gigantea* MTs

As mentioned, mollusc MTs are going to be a main character in this thesis and this section starts with a system of two mollusc MTs. *L. gigantea* is a marine limpet with two MT isoforms reported: LgiMT1 and LgiMT2. The interest of this set of MTs resides in their Cys arrangement (**Annex 7.3.4: Article 4**). As most of mollusc MTs, LgiMTs show a nine Cys motif at C-terminal, called  $\beta$  domain (**Figure 3.30A**), but, interestingly, contain a ten Cys motif at N-terminal arranged in duplets of Cys (CC), called  $\gamma$  domain (**Figure 3.30A**). This novel motif unveils a new metallic cluster with peculiar metal-binding abilities, as exposed next.

From the study of LgiMTs (**Annex 7.1.8** and **7.1.9**), the first discrepancy obtained in comparison to the proteins described in the last section is the detection of a mixture of Zn-MT species in the samples purified from the Zn(II)-enriched cultures (**Figure 3.30B** and **D**). As observed, and as expected from two proteins only differing by three amino acids, both MTs display analogous results. The recovery of this mixture of Zn-MT complexes denotes poor Zn-thionein behaviour for the LgiMTs, as well as the faint CD envelope rendered by the heterogenous samples (**Figure 3.30H**). These low intense Gaussian bands centred at *ca.* 240 nm reveal the expected tetrahedral coordination geometry of the Zn-(S<sub>Cys</sub>)<sub>4</sub> chromophores, although poorly structured. Besides the abundant variety of Zn-LgiMT complexes, it is remarkable that Zn<sub>7</sub>- and Zn<sub>4</sub>-LgiMTs are the most intense peaks detected by ESI-MS. These numbers gain relevance if we consider the Cys arrangement of LgiMTs: structured in two motifs of ten and nine Cys each. It is well known that a  $\beta$  domain (nine Cys) binds three divalent metal ions [55, 56] but

it is not described yet the number of divalent metal ions that a motif of ten Cys can bind. The results obtained from the production of the  $\gamma$  fragment assisted to elucidate this unknown. When the  $\gamma$ LgiMT2 fragment is synthesised under Zn(II) surplus, it mostly yields  $Zn_4$ - $\gamma$ LgiMT2 complexes, showing that this number is important (Figure 3.30F).

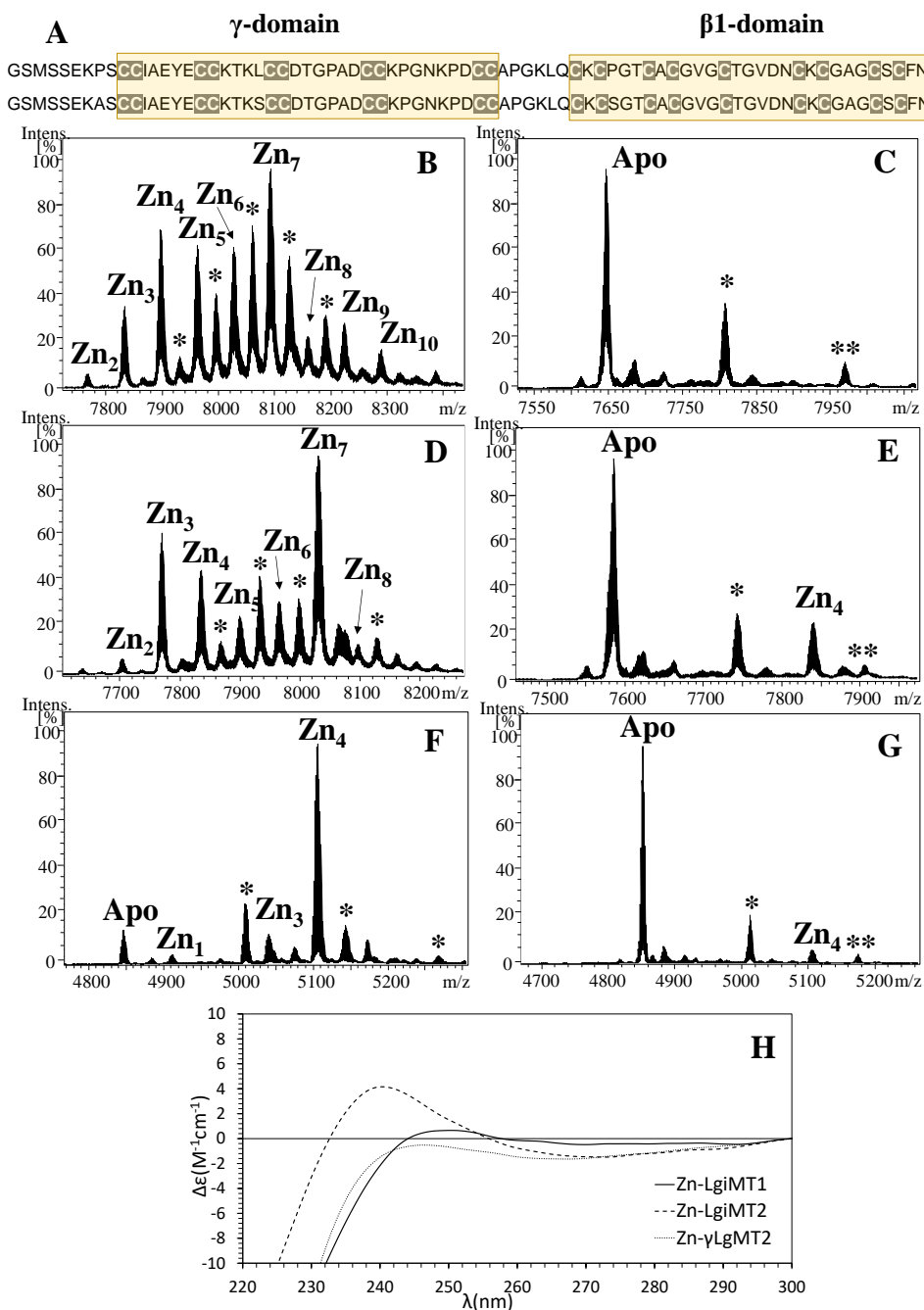


**Figure 3.30.** (A) Architecture of LgiMTs amino acid sequences, Cys residues are shadowed, and yellow boxes highlight the 10-Cys ( $\gamma$ -domain) and 9-Cys ( $\beta$ -domain) motifs of the sequence. Deconvoluted ESI-MS spectra at pH 7.0 of (B) Zn-LgiMT1, (D) Zn-LgiMT2 and (F) Zn- $\gamma$ LgiMT2 productions. Deconvoluted ESI-MS spectra at pH 2.4 of (C) Zn-LgiMT1, (E) Zn-LgiMT2 and (G) Zn- $\gamma$ LgiMT2 productions. Glycosylated species are signalled with an asterisk (\*). (H) CD envelopes of Zn-LgiMT1 (solid line), Zn-LgiMT2 (dashed line) and Zn- $\gamma$ LgiMT2 (dotted line) productions.

In addition, the intensity of the CD envelope of this fragment is very low as well, denoting a non-compact structure. Probably, those important Zn<sub>7</sub>-LgiMT2 species are organised as Zn<sub>3</sub>(S<sub>Cys</sub>)<sub>9</sub> and Zn<sub>4</sub>(S<sub>Cys</sub>)<sub>10</sub> clusters. Finally, a trait of major interest is the high number of glycosylated species present in the samples. Glycosylated species have already been found in protein productions of anterior sections but, in this case, they are of utmost relevance. These species are detected by ESI-MS at either pH 7.0 or 2.4 (**Figure 3.30**), adding up to three monomers of hexoses to the same protein. This phenomenon is widely explained in **Section 3.5**, but, in short, glycosylation is of great use to classify MTs by their metal-preference, since glycosylation only occurs in very mobile polypeptide sequences with highly labile metal clusters. Finding these modifications in the samples suggests that the Zn-LgiMTs complexes are instable, denoting their poor Zn-thionein behaviour.

While the samples obtained from the *E. coli* cultures supplemented with Zn(II) present species with high degree of heterogeneity, the samples produced under Cd(II) surplus yield unique Cd<sub>7</sub>-LgiMTs complexes (**Figure 3.31A** and **C**). Thus, LgiMTs nicely bind seven Cd(II) ions, with a unique energetically favoured form, but they are not so efficient binding Zn(II) ions. However, as mentioned before, seven (divalent metal ions) is an interesting number. Both LgiMTs maintain four Cd(II) ions at pH 2.4 (**Figure 3.31B** and **D**), and parallelly  $\gamma$ LgiMT2 renders Cd<sub>4</sub> species as well, also maintaining four Cd(II) ions at pH 2.4 (**Figure 3.31E** and **F**). Certainly, this confirms that the Cd<sub>4</sub>-LgiMTs species found at pH 2.4 correspond to the Cd<sub>4</sub>- $\gamma$ LgiMT species found at pH 7.0 and pH 2.4. Bearing in mind the aforementioned Cys arrangement, LgiMTs must form two clusters (one in the  $\gamma$  domain and another in the  $\beta$  domain): Cd<sub>4</sub>(S<sub>Cys</sub>)<sub>10</sub> and Cd<sub>3</sub>(S<sub>Cys</sub>)<sub>9</sub>. Moreover, the clusters of three Cd(II) ions are more susceptible to pH variations, as they readily exchange the metals by protons, while the Cd<sub>4</sub>(S<sub>Cys</sub>)<sub>10</sub> cluster of the  $\gamma$  domain resists at pH 2.4. The CD spectra of Cd- $\gamma$ LgiMT2 is equivalent to the Cd-LgiMTs' CD envelopes, suggesting a dominant optical activity from the  $\gamma$  domain cluster over the one built by the  $\beta$  domain (**Figure 3.31G**). The CD envelopes are of high intensity, showing an *exciton coupling* centred at *ca.* 250 nm that is overlapped by a higher signal at 265 nm, which may be given by the aromatic amino acids. The proposed structure for this  $\gamma$  domain, due to the number of ligands and metal ions, is an adamantane-like structure [238], which would be a new structural motif in the MTs field. This structure should be confirmed by NMR.

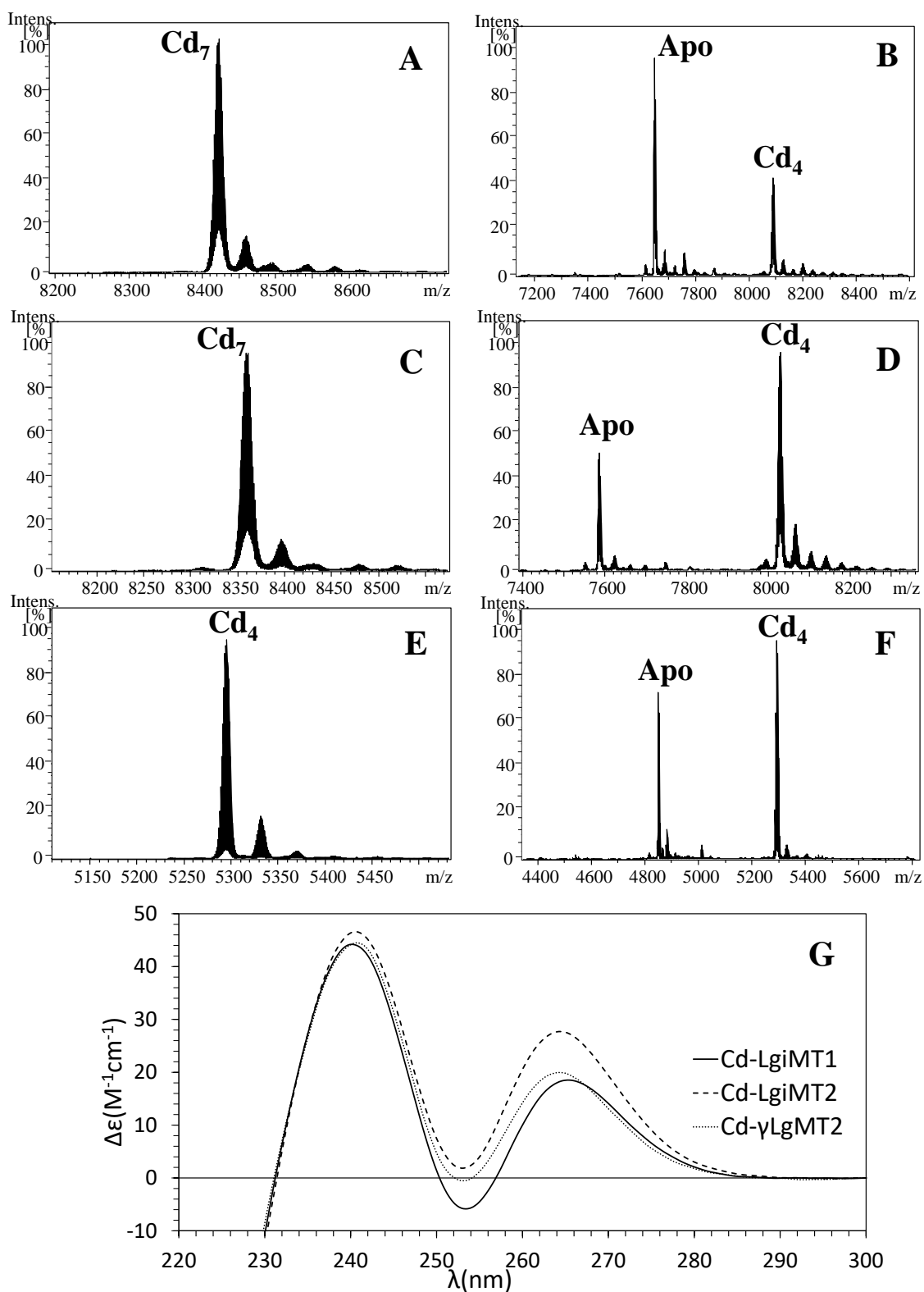


**Figure 3.31.** Deconvoluted ESI-MS spectra at pH 7.0 of (A) Cd-LgiMT1, (C) Cd-LgiMT2, and (E) Cd- $\gamma$ LgiMT2 productions. Deconvoluted ESI-MS spectra at pH 2.4 of (B) Cd-LgiMT1, (D) Cd-LgiMT2, and (F) Cd- $\gamma$ LgiMT2 productions. (G) CD envelopes of Cd-LgiMT1 (solid line), Cd-LgiMT2 (dashed line) and Cd- $\gamma$ LgiMT2 (dotted line) productions.

As regards to LgiMTs metal-binding preferences towards Cu(I) ions, the samples obtained from the Cu(II)-supplemented *E. coli* cultures also show high degree of heterogeneity in the speciation (Figure 3.32).

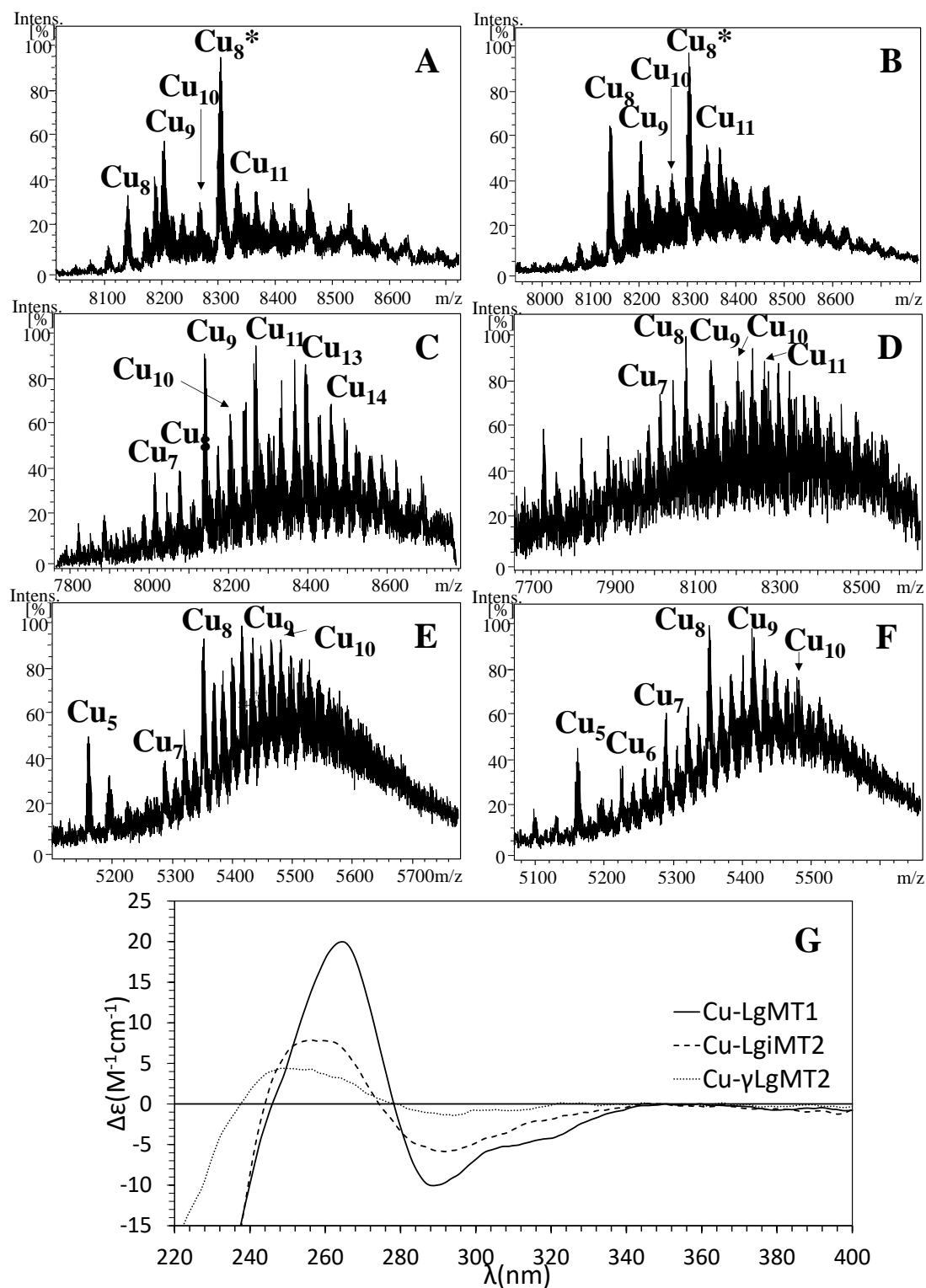


**Figure 3.32.** Deconvoluted ESI-MS spectra at pH 7.0 of (A) Cu-LgiMT1, (C) Cu-LgiMT2, and (E) Cu-γLgiMT2 productions. Deconvoluted ESI-MS spectra at pH 2.4 of (B) Cu-LgiMT1, (D) Cu-LgiMT2, and (F) Cu-γLgiMT2 productions. (G) CD envelopes of Cu-LgiMT1 (solid line), Cu-LgiMT2 (dashed line) and Cu-γLgiMT2 (dotted line) productions. Glycosylated species are marked with asterisks (\*).

The lack of unique metal-MT complexes denotes poor preference of these proteins for Cu(I) ions. However, and very interestingly, these metal-MT complexes are homometallic, as ICP-AES only detected Cu(I) (**Annex 7.1.8** and **7.1.9**). This trait differs from other MTs that displays a strong preference for divalent metal ions (see **Section 3.3**), which yield heterometallic Zn,Cu-MT complexes when synthesised in Cu(II)-enriched cultures (more information about these differences in **Section 3.6**). Thus, LgiMTs do not show Zn-thionein features but neither they show Cu(I)-preference. The CD spectra of these heterogenous samples are equivalent in regard to their absorption maxima, which coincide with those found in other Cu-MT preparations (**Figure 3.32G**). The low intensity of this CD fingerprints confirms the low degree of robustness of the clusters formed. As already observed in the Zn-LgiMTs, the samples purified from the Cu(II)-supplemented cultures show glycosylated species as well. Once again, this phenomenon relates to very labile metal clusters and mobile polypeptide chains, which confirms the poor Cu-thionein behaviour of LgiMTs.

In conclusion, the characterisation of LgiMT1, LgiMT2, and of the  $\gamma$ LgiMT2 fragment allowed to discover a new MT domain that shows high resistance to be demetallated at low pH. It also demonstrates that some MTs can form nice and unique Cd(II)-MT complexes but not behave equally towards Zn(II) ions. This is the first example of an MT in this thesis that exhibits Cd-selectivity but not Zn-specificity.

### 3.4.2. Study of *Nautilus pompilius* MT

*Nautilus pompilius* only possess one reported MT isoform so far and its amino acid sequence bears a keen interest for this thesis. *N. pompilius* MT (NpoMT1) is a representative sample for cephalopod MTs and those molluscs whose MTs share the bidomain structure  $\alpha/\beta$  with NpoMT1. This structure is arranged in one conserved nine Cys motif ( $\beta$  domain) at C-terminal (shared with the rest of mollusc MTs) and a twelve Cys motif ( $\alpha$  domain) at N-terminal.

When NpoMT1 (**Annex 7.1.10**) is produced in Zn(II) surplus it renders Zn<sub>6</sub>- and Zn<sub>7</sub>-NpoMT1 as major species (**Figure 3.33A**). The stoichiometry of 6-7 Zn(II) ions per protein is corroborated by the ICP-AES results ( $1.3 \cdot 10^{-4}$  M and 6.5 Zn/MT) (**Annex 7.1.10**). Comparing NpoMT1 with other MTs with 21 Cys and a bidomain  $\alpha/\beta$  architecture (*e.g.*, mammalian MTs, with 20 Cys), it is evident that seven divalent metal ions is a common and expectable stoichiometry [33]. Consequently, the CD spectrum of the Zn-NpoMT1 sample depicts a positive Gaussian band centred at *ca.* 235 nm, displaying the usual fingerprint of Zn-thiolate

chromophores (**Figure 3.33F**). The poor Zn-thionein behaviour of NpoMT1 is shared with its  $\alpha$  fragment, which renders  $Zn_4$ -(major) and  $Zn_3$ -(minor)  $\alpha$ NpoMT1 species in the presence of Zn(II) and shows a faint CD envelope (**Figure 3.33C and F**). It is, once again, remarkable the presence of glycosylated species for both the whole protein and its independently synthesised  $\alpha$  domain, denoting a labile cluster.

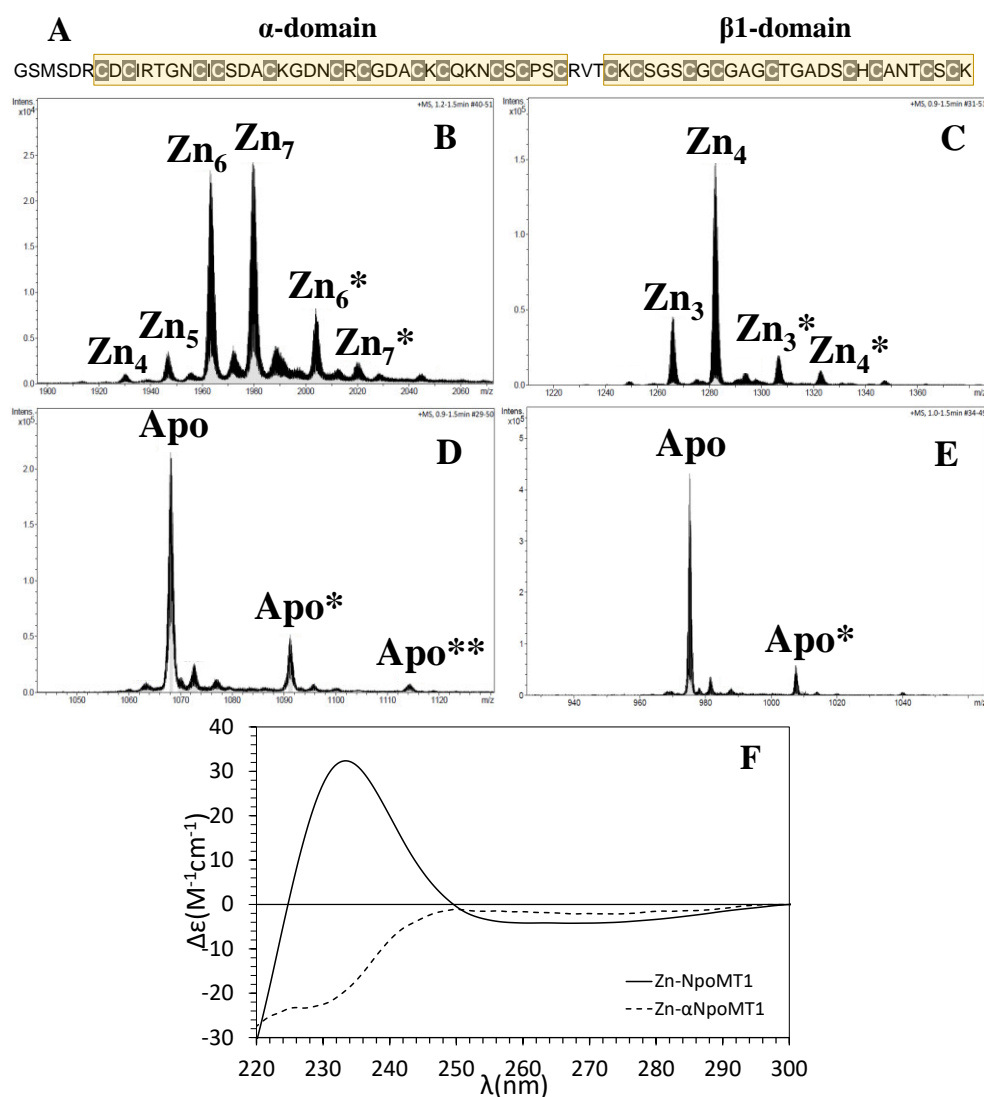


**Figure 3.33.** (A) Architecture of NpoMT1 amino acid sequence, Cys residues are shadowed, and yellow boxes highlight the 12-Cys ( $\alpha$ -domain) and 9-Cys ( $\beta$ -domain) motifs of the sequence. ESI-MS spectra at pH 7.0 of (B) Zn-NpoMT1 ( $Q^+ = +4$ ) and (C) Zn- $\alpha$ NpoMT1 ( $Q^+ = +4$ ) productions. ESI-MS spectra at pH 2.4 of (D) Zn-NpoMT1 ( $Q^+ = +7$ ) and (E) Zn- $\alpha$ NpoMT1 ( $Q^+ = +5$ ) productions. Glycosylated species are signalled with an asterisk (\*). (F) CD envelopes of Zn-NpoMT1 (solid line), and Zn- $\alpha$ NpoMT1 (dashed line) productions.

In contrast to the results obtained for the production supplemented with Zn(II), NpoMT1 renders a unique  $Cd_7$ -NpoMT1 species (**Figure 3.34A**) when synthesised in Cd(II) surplus. This same situation is found in other MTs with the same domain



arrangement (*e.g.*, the aforementioned mammal MTs), which leads to suggest that NpoMT1 might be structured as a dumbbell-like bidomain MT that sustains a  $\text{Cd(II)}_3(\text{S}_{\text{Cys}})_9$  and a  $\text{Cd(II)}_4(\text{S}_{\text{Cys}})_{12}$  clusters. That hypothesis is supported by the fact that a  $\text{Cd}_4$ -NpoMT1 species is detected at pH 2.4 (**Figure 3.34C**) and also a unique  $\text{Cd}_4$ - $\alpha$ NpoMT1 species is found in the independent fragment synthesis (**Figure 3.34B**). Probably, both species correspond to the same  $\text{Cd(II)}_4(\text{S}_{\text{Cys}})_{12}$  cluster, that means that (1)  $\alpha$ NpoMT1 fragment is able to bind four Cd(II) ions by itself and, thus, it is a functional domain and that (2) the  $\text{Cd}_4$ -NpoMT1 species found at pH 2.4 correspond to the cluster formed by this  $\alpha$  domain. Moreover, both full protein and the independent  $\alpha$ NpoMT1 fragment display analogous CD envelopes, showing an *exciton coupling* centred at *ca.* 250 nm and, thus, denoting a highly compact metal cluster (**Figure 3.34E**). This protein shows great ability to perform unique well-formed complexes with Cd(II), which reveals great metal-binding abilities for this metal.

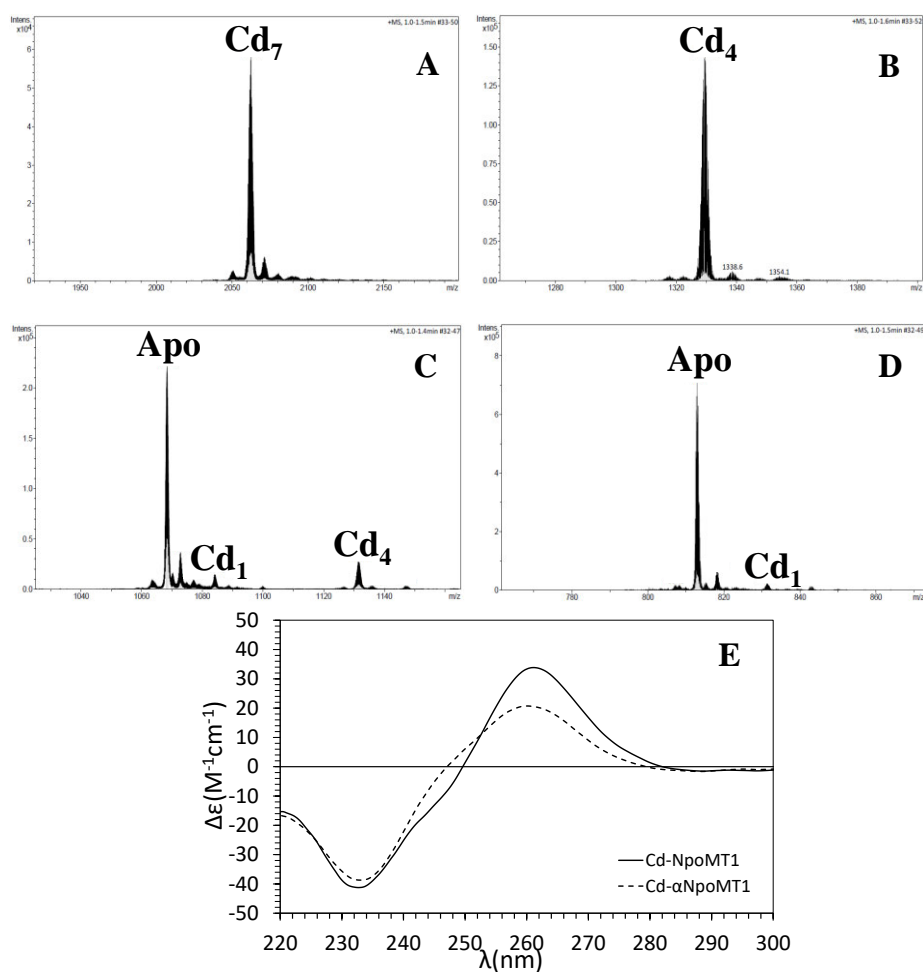


**Figure 3.34.** ESI-MS spectra at pH 7.0 of (A) Cd-NpoMT1 ( $Q^+ = +4$ ) and (B) Cd- $\alpha$ NpoMT1 ( $Q^+ = +4$ ) productions. ESI-MS spectra at pH 2.4 of (C) Cd-NpoMT1 ( $Q^+ = +7$ ) and (D) Cd- $\alpha$ NpoMT1 ( $Q^+ = +6$ ) productions. (E) CD envelopes of Cd-NpoMT1 (solid line), and Cd- $\alpha$ NpoMT1 (dashed line) productions.

With regards to the samples obtained from Cu(II)-enriched media, a great variety of Cu-NpoMT1 complexes, at very low concentrations were detected by ESI-MS (Figure 3.35). The experience says that, normally, when the preparation recovered from a production shows low concentrations, the metal-MT complexes are not much favoured in those synthesis conditions, denoting the poor metal-binding affinity of the protein for these specific metal ions. Besides, the CD spectrum of this production confirmed that the complexes in the sample possessed low degree of structuration, displaying a faint CD envelope (Figure 3.35E). Therefore, we can say that NpoMT1 displays poor Cu-thionein features, despite that the ICP-AES only detected Cu in the sample and no trace of Zn ( $<0.1 \cdot 10^{-4}$  M and  $>14.16$  Cu) (Annex 7.1.10).

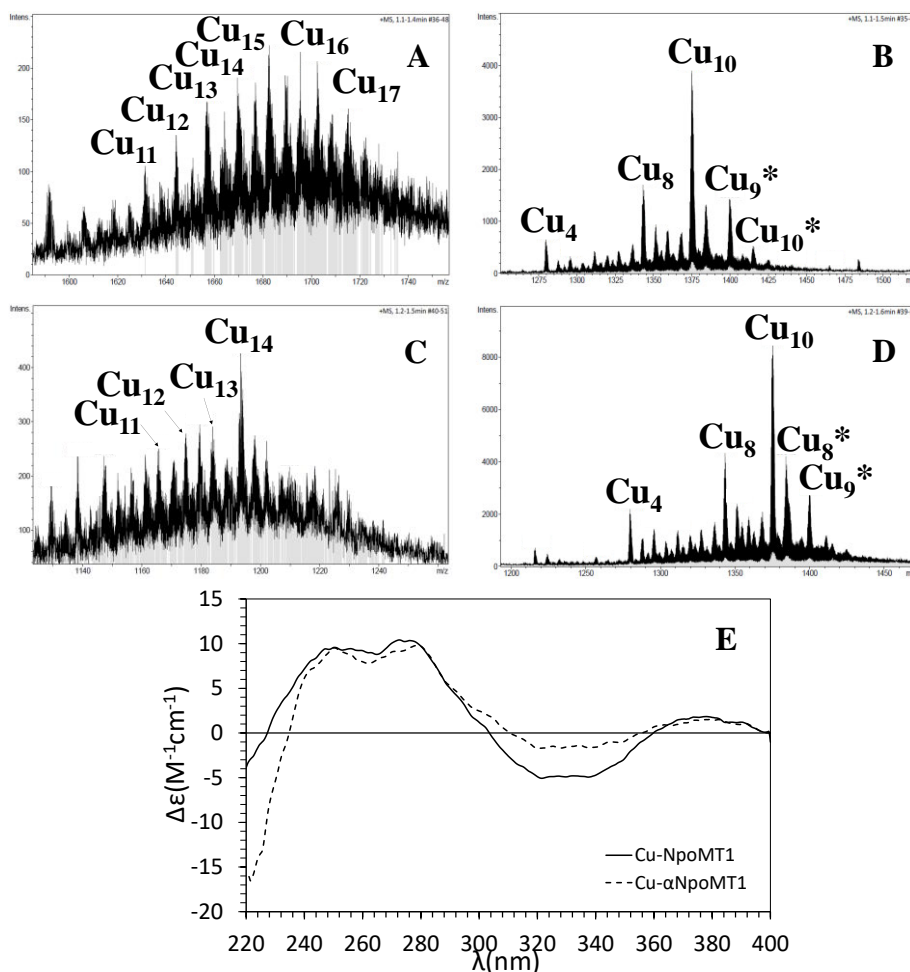


**Figure 3.35.** ESI-MS spectra at pH 7.0 of (A) Cu-NpoMT1 ( $Q^+ = +5$ ) and (B) Cu- $\alpha$ NpoMT1 ( $Q^+ = +4$ ) productions. ESI-MS spectra at pH 2.4 of (C) Cu-NpoMT1 ( $Q^+ = +7$ ) and (D) Cu- $\alpha$ NpoMT1 ( $Q^+ = +4$ ) productions. (E) CD envelopes of Cu-NpoMT1 (solid line), and Cu- $\alpha$ NpoMT1 (dashed line) productions. Glycosylated species are marked with asterisks (\*).

Interestingly, the ESI-MS (Figure 3.35B and D) and ICP-AES (Annex 7.1.10) results revealed that the  $\alpha$ NpoMT1 fragment exhibits less heterogeneity in the

speciation of its Cu-MT complexes than the whole protein, showing a dominant Cu<sub>10</sub>-MT complex, but, more importantly, it is confirmed the presence of homometallic Cu-species, which settles that NpoMT1 has poor Zn-preference. This fact is also confirmed by the results obtained by CD, where the αNpoMT1 fragment shows an equivalent fingerprint with the full protein (**Figure 3.35E**).

In conclusion, this section presents another mollusc protein that is well-structured when binds Cd(II) ions but not when it is coordinating Zn(II) ions. Additionally, the high degree of heterogeneity in the speciation of the Cu-complexes synthesised confirms also the poor Cu-thionein behaviour of NpoMT1. A different protein with different Cys arrangement generates similar results to those found for LgiMTs.

### 3.4.3. Study of *Nerita peloronta* MT2

This section aims to describe the metal-binding abilities of NpeMT2 isoform and discusses why NpeMT2 is under **Section 3.4**. As explained in **Section 3.3.2**, *Nerita peloronta* is a marine snail that has two MTs (**Annex 7.3.4: Article 4**). Both MTs exhibit highly similar metal-binding features. However, there is a particular trait worth to consider separating them into two different metal-binding behaviours as will be discussed here and, extendedly, in **Section 3.6**. Both isoforms share the same bidomain β/β arrangement (9 Cys +9 Cys) with 19 Cys in NpeMT1 and 18 Cys in NpeMT2. However, NpeMT2 contains two His residues in its polypeptide chain. This particular residue might have some impact on the metal-binding features of this isoform. In addition to the characterisation of NpeMT2, and to have a record of all variable domains of bidomain mollusc MTs, βNpeMT2 domain has been independently synthesised and its biochemical properties studied.

NpeMT2 (**Annex 7.1.11**), as NpeMT1, yields unique Zn<sub>6</sub>-NpeMT2 species when synthesised in *E. coli* cultures supplemented with Zn(II) (**Figure 3.36B**). This 6-to-1 Zn(II)-to-protein stoichiometry is corroborated by ICP-AES (2.9·10<sup>-4</sup> M and 5.9 Zn/MT) (**Annex 7.1.11**). Probably, as speculated with NpeMT1, NpeMT2 is structured in two domains forming two Zn(II)<sub>3</sub>(S<sub>Cys</sub>)<sub>9</sub> clusters. These speculations are backed on the results obtained from the characterisation of β3NpeMT2, which show that the fragment yields an almost unique Zn<sub>3</sub>-β3NpeMT2 species (**Figure 3.36C**), meaning that this domain is able to perform a Zn(II)<sub>3</sub>(S<sub>Cys</sub>)<sub>9</sub> cluster independently and suggesting that the other β domain forms an equivalent cluster. The Zn(II) coordination geometry is the classical tetrahedral, as denoted by the broad Gaussian band centred at *ca.* 235 nm, usually seen in Zn-(S<sub>Cys</sub>)<sub>4</sub> chromophores

(Figure 3.36F). In this case, as happens with NpeMT1, the incidence of glycosylated species is almost negligible, denoting higher stability in their Zn-MT complexes with respect to the other proteins described in this section.

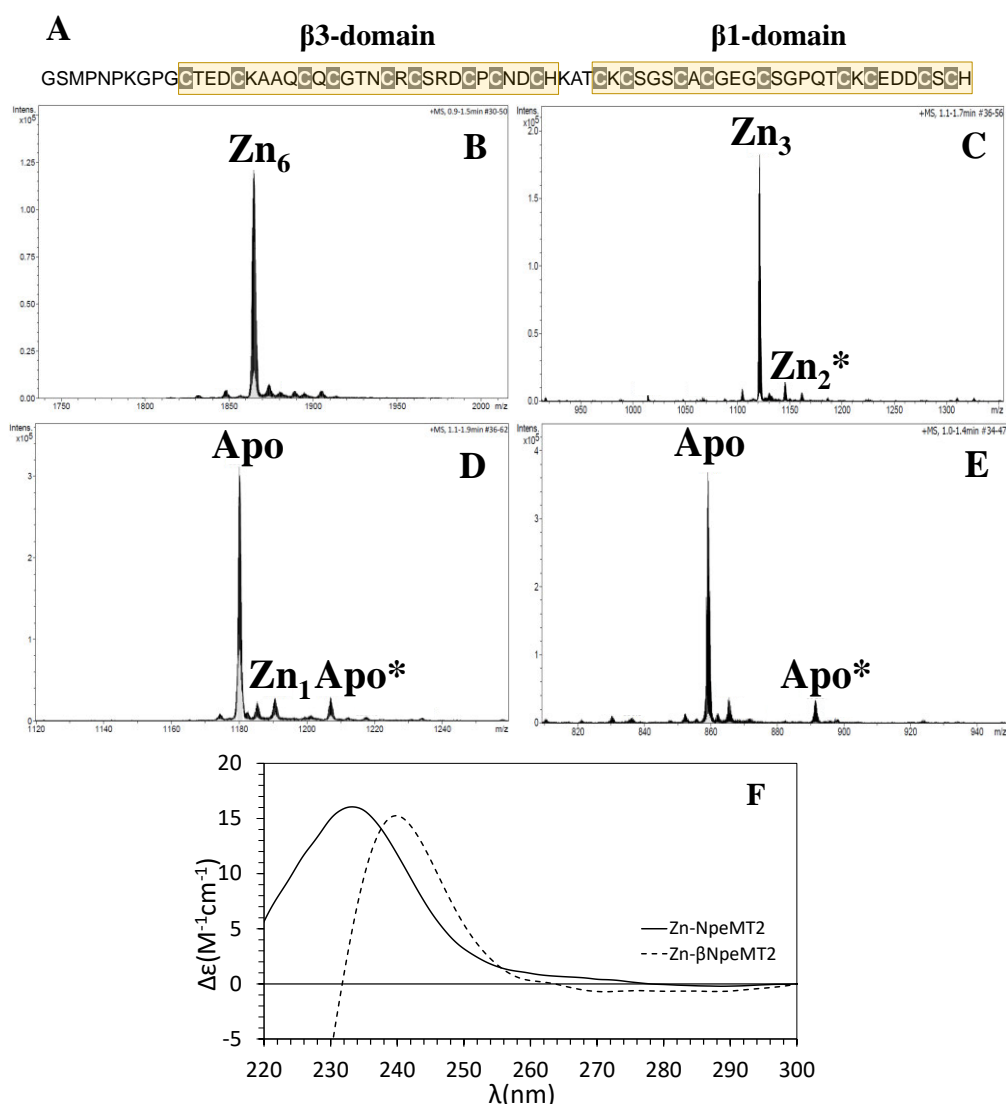


**Figure 3.36.** (A) Architecture of NpeMT2 amino acid sequence, Cys residues are shadowed, and yellow boxes highlight the two 9-Cys ( $\beta$ -domain) motifs of the sequence. ESI-MS spectra at pH 7.0 of (B) Zn-NpeMT2 ( $Q^+ = +4$ ) and (C) Zn- $\beta$ 3NpeMT2 ( $Q^+ = +4$ ) productions. ESI-MS spectra at pH 2.4 of (D) Zn-NpeMT2 ( $Q^+ = +6$ ) and (E) Zn- $\beta$ 3NpeMT2 ( $Q^+ = +5$ ) productions. Glycosylated species are signalled with an asterisk (\*). (F) CD envelopes of Zn-NpeMT2 (solid line), and Zn- $\beta$ 3NpeMT2 (dashed line) productions.

As its homologue, NpeMT2 renders a unique  $Cd_6$ -NpeMT2 complex when purified from the *E. coli* cultures supplemented with Cd(II) (Figure 3.37A). The stoichiometry is corroborated by ICP-AES, as usual ( $1.4 \cdot 10^{-4}$  M and 5.5 Cd/MT) (Annex 7.1.11). Additionally, it is demonstrated that the  $\beta$ 3NpeMT2 fragment builds stable three metal clusters by itself (Figure 3.37B). Certainly, NpeMT2 exhibits an unusual CD envelope, as it represents a simple Gaussian band centred

at *ca.* 250 nm, typical absorption band of Cd-(S<sub>Cys</sub>)<sub>4</sub> chromophores, with some extra optical activity at wavelengths lower than 240 nm (**Figure 3.37E**). In contrast, the  $\beta$ 3 fragment's CD spectra exhibits an interesting envelope. It shows a classical *exciton coupling* centred at *ca.* 250 nm that is modified with a shoulder at *ca.* 245 nm. This shoulder has been previously reported as arising from an interaction between His residues and the Cd(II) ions of the cluster [186]. This interaction is clear in this simplified mono-domain system but it could explain some features of NpeMT2's CD envelope and its whole bidomain system, suggesting that maybe His could participate in the coordination of the Cd(II) ions. However, this interesting topic deviates from our main goal and we did not study it in depth. In the future, we believe that this case should be analysed since it might contribute to understand better the role of His residues in the metal cluster formation. Overall, these results are those of a protein with Zn-thionein features. However, all biochemical traits should be considered before taking any conclusions.

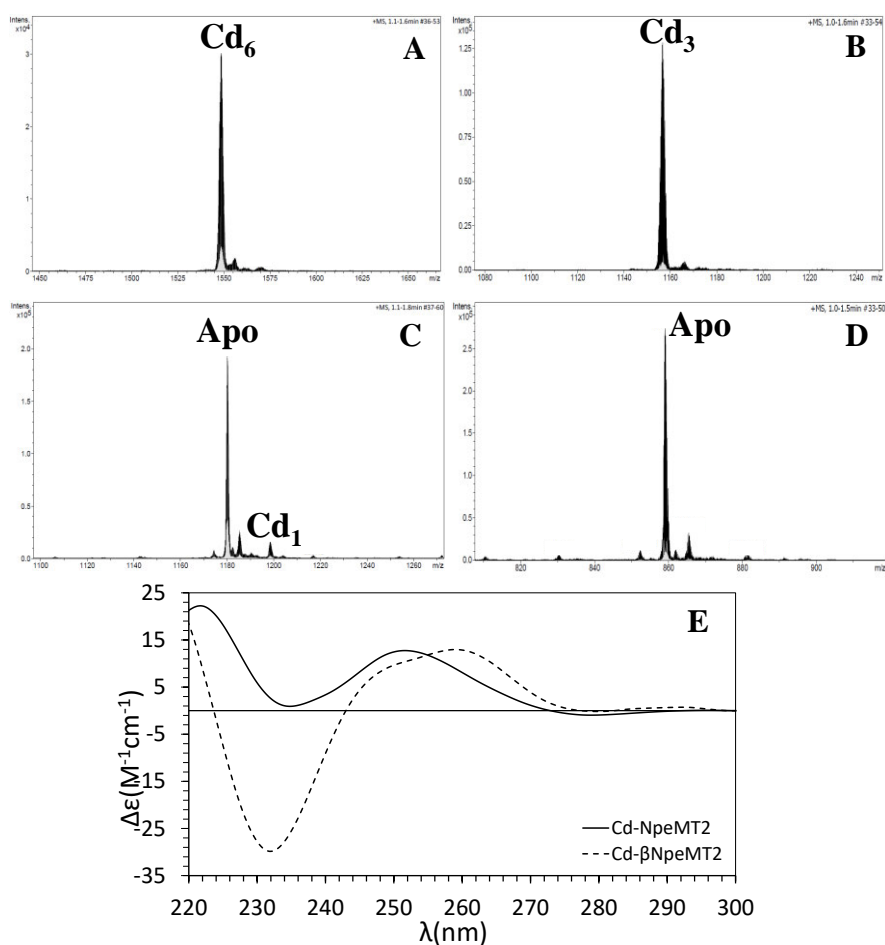


**Figure 3.37.** ESI-MS spectra at pH 7.0 of (A) Cd-NpeMT2 ( $Q^+ = +5$ ) and (B) Cd- $\beta$ 3NpeMT2 ( $Q^+ = +4$ ) productions. ESI-MS spectra at pH 2.4 of (C) Cd-NpeMT2 ( $Q^+ = +6$ ) and (D) Cd- $\beta$ 3NpeMT2 ( $Q^+ = +5$ ) productions. (E) CD envelopes of Cd-NpeMT2 (solid line), and Cd- $\beta$ 3NpeMT2 (dashed line) productions.

NpeMTs differ in their Cu(I)-binding abilities. While NpeMT1 renders heterometallic Zn,Cu-MT complexes when synthesised in Cu(II) surplus (Section 3.3.2), NpeMT2 yields mixtures of homometallic Cu-MT complexes (Figure 3.38A and Annex 7.1.11). Certainly, the sample obtained from the production enriched with Cu(II) still shows high degree of heterogeneity in the speciation, showing species ranging from  $\text{Cu}_8^-$  to  $\text{Cu}_{14}$ -NpeMT2. Equal is the case of  $\beta 3$ NpeMT2, that renders a mixture of homometallic species as the full protein (Figure 3.38B and Annex 7.1.11). Moreover, the synthesis of Cu- $\beta 3$ NpeMT2 produced two families of complexes that were separated by FPLC and characterised independently (Annex 7.1.11). The appearance of two families of complexes already denotes high heterogeneity in the sample. The first of the two peaks shows that one family yields dimers and even trimers of Cu-MT complexes, suggesting that the fragment struggles to form complexes by itself and has to pair with other peptides. The second peak exhibits glycosylated species, as occurs in NpeMT2, and denotes flexibility of the polypeptide chain that is not stabilized by an adequate metal cluster (see Section 3.5), as proved by the mixture of complexes present in the sample.

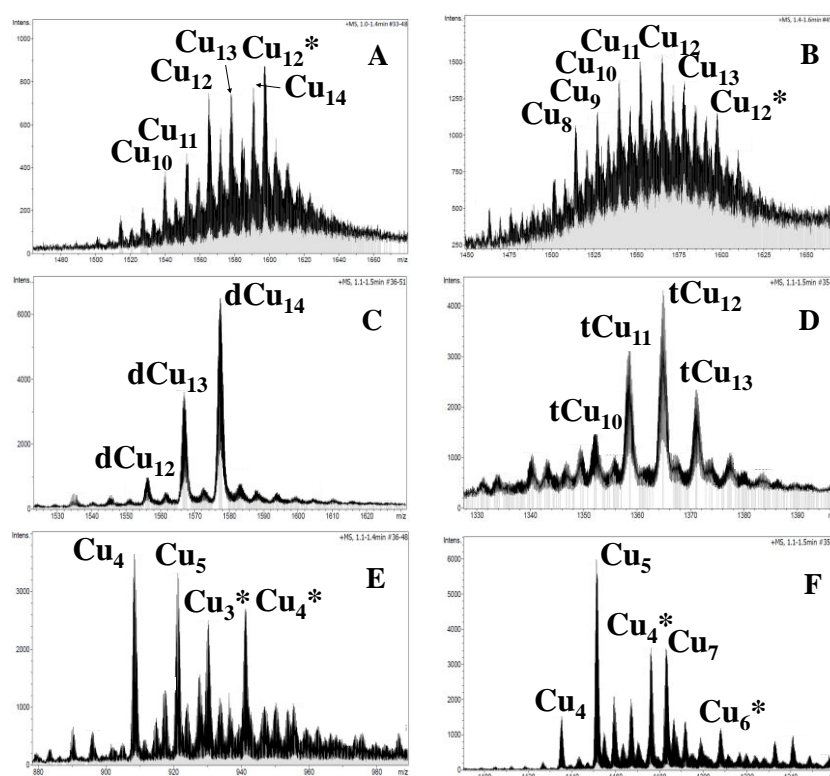


**Figure 3.38.** ESI-MS spectra at pH 7.0 of (A) Cu-NpeMT2 ( $Q^+ = +5$ ), (C) Cu- $\beta 3$ NpeMT2 (first FPLC peak) ( $Q^+ = +5$ ) and (E) Cu- $\beta 3$ NpeMT2 (second FPLC peak) ( $Q^+ = +5$ ) productions. ESI-MS spectra at pH 2.4 of (B) Cu-NpeMT2 ( $Q^+ = +5$ ), (D) Cu- $\beta 3$ NpeMT2 (first FPLC peak) ( $Q^+ = +6$ ) and (F) Cu- $\beta 3$ NpeMT2 (second FPLC peak) ( $Q^+ = +4$ ) productions. Glycosylated species are signalled with an asterisk (\*), dimers with a (d-) and trimers with a (t-).

These results clearly show that none of the NpeMTs is a genuine Cu-thionein, however, NpeMT2 exhibits more of this behaviour (or less of a Zn-thionein) than NpeMT1. In fact, and this is the reason why NpeMT2 has been included in this section, NpeMT2 behaves as the rest of the proteins presented in this section when binding Cu(I), while NpeMT1 behaves as the rest of Zn-thioneins. This unique difference between both proteins have been an inflexion point to separate two proteins that share traits of a genuine Zn-thionein and to propose a new concept to classify MTs: a genuine Cd-thionein behaviour (**Annex 7.3.7: Article 7**).

#### 3.4.4. Study of *Oikopleura dioica* MT system

The study of zooplankton *Oikopleura dioica*'s MT system entailed a prime contact with MTs in urochordates. Two metallothioneins are expressed by *O. dioica*: OdiMT1, a 72 amino acid MT (equivalent to a mammal MT) and OdiMT2, a 399 amino acid MT, one of the longest MT reported to date. The genetical studies performed on these MTs revealed that OdiMT2 is formed by six consecutive sequences that each one conserve the Cys pattern of OdiMT1. In turn, OdiMT1 seems to have suffered several evolutionary events that brought it to become a bidomain MT composed by a 12C domain and a truncated 12C domain (t12C) (see **Section 3.1.2**). This section, then, exposes and discusses the results that support these genetic conclusions by characterising the metal-binding abilities of the OdiMT1 fragments and, of course, exposes the biochemical features of the whole sequence of OdiMT1 and OdiMT2.

The characterisation of OdiMT1 fragments (**Table 3.1**) revealed that the particular modular structure of the protein firstly proposed as two C7 motifs (see **Section 3.1.2**) was, in fact, more complex than expected. The C-terminal fragment of OdiMT1, comprising from aa 31 to 72, is composed by a C7 motif plus a carboxyl-end with four Cys (7C+4C), while the N-terminal fragment (from aa 1 to 30) contains a C7 motif and an amino-end with two Cys (7C+2C). While the C-terminal displays an autonomous stable metal cluster, yielding unique  $M(II)_4$ -MT complexes, the N-terminal, renders  $Zn(II)_3$ - and  $Cd(II)_4$ -MT complexes as major species (**Annex 7.2.3: Sheet 7.2.3.1**). Moreover, the samples of the latter fragment show high heterogeneity in the degree of speciation and the presence of sulphide labile ions, which suggest that this fragment struggles to form a unique energetically favoured metal-cluster by itself. Probably, the C-terminal fragment is an independent domain and N-terminal needs of the C-terminal domain to be stabilised. Moreover, the sequence alignment of OdiMT1, OdiMT2 and other *Oikopleura* species' MTs showed that the N-terminal domain of OdiMT1 is

truncated, missing some Cys that would complete a protein with two domains with equivalent Cys motifs, as *O. vanhoeffeni* or *O. albicans* MTs. For that reason, we concluded that the prototypical domain of *Oikopleuras* MTs is formed by 12 conserved Cys arranged in specific motifs, which in the case of OdiMT1, its N-terminal domain is truncated, missing three Cys, and, in its C-terminal domain, it has been a replacement of a Cys to a Ser (more information about these fragments in **Annex 7.3.5: Article 5**).

**Table 3.1.** Design of the constructs synthesised from OdiMT1 and OdiMT2. Coloured boxes represent the initially stated 7C conserved motifs, while OdiMT1 fragments represent the actual 12C conserved motifs.

Structure	Construct name	Number of aa <sup>a</sup>	Cys content	Major metal-protein species <sup>b</sup>
	OdiMT1	74 aa	20 CYS	Cd <sub>7</sub> /Zn <sub>7</sub> /Cu <sub>12</sub>
	t12C	32 aa	9 CYS	Cd <sub>4</sub> /Zn <sub>3</sub> /nd
	12C	44 aa	11 CYS	Cd <sub>4</sub> /Zn <sub>4</sub> /Cu <sub>9</sub>
	OdiMT2	399 aa	123 CYS	nd/nd/nd
	OdiMT2.1	203 aa	63 CYS	nd/Cd <sub>22</sub> /nd
	OdiMT2.2	199 aa	62 CYS	Zn <sub>20</sub> /Cd <sub>22</sub> /nd

<sup>a</sup> These numbers consider the artificially included amino acid residues GS from the recombinant production.

<sup>b</sup> nd stands for no data.

After consolidating that OdiMT1 is probably structured in two domains, a conserved 12C domain and a truncated 12C domain (t12C), its metal-binding features have been characterised. OdiMT1 (**Annex 7.1.12**) share the same results as most of the MTs presented in this section. The samples recovered from the Zn(II)-enriched *E. coli* cultures rendered from Zn<sub>5</sub>- to Zn<sub>7</sub>-OdiMT1 complexes, being seven Zn(II) ions per protein the most abundant stoichiometry detected by ESI-MS (**Figure 3.39A**) and confirmed by ICP-AES (6.5 Zn/MT) (**Annex 7.1.12**). From this data, it is evident that OdiMT1 do not show a Zn-thionein behaviour. However, the



numbers obtained in the whole protein coincide with the results of its fragments ( $Zn_3$ -tC12 plus  $Zn_4$ -12C =  $Zn_7$ -OdiMT1), which supports the idea of a bidomain MT and the contribution to the metal binding of the respective domains. This idea was evidenced by the results obtained from the forms purified from the Cd(II)-supplemented cultures, which rendered unique well-structured  $Cd_7$ -OdiMT1 complexes (Figure 3.39B). The metal-cluster stabilization is corroborated by the CD spectra, which displays a nice and intense *exciton coupling* centred at *ca.* 240 nm (Figure 3.39D), denoting high robustness and compactness of the Cd-(S<sub>Cys</sub>) chromophores. The discrimination in the metal-preference of OdiMT1 between divalent metal ions is observed in others MTs presented in this section and it is one of the keystones of this thesis.

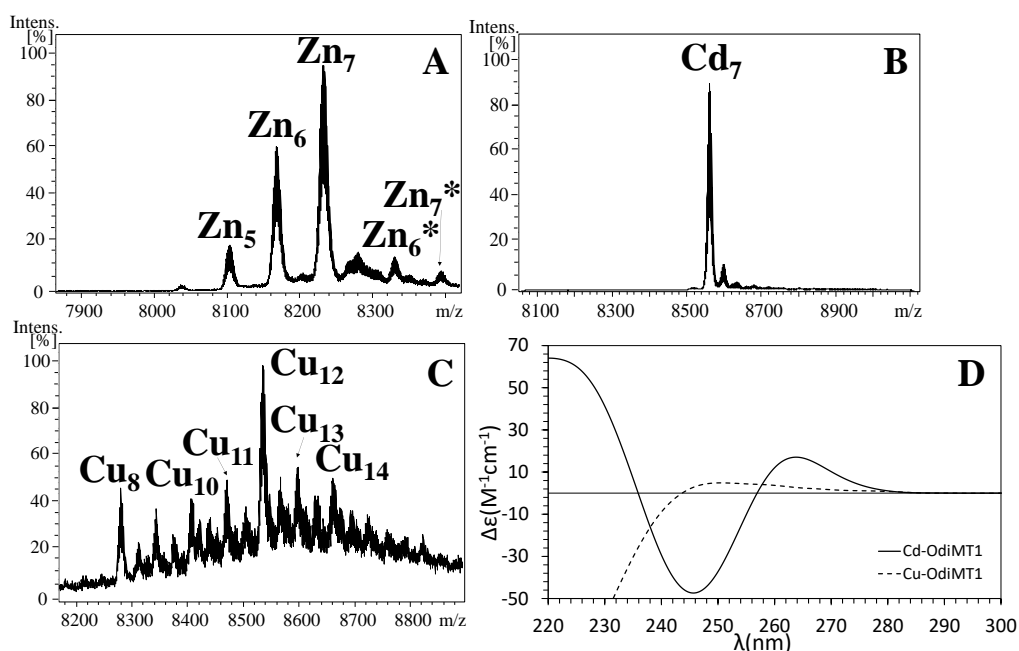


**Figure 3.39.** Deconvoluted ESI-MS spectra at pH 7.0 of (A) Zn-OdiMT1, (B) Cd-OdiMT1 and (C) Cu-OdiMT1 productions. Glycosylated species are signalled with an asterisk (\*). (D) CD envelopes of Cd-OdiMT1 (solid line), and Cu-OdiMT1 (dashed line) productions.

The mixture of species obtained from the samples purified from the cultures with Cu(II) surplus confirmed the Cd-selectivity of OdiMT1 (Figure 3.39C). The synthesis of the MT was performed twice at normal aeration conditions and once under low-aeration conditions. However, only was detected on one peak of one of the productions run at normal aeration conditions (Annex 7.1.12), which denote the difficulty of obtaining a valid complex of Cu(I) with this isoform. The values obtained from CD denote the low profile of structuration of these complexes (Figure 3.39D). It is worth to be mentioned that the species rendered by OdiMT1

were homometallic, as the rest of MTs of this section, which contrast with the usual heterometallic forms obtained by genuine Zn-thioneins.

It is interesting to understand OdiMT1's biochemical features before characterising OdiMT2, since, as mentioned, OdiMT2 is a multi-modular MT constructed by OdiMT1-like-units repeated in tandem. Thus, it is expectable that OdiMT2 reproduces OdiMT1's metal-binding behaviour and enlarges its metal binding capacity as many times as repeated units form OdiMT2 (*i.e.*, 6 times). Unluckily, the massive dimensions of this MT hindered the synthesis and obtention of valid samples to be characterised (**Annex 7.1.13**). However, it was possible to extract some valuable hints that allowed us to characterise this enormous protein. First, it was remarkable that for the three metals used in the production of OdiMT2, only Cd(II)-enriched cultures allowed the recovery of reasonable samples. In fact, only Cd-OdiMT2 samples provided any results, since both Zn-OdiMT2 and Cu-OdiMT2 complexes were under the limit of detection for ESI-MS and ICP-AES (**Annex 7.1.13**). From the Cd-OdiMT2 complexes we observed that the stoichiometry found by ICP-AES (from 40.4 Cd/MT to 55.3 Cd/MT) was about 5-6 times the stoichiometry detected from the Cd-OdiMT1 samples (**Figure 3.39B** and **Annex 7.1.12**). Additionally, some metallated species were detected by ESI-MS, although the unique concluding species detected was the apo form, confirming that OdiMT2 was synthesised (**Figure 3.40A**).

In addition to the results obtained from the entire protein, two fragments based on the N-terminal and the C-terminal half of OdiMT2 were designed and characterised: OdiMT2.1 and OdiMT2.2 (**Table 3.1**). Both fragments contain three OdiMT1-like-units (RU). The individual characterisation of these constructs added information about the biochemical features of the whole system, considering the difficulties of characterising the enormous OdiMT2. The recombinant synthesis of both OdiMT2.1 and OdiMT2.2 in Zn(II)- and Cd(II)-enriched *E. coli* cultures rendered equivalent species (**Figure 3.40**), showing a nice symmetry between the two halves of OdiMT2 and suggesting that this is a modular system in which each module (*i.e.*, RU) is independent from the other. From one side, OdiMT2.1 and OdiMT2.2 render a mixture of Zn-MT complexes, where the stoichiometry range goes from Zn<sub>16</sub> to Zn<sub>25</sub> (**Figure 3.40B** and C). These numbers are interesting since OdiMT1 binds up to seven divalent metal ions and these OdiMT2 constructs contain three OdiMT1-like-units. Therefore, it is consistent that three repeat units (RU) binding 7 M(II) render 21 M(II)-species.

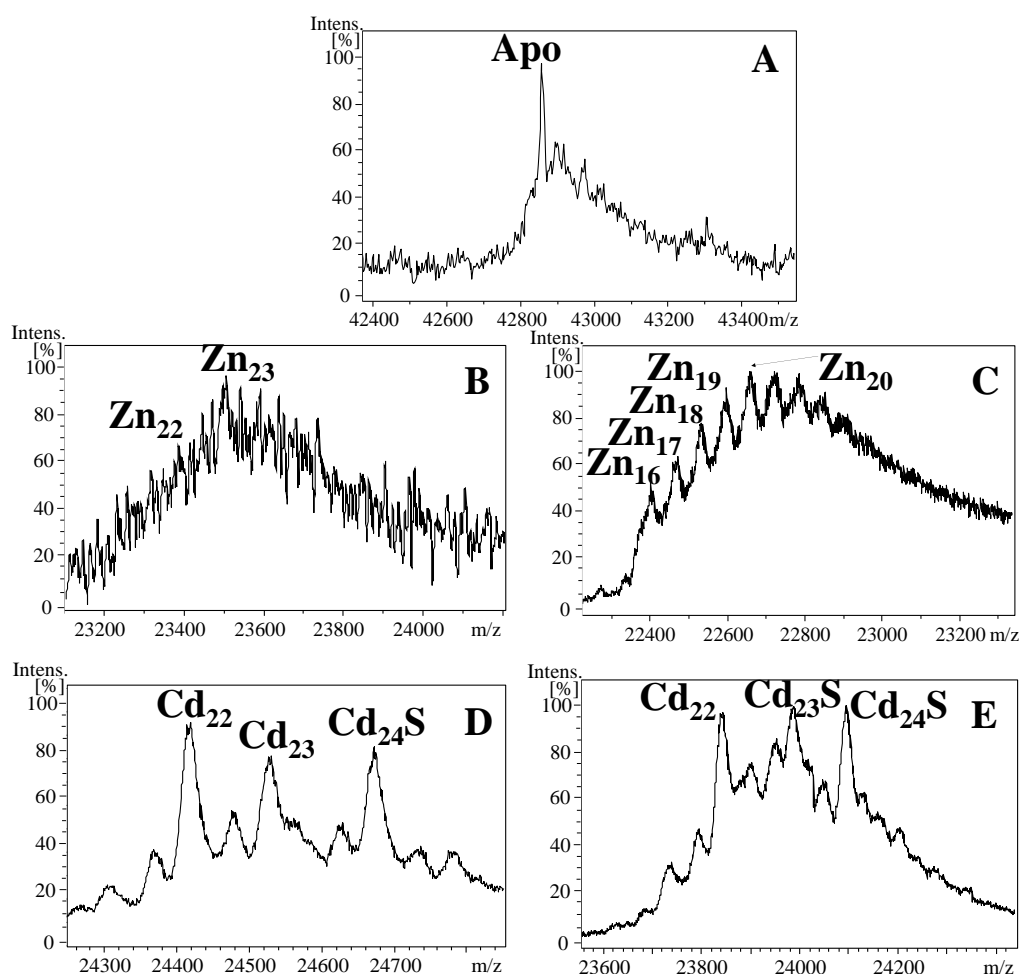


**Figure 3.40.** Deconvoluted ESI-MS spectra at pH 2.4 of (A) Cd-OdiMT2 production. Deconvoluted ESI-MS spectra at pH 7.0 of (B) Zn-OdiMT2.1, (C) Zn-OdiMT2.2, (D) Cd-OdiMT2.1 and (E) Cd-OdiMT2.2 productions.

Similarly, both OdiMT2 constructs yield major Cd<sub>22</sub>- and Cd<sub>24</sub>S-MT complexes, although Cd<sub>23</sub>- and Cd<sub>23</sub>S-MT are important species too (Figure 3.40D and E). As mentioned, these artefactual Cd<sub>x</sub>-S<sup>2-</sup>-MT complexes are produced as a consequence of the recombinant synthesis of an artificial MT design. The most plausible explanation of these Cd<sub>x</sub>-S<sup>2-</sup>-MT complexes is that the large size of the constructs allow the incorporation of additional ions present in the intracellular medium of the cell such as S<sup>2-</sup> ions, whose acidic properties provides them with high affinity to coordinate metals, interacting with the formed clusters and integrating extra Cd(II) ions. The fact that there are some outlined species in the ESI-MS spectra of the Cd-OdiMT2.1/2.2 samples suggests that these species are more favoured than the rest, contrasting with the ESI-MS spectra of the Zn-samples in which any species stands out among the rest. Probably this is a hint about the Cd-specific abilities of OdiMT2 provided by the nature of its individual RU, that is similar to OdiMT1's. Also, the compartmentalisation of OdiMT2 is evidenced once more in terms of

numbers, since the fragments bind about the 21 divalent metal ions expected from three RU in which each RU binds seven M(II). This idea is reinforced by the ESI-MS spectra at pH 2.4, which display (a part of Apo species) metal-species loaded with multiples of four M(II) ions (**Figure 3.41**). These species are detected for both Zn(II) and Cd(II) metals and resemble to those observed in OdiMT1 C-terminal fragment, corresponding to the C12 motif. It seems that the C12 motif is more reluctant to release its coordinated metal ions than the other (tC12 motif), which in turn, is compatible with the aforementioned postulation that tC12 is less autonomous than C12 and needs of the latter to ensemble in a stable complex. Additionally, OdiMT2's large size and folding would protect some of the inner metal clusters from the external acidic medium and this could explain that the reluctance to exchange some metal ions by protons is detected only for OdiMT2 and not for OdiMT1.

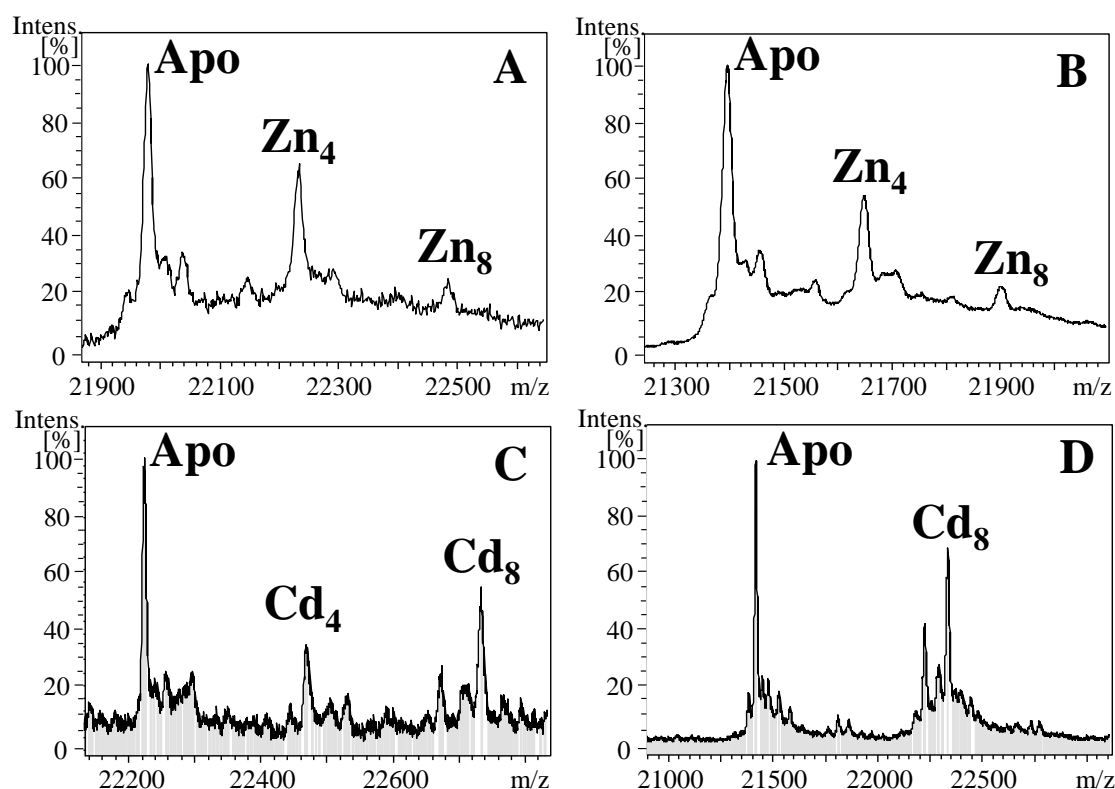


**Figure 3.41.** Deconvoluted ESI-MS spectra at pH 2.4 of (A) Zn-OdiMT2.1, (B) Zn-OdiMT2.2, (C) Cd-OdiMT2.1 and (D) Cd-OdiMT2.2 productions.

In conclusion, OdiMT1 shows high metal-selectivity towards Cd(II) ions as demonstrated by the results obtained by ESI-MS. The study of the fragments of OdiMT1 allowed to understand the nature of the structure of the MT, learning that is probably a bimodular protein in which there is a core domain that binds four M(II) ions and a dependent domain that contributes with the union of three extra

M(II) ions. Interestingly, the results obtained from OdiMT1 are concordant with those obtained from OdiMT2. OdiMT2 is the longest MT reported to date and it is constructed by the repetition of units whose sequence is well-conserved to OdiMT1. Concordantly, OdiMT2's metal binding abilities are those of an agglomeration of individual OdiMT1-like-units. Its large size hindered its characterisation but the design of smaller fragments that separated the protein in two pieces, allowed its characterisation.

#### 3.4.5. Study of some ascidian MTs: *Ciona robusta*, *Hallocynthia roretzi* and *Botryllus schlosseri* MT systems

After introducing tunicates MTs with the characterisation of *Oikopleura dioica* MTs, we explored other tunicate MTs from other classes such as Ascidiacea and Thaliacea. The prototypical mono-modular structure of ascidian MTs (CroMT1, HroMTs and BscMT1 fragment, BscMT1R4) shows high similarities with the 12C domain of OdiMT1 and to the  $\alpha$  domain of vertebrate MTs in terms of metal-binding capacity (**Annex 7.3.6: Article 6**). All these peptides render unique  $M(II)_4$ -MT complexes, displaying equivalent ESI-MS results (**Figure 3.42**). Additionally, the perfect *exciton coupling* centred at *ca.* 250 nm yielded for all Cd-MT complexes denote equal  $Cd-(S_{Cys})$  chromophores and compact  $Cd_4(S_{Cys})_{12}$  clusters for all ascidian MTs, even for the enormous BscMT1 (**Figure 3.42E**). However, CroMT1 display some divergences when binding Zn(II) ions and, although  $Zn_4$ -CroMT1 is the predominant species, the glycosylated species detected in the sample contrast with the unique  $Zn_4$ -MT complexes found for HroMTs and BscMT1R4 (**Annex 7.2.3: Sheet 7.2.3.2**). This divergence denotes certain instability of CroMT1 when binding Zn(II), since the flexibility of the MT without a compact metal cluster makes it more accessible for the glycosylation machinery (**Section 3.5**). This phenomenon is also present in the samples of all ascidian MTs recovered from the Cu(II)-enriched cultures, in this case, with higher intensity. The high degree of speciation found for all the MTs (and BscMT1R4 module) and the important presence of glycosylated species, suggest a poor Cu-thionein behaviour from ascidian MTs. However, it is important to mention that the species rendered are homometallic Cu-species (**Annex 7.2.3: Sheet 7.2.3.2**), which differ to the heterometallic Zn,Cu-MT complexes yielded by genuine Zn-thioneins. With these results, it can be stated that ascidian MTs are mostly Cd-selective MTs that render single well-folded  $Cd_4$ -MT complexes.

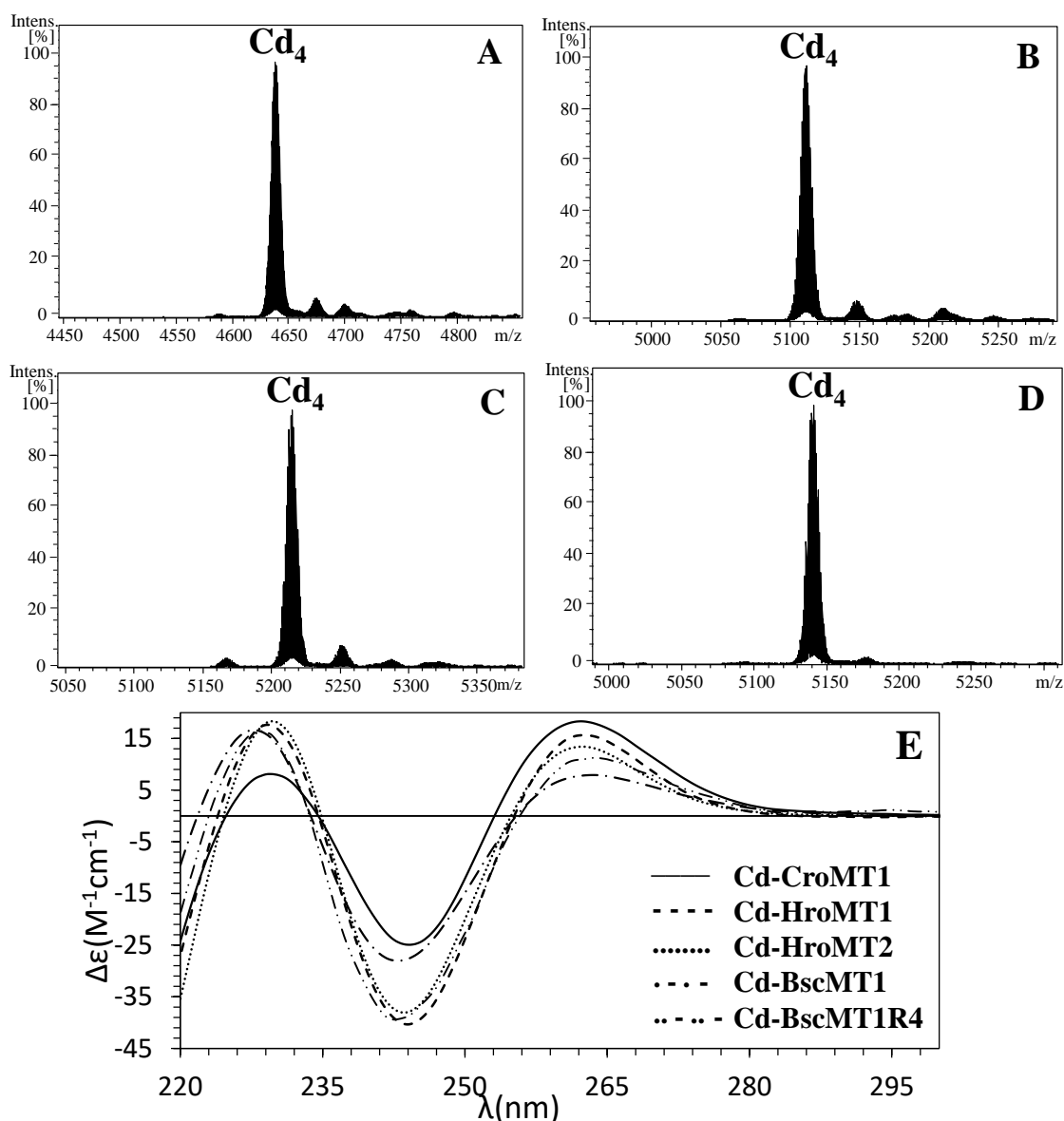


**Figure 3.42.** Deconvoluted ESI-MS spectra at pH 7.0 of (A) CroMT1, (B) HroMT1, (C) HroMT2 and (D) BscMT1R4 Cd-productions. (E) CD envelopes of the products recovered from the Cd-supplemented cultures of CroMT1, HroMT1, HroMT2, BscMT1 and BscMT1R4.

With regards to the compartmentation of BscMT1, the characterisation of BscMT1R4 has been of great use to understand it. BscMT1, as OdiMT2, is a massive MT and its complete process of synthesis, purification and characterisation has been difficult to achieve. Luckily, BscMT1's biochemical features have been described by gathering partial results of its characterisation and completing these results with fragment BscMT1R4 characterisation. Considering that BscMT1R4 renders unique  $\text{M(II)}_4$ -MT complexes and that  $\text{Zn}_{36}$ -BscMT1 species have been detected by ESI-MS (**Figure 3.43**), it can be stated that BscMT1 is a multi-modular protein structured in nine conserved units of 12C motifs. As mentioned before, the CD envelope of both the whole protein and its fragment binding Cd(II) are equal, confirming that the metal clusters of all nine modules in BscMT1 are equally

structured. This equivalence in the metal-binding behaviour and the fact that the sequences of the modules are highly conserved also supports the idea that the behaviour found in BscMT1R4 can be extrapolated to the rest of modules.

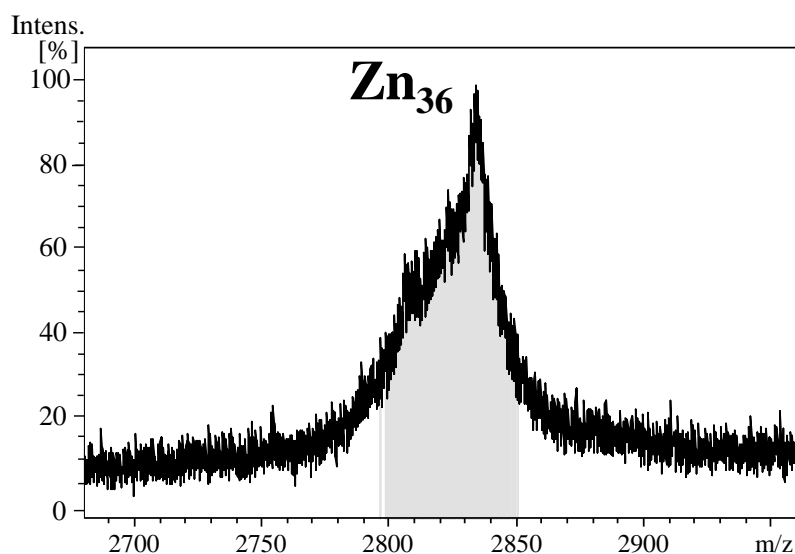
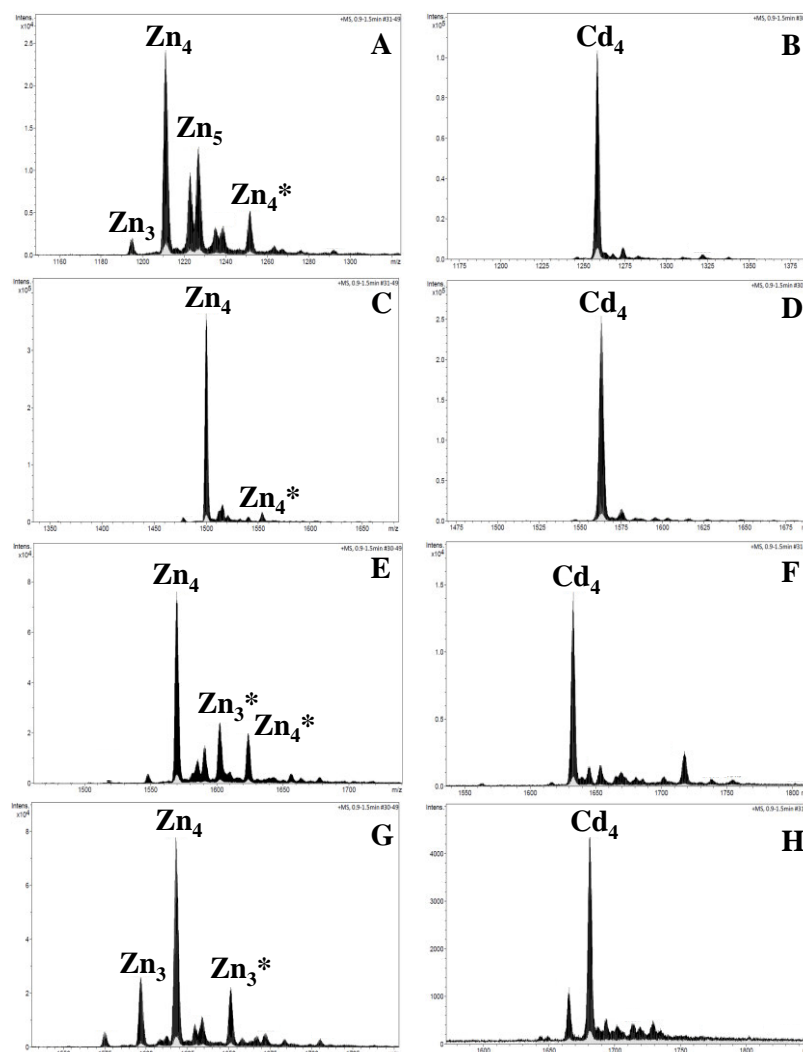


Figure 3.43. ESI-MS spectrum at pH 7.0 and +14 charge state of Zn-BscMT1 production.

In conclusion, ascidian MTs possess a conserved 12C motif that share metal-binding features with other chordate MTs and render mostly unique  $M(II)_4$ -MT complexes. Even the difficulties of synthesising and characterising a large MT, the biochemical features of BscMT1 have been determined through the evidence found from other ascidian MTs and its BscMT1R4 fragment.

#### 3.4.6. Study of *Salpa thompsoni* MT system

The third and last class of urochordate studied is Thaliacea. These filtering organisms share physiological and ecological traits with the other tunicates. The SthMTs samples produced in Zn(II)-enriched cultures show some variations in their speciation between them. All SthMTs rendered major Zn<sub>4</sub>-MT complexes but only in SthMT2 this species is unique (Figure 3.44). The rest of MTs show other metallated-species, even glycosylated species, denoting that the stabilisation of the peptides about the Zn-clusters is highly flexible and permits more than a unique energetically favoured form. On the other hand, when SthMTs are bound to Cd(II), only Cd<sub>4</sub>-MT complexes are detected (Figure 3.44).



**Figure 3.44.** ESI-MS spectra at pH 7.0 of the products recovered from the Zn(II)-supplemented cultures of (A) SthMT1 ( $Q^+ = +4$ ), (C) SthMT2 ( $Q^+ = +3$ ), (E) SthMT3 ( $Q^+ = +3$ ) and (G) SthMT4 ( $Q^+ = +3$ ) and the products recovered from the Cd(II)-supplemented cultures of (B) SthMT1 ( $Q^+ = +4$ ), (D) SthMT2 ( $Q^+ = +3$ ), (F) SthMT3 ( $Q^+ = +3$ ) and (H) SthMT4 ( $Q^+ = +3$ ).

These results are concordant to those of other MTs with 12 Cys (such as ascidian MTs) or other 12 Cys domains (such as mammalian and invertebrate  $\alpha$  domain), which all of them bind four M(II) ions [32]. This behaviour denotes that SthMTs possess strong Cd-selectivity rather than Zn-thionein features. Additionally, the species rendered by SthMT1 and SthMT3 when synthesised in Cu(II)-supplemented cultures, the only isoforms that yielded valid samples, are homometallic Cu-species (**Annex 7.1.18** and **7.1.20**), contrarily to the expected heterometallic Zn,Cu-species that yield genuine Zn-thioneins. These results reinforce the idea that SthMTs, as all the tunicate MTs studied, display a high metal-preference towards Cd(II).

Overall, the sequence features of urochordates converge in the fact that all of them are built around a conserved 12C domain. Additionally, this domain exhibits



high selectivity towards Cd(II) ions, which seems to be a common trait for those marine animals [54, 78, 148]. This supports the idea that Cd(II) concentration in those organisms' habitats was an important factor that drove MTs evolution.

#### 3.4.7. Common traits in the described Cd-thioneins

The variety and abundance of the MTs presented in this section permits to state with high robustness some of the common traits that these proteins display. The first characteristic, and logical, trait is that all the MTs render unique Cd-MT complexes with marked *exciton coupling* effects in the CD envelopes at the expected wavelengths. These results denote that the MTs build compact and well-structured Cd(II) clusters, being the most and unique favourable energetic conformation of these proteins. Secondly, all putative Cd-thioneins show glycosylation when are produced in Zn(II)- or Cu(II)-enriched culture medium, some of these glycosylated species are produced in great measure (*e.g.*, LgiMTs, OdiMT1, NpoMT1, etc...). This phenomenon will be discussed in the following section; however, it is remarkable its appearance in the MTs described here. Thirdly, and another critical point to be discussed, all the Cd-thioneins render homometallic Cu(I)-MT complexes. This feature diverges from the heterometallic Zn,Cu-MT complexes yielded by genuine Zn-thioneins and, for that reason, it becomes a necessary checkpoint to distinguish between Zn-thioneins and the proposed Cd-thioneins. Surely, these common traits found in putative Cd-thioneins differ to the common traits found in genuine Zn-thioneins and as discussed in **Section 3.6**, they are critical to the new proposal of classification of MTs.

### 3.5. Glycosylation: The Zn<sub>2</sub>S enigma

After all these years, our group has characterised the MT systems of a great number of organisms, compiling their biochemical features [6]. To obtain a pure and concentrated sample that reproduces the natural MT system, the proteins are synthesised by means of the well-accepted reliable recombinant protein expression in *Escherichia coli* [33]. In general, the study of MTs is based on the recombinant production of the putative MTs using *E. coli* BL21(DE3) as a vector [32]. After that, the protein is purified and characterised. Additionally, this methodology allows the *in vivo* replication of the three-dimensional structures yielded by the MTs, a handy tool considering that the same MT sequence may exhibit polymorphism in its structure depending on the coordinating metal [2], displaying distinct conformations. By supplementing the *E. coli* cultures with Zn(II), Cd(II) or Cu(II), the native metal-MT complexes are recovered. After that, their three-dimensional

structure and metal-binding abilities towards essential (such as Zn or Cu) or toxic transition metals (as Cd) are characterised. One of the most powerful characterisation methods is ESI-MS [14]. The mild ionizing conditions of the instrument permit the detection of metallated proteins (holo form) [239]. Normally, the functional native metal-MT species are identified at physiological pH (*ca.* 7.0) and, complementarily, the demetallated protein (apo form) is observed at acidic pH (*ca.* 2.4) [240]. At acidic pH, the thiolate groups are protonated, releasing the bound metals and obtaining the signal of the bare protein. Through more than 30 years this group has devoted its research efforts to the study of MTs (see **Section 1.2**), always applying the same methodology. Thanks to these conditions, it has been possible to identify an intriguing peak that does not correspond to the expected MT mass and that, eventually, has been of use for this thesis.

### 3.5.1. Surveying an intriguing additional mass of 162 Da

During this thesis, we have managed plenty of ESI-MS spectra of MTs and we have realized that an important number of the MT productions exhibited, along with the expected MT mass, an unexpected additional mass. At first, this extra peak was detected at acidic pH and in proteins recovered from Zn(II)-supplemented productions. Applying maths, since there was no other metal combination that matched that additional mass, we considered for a long period that the most plausible option was an unusual resistant  $Zn_2S$  cluster (~160 Da). This formation is very uncanny, but it was proved that sulphide labile ligands aided in the stability of the metal clusters of those MTs loaded with non-cognate metal ions (**Section 3.2**). Besides, these species were precisely found in protein productions that rendered a mixture of metal-MT complexes and the presence of sulphide ligands was not a surprising fact.

The trigger that made us consider this an intriguing phenomenon was that in all the ESI-MS experiments performed at pH 2.4 (when all the metal is normally released) the separation between apo and the extra peak was always of 162 Da, independently of the MT studied. This was observed for almost all the MTs, no matter their molecular weight. Certainly, the first impression was that these peaks might be some residual metallated-MT species at pH 2.4. However, in those cases, pH was lowered till 1.0 to release the most resistant metal clusters. Despite this extreme pH, the additional mass was still detected, suggesting that these extra 162 Da corresponded to a moiety covalently bound to the protein. From that moment onwards we called this extra mass Apo', since it was an apo form that did not correspond to our MT of interest.

As mentioned, it was only detected in MT productions obtained under Zn(II)-surplus, although later it was found in those productions supplemented with Cu(II), as well. Extraordinarily, on one occasion, a production supplemented with Zn(II) did not show this peak but it did after repeating the production (**Figure 3.45**).

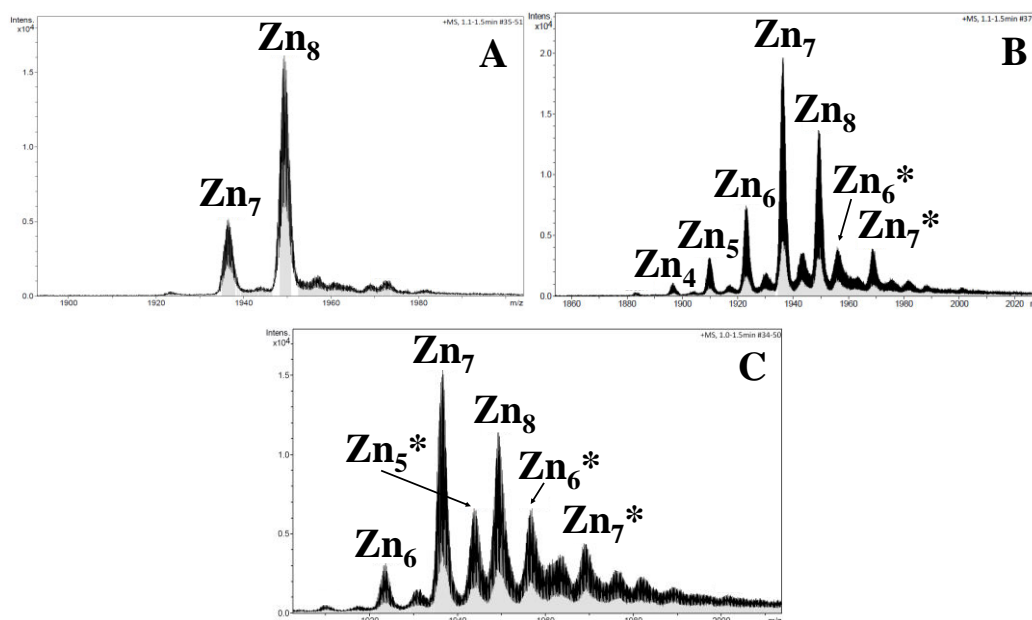


**Figure 3.45.** ESI-MS spectra measured at pH 7.0 of the Zn-PbrMT1 (A) first production ( $Q^+ = +5$ ), (B) second production ( $Q^+ = +5$ ) and (C) third production ( $Q^+ = +5$ ). Asterisks (\*) mark those metallated species built by Apo'. Only the first production did not show Apo' metallated species as an exceptional case.

Since this extra mass did not depict a metallated form of our MT, a cleavage error of the thrombin during the purification process was considered, adding extra amino acids to the MT. This hypothesis was discarded for two reasons: (1) the only possible amino acid whose molecular weight is close to 162 is tyrosine (163.2 Da once is bound to the protein, and a molecule of water released during the peptide bond formation). This amino acid is not included in the plasmid design of any of the MTs characterised, for this option was rejected. (2) Some of the ESI-MS spectra show extra apo' (*i.e.*, apo'', apo''',...), all of them separated by 162 Da between adjacent peaks (**Figure 3.46**). Thus, a certain mass of *ca.* 162 Da is being sequentially attached to the protein, which definitely discards an error during the cleavage, since there are no designs of consecutive tyrosine residues. Interestingly, numbers are concordant if this moiety is a carbohydrate, a hexose of empiric formula C<sub>6</sub>H<sub>12</sub>O<sub>6</sub> and 180.1 Da of molecular weight. When the hexose (180.1 Da) is attached to the protein, a water molecule (18 Da) is released, and the glycosylated MT final weight is increased in 162.1 Da.

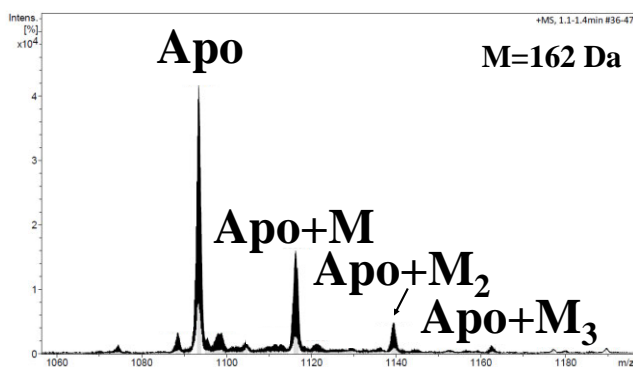


**Figure 3.46.** ESI-MS spectrum at pH 2.4 of Zn-LgiMT1 ( $Q^+ = +7$ ) production. It is observable that the highest peak corresponds to Apo and the successive peaks correspond to Apo with additional  $M=162$  Da.

### 3.5.2. Proposing glycosylation as a justification of the extra mass

Apparently, with this data on the table, the most plausible hypothesis about this extra mass is that the protein is being glycosylated. Glycosylation is one of the most common posttranslational modifications in proteins, which is known for the covalent union of a glycan to the lateral chain of an amino acid of a protein [241]. Despite that *E. coli* BL21(DE3) has been considered a reliable tool to synthesise recombinant proteins due to the minimal interference of the bacteria into the heterologous protein [242], in this chapter it is stated that this strain is able to glycosylate – and glycosylates – the MTs studied in this thesis.

Historically, glycosylation has been attributed to eukaryote realm, however, nowadays it is well accepted that this process occurs in archaea [243, 244] and bacteria [245, 246] as well. In fact, numerous cases report that exists glycosylation machinery and glycosylated proteins in bacteria [247], most of them related to pathogenic bacteria, which present glycosylated proteins on their surface to enhance their adherence to the host cell [248, 249]. At any rate, the findings in the data presented in this thesis will reconsider our current insights into the abilities to glycosylate of *E. coli* BL21(DE3).

### 3.5.3. Demonstrating that the MTs are glycosylated

The determinant experiment to elucidate whether we have sugar in the sample or not has been Enzyme-linked lectin assay (ELLA) experiments, which have been performed to detect if there are possible glycosylated proteins and which carbohydrates are attached. These experiments have been performed in collaboration with Pr. José Manuel Domínguez from Universidad de Granada. Proteins with a high specificity for sugars (lectins) are used in this procedure. In this case, tests were performed for galactose, mannose and fructose using PNA

(peanut agglutinin), ConA (Concavalin A) and UEA (*Ulex europaeus* agglutinin) to detect, respectively, those carbohydrates. A total of 19 MTs samples were blind-measured: six produced with Zn(II), five with Cd(II) and eight with Cu(I). Proteins produced in Zn(II) or Cu(II)-enriched medium tested positive for some of the carbohydrates (Table 3.2). In some cases, the concentration of protein was so low that carbohydrate was undetectable. However, some of the proteins did test positive and, therefore it was confirmed that the proteins are glycosylated. For that reason, from now on, Apo' and the metallic complexes formed by this modified protein will be named Apo\* or M<sub>x</sub>\*.

**Table 3.2.** Summary of the ELLA experiment results. Samples have been grouped by the metal supplemented in the synthesis. “X” marks the presence of any of the three hexoses studied in the sample.

Metal-binding Character	Metal Supplemented	Name	Mannose	Galactose	Fructose
Cd-th	Cd	alfaNpoMT1-Cd			
Zn-th	Cd	NpeMT1-Cd			
Cd-th	Cd	LgiMT2-Cd			
Zn-th	Cd	FcaMT1-Cd			
Cu-th	Cd	Mper1-Cd			
Cd-th	Cu	alfaNpoMT1-Cu			
Cd-th	Cu	gammaLgiMT2-Cu			
Zn-th	Cu	FcaMT1-Cu			
Zn-th	Cu	NpeMT1-Cu		X	
Cd-th	Cu	CroMT1-Cu			
Cu-th	Cu	CaCuMT-Cu	X	X	X
Cu-th	Cu	HpCuMT-Cu			
Cu-th	Cu	mMT3-Cu		X	
Cd-th	Zn	alfaNpoMT1-Zn	X	X	X
Cd-th	Zn	LgiMT2-Zn	X	X	X
Zn-th	Zn	FcaMT1-Zn		X	X
Zn-th	Zn	NpeMT1-Zn	X	X	X
Cu-th	Zn	mMT3-Zn			
Cu-th	Zn	Mper1-Zn		X	

As observed in Table 3.2, most of the positive cases come from the Zn-supplemented samples. Those samples, along with the Cd(II)-supplemented ones, are the most concentrated and, therefore, the detection of glycosylated species, if any, has been possible. These results demonstrate that Cd(II)-enriched cultures do not yield glycosylated species, while Zn(II)- and Cu(II)-supplemented cultures do, independently of the MTs' metal-binding abilities.

#### 3.5.4. Characterisation of *Escherichia coli* glycosylation

After ensuring that the additional mass found in the proteins is a hexose, it is convenient to learn about the glycosylation machinery of *E. coli* BL21, characterising its most important features (*i.e.*, type of substrate used, attachment process and substrate-MT bonding).

Clearly, the experimental conditions under which recombinant production occurs are key to explain how proteins are glycosylated. A simple experiment in which the only change is the supplemented carbohydrate of the bacterial cultures allows to learn the limitations of the glycosylation machinery with regards to the substrate. Therefore, the culture medium in which the bacteria grow has been changed, using a minimum medium with glycerol instead of the usual LB medium, which contains carbohydrates and amino acids. The results show no posttranslational changes or additions of any kind of carbohydrate (**Figure 3.47**). Glycerol, which contains three carbons, requires many more steps to be transformed to hexoses, as the ones detected in glycosylated proteins. This experiment demonstrates as well that glycosylation is a biological process that occurs during protein production and not a product of purification or any artefact of the techniques used during characterization. Additionally, the results demonstrate the inability of *E. coli* to glycosylate proteins when the substrate is glycerol.

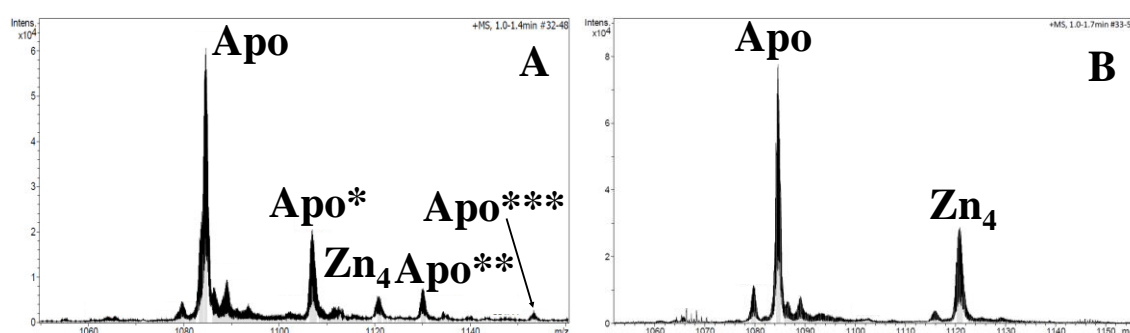


**Figure 3.47.** ESI-MS spectra measured at pH 2.4 of LgiMT2 produced in (A) LB culture supplemented with Zn(II) ( $Q^+ = +7$ ) and (B) in minimum media with glycerol supplemented with Zn(II) ( $Q^+ = +7$ ).

Returning to the spectrometric data, all the mass spectra exhibited the same pattern: Apo has a higher intensity than Apo\*, which in turn is more intense than Apo\*\* and so on (**Figure 3.46** and **3.47**). Although the intensities of the  $m/z$  values do not depend only on the concentration of the species, but also on the ionisation efficiency of the protein [250, 251], it can be considered that the most abundant species is the non-glycosylated species, the second most abundant is the mono-glycosylated, etc., since the relationship between intensities remains constant in different proteins with different properties. Having clarified that, it has to be highlighted that, in glycosylation, there are two ways for which carbohydrates can be bound to the protein: (1) *en bloc*, in which carbohydrates are first attached to a carrier lipid (LLO) and then transferred from the lipid to the peptide as a block [252] or (2) sequentially, in which the carbohydrate is directly bound to the protein

by successive additions of the monosaccharide, using the enzymes glycosyltransferases (GT) [253]. The fact that consecutive Apo\*, Apo\*\*, etc. species are detected, and that the mono-glycosylated species is more abundant than the di-glycosylated and so forth, makes the sequential addition the approach that best fits in our system. A block addition would cause the union of the same number of monomers in every case or, at least, the pattern of abundance of the species would vary between samples.

Another feature of glycosylation machinery to characterise is the type of bond that sugars form with the peptides. The two most common enzymatic pathways to bind carbohydrates into proteins are those that bind to asparagine (N) residues (N-linked glycosylation) and to serine (S) or threonine (T) residues (O-linked glycosylation) [254, 255]. To detect which kind of bond was occurring in our system, Zn-LgiMT2 was digested with trypsin (**Section 5.2.6**), that preferentially cleaves at the carboxy group of Lys and Arg [256]. Considering the biochemical features of trypsinisation, the following table shows the theoretical fragments obtained from this procedure:

**Table 3.3.** Theoretical products of trypsinisation. “Mass” column exposes the theoretical mass of the non-glycosylated form of the fragment, while “Mass\*” displays the molecular weights of the glycosylated forms of the fragments.

Mass (Da)	Mass* (Da)	Fragment	Peptide sequence
2371.71	2533.81	22-45	SCCDTGPADCCCKPGNKPDCCAPGK
1678.92	1841.02	50-67	CSGTCACGVGCTGVDNCK
1323.55	1485.65	8-19	ASCCIAEYECCK
861.98	1024.08	68-76	CGAGCSCFN
725.79	887.89	1-7	GSMSEK

With this experiment, it was intended to elucidate whether the glycosylation was either N- or O-bonded. Only a fragment that contains either Ser and Thr residues or Asn, but not both, would permit to extract any information about this bonding. However, the only fragments obtained from the digestion that were detected by the ESI-MS conditions used were fragment 22-45 and 8-19 (**Figure 3.48**).

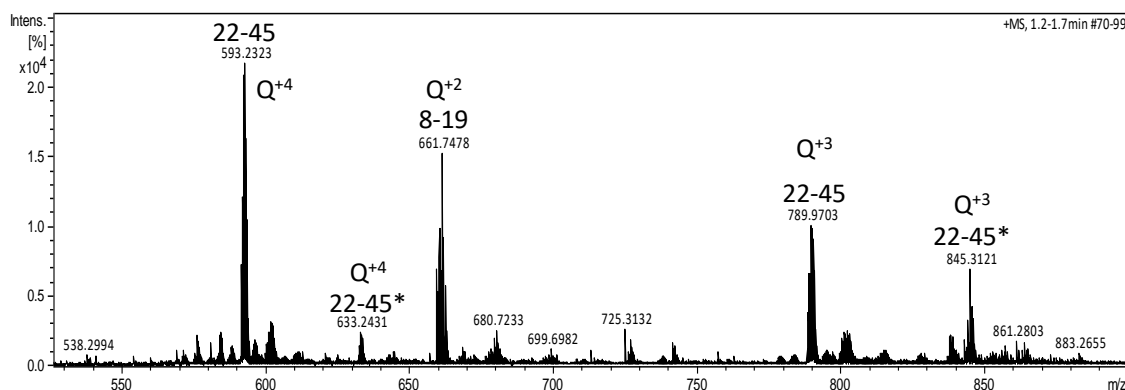


**Figure 3.48.** ESI-MS spectrum performed at pH 2.4 of Zn-LgiMT2 production.  $Q^{n+}$  indicates the charge state of the species.

It was clear that the longest fragment was glycosylated, as observed these modified species at different charge states, unluckily, this fragment contains both types of amino acid, for it was not possible to discern whether there is N- or O-glycosylation in this system. Thus, this feature of our glycosylation system could not be elucidated. It is necessary to continue studying and using more accurate methods, such as using N-glycosidase [257], to understand better this characteristic.

### 3.5.5. Cadmium inhibits glycosylation

Intriguingly, and as it has been stated above (**Section 3.5.1**), the presence of glycosylated species is only detected in productions supplemented with Zn(II) or Cu(II) (**Figure 3.49**). These glycosylated species are easier to detect on the proteins obtained from Zn(II)-enriched productions because Zn(II) ions exhibit less affinity for thiolate groups than Cu(I) ions [94]. Therefore, Zn(II) is exchanged by protons easily at low pH and the resultant mass spectra of these productions at these conditions are clearer and less crowded. However, it is certain that none of the proteins obtained from cultures supplemented with Cd(II) display glycosylation, suggesting that glycosylation is a metal-dependent process.



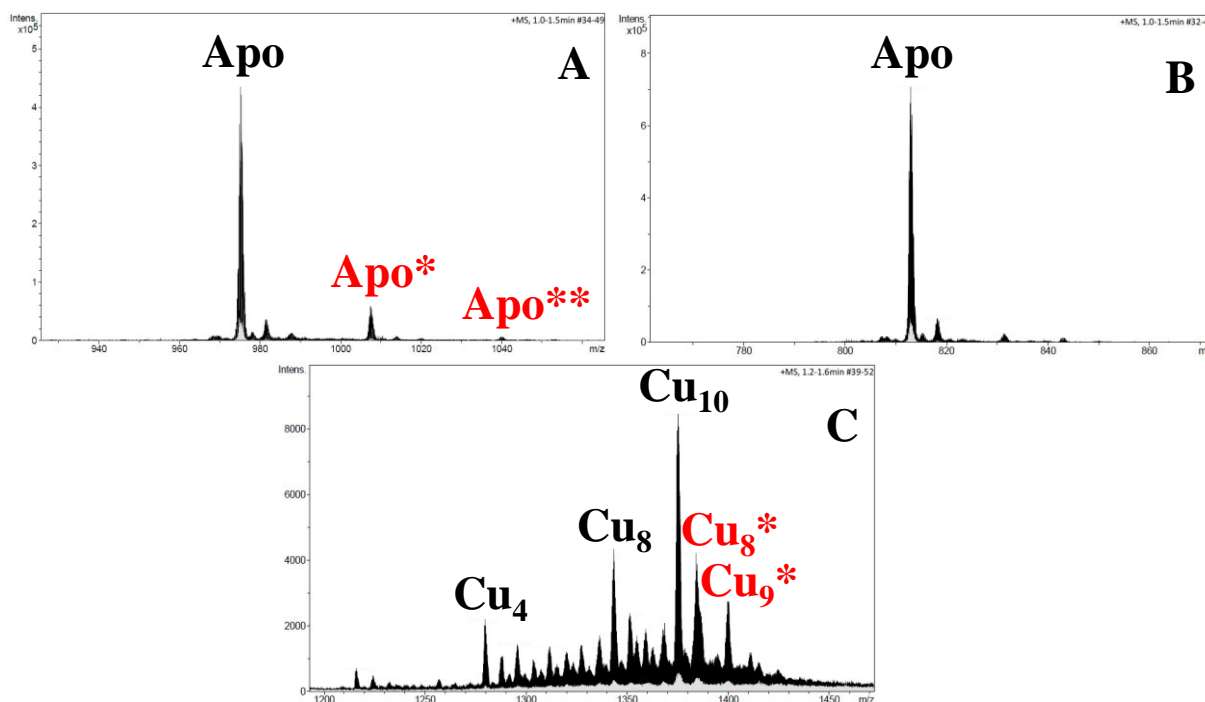


**Figure 3.49.** ESI-MS spectra measured at pH 2.4 of  $\alpha$ NpoMT1 fragment products synthesised in (A) Zn(II)- ( $Q^+ = +5$ ), (B) Cd(II)- ( $Q^+ = +6$ ) and (C) Cu(II)- ( $Q^+ = +4$ ) enriched cultures. Glycosylated species are marked with an asterisk and coloured red.

After more than 22 MT sequences characterised three times, once for each metal supplemented, during this PhD thesis, none of the products obtained from Cd(II)-enriched cultures rendered glycosylated species at a detectable level, while all of the proteins (except two cases) synthesised in Zn(II)-supplemented cultures displayed glycosylation in some degree. These significant differences in the glycosylation activity and the fact that Zn(II) and Cd(II) are chemically similar substances, suggests that Cd(II) might be interacting with a Zn(II)-dependant enzyme [105]. After some bibliographic research, two metalloproteins involved on glycosylation that can explain why only some MT productions render glycosylated species were found. First, glycosyltransferases (GT) enzymes are proteins that catalyse the union of the saccharide with the protein. Although, there are many GT isoforms, most of them use Mn(II) to stabilise their native structure [258] and an interaction with Cd(II) would not be probable. However, nucleotidyltransferase, an enzyme that activates monosaccharides by adding two nucleoside monophosphates [259], is crucial to GTs, that need an activated substrate to perform their function. Bacterial nucleotidyltransferases (Protein Data Bank ID: 1GUQ) are metalloproteins that catalyse the synthesis of UDP (uridine diphosphate)-glucose or UDP-galactose and, more importantly, their native structure is stabilised with a Zn(II) ion [260], for Cd(II) ions potentially interact with this site. Therefore, it is evidenced that the recombinant synthesis render

glycosylated species and that this posttranslational process can be switched by Cd(II) ions.

### 3.5.6. Glycosylation relies on MTs flexibility

Another experiment performed to demonstrate that glycosylation is a metal-dependant process consisted in studying glycosylation intensity at different concentration levels of Zn(II) supplementation. Thus, culture media were supplemented at the Zn(II) concentration usually employed in our studies (300  $\mu\text{M}$ ), at the same Zn(II) concentration as the intracellular levels (100  $\mu\text{M}$ ) [261], and without Zn(II) supplementation (0  $\mu\text{M}$ ). The first two conditions rendered equivalent species, ensuring that maintaining the intracellular levels of Zn(II) is enough to build the same metal-MT complexes than with an excess of metal. Interestingly, the sample obtained from the biosynthesis without supplementation showed different, yet enlightening, results from the other two conditions (**Figure 3.50**). Without metal supplementation, the glycosylation machinery is still active and there are modified proteins in the sample (**Figure 3.50E**). However, since Zn(II) levels are too low, MTs are not fully loaded of metal. One of the most remarkable features of this synthesis is that the glycosylated species increase their intensity ratios in comparison to Apo (**Figure 3.50F**). This increment of glycosylated species leads to an important postulation: the glycosylation machinery is more active in labile protein configurations in which potentially “glycosylable” amino acids are exposed to this machinery. MTs’ three-dimensional structure gain stability when are in association with metals, in fact, MTs only display a defined tertiary structure in this situation [2]. Therefore, a strong, well-structured cluster stabilises the backbone folding and, therefore, the metal-MT complex loses flexibility, hindering the action of the glycosylation enzymes. This is exactly what occurs in the preparation of Zn-MT complexes of genuine Zn-thioneins, in which the samples barely show detectable levels of glycosylation. In contrast, some Zn-MT complexes obtained from the non-supplemented cultures are semi-loaded (**Figure 3.50E**) and, structurally incomplete, so their highly mobile and flexible polypeptide chain is prone to be modified and the glycosylation rate in this sample is very high. Likewise, putative Cd-thioneins show very labile Zn-MT complexes and, thus, very flexible backbone chains, which provokes similar results to those obtained from the non-supplemented cultures. Taking advantage of this feature, it is possible to determine the robustness of a metal-MT complex and its cluster by detecting glycosylated species in the sample.

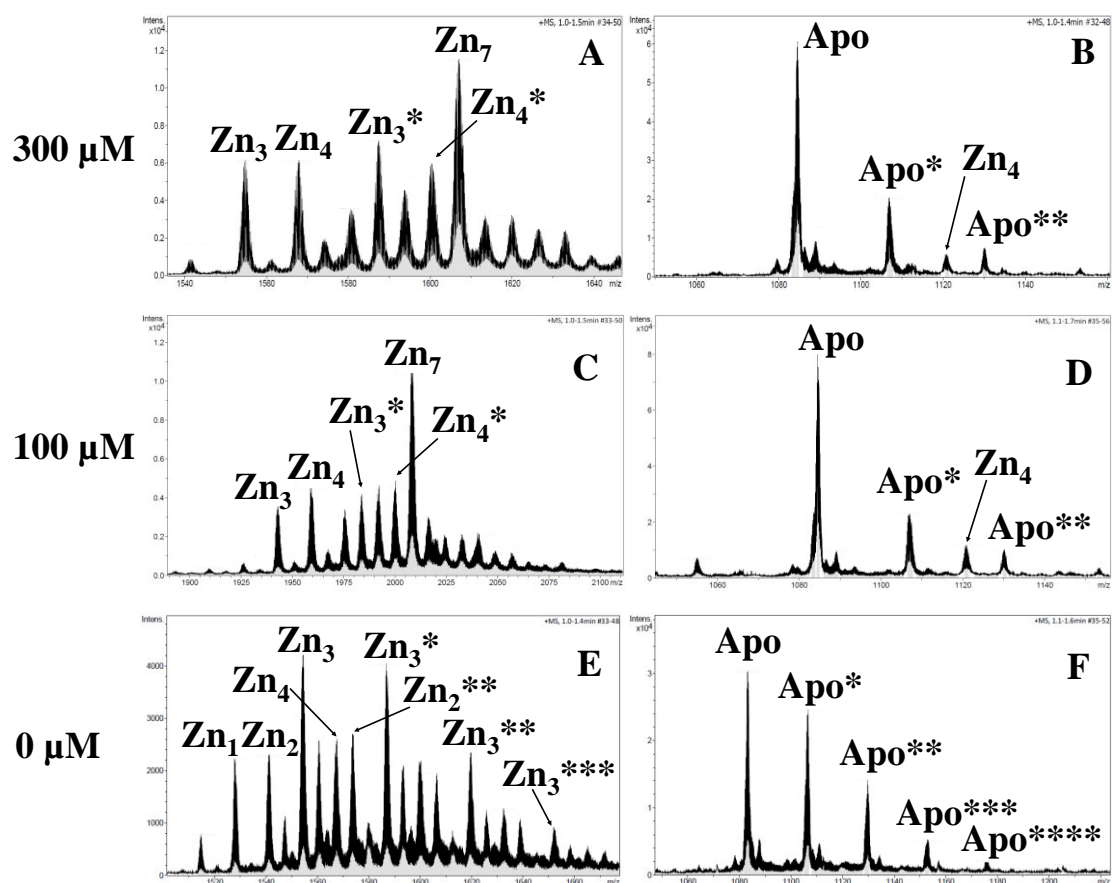


**Figure 3.50.** ESI-MS spectra of the products of the synthesis of LgiMT2 under three different Zn(II) concentrations: 300, 100 and 0  $\mu\text{M}$ . ESI-MS measured at pH 7.0 (A ( $Q^+ = +5$ ), C ( $Q^+ = +4$ ) and E ( $Q^+ = +5$ )) and at pH 2.4 (B ( $Q^+ = +7$ ), D ( $Q^+ = +7$ ) and F ( $Q^+ = +7$ )).

### 3.5.7. Glycosylation affects metal-binding of MTs

The initial drawback of discovering that our samples contained glycosylated proteins has become nowadays into an important hint when characterising the metal-binding abilities of MTs, as it can be used to ascertain their Zn-, putative Cd- or Cu-thionein behaviour. Firstly, as mentioned before, unstable clusters are more susceptible to be glycosylated than the well-structured ones. This is very interesting since genuine Zn-thioneins, although they render glycosylated species, they do it in very low amounts. More importantly, and connecting with the next point, the speciation of genuine Zn-thioneins is not affected by glycosylation when synthesised in Zn(II)-supplemented cultures. Considering **Figure 3.51**, which depicts a genuine Zn-thionein and a putative Cd-thionein produced in Zn(II)-supplemented cultures with and without glycosylated species in the sample, two features are observed: (1) non-glycosylated species of genuine Zn-thioneins remain equal whether the sample contains glycosylated species or not (**Figure 3.51A** and **B**), while the speciation of putative Cd-thioneins is affected by glycosylation, displaying different metal-MT complexes in each situation (**Figure 3.51C** and **D**).

(2) glycosylated-MTs render heterogenous species that normally cope with less metal ions than the non-glycosylated ones. The first feature is a reliable trait to distinguish Zn-thioneins from putative Cd-thioneins and it should be adopted as a new characterisation method to classify MTs by their metal-binding abilities (*vide infra*). As for the fact that glycosylated proteins cope with less metal ions than non-glycosylated-MTs, it could be used to study MTs' metal-binding abilities if it is considered that glycosylation is affecting essential amino acids that stabilise the metal cluster. Surely, as a future perspective, directing glycosylation to specific amino acids would help to determine whether those residues intervene in metal coordination or not and provide new insights into MTs and metalloproteins biochemistry.

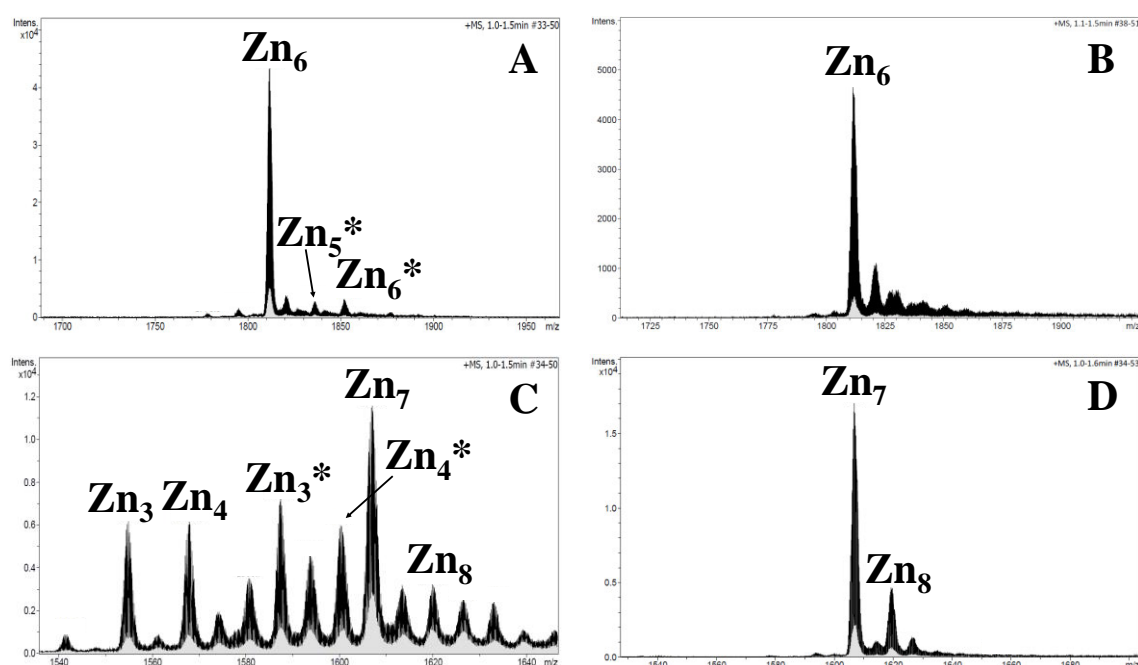


**Figure 3.51.** ESI-MS spectra measured at pH 7.0 of NpeMT1 (Zn-thionein) and LgiMT2 (Cd-thionein) synthesised in LB medium containing glucose (A ( $Q^+ = +4$ ) and C ( $Q^+ = +5$ )) and in minimum medium containing glycerol (B ( $Q^+ = +4$ ) and D ( $Q^+ = +5$ )). The first medium promotes glycosylation, while the latter avoids it. Glycosylated species are marked with an asterisk (\*).

Finally, a last feature of glycosylation was deduced from the results. If glycosylation, as demonstrated, depends on the stability of the metal cluster (as Zn-MT complexes of genuine Zn-thioneins are less affected than putative Cd-thioneins by glycosylation), this glycosylation occurs after metal-binding. Otherwise, Zn-MT complexes of genuine Zn-thioneins would not render the same species in glycosylating and non-glycosylating conditions, since, as mentioned before, glycosylated MTs cope with less metal ions than non-glycosylated MTs.

### 3.5.8. Final remarks of glycosylation

From the data compiled along all these years characterising MTs, it has been thoroughly detailed how *E. coli* glycosylation machinery works. All the data gathered in this section permitted to build a manuscript to be published (**Annex 7.3.8: Manuscript 1**). In this section, it has been demonstrated that the additional peaks found in the MS spectra correspond to glycosylated MTs that include hexoses to their sequence. After that, some experiments allowed to characterise the glycosylation process occurring in this system. First, by changing the substrate of the cultures, it was demonstrated that this glycosylation was a biological process rather than an *in vitro* modification, nor an experimental artefact. Moreover, it has been assured that there is a sequential addition of hexoses by means of a glycosylation machinery dependent of Zn(II), which is affected by Cd(II), inhibiting its activity. Thanks to glycosylation, it has been possible to study the metal-binding abilities of MTs, proposing a new characterisation method to distinguish between Zn- and putative Cd-thioneins. As a final fact, this is actually a shocking finding that provides new insights into recombinant production of proteins, since glycosylation was not expected to occur in this technique till now.

## 3.6. A new MT classification proposal

MTs functionality is still a topic of debate [85, 262]. The importance of finding this function lies on the necessity of locating a common evolutionary origin that connects all MTs across the phyla, defining “metallothionein” concept and understanding their function. Two features provide essential information of MT functions: the metal-binding capabilities of MTs and the affinity of the protein for these metal ions. As explained in **Section 1.1.4**, our group developed a functional classification based on the metal-binding abilities of MTs [13], separating them between genuine Zn-thioneins (high preference and specificity to bind Zn(II) metal ions) and genuine Cu-thioneins (extreme affinity to Cu(I) metal ions). Recently, it was demonstrated that Cd(II) drove mollusc MTs evolution [210]. This postulation was the starting point of this thesis, proposing a new classification scheme in which the putative Cd-thionein behaviour is independent from the Zn-thionein one. In this section it is compiled and synthesised the specific features of all the MTs studied in this thesis that are grouped into three metal-binding behaviours: Zn-thioneins, putative Cd-thioneins and unspecific MTs. Genuine Cu-thioneins are not included for two reasons: none of the MTs reported in this thesis present this behaviour and the differentiation between Cd/Zn-thioneins and Cu-thioneins was

extensively reported by our group in the past, so we decided to focus on the distinction between Zn- and Cd-thioneins.

### 3.6.1. Comparison of Zn- and Cd-thioneins metal-binding abilities towards Zn(II) ions

The analogous physicochemical properties of Zn(II) and Cd(II) entails that some MTs react similarly to these two ions (*i.e.*, equivalent selectivity and metal affinity). For that reason, during a period of time, Cd-MT complexes have been considered protein models of Zn-thioneins and led our group to think about a dichotomic functional classification of MTs. Therefore, in this thesis, some MTs proposed in different groups might exhibit similar metal-binding behaviour towards Zn(II) and Cd(II) but the key to separate them is in their differences. When it comes to bind Zn(II), Zn-thioneins and some Cd-thioneins share metal-binding features, rendering unique Zn-MT complexes. As mentioned, Zn(II) and Cd(II) are chemically equivalent, coordinating to the MTs as divalent ions. The principal difference between both ions is their radius. Thus, a flexible MT with high preference for divalent metal ions might render similar structures for both Zn(II) and Cd(II) metal ions, such is the case of NpeMTs, FcaMT1, HroMTs or AvuMT1 (**Table 3.4**). However, those polypeptide sequences whose amino acids features restrict their movement and cannot adapt to the distinct sizes of Zn(II) and Cd(II) are unable to render unique species for both metal ions. For example, Cd-thioneins that clearly do not exhibit Zn-thionein behaviour, rendering mixtures of Zn-MT complexes when synthesised in Zn(II)-supplemented cultures, such as CroMT1, LgiMTs, NpoMT1, OdiMT1 and SthMTs (**Table 3.4**).

Then, all Zn-thioneins render unique Zn-MT complexes, as well as some Cd-thioneins. On the other hand, there is a group of Cd-thioneins that yield a mixture of Zn-MT complexes, denoting poor affinity towards this metal. This first difference allows to distinguish between extreme Zn-thioneins and extreme Cd-thioneins and confirms the existence of this new metal-binding behaviour.

**Table 3.4.** Summary of the MT isoforms studied in this thesis classified by their metal-binding behaviours (blue, Zn-thioneins; yellow, Cd-thioneins; red, unspecific MTs; white, not enough data) and the properties detected during their characterisation (unique species with Zn(II), Cd(II), or Cu(I), glycosylation modifying speciation, labile sulphide ligands in Cd(II)-MT productions and hetero- or homonuclear properties of the Cu(I)-MT productions). OdiMT2 (nor their partial constructions) are not sorted in any metal-binding behaviour due to the lack of data.

Protein	Metal-binding behaviour					Results characterisation						
	Zn-th	Zn/Cd-th	Cd-th	Cu-th	Unspecific	Zn unique	Cd unique	Cu unique	Zn-glyco	Cd-S	Heteronuclear Cu/Zn	Homonuclear Cu
AvMT1	X	X				X	X				X	
BsMTR4		X	X			X	X					X
CaCUP1	X					X				X		X
FcaMT1	X	X				X	X				X	
δFcaMT1	X	X				X					X	
NpeMT1	X	X				X	X				X	
HrMT1		X	X			X	X					X
HrMT2		X	X			X	X					X
LgiMT1			X				X		X			X
LgiMT2			X				X		X			X
γLgiMT2			X				X		X			X
NpoMT1			X				X		X			X
αNpoMT1			X				X		X			X
NpeMT2		X	X			X	X					X
βNpeMT2		X	X			X	X					X
OdiMT1			X				X		X			X
CroMT1			X				X		X			X
SthMT1			X				X		X			X
SthMT2		X				X	X					
SthMT3			X				X		X			X
SthMT4			X				X		X			
AvMT2					X				X	X		X
PbrMT1					X				X	X	X	
PbrMT2					X				X	X		X
βLliMT1	X	X	X			X	X					X
OdiMT2.1										X		
OdiMT2.2										X		
OdiMT2												

Another feature worth to mention is the yielding of glycosylated species. Glycosylation has been a phenomenon that has permitted to understand better the synthesis and construction of the metal-MT complexes and, *vice versa*, metal-MT complexes have permitted to understand glycosylation mechanism. For what concerns to this section, glycosylation is of use to detect highly labile complexes. All the examples of putative Cd-thioneins synthesised in LB medium supplemented with Zn(II) salts exhibit glycosylation (**Section 3.4**). The metal-binding of these glycosylated proteins is affected by the attached carbohydrates, modifying the speciation of the sample (**Section 3.5.7**). This causes that non-glycosylated species render complexes with less metals than expected and this is easily detected by ESI-MS. In contrast, Zn-thioneins exhibit very low amounts of glycosylated species when synthesised in Zn(II)-enriched media and, more importantly, the metal-binding capacity of non-glycosylated species is not affected by glycosylation. Therefore, the biochemical properties of the different kinds of MTs that makes

them prone to be glycosylated in some measure is another differential trait between Zn- and Cd-thioneins worth to be considered.

### 3.6.2. Comparison of Zn- and Cd-thioneins metal-binding abilities towards Cd(II) ions

Despite the high variety of MTs of different species studied in this PhD thesis, most of them belonged to molluscs or urochordates. Curiously, the respective archetype MTs of these two evolutive groups exhibited more Cd-selectivity than Zn- or Cu-thionein behaviour (**Annex 7.3.6: Article 6**, and Ref. 210), and most of the MTs presented in this thesis evolved from these two archetypes, therefore, it is understandable that the metal-binding behaviours found are very similar. This explains that most of the proteins characterised rendered unique Cd-MT complexes when synthesised in Cd(II)-enriched culture media, even if they exhibited Zn-thionein behaviour. However, most of the genuine Zn-thioneins still show preference to Cd(II) in some extension. As reported by our group [13], Zn-thioneins might render *in vivo* hybrid Zn,Cd-MT complexes but in this thesis, this case has not been found. All the MTs considered Zn- or Cd-thioneins (except CaCUP1 and  $\delta$ FcaMT1) have rendered unique Cd-MT complexes in this thesis (**Table 3.4**), for this feature is not informative to distinguish between these two behaviours. However, this feature has been handy to understand that it exists a gradation between extreme Zn-thioneins and extreme Cd-thioneins, as there is a gradation between extreme Zn-thioneins and extreme Cu-thioneins [13]. In this case, the intermediate feature that locates an MT between Zn- and Cd-thioneins is their unique speciation with both Zn(II) and Cd(II) ions. Therefore, the determinant factor to distinguish between genuine Zn- and putative Cd-thioneins is their metal-binding capabilities towards Cu(I).

### 3.6.3. Comparison of Zn- and Cd-thioneins metal-binding abilities towards Cu(I) ions

This section shows one of the most helpful metal-binding features to distinguish between Zn- and Cd-thionein behaviours. Cu(I) chemistry differs with that of the previously assayed divalent metal ions Zn(II) and Cd(II). For that reason, MTs show more differences in their metal-binding towards Cu(I) than to Zn(II) or Cd(II). As most of the MTs in this thesis exhibit Zn- or/and Cd-thionein behaviour and considering the physicochemical differences between these elements, it is not strange finding that these proteins well adapted to bind divalent metal ions render a mixture of species when synthesised in Cu(II)-supplemented cultures. None of



the MTs studied rendered unique Cu-MT complexes and this should be marked as one of the main characteristics of Zn- and Cd-thioneins. After pointing this, it should be clarified that the MTs of these two divalent metal-binding behaviours yield different complexes when synthesised in Cu(II)-supplemented cultures. From one side, Zn-thioneins render heterometallic Zn,Cu-MT complexes, using Zn(II) ions from the inner medium of the cell to stabilize the metal cluster. This phenomenon was already observed [13] and has been an essential feature during characterisation to verify Zn-thioneins. From the other side, Cd-thioneins render homometallic Cu-MT complexes. This feature differs from the Zn-thioneins one, denoting that Cd-thioneins do not exhibit preference to Zn(II), since this metal ion is not used as structural ion in the Cu-MT complexes formation. This fact has been used as a determinant factor to establish whether a MT exhibits more Zn- or Cd-thionein behaviour. A final point to mention is, once again, glycosylation. As neither Zn- or Cd-thioneins render stable complexes with Cu(I), glycosylation machinery acts and glycosylates part of the complexes. Glycosylated Cu-MT complexes of these proteins are harder to characterise than Zn-MT complexes, mainly, because Zn-MT complexes are demetallated at pH 2.4 and because Cu-samples render much more species that hinder the detection of glycosylated species by ESI-MS.

#### *3.6.4. Final remarks on the proposal of a new scheme of MT classification*

Along the last sections the principal features of Zn- and putative Cd-thioneins when binding Zn(II), Cd(II) or Cu(I) have been described. There are important differences between these two metal-binding behaviours, especially when binding Zn(II) or Cu(I). For that reason, it can be stated that Zn- and putative Cd-thionein, although similar, are different metal-binding behaviours and the current dichotomic MT classification should be updated to a three-branch MT classification, adding Cd-thioneins as an independent metal-binding behaviour. During this process of evaluation, additional traits in the metal-binding abilities of the MTs have been observed and should be considered. For example, the fact that some putative Cd-thioneins render unique Zn-MT complexes but not heterometallic Zn,Cu-MT complexes suggests that there are intermediate metal-binding abilities between Zn- and Cd-thioneins behaviours. Although some MTs build nice metal complexes with divalent metal ions, their polypeptide sequence does not include Zn(II) ions in the Cu(I) metal clusters, denoting less dependence or preference for these metal ions than genuine Zn-thioneins. These intermediate steps have been observed in the first classification proposal as well. Not only an

extreme Zn- or Cu-thionein behaviour was proposed but several intermediate behaviours whose metal-binding abilities gradually jump between both states. Importantly, the chemical similarities between Zn(II) and Cd(II) makes usual to encounter many MTs that display an intermediate Zn/Cd-thionein behaviour. Last, it should be mentioned that a key criterion to determine whether a protein displays more of one metal-binding behaviour, or another is the levels of glycosylation found in the sample, which indicates the lability of the metal clusters.

The following table summarises the features of Zn- and the novel Cd-thioneins proposed in this PhD Thesis:

**Table 3.5.** Comparison of the features of the products rendered by genuine Zn-thioneins and genuine Cd-thioneins.

Genuine Zn-thioneins	Genuine Cd-thioneins
Render unique Zn(II)-MT species when synthesised in Zn(II)-enriched media	Render mixtures of Zn(II)-MT complexes when produced in Zn(II)-supplemented media
Might yield heterometallic Zn,Cd-MT complexes when produced in Cd(II)-supplemented <i>E. coli</i> cultures	Yield unique Cd(II)-MT complexes from the biosynthesis in Cd(II)-enriched <i>E. coli</i> cultures
Are reluctant to <i>in vitro</i> exchange Zn(II) by Cd(II)	No resistance to fully exchange Zn(II) by Cd(II) <i>in vitro</i>
Mixture of heterometallic Zn,Cu-MT species when recombinantly synthesised in Cu(II) supplemented media (process dependent on the oxygenation degree of the culture)	Mixture of homometallic Cu-MT species when biosynthesised in Cu(II)-enriched media (independently of the oxygenation degree of the culture)
Speciation of the Zn(II)-MT complexes not affected by glycosylation	Glycosylation do affect the speciation of the Zn(II)-MT complexes



## 4. CONCLUSIONS

---



## 4. Conclusions

---

The results achieved in this PhD thesis have permitted to reach some conclusions, which are exposed next, following the same order as the partial objectives were proposed in **Section 2**. The answer to the main objective (questioning whether the current MT classification is nowadays still valid) is stated at the end of this section after considering all the achieved partial conclusions.

### 1. Metal-binding features of different mollusc MTs

- *The evolutionary study and biochemical characterisation of the ten new MT isoforms of different Mollusca phylogenetic groups have permitted to understand better how mollusc MTs evolved and, thus, the MTs functionality along the evolution of these organisms.*
- *The results obtained from both in vivo and in vitro conditions show that mollusc MTs display heterogeneous, although marked, metal-binding features towards Zn(II), Cd(II) or Cu(I) ions. This heterogeneity in their biochemistry confirms mollusc MTs as a suitable model for this study.*
- *Three different coordinating capabilities have been detected from the studied mollusc MTs: high specificity for Zn(II) ions, high preference for Cd(II) ions and unspecific metal-binding preference for any of the metal ions explored.*
- *All except two of the mollusc MTs explored rendered a unique well-structured M(II)-MT species with at least one of the two divalent metal ions (Zn(II) or Cd(II)), denoting a great relevance of these ions in the mollusc MTs' evolution.*

### 2. Metal-binding abilities of the independent mollusc MT domains

- *The characterisation of new MTs of unexplored mollusc phylogenetic groups revealed a new functional domain of 10 Cys residues in Patellogastropoda*

named  $\gamma$  domain (**Section 3.4.1**). and one of 14 Cys residues in Caudofoveata called  $\delta$  domain (**Section 3.3.3**).

- The characterisation of the independent sequences of mollusc MT domains:  $\alpha$  (11/12 Cys),  $\beta$  (9 Cys),  $\gamma$  (10 Cys) and  $\delta$  (14 Cys), demonstrated that these domains fold and form metal clusters autonomously.
- Mollusc domains possess metal-binding preferences that resemble to those of the entire sequences, which in most of the cases show either a Zn(II)- or a putative Cd(II)-thionein behaviour, each independent module providing with specific metal-binding traits to the whole protein.
- Mollusc MTs are compartmentalised structures in which each module possesses specific metal-binding affinities. This is exemplified in LgiMTs in which each domain has different susceptibilities to pH variations (**Section 3.4.1**).

### 3. Metal-binding abilities of Ascidiacea, Thaliacea, and Appendicularia MTs

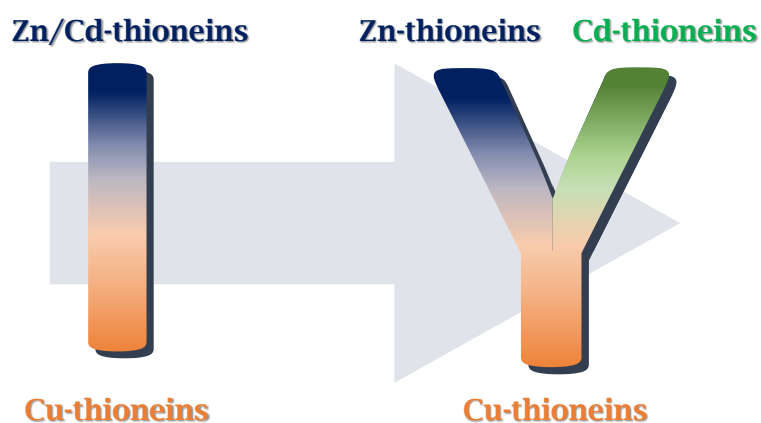
- The evolutionary study and biochemical characterisation of ten new MTs including at least one representative MT of all Tunicata phylogenetic groups has permitted to understand better how tunicate MTs evolved and, thus, contribute with new insights into the evolutive origin of chordate MTs.
- The results obtained from both *in vivo* and *in vitro* conditions show that tunicate MTs, in contrast with mollusc MTs, display homogeneous metal-binding features towards Zn(II), Cd(II) or Cu(I) ions.
- All tunicate MTs are constituted by 12C domains, multiple 12C domains or a combination of a 12C and a 12C domain variation, demonstrating that the MTs of this phylogenetical group lost the 9 Cys domain that the sister groups of tunicates (cephalochordates and vertebrates) possess.
- The prototypical ascidian/thaliacean MT (unique 12C domain) and the appendicularian MT (12C+t12C domains) render unique well-structured Cd(II)<sub>4</sub>-MT and Cd(II)<sub>7</sub>-MT complexes, respectively, when synthesised in Cd(II)-enriched *E. coli* cultures, reproducing equivalent metal clusters as vertebrates  $\alpha$  domains and vertebrates  $\alpha\beta$  MTs. In contrast, most MTs yielded a mixture of Zn(II)-MT species in the productions supplemented with Zn(II) salts. This clearly marks a predominant tendency in the biochemical traits of the prototypical tunicate MTs towards a Cd-selectivity.
- The evolutionary studies also revealed that the enormous multi-modular OdiMT2 and BscMT1 are composed by repetitive units whose sequences are well-aligned with each other.

- *The biochemical characterisation of the studied multi-modular MTs revealed that each repetitive unit forms an independent metal cluster and, thus, OdiMT2 and BscMT1 cope with as many metal ions as the number of repetitive units they contain and the coordinating capacity of each module.*
4. Sorting all the characterised MTs into the two existing metal-binding behaviours and the newly proposed one.
- *Thanks to the newly proposed classification, the 21 MT sequences characterised in this PhD thesis have been sorted in three groups, considering three distinguished metal-binding preferences towards Zn(II), Cd(II) or Cu(I) ions: 4 MT sequences have been classified as Zn-thioneins, 15 as putative Cd-thioneins, 2 as non-specific MTs and none as Cu-thionein.*
  - *All the MTs classified as Zn-thioneins yielded unique and well-structured Zn(II)-MT complexes, major Cd(II)-MT species with possible presence of minor species and, importantly, mixture of heterometallic Zn,Cu-MT complexes.*
  - *The putative Cd-thioneins rendered mixtures or unique Zn(II)-MT species, always a unique and well-structured Cd(II)-MT complex and, importantly, mixtures of homometallic Cu-MT species, contrasting with the Zn-thioneins.*
  - *The two non-specific MTs displayed none of the specific traits of the other two groups nor the relevant traits of the genuine Cu-thioneins.*
5. Towards an updated functional MT classification
- *Zn-thioneins and putative Cd-thioneins extremely differ in their in vivo metal-binding behaviour towards Cu(I) ions, i.e., Zn-thioneins always render heterometallic Zn,Cu-MT complexes and Cd-thioneins yield homometallic Cu-MT species.*
  - *Several putative Cd-thioneins showed a unique metal-binding behaviour by rendering samples with a mixture of Zn(II)-MT species when synthesised in Zn(II)-enriched culture media.*
  - *Despite that none of the MTs characterised here could be regarded as a Cu-thionein, leaving no possible experimental comparison with the rest of metal-binding behaviours, the results obtained in this PhD thesis have permitted to separate the “genuine Zn/Cd-thioneins” class into two new classes: “genuine Zn-thioneins” and “genuine Cd-thioneins”.*
  - *Those Zn- and Cd-thioneins that rendered both unique well-structured Zn(II)- and Cd(II)-MT complexes, and only differed in the hetero- or homometallic nature of their Cu(I) complexes, permitted to realise that there is a stepwise*



*gradation between genuine Zn- and Cd-thioneins, existing intermediate states in which some features are shared with the two behaviours, just as previously proposed for the dichotomic Zn- to Cu-thioneins classification.*

- *Overall, we can conclude that there is a differential metal-binding behaviour among the three classes of MTs, and the current dichotomic MT classification should be replaced by a three-branch functional MT classification, considering genuine Zn-, Cd- and Cu-thioneins as extreme behaviours.*



- *This novel three-branch classification can be applied to any MT reported from now on or in the past, if the proper biochemical characterisation is or has been performed.*

# 5. EXPERIMENTAL PROCEDURES

---



# 5. Experimental procedures

---

This section is aimed to explain all the techniques and procedures followed to synthesise, to purify, and to characterise all the MTs presented in this PhD thesis.

As a general consideration, all glassware material employed in this thesis was washed with HNO<sub>3</sub> 20% (v/v) and thoroughly rinsed with milli-Q water before use it. The purpose of this procedure is to eliminate any metal ion present in the material that could contaminate the samples. As for the disposable plastic material used, no previous decontamination was required. All solvents and solutions were spectroscopic quality.

## 5.1. Protein synthesis and purification

All proteins studied in this doctoral thesis were synthesised and purified by Dr. Ricard Albalat's research group, based in the University of Barcelona and part of the Genetics Department of the Biology Faculty. However, the UAB team occasionally performed some protein synthesis to get involved in the whole procedure. MTs were recombinantly synthesised by means of protease-deficient *E. coli* BL21 cells transformed with the plasmid containing the heterologous MT gene. Plasmid synthesis and cell transformation was performed by UB research group following their own cloning protocol [32]. *E. coli* cells were grown overnight in 300 mL or 500 mL of LB medium with 100 µg·mL<sup>-1</sup> of ampicillin at 37 °C. Afterwards, this culture was inoculated to a 3-5 L of fresh LB-100 µg·mL<sup>-1</sup> ampicillin medium and it was incubated for 1.5 h (till A<sub>600</sub>= 0.6-0.8). Then, β-D-thiogalactopyranoside (IPTG) (100 µM) was added to induce gene expression for 3 h, shaking the solution at 250 rpm (aeration conditions) or at 150 rpm (low-oxygen conditions). After 30 minutes of expression, the culture was supplemented with Zn(II) (300 µM of ZnCl<sub>2</sub>), Cd(II) (300 µM of CdCl<sub>2</sub>) or Cu(II) (500 µM of CuSO<sub>4</sub>). Despite that the culture medium is supplemented with divalent Cu(II) ions, the recovered complexes

contain monovalent Cu(I) ions. Bacteria only have mechanisms to introduce divalent Cu(II), however, reducing conditions are applied inside the cell to achieve the necessary monovalent Cu(I) ions to form Cu(I)-MT complexes. When higher protein concentrations were required, the synthesis was performed in a 30 L fermenter, following the same conditions aforementioned, except that bacterial growth is performed in one single step.

Once the synthesis process is finished, cells were harvested by centrifugation (Sorvall; ThermoFisher Scientific, USA) at 7700 rpm for 5 minutes and supernatant was discarded. Bacterial pellet was resuspended in ice-cold phosphate-buffered saline (PBS; 1.4 M NaCl, 27 mM KCl, 101 mM Na<sub>2</sub>HPO<sub>4</sub>, 18 mM KH<sub>2</sub>PO<sub>4</sub> and 0.5% v/v β-mercaptoethanol). Cells were disrupted by sonication (Sonifier Ultrasonic Cell Disruptor) for 8 minutes at 6 V with 0.6 s pulses, and then cell detritus was precipitated by centrifugation (12000 rpm during 40 min at 4 °C). Supernatant was collected and incubated with Glutathione Sepharose 4B (GE Healthcare, USA) for 1 h at room temperature with gentle rotation. Glutathione Sepharose beads bound to glutathione S-transferase (GST)-MT fusion protein were washed with 20-30 mL of cold PBS previously bubbled with argon to prevent MTs oxidation. GST-MT fusion proteins were digested with 25 U·L<sup>-1</sup> thrombin (GE Healthcare, USA) overnight at 17 °C. This process cleaves metal-MT complexes from the GST bound to the Sepharose beads. Metal-MT complexes remaining in solution were concentrated using Centriprep Low Concentrators (Amicon, Merck, Germany) and fractionated through a Superdex-75 FPLC column (GE Healthcare, USA) running at 0.8 mL·min<sup>-1</sup>, being 20 mM Tris-HCl (pH 7.0) the mobile phase. Protein-containing fractions were identified by their absorbance at 254 nm, pooled in aliquots and stored at -80 °C until used.

## 5.2. Protein characterisation

An important fact to be considered when using recombinant DNA technology is that, although *E. coli* expression system is a good approximation [32, 33], the products obtained through this technique do not proceed from the organism of study, which may mean that the resulting proteins may not have the expected quality (*e.g.*, unexpected MW, insufficient protein concentration, etc.). With this object, an accurate characterisation of all samples was carried out. The first evidence to verify the integrity of the amino acid sequence was acidic (pH 2.4) ESI-MS results. Acidic pH demetallates Zn(II)- and Cd(II)-loaded MTs, allowing the determination of apo-form molecular weight, so theoretical and experimental masses can be compared. In addition to that measure, this section describes all the

techniques used to characterise the structural and metal-binding properties of MTs, as well as the nomenclature used to refer to each protein.

### 5.2.1. Proteins' nomenclature

An inconvenience encountered during this PhD thesis was the nomenclature used to tag such number of sequences. Up to the present, MTs have been named by the discoverer's criteria, with a few indications convened in the international meeting held in Zürich in 1978 [263]. This convention stipulates that MTs should be termed as *metallothionein* followed by Arabic numbers to differentiate between different isoforms (*e.g.*, metallothionein-1). Only distinct amino acid sequences are to be mentioned with a unique nomenclature, therefore, the same amino acid sequence forming two different metal complexes only has one nomenclature. In addition, before that, the organism which possesses the mentioned MT should be indicated. This agreement has evolved to a more pragmatic terminology, shorting the whole term to a few representative characters (*i.e.*, mammalian metallothionein-1 equals to mMT-1). As a rule of thumb, the nomenclature follows this structure: "Characters that reference the species Latin name" followed by "MT" (as for metallothionein) continued by an "Arabic number" (as for the isoform). This terminology applies to most of the MTs reported except for a few cases, such as CUP1, which is named after the yeast gene of a resistance copper protein and, afterwards, it was considered an MT [264].

Our group has historically used two letters to refer to the species of the MT (*e.g.*, *Helix pomatia* copper MT is named HpCuMT). However, the introduction of more MT sequences and more species have led to coincidences in the tagging of some MTs. To avoid these situations, in this PhD thesis, the MTs' nomenclature is built with three letters: the first character of the genus name and the two first letters of the species name (*e.g.*, *Arion vulgaris* MT1 is AvuMT1).

### 5.2.2. Inductively coupled plasma atomic emission spectroscopy (ICP-AES)

ICP-AES analysis is based on the measure of photons emitted by ionised elements that have been excited by a high radiofrequency (RF) discharge [265]. Liquid samples are introduced in the instrument through a nebulizer. They are quickly vaporized by the inductively coupled plasma (ICP) core (sustaining a temperature of 10000 K), liberating free atoms in gaseous state. These atoms or ions are excited within the plasma. Then, those excited species may relax emitting a photon. The characteristic energy of the photon (wavelength) permits to identify

the element from which they were originated. The total amount of photons detected are proportional to the concentration of the originating element.

Therefore, this technique allowed to simultaneously measure the total content of metals (Zn, Cd and Cu) and sulphur present in the samples. Sulphur atoms proceed from cysteine (Cys) and methionine (Met) residues. Protein concentration was calculated dividing the total sulphur content of the sample by the number of Cys and Met of the protein. This methodology is referenced in this doctoral thesis as “conventional ICP”. However, some metal-MT complexes may include labile  $S^{2-}$  ligands [155]. These ions interfere in the protein concentration quantification, to eliminate those ligands and to analyse these samples, concentrated formic acid was added in the aliquot before the experiment. The formation of  $H_2S$  gas was evident because of its characteristic odour. Throughout this thesis, this procedure is called “acid ICP”.

ICP-AES measures were carried out in an Optima 4300DV spectrometer (PerkinElmer, USA) by Servei d'Anàlisi Química (SAQ) in the Universitat Autònoma de Barcelona (UAB). All samples were diluted with  $HNO_3$  1% (v/v) and measured at 182.04 nm, 213.85 nm, 324.75 nm and 228.80 nm for determining S, Zn, Cd and Cu concentrations, respectively.

### 5.2.3. *Electrospray Ionisation Mass Spectrometry Time-of-Flight (ESI-MS-TOF)*

A key aspect when characterising MTs is to evaluate their native structure. That means that it is important to conserve the physiological features of metal-MT complexes during their examination. The use of electrospray ionisation mass spectrometry (ESI-MS) has been established as an essential approach in the study of metalloproteins, concretely, MTs [239]. ESI-MS is a procedure in which its mild ionisation conditions preserve the three-dimensional structure of the proteins studied and, more importantly, it maintains the structure of metal-MT clusters. Consequently, the stoichiometry of the complexes may be determined. In addition, high resolution Time-of-Flight (TOF) analyser permits to accurately identify mass-to-charge ratio ( $m/z$ ) values.

As for this essay, the instrument used was a Micro Tof-Q instrument (Bruker, USA) coupled to a Series 1200 HPLC pump (Agilent technologies, USA) that drove the sample from the injector to the nebuliser. This setting allowed using two different conditions: pH 7.0 and pH 2.4. At physiological conditions (pH 7.0), folded metal-MT complexes were detected while at acid conditions (pH 2.4), Zn(II) and Cd(II) are released and only unfolded apo-MT peptides and resistant Cu(I)-MT complexes were detected. Instrument calibration was attained with a NaI solution

(0.2 g NaI in 100 mL of 1:1 H<sub>2</sub>O:Isopropanol mixture). Instrument was calibrated and prepared by SAQ staff, and the UAB team performed the measures.

Samples of MT complexes containing Zn(II) and Cd(II) were analysed under the next experimental conditions: 20  $\mu$ L of protein solution injected through a polyether heteroketone (PEEK) column (1.5 m x 0.18 mm i.d.) at 40  $\mu$ L $\cdot$ min<sup>-1</sup>; capillary voltage 5000 V; dry temperature 100 °C; dry gas 6 L $\cdot$ min<sup>-1</sup>;  $m/z$  range 800-3000. The carrier used under these conditions was a 5:95 mixture of acetonitrile:ammonium acetate/ammonia 15 mM at pH 7.0. Otherwise, samples of MT complexes containing Cu(I) were measured as follows: 20  $\mu$ L of protein solution injected at 40  $\mu$ L $\cdot$ min<sup>-1</sup>; capillary voltage 4400 V; dry temperature 90 °C; dry gas 6 L min<sup>-1</sup>;  $m/z$  range 800-2500. In this case, the carrier was a mixture of 10:90 acetonitrile:ammonium acetate/ammonia 15 mM at pH 7.0. For apo-MT peptides and Cu-MT complexes analyses at acidic pH, 20  $\mu$ L of sample was injected under the same conditions as those used for divalent metal measures, excepting that the carrier was a 5:95 mixture of acetonitrile:formic acid at pH 2.4.

#### 5.2.4. Ultraviolet-Visible absorption spectroscopy (UV-Vis)

UV-Vis absorption spectroscopy is a classic method used to characterise molecules by measuring their interaction with electromagnetic radiation. Then, UV-Vis absorption spectroscopy measures the difference of intensity of electromagnetic radiation passing through a certain medium at a certain wavelength. Light absorption results from electrons' excitation to higher energy levels. The energy irradiated at the UV-Vis range (200-700 nm) involves energy transitions of nonbonding  $n$  electrons and  $\pi$  electrons to  $\pi^*$  excited states [266]. Molecules capable of absorbing at these wavelengths are called chromophores.

Due to their aromatic residue scarcity, free metal apo-MTs only show significant absorption bands in the peptide bond region (180-260 nm). Carbonyl  $n$ - $\pi^*$  transition state at 213 nm displays the highest absorbance. When metal-MT complexes are formed (*e.g.*, Zn(II)-MT, Cd(II)-MT, Cu(I)-MT...), new bands appear in the range of 220 to 400 nm [42]. In general, when MTs show absorption bands to the red of 220 nm, they can be directly related to metal-MT complexes. Although Zn(II), Cd(II) and Cu(I) are spectroscopically silent, the effect of the ligand to these metals permit the detection of ligand to metal charge transfer (LMCT) bands. Thus, absorption arisen from the ligand (generally thiolates) to cadmium, zinc or copper charge transfer is well characterised and UV-Vis spectroscopy, in this thesis, is used to this end, evaluate the viability of the different metal-MT complexes. In addition, UV-Vis spectroscopy was used for monitoring metal-exchange



experiments, generating a spectrum at each metal addition. By subtracting two consecutive steps spectra, the contribution of this metal addition step to the formation or disappearance of certain chromophore can be evaluated.

UV-Vis absorption spectra were generated by means of a Diode array HP8452A UV-Vis spectrophotometer (Hewlett-Packard, USA) with an integration time of 15 seconds and using 1 cm quartz cuvettes. Tris-HCl solution (at the same concentration as in the samples) was recorded as blank. All spectra were processed correcting background and sample concentration using GRAMS32 software (GRAMS/AI v.7.02, Thermofisher Scientific, USA).

#### 5.2.5. Circular Dichroism (CD)

Circular dichroism (CD) spectroscopy is a technique employed to characterise optically active (chiral) compounds by means of polarised light (composed by right- and left-circularly polarised light). Two superposed circularly polarised light beams, rotating in opposite directions, pass through a solution containing a chiral compound. Optical active chromophores possess distinct refractive index for right and left polarisations, which means, both beams travel at different velocities, which leads to a rotation of the plane of the light [267]. In the same way, one polarised beam is absorbed (as in intensity) distinctly to its opposite and the resultant radiation traces an ellipse [268]. This effect is known as circular dichroism. Normally, CD instruments measure *ellipticity*  $\theta$  (in mdeg) but data is reported as *molar extinction* variation  $\Delta\epsilon$  (in  $M^{-1}cm^{-1}$ ), that is, differential absorbance of right- and left- circularly polarised light ( $\epsilon_R - \epsilon_L$ ) corrected by the sample concentration. A CD spectrum is yielded when  $\Delta\epsilon$  is plotted against wavelength  $\lambda$  (in nm). This spectrum depicts positive and negative bands, called Cotton effects, at those wavelengths where the sample is CD active. These bands are coincident with the corresponding UV absorption bands [268]. CD signals draw a Gaussian distribution curve (positive or negative), representing a CD absorption band of a unique chiral species. However, in a system, it is common to find more than one chromophore. When two or more close-in-space chromophores are excited at a similar wavelength and in a similar intensity, their excitation states are asymmetrically coupled describing a characteristic sigmoidal curve (*exciton coupling*).

As regard to MTs, metal-thiolate  $[M-(SCys)_x]$  chromophores are optically active because achiral metal centres receive their asymmetry from the intrinsically chiral cysteines [269]. Thus, despite CD spectroscopy has been historically used to assess three-dimensional protein structures considering their amide bond signals, in MTs'

field, CD has proved utility for characterising metal clusters. In fact, MTs only present a specific three-dimensional structure and a strong chiral field when metals are coordinated [6]. Therefore, MTs' CD spectrum displays their folding information and their metal coordination environment. As a drawback, when there is more than a unique stable species in the medium, the resulting CD spectrum represents a global measure of the whole metal-MTs' system. At any rate, CD is a valuable tool for monitoring MTs' metal clusters during metal exchange experiments, giving information about protein metallic centres while experimental conditions change.

CD spectra were registered at 50 nm·min<sup>-1</sup> and 0.5 nm of resolution by means of a Jasco-715 spectropolarimeter (Jasco Inc., Easton, USA) interfaced to a computer (J700 software). Samples were recorded in 1 cm quartz cuvettes and kept at 25 °C by a Peltier PTC-351S apparatus (TE Technology Inc., USA). A Tris-HCl solution at the same concentration as the sample was used as a blank. All spectra were processed, correcting blank and dilution effects using GRAMS32 software (GRAMS/AI v.7.02, Thermo Scientific, USA).

#### 5.2.6. Protein digestion

This methodology is widely used in proteomics for protein identification and characterisation, specially complemented with mass spectrometry [270]. The MS profile elaborated from the digested proteins permit to determine specific fingerprints that can be used to identify these proteins in complex samples that contain a whole proteome [271]. This method is based on the controlled cleavage of a protein in specific amino acids or sequence of amino acids in order to obtain smaller peptides of the full protein that will aid in its characterisation, especially in the detection of posttranslational modifications and their sites [272, 273]. In this PhD thesis, the enzyme employed to perform the protein digestion is trypsin (Promega Biotech Ibérica S.L., Spain). This enzyme is prone to cleave the polypeptide chain after lysine or arginine amino acids [274]. Moreover, it must be considered that metallated MTs are protected against the action of trypsin [275], for this reason, MTs are to be demetallated with EDTA before the digestion.

The procedure followed here is an adaptation from [276]. Starting with an Eppendorf tube containing 200 µL of Zn(II)-loaded LgiMT2 at a concentration of  $8.42 \cdot 10^{-5}$  M, 100 µL of EDTA at  $3.2 \cdot 10^{-3}$  M were added to dispose of all Zn(II) ions coordinated to the protein. After that, the protein solution was mixed with a trypsin 10 µg/mL solution in a 1:20 protein:trypsin ratio (pH ~7.5-8.0). This mixture was incubated at 37°C for four hours. The digestion was stopped by

lowering the pH to 1.5 with formic acid (HCOOH) and the sample was measured by ESI-MS.

### 5.3. Cd(II) and Cu(I) titrating agents

The Cd(II) or Cu(I) substitution experiments were performed on metal-MT complexes (generally Zn-MT complexes) to complement the biochemical characterisation of the MTs. These experiments are also referred as titration experiments during this PhD Thesis and provided a deeper perspective on the metal-binding features and the metal cluster formation. They allowed the comparison between *in vivo* and *in vitro* Cd(II)- and Cu(I)-metal clusters formation.

As the rest of the spectroscopic measures, these metal-exchange experiments were performed under argon atmosphere, at 25 °C in a 1 cm quartz cuvette and they were monitored by means of UV-Vis and CD spectroscopy. In addition, aliquots were taken in some of the metal-addition steps to perform ESI-MS analysis.

#### 5.3.1. Cd(II) solution

To perform metal-exchange experiments with Cd(II), a solution of CdCl<sub>2</sub> 1 mM was prepared with milli-Q water. Concentration was corroborated by ICP-AES under the same conditions explained in **Section 5.2.2**.

#### 5.3.2. Cu(I) solution

An aqueous (30% CH<sub>3</sub>CN) solution of [Cu(CH<sub>3</sub>CN)<sub>4</sub>]ClO<sub>4</sub> complex was employed as agent for metal-exchange experiments with Cu(I). This complex is highly resistant to oxidation and its counter-ion (ClO<sub>4</sub><sup>-</sup>) has low coordinating capacity.

Cu(I)-complex synthesis was performed following Kubas, Monzyc and Crumbliss instructions [277]. All the procedure was carried out under argon atmosphere and all solutions were degassed before its use. On a suspension of 4.0 g Cu<sub>2</sub>O in 80 mL CH<sub>3</sub>CN, 24.6 mL HClO<sub>4</sub> 4.6 M were gradually added. The solution was agitated at 100 °C under reflux till there was no white precipitate and it became transparent blueish. The solution was filtered while it still was hot and the filtrate is let to cool, first, at room temperature, after, in the fridge and finally in the freezer overnight. Complex white crystals were gathered by filtration and washed with 3 portions of 5-10 mL cold Et<sub>2</sub>O. After drying, the crystals are used to prepare 1 mM complex dilution with aqueous (30% CH<sub>3</sub>CN) solution under argon atmosphere. Aliquots of 1-1.5 mL were prepared and frozen. One aliquot was used to verify the correct concentration of the solution by ICP-AES.

## 6. BIBLIOGRAPHY

---



## 6. Bibliography

- 
- [1] J.H. Kägi & B.L. Vallee, "Metallothionein: a cadmium- and zinc-containing protein from equine renal cortex" *J. Biol. Chem.* **235**, 3460-3465 (1960).
- [2] K.B. Nielson, C.L. Atkin, D.R. Winge, "Distinct metal-binding configurations in metallothioneins" *J. Biol. Chem.* **260**, 5342-5350 (1985).
- [3] H. Willner, M. Vasák, J.H. Kägi, "Cadmium-thiolate clusters in metallothionein: spectrophotometric and spectropolarimetric features" *Biochemistry* **26**, 6287-6292 (1987). doi: 10.1021/bi00393a049.
- [4] G. Isani, E. Carpenè E, "Metallothioneins, unconventional proteins from unconventional animals: a long journey from nematodes to mammals" *Biomolecules* **4**, 435-457 (2014). doi: 10.3390/biom4020435.
- [5] M. Margoshes, B.L. Vallee, "A Cadmium Protein from Equine Kidney Cortex" *J. Am. Chem. Soc.* **79**, 4813-4814 (1957).
- [6] M. Capdevila, R. Bofill, Ò. Palacios, S. Atrian, "State-of-the-art of metallothioneins at the beginning of the 21st century" *Coord. Chem. Rev.* **256**, 46- 62 (2012).
- [7] A. Sekovanić, J. Jurasović, M. Piasek, "Metallothionein 2A gene polymorphisms in relation to diseases and trace element levels in humans" *Arh. Hig. Rada. Toksikol.* **71**, 27-47 (2020). doi:10.2478/aiht-2020-71-3349
- [8] K. Subramanian Vignesh, G.S. Jr. Deepe, "Metallothioneins: Emerging Modulators in Immunity and Infection" *Int. J. Mol. Sci.* **18**, 2197 (2017). Published 2017 Oct 23. doi:10.3390/ijms18102197
- [9] M. Cesani, E. Cavalca, R. Macco, G. Leoncini, M.R. Terreni, L. Lorioli, R. Furlan, G. Comi, C. Doglioni, D. Zacchetti, M. Sessa, C.R. Scherzer, A. Biffi, "Metallothioneins as dynamic markers for brain disease in lysosomal disorders" *Ann. Neurol.* **75**, 127-137 (2014). doi:10.1002/ana.24053
- [10] J.C. Gutiérrez, F. Amaro, A. Martín-González, "From heavy metal-binders to biosensors: ciliate metallothioneins discussed" *Bioessays* **31**, 805-816 (2009). doi: 10.1002/bies.200900011
- [11] A.M.S. Hertika, K. Kusriani, E. Indrayani, R. Nurdiani, R.B.D.S. Putra, "Relationship between levels of the heavy metals lead, cadmium and mercury, and metallothionein in the gills and stomach of *Crassostrea iredalei* and *Crassostrea glomerata*" *F1000Res.* **7**, 1239 (2018). Published 2018 Aug 10. doi:10.12688/f1000research.14861.1

- [12] C. Zhang, M. Jansen, L. De Meester, R. Stoks, "Thermal evolution offsets the elevated toxicity of a contaminant under warming: A resurrection study in *Daphnia magna*" *Evol. Appl.* **7**, 1425-1436. doi: 10.1111/eva.12637
- [13] O. Palacios, S. Atrian, M. Capdevila "Zn- and Cu-thioneins: a functional classification for metallothioneins?" *J. Biol. Inorg. Chem.* **16**, 991-1009 (2011). doi: 10.1007/s00775-011-0827-2
- [14] C.A. Blindauer, O.I. Leszczyszyn, "Metallothioneins: unparalleled diversity in structures and functions for metal ion homeostasis and more" *Nat. Prod. Rep.* **27**, 720-741 (2010). doi: 10.1039/b906685n
- [15] A. Ziller, L. Fraissinet-Tachet, "Metallothionein diversity and distribution in the tree of life: a multifunctional protein" *Metallomics* **10**, 1549-1559 (2018). doi: 10.1039/c8mt00165k
- [16] J.F. Riordan, B.L. Vallee, *Methods in Enzymology Metallobiochemistry part B Metallothionein and Related Molecules*, vol. 205, Academic Press, San Diego, 1991.
- [17] E. Hödl, E. Felder, M. Chabicovsky, R. Dallinger, "Cadmium stress stimulates tissue turnover in *Helix pomatia*: increasing cell proliferation from metal tolerance to exhaustion in molluscan midgut gland" *Cell Tissue Res.* **341**, 159-171 (2010). doi: 10.1007/s00441-010-0980-x.
- [18] S. R. Davis and R. J. Cousins, "Metallothionein expression in animals: a physiological perspective on function" *J. Nutr.* **130**, 1085-1088 (2000).
- [19] K.E. Rigby Duncan, M.J. Stillman, "Metal-dependent protein folding: metallation of metallothioneins" *J Inorg Biochem.* **100**, 2101-2107 (2006). doi: 10.1016/j.jinorgbio.2006.09.005
- [20] R. Orihuela, F. Monteiro, A. Pagani, M. Capdevila, S. Atrian, "Evidence of native metal-S<sup>2</sup>-metallothionein complexes confirmed by the analysis of Cup1 divalent-metal-ion binding properties" *Chem. Eur. J.* **16**, 12363-12372 (2010). doi: 10.1002/chem.201001125.
- [21] Y. Nishiyama, S. Nakayama, Y. Okada, K.S. Min, S. Onosaka, K. Tanaka "Amino acids and peptides. XXVI. Synthesis of *Agaricus bisporus* metallothionein and related peptides and examination of their heavy metal-binding properties" *Chem. Pharm. Bull.* **38**, 2112-2117 (1990). doi: 10.1248/cpb.38.2112
- [22] F.J. Kull, M.F. Reed, T.E. Elgren, T.L. Ciardelli, D.E. Wilcox. "Solid-phase peptide synthesis of the alpha and beta domains of human liver metallothionein 2 and the metallothionein of *Neurospora crassa*" *J. Am. Chem. Soc.* **112**, 2291-2298 (1990). Doi: 10.1021/ja00162a033
- [23] Y. Okada, N. Ohta, S. Iguchi, Y. Tsuda, H. Sasaki, T. Kitagawa, M. Yagyu, K.S. Min, S. Onosaka, K. Tanaka "Amino acids and peptides. XIII. Synthesis of a nonacosapeptide corresponding to the N-terminal sequence 1-29 (beta-fragment) of human liver metallothionein II (hMT II) and its heavy metal-binding properties" *Chem. Pharm. Bull.* **34**, 986-98 (1986). doi: 10.1248/cpb.34.986
- [24] H.J. Hartmann, Y.J. Li, U. Weser, "Analogous copper(I) coordination in metallothionein from yeast and the separate domains of the mammalian protein" *Biometals* **5**, 187-191 (1992). doi: 10.1007/BF01061327
- [25] Y.J. Liu, U. Weser, "Circular dichroism, luminescence, and electronic absorption of copper binding sites in metallothionein and its chemically synthesized alpha and beta domains" *Inorg. Chem.* **31**, 5526-5533 (1992). doi: 10.1021/ic00052a031

- [26] A.K. Sewell, L.T. Jensen, J.C. Erickson, R.D. Palmiter, D.R. Winge, "Bioactivity of Metallothionein-3 Correlates with Its Novel beta. Domain Sequence Rather Than Metal Binding Properties" *Biochemistry* **34**, 4740-4747 (1995). doi: 10.1021/bi00014a031
- [27] Y. Okada, K. Tanaka, J.-I. Sawada, Y. Kikuchi, in: M.J. Stillman, C.F. Shaw III, K.T. Suzuki (Eds.), *Metallothioneins Synthesis, Structure and Properties of Metallothioneins, Phytochelatins and Metal-Thiolate complexes*, VCH Publishers Inc, New York, 1992, 195.
- [28] J.D. Watson, R.M. Myers, A.A. Caudy, J.A. Witkowski, in: W.H. Freeman (Eds.), *Recombinant DNA: Genes and Genomes: A Short Course*, W.H. Freeman and Company, Gordonsville, 2007.
- [29] F.M. Romeyer, F.A. Jacobs, L. Masson, Z. Hanna, R. Brousseau, "Bioaccumulation of heavy metals in *Escherichia coli* expressing an inducible synthetic human metallothionein gene" *J. Biotechnol.* **8**, 207-220 (1988). doi: 10.1016/0168-1656(88)90003-X
- [30] F.A. Jacobs, F.M. Romeyer, M. Beauchemin, R. Brousseau, "Human metallothionein-II is synthesized as a stable membrane-localized fusion protein in *Escherichia coli*" *Gene* **83** 95-103. doi: 10.1016/0378-1119(89)90407-1.
- [31] S. Yamazaki, M. Nakanishi, T. Hamamoto, H. Hirata, A. Ebihara, A. Tokue, Y. Kagawa, "Expression of human metallothionein-II fusion protein in *Escherichia coli*" *Biochem. Intern.* **28**, 451-460 (1992).
- [32] M. Capdevila, N. Cols, N. Romero-Isart, R. González-Duarte, S. Atrian, P. González-Duarte, "Recombinant synthesis of mouse Zn<sub>3</sub>-β and Zn<sub>4</sub>-α metallothionein 1 domains and characterization of their cadmium(II) binding capacity" *Cell. Mol. Life Sci.* **53**, 681-688 (1997). doi: 10.1007/s000180050088
- [33] N. Cols, N. Romero-Isart, M. Capdevila, B. Oliva, P. González-Duarte, R. González-Duarte, S. Atrian, "Binding of Excess Cadmium(II) to Cd<sub>7</sub>-metallothionein from Recombinant Mouse Zn<sub>7</sub>-metallothionein 1. UV-VIS Absorption and Circular Dichroism Studies and Theoretical Location Approach by Surface Accessibility Analysis" *J. Inorg. Biochem.* **68**, 157-166 (1997). doi: 10.1016/s0162-0134(97)00085-8
- [34] I. Dance, K. Fisher, G. Lee, in: M.J. Stillman, C.F. Shaw III, K.T. Suzuki (Eds.), *Metallothioneins Synthesis, Structure and Properties of Metallothioneins, Phytochelatins and Metal-Thiolate complexes*, VCH Publishers Inc, New York, 1992, 284.
- [35] J.S. Scheller, G.W. Irvine, M.J. Stillman, "Unravelling the mechanistic details of metal binding to mammalian metallothioneins from stoichiometric, kinetic, and binding affinity data" *Dalton Trans.* **47**, 3613-3637 (2018). doi: 10.1039/c7dt03319b
- [36] G. Digilio, C. Bracco, L. Vergani, M. Botta, D. Osella, A. Viarengo, "The cadmium binding domains in the metallothionein isoform Cd<sub>7</sub>-MT10 from *Mytilus galloprovincialis* revealed by NMR spectroscopy" *J. Biol. Inorg. Chem.* **14**, 167-178 (2009). doi: 10.1007/s00775-008-0435-y
- [37] C.A. Blindauer, M.T. Razi, D.J. Campopiano, P.J. Sadler, "Histidine ligands in bacterial metallothionein enhance cluster stability" *J. Biol. Inorg. Chem.* **12**, 393-405 (2007). doi: 10.1007/s00775-006-0196-4



- [38] C.A. Blindauer, "Metallothioneins with unusual residues: histidines as modulators of zinc affinity and reactivity" *J. Inorg. Biochem.* **102**, 507-521 (2008). doi: 10.1016/j.jinorgbio.2007.10.032
- [39] M. Tomas, M.A. Pagani, C.S. Andreo, M. Capdevila, R. Bofill, S. Atrian, "His-containing plant metallothioneins: comparative study of divalent metal-ion binding by plant MT3 and MT4 isoforms" *J. Biol. Inorg. Chem.* **19**, 1149-1164 (2014). doi: 10.1007/s00775-014-1170-1
- [40] S. Pérez-Rafael, A. Pagani, Ò. Palacios, R. Dallinger, M. Capdevila, S. Atrian "The role of histidine in a copper-specific metallothionein" *Z. Anorg. Allg. Chem.* **639**, 1356-1360 (2013). doi: 10.1002/zaac.201300053
- [41] P.C. Wilkins, R.G. Wilkins, in: R.G. Compton, S.G. Davies, J. Evans, L.F. Gladden (Eds.), *Inorganic Chemistry in Biology*, Oxford Higher Education, Oxford, 2015, 10
- [42] C.F. Shaw III, M.J. Stillman, K.T. Suzuki, in: M.J. Stillman, C.F. Shaw III, K.T. Suzuki (Eds.), *Metallothioneins Synthesis, Structure and Properties of Metallothioneins, Phytochelatins and Metal-Thiolate complexes*, VCH Publishers Inc, New York, 1992, 1.
- [43] J. Hidalgo, R. Chung, M. Penkowa, M. Vasák, in: A. Sigel, H. Sigel, R.K.O. Sigel (Eds.) *Metal Ions in Life Sciences (Vol. 5)*, The Royal Society of Chemistry, Cambridge, 2009, 279-317
- [44] A. Krezel, Q. Hao, W. Maret, "The zinc/thiolate redox biochemistry of metallothionein and the control of zinc ion fluctuations in cell signaling" *Arch. Biochem. Biophys.* **463**, 188-200 (2007). doi: 10.1016/j.abb.2007.02.017
- [45] S.L. Tucker, C.R. Thornton, K. Tasker, C. Jacob, G. Giles, M. Egan, N.J. Talbot, "A fungal metallothionein is required for pathogenicity of *Magnaporthe grisea*" *Plant Cell.* **16**, 1575-1588 (2004). doi: 10.1105/tpc.021279
- [46] A. Espart, M. Marín, S. Gil-Moreno, Ò. Palacios, F. Amaro, A. Martín-González, J.C. Gutiérrez, M. Capdevila, S. Atrian, "Hints for metal-preference protein sequence determinants: different metal binding features of the five *Tetrahymena thermophila* metallothioneins" *Int. J. Biol. Sci.* **11**, 456-471 (2015). doi: 10.7150/ijbs.11060
- [47] A. Ziller, R.K. Yadav, M. Capdevila, M.S. Reddy, L. Vallon, R. Marmeisse, S. Atrian, Ò. Palacios, L. Fraissinet-Tachet, "Metagenomics analysis reveals a new metallothionein family: Sequence and metal-binding features of new environmental cysteine-rich proteins" *J. Inorg. Biochem.* **167**, 1-11 (2017). doi: 10.1016/j.jinorgbio.2016.11.017
- [48] W. Braun, M. Vasák, A.H. Robbins, C.D. Stout, G. Wagner, J.H. Kägi, K. Wüthrich, "Comparison of the NMR solution structure and the x-ray crystal structure of rat metallothionein-2" *roc. Natl. Acad. Sci. U S A.* **89**, 10124-10128 (1992). doi: 10.1073/pnas.89.21.10124
- [49] C.W. Peterson, S.S. Narula, I.M. Armitage, "3D solution structure of copper and silver-substituted yeast metallothioneins" *FEBS Lett.* **379**, 85-93 (1996). doi: 10.1016/0014-5793(95)01492-6
- [50] E.A. Peroza, R. Schmucki, P. Güntert, E. Freisinger, O. Zerbe, "The beta(E)-domain of wheat E(c)-1 metallothionein: a metal-binding domain with a distinctive structure" *J. Mol. Biol.* **387**, 207-218 (2009). doi: 10.1016/j.jmb.2009.01.035

- [51] O. Palacios, A. Pagani, S. Pérez-Rafael, M. Egg, M. Höckner, A. Brandstätter, M. Capdevila, S. Atrian, R. Dallinger, “Shaping mechanisms of metal specificity in a family of metazoan metallothioneins: evolutionary differentiation of mollusc metallothioneins” *BMC Biol.* **9**:4 (2011). doi: 10.1186/1741-7007-9-4.
- [52] W. Braun, G. Wagner, E. Worgotter, M. Vasák, J.H. Kägi, K. Wüthrich “Polypeptide fold in the two metal clusters of metallothionein-2 by nuclear magnetic resonance in solution” *J Mol Biol.* **187**, 125–129 (1986). doi: 10.1016/0022-2836(86)90412-2
- [53] R. Riek, B. Prêcheur, Y. Wang, E.A. Mackay, G. Wider, P. Güntert, A. Liu, J.H. Kägi, K. Wüthrich “NMR structure of the sea urchin (*Strongylocentrotus purpuratus*) metallothionein MTA” *J. Mol. Biol.* **291**, 417-428 (1999). doi: 10.1006/jmbi.1999.2967
- [54] A. Muñoz., F.H. Forsterling, C.F. Shaw III, D.H. Petering “Structure of the  $^{113}\text{Cd}_3\beta$ domains from *Homarus americanus* metallothionein-1: hydrogen bonding and solvent accessibility of sulfur atoms” *J. Biol. Inorg. Chem.* **7**, 713–724 (2002). doi: 10.1007/s00775-002-0345-3
- [55] C. Baumann, A. Beil, S. Jurt, M. Niederwanger, O. Palacios, M. Capdevila, S. Atrian, R. Dallinger, O. Zerbe “Structural Adaptation of a Protein to Increased Metal Stress: NMR Structure of a Marine Snail Metallothionein with an Additional Domain” *Angew Chem Int Ed Engl.* **56**, 4617-4622 (2017). doi: 10.1002/anie.201611873
- [56] A. Beil, S. Jurt, R. Walser, T. Schönhut, P. Güntert, Ò. Palacios, S. Atrian, M. Capdevila, R. Dallinger, O. Zerbe “The Solution Structure and Dynamics of Cd-Metallothionein from *Helix pomatia* Reveal Optimization for Binding Cd over Zn” *Biochemistry* **58**, 4570-4581 (2019). doi: 10.1021/acs.biochem.9b00830
- [57] J. Domènech, R. Orihuela, G. Mir, M. Molinas, S. Atrian, M. Capdevila, “The Cd(II)-binding abilities of recombinant *Quercus suber* metallothionein: bridging the gap between phytochelatins and metallothioneins” *J. Biol. Inorg. Chem.* **12**, 867-882 (2007). doi: 10.1007/s00775-007-0241-y
- [58] X. Wan, E. Freisinger, “The plant metallothionein 2 from *Cicer arietinum* forms a single metal-thiolate cluster” *Metallomics* **1**, 489-500 (2009). doi: 10.1039/b906428a
- [59] S. Gil-Moreno, E. Jiménez-Martí, Ò. Palacios, O. Zerbe, R. Dallinger, M. Capdevila, S. Atrian “Does Variation of the Inter-Domain Linker Sequence Modulate the Metal Binding Behaviour of *Helix pomatia* Cd-Metallothionein?” *Int. J. Mol. Sci.* **17**:6 (2015). doi: 10.3390/ijms17010006
- [60] M. Nemer, D.G. Wilkinson, E.C. Travaglini, E.J. Sternberg, T.R. Butt, “Sea urchin metallothionein sequence: key to an evolutionary diversity” *Proc. Natl. Acad. Sci. USA.* **82**, 4992-4994 (1985). doi: 10.1073/pnas.82.15.4992
- [61] A.H. Robbins, D.E. McRee, M. Williamson, S.A. Collett, N.H. Xuong, W.F. Furey, B.C. Wang, C.D. Stout, “Refined crystal structure of Cd, Zn metallothionein at 2.0 Å resolution” *J. Mol. Biol.* **221**, 1269-1293 (1991).
- [62] V. Calderone, B. Dolderer, H.J. Hartmann, H. Echner, C. Luchinat, C. Del Bianco, S. Mangani, U. Weser, “The crystal structure of yeast copper thionein: the solution of a long-lasting enigma” *Proc. Natl. Acad. Sci. U S A.* **102**,51-56 (2005). doi: 10.1073/pnas.0408254101
- [63] R. Bofill, R. Orihuela, M. Romagosa, J. Domènech, S. Atrian, M. Capdevila, “*Caenorhabditis elegans* metallothionein isoform specificity-metal binding abilities

- and the role of histidine in CeMT1 and CeMT2" *FEBS J.* **276**, 7040-7056 (2009). doi: 10.1111/j.1742-4658.2009.07417
- [64] O. Palacios, K. Polec-Pawlak, R. Lobinski, M. Capdevila, P. González-Duarte, "Is Ag(I) an adequate probe for Cu(I) in structural copper-metallothionein studies? The binding features of Ag(I) to mammalian metallothionein 1" *J. Biol. Inorg. Chem.* **8**, 831-842 (2003). doi: 10.1007/s00775-003-0481-4
- [65] M.J. Stillman, "Metallothioneins", *Coord. Chem. Rev.* **144**, 461-511 (1995). [https://doi.org/10.1016/0010-8545\(95\)01173-M](https://doi.org/10.1016/0010-8545(95)01173-M)
- [66] M. Vasák, J.H. Kägi, H.A. Hill, "Zinc(II), cadmium(II), and mercury(II) thiolate transitions in metallothionein" *Biochemistry* **20**, 2852-2856 (1981). doi: 10.1021/bi00513a022
- [67] W.F. Furey, A.H. Robbins, L.L. Clancy, D.R. Winge, B.C. Wang, C.D. Stout, "Crystal structure of Cd,Zn metallothionein" *Science* **231**, 704-710 (1986). doi: 10.1126/science.3945804.
- [68] K.A. Melis, D.C. Carter, C.D. Stout, D.R. Winge, "Single crystals of cadmium, zinc metallothionein" *J. Biol. Chem.* **258**, 6255-6257 (1983).
- [69] E. Wörgötter, G. Wagner, M. Vasák, J.H. Kägi, K. Wüthrich, "Sequence-specific 1H-NMR assignments in rat-liver metallothionein-2" *Eur. J. Biochem.* **167**, 457-466 (1987). doi: 10.1111/j.1432-1033.1987.tb13359.x.
- [70] M. Vasák, E. Wörgötter, G. Wagner, J.H. Kägi, K. Wüthrich, "Metal coordination in rat liver metallothionein-2 prepared with or without reconstitution of the metal clusters, and comparison with rabbit liver metallothionein-2" *J. Mol. Biol.* **196**, 711-719 (1987). doi: 10.1016/0022-2836(87)90042-8
- [71] P. Schultze, E. Wörgötter, W. Braun, G. Wagner, M. Vasák, J.H. Kägi, K. Wüthrich, "Conformation of [Cd<sub>7</sub>]-metallothionein-2 from rat liver in aqueous solution determined by nuclear magnetic resonance spectroscopy" *J. Mol. Biol.* **203**, 251-268 (1988). doi: 10.1016/0022-2836(88)90106-4
- [72] B.A. Messerle, A. Schäffer, M. Vasák, J.H. Kägi, K. Wüthrich, "Three-dimensional structure of human [<sup>113</sup>Cd<sub>7</sub>]-metallothionein-2 in solution determined by nuclear magnetic resonance spectroscopy" *J. Mol. Biol.* **214**, 765-779 (1990). doi: 10.1016/0022-2836(90)90291-S
- [73] B.A. Messerle, A. Schäffer, M. Vasák, J.H. Kägi, K. Wüthrich "Comparison of the solution conformations of human [Zn<sub>7</sub>]-metallothionein-2 and [Cd<sub>7</sub>]-metallothionein-2 using nuclear magnetic resonance spectroscopy" *J. Mol. Biol.* **225**, 433-443 (1992). doi: 10.1016/0022-2836(92)90930-i
- [74] H. Wang, Q. Zhang, B. Cai, H. Li, K.H. Sze, Z.X. Huang, H.M. Wu, H. Sun, "Solution structure and dynamics of human metallothionein-3 (MT-3)" *FEBS Lett.* **580**, 795-800 (2006). doi: 10.1016/j.febslet.2005.12.099
- [75] G. Oz, K. Zangger, I.M. Armitage, "Three-dimensional structure and dynamics of a brain specific growth inhibitory factor: metallothionein-3" *Biochemistry* **40**, 11433-11441 (2001). doi: 10.1021/bi010827l.
- [76] M.H. Frey, G. Wagner, M. Vasák, O.W. Sørensen, D. Neuhaus, E. Wörgötter, J.H.R. Kägi, R.R. Ernst, K. Wüthrich, "Polypeptide-metal cluster connectivities in metallothionein 2 by novel proton-cadmium-113 heteronuclear two-dimensional NMR experiments" *J. Am. Chem. Soc.* **107**, 6847-6851 (1985). doi: 10.1021/ja00310a017

- [77] C. Capasso, V. Carginale, O. Crescenzi, D. Di Maro, E. Parisi, R. Spadaccini, P.A. Temussi, "Solution Structure of MT<sub>nc</sub>, a Novel Metallothionein from the Antarctic Fish *Notothenia coriiceps*" *Structure* **11**, 435-443 (2003). doi: 10.1016/S0969-2126(03)00044-3
- [78] S.S. Narula, M. Brouwer, X.Y. Hua, I.M. Armitage, "Three-dimensional solution structure of *Callinectes sapidus* metallothionein-1 determined by homonuclear and heteronuclear magnetic resonance spectroscopy" *Biochemistry* **34** 620-631 (1995). doi: 10.1021/bi00002a029
- [79] I. Bertini, H.J. Hartmann, T. Klein, G.H. Liu, C. Luchinat, U. Weser, "High resolution solution structure of the protein part of Cu<sub>7</sub> metallothionein" *Eur. J. Biochem.* **267**, 1008-1018 (2000). doi: 10.1046/j.1432-1327.2000.01093.x
- [80] P.A. Cobine, R.T. McKay, K. Zangger, C.T. Dameron, I.M. Armitage, "Solution structure of Cu<sub>6</sub> metallothionein from the fungus *Neurospora crassa*" *Eur. J. Biochem.* **271**, 4213-4221 (2004). doi: 10.1111/j.1432-1033.2004.04361.x
- [81] J. Loebus, E.A. Peroza, N. Blüthgen, T. Fox, W. Meyer-Klaucke, O. Zerbe, E. Freisinger, "Protein and metal cluster structure of the wheat metallothionein domain  $\gamma$ -E(c)-1: the second part of the puzzle" *J. Biol. Inorg. Chem.* **16**, 683-694 (2011). doi: 10.1007/s00775-011-0770-2
- [82] K. Tarasava, S. Johannsen, E. Freisinger, "Solution structure of the circular  $\gamma$ -domain analog from the wheat metallothionein E(c)-1" *Molecules* **18**, 14414-14429 (2013). doi: 10.3390/molecules181114414
- [83] J. Habjanič, O. Zerbe, E. Freisinger, "A histidine-rich *Pseudomonas* metallothionein with a disordered tail displays higher binding capacity for cadmium than zinc" *Metallomics*. **10**, 1415-1429 (2018). doi: 10.1039/c8mt00193f
- [84] C.A. Blindauer, M.D. Harrison, J.A. Parkinson, A.K. Robinson, J.S. Cavet, N.J. Robinson, P.J. Sadler, "A metallothionein containing a zinc finger within a four-metal cluster protects a bacterium from zinc toxicity" *Proc. Natl. Acad. Sci. U.S.A.* **98**, 9593-9598 (2001). doi: 10.1073/pnas.171120098
- [85] R.D. Palmiter, "The elusive function of metallothioneins" *Proc Natl Acad Sci U S A.* **95**, 8428-8430 (1998). doi: 10.1073/pnas.95.15.8428
- [86] A.Y. Abdin, C. Jacob, L. Kästner, "The Enigmatic Metallothioneins: A Case of Upward-Looking Research" *Int. J. Mol. Sci.* **22**:5984. doi: 10.3390/ijms22115984
- [87] N. Romero-Isart, M. Vasák, "Advances in the structure and chemistry of metallothioneins" *J. Inorg. Biochem.* **88**, 388-396 (2002). doi: 10.1016/s0162-0134(01)00347-6
- [88] S. Atrian, M. Capdevila, "Metallothionein-protein interactions" *Biomol. Concepts* **4**, 143-160 (2013). doi: 10.1515/bmc-2012-0049
- [89] N. Darby, T.E. Creighton "Disulfide bonds in protein folding and stability" *Methods Mol. Biol.* **40**, 219-252 (1995). doi: 10.1385/0-89603-301-5:219
- [90] S.G. Bell, B.L. Vallee, "The metallothionein/thionein system: an oxidoreductive metabolic zinc link" *Chembiochem.* **10**, 55-62 (2009). doi: 10.1002/cbic.200800511
- [91] W. Maret, "Redox biochemistry of mammalian metallothioneins" *J. Biol. Inorg. Chem.* **16**, 1079-1086 (2011). doi: 10.1007/s00775-011-0800-0.
- [92] Y. Yang, W. Maret, B.L. Vallee, "Differential fluorescence labeling of cysteinyl clusters uncovers high tissue levels of thionein" *Proc. Natl. Acad. Sci. U.S.A.* **98**, 5556-5559 (2001). doi: 10.1073/pnas.101123298

- [93] A. Krezel, W. Maret "Thionein/metallothionein control Zn(II) availability and the activity of enzymes" *J. Biol. Inorg. Chem.* **13**, 401-409 (2008). doi: 10.1007/s00775-007-0330-y.
- [94] H. Irving, R.J.P. Williams, "The stability of transition-metal complexes" *J. Chem. Soc.* **0**, 3192-3210 (1953). doi:10.1039/JR9530003192
- [95] J.D. Otvos, H.R. Engeseth, D.G. Nettesheim, C.R. Hilt "Interprotein metal exchange reactions of metallothionein" *Experientia Suppl.* **52**:171-178 (1987).
- [96] I. El Ghazi, B.L. Martin, I.M. Armitage, "New proteins found interacting with brain metallothionein-3 are linked to secretion" *Int. J. Alzheimer's Dis.* **2011**:208634 (2010). doi: 10.4061/2011/208634
- [97] A. Mahim, M. Mahim, D.H. Petering "Zinc Trafficking 1. Probing the Roles of Proteome, Metallothionein, and Glutathione" *Metallomics*. mfab055 (2021). doi: 10.1093/mtomcs/mfab055.
- [98] W. Maret, G. Heffron, H. A. O. Hill, D. Djuricic, L.-J. Jiang, B. L. Vallee, "The ATP/metallothionein interaction: NMR and STM" *Biochemistry* **41**, 1689-1694 (2002). doi: 10.1021/bi0116083
- [99] L.-J. Jiang, W. Maret and B. L. Vallee, The glutathione redox couple modulates zinc transfer from metallothionein to zinc-depleted sorbitol dehydrogenase, *Proc. Natl. Acad. Sci. U. S. A.* **95**, 3483-3488 (1998). doi:10.1073/pnas.95.7.3483
- [100] R.J.P. Williams, J.J.R. Frausto Da Silva, in: R.J.P. Williams, J.J.R. Frausto Da Silva (Eds.), *The biological chemistry of the elements: the inorganic chemistry of life*, Oxford University Press, New York, 2001, 299-341.
- [101] C.A. Blindauer, P.J. Sadler, "How to hide zinc in a small protein" *Acc. Chem. Res.* **38**, 62-69 (2005). doi: 10.1021/ar030182c
- [102] H. Shen, H. Qin, J. Guo "Cooperation of metallothionein and zinc transporters for regulating zinc homeostasis in human intestinal Caco-2 cells" *Nutr. Res.* **28**, 406-413 (2008). doi: 10.1016/j.nutres.2008.02.011
- [103] W. Maret, "Fluorescent probes for the structure and function of metallothionein" *J. Chromatogr. B. Analyt. Technol. Biomed. Life Sci.* **877**, 3378-3383 (2009). doi: 10.1016/j.jchromb.2009.06.014
- [104] W. Maret, "Zinc and Sulfur: A Critical Biological Partnership" *Biochemistry* **43**, 3301-3309 (2004). doi: 10.1021/bi036340p
- [105] A. Martelli, E. Rousselet, C. Dycke, A. Bouron, J.M. Moulis, "Cadmium toxicity in animal cells by interference with essential metals" *Biochimie.* **88**, 1807-1814 (2006). doi: 10.1016/j.biochi.2006.05.013
- [106] C.D. Klaassen, J. Liu, S. Choudhuri, "Metallothionein: an intracellular protein to protect against cadmium toxicity" *Annu. Rev. Pharmacol. Toxicol.* **39**, 267-294 (1999). doi: 10.1146/annurev.pharmtox.39.1.267
- [107] B.A. Masters, E.J. Kelly, C.J. Quaipe, R.L. Brinster, R.D. Palmiter, "Targeted disruption of metallothionein I and II genes increases sensitivity to cadmium" *Proc. Natl. Acad. Sci. U.S.A.* **91**, 584-588 (1994). doi: 10.1073/pnas.91.2.584
- [108] J.C. Amiard, C. Amiard-Triquet, S. Barka, J. Pellerin, P.S. Rainbow, "Metallothioneins in aquatic invertebrates: their role in metal detoxification and their use as biomarkers" *Aquat. Toxicol.* **76**, 160-202 (2006). doi: 10.1016/j.aquatox.2005.08.015

- [109] P. Simoniello, C.M. Motta, R. Scudiero, F. Trinchella, S. Filosa, "Cadmium-induced teratogenicity in lizard embryos: correlation with metallothionein gene expression" *Comp. Biochem. Physiol. C. Toxicol. Pharmacol.* **153**, 119-127 (2011). doi: 10.1016/j.cbpc.2010.09.007
- [110] E. Moltó, E. Bonzón-Kulichenko, A. del Arco, D.M. López-Alañón, O. Carrillo, N. Gallardo, A. Andrés "Cloning, tissue expression and metal inducibility of an ubiquitous metallothionein from *Panulirus argus*" *Gene* **361**, 140-148 (2005). doi: 10.1016/j.gene.2005.07.026
- [111] R. Dallinger, Y. Wang, B. Berger, E.A. Mackay, J.H. Kägi, "Spectroscopic characterization of metallothionein from the terrestrial snail, *Helix pomatia*" *Eur J Biochem.* **268**, 4126-4133 (2001). doi: 10.1046/j.1432-1327.2001.02318.x
- [112] S. Pérez-Rafael, F. Monteiro, R. Dallinger, S. Atrian, O. Palacios, M. Capdevila, "Cantareus aspersus metallothionein metal binding abilities: the unspecific CaCd/CuMT isoform provides hints about the metal preference determinants in metallothioneins" *Biochim. Biophys. Acta.* **1844**, 1694-1707 (2014). doi: 10.1016/j.bbapap.2014.06.018
- [113] G.K. Andrews, "Regulation of metallothionein gene expression by oxidative stress and metal ions" *Biochem. Pharmacol.* **59**, 95-104 (2000). doi: 10.1016/s0006-2952(99)00301-9
- [114] V. Pedrini-Martha, M. Niederwanger, R. Kopp, R. Schnegg, R. Dallinger, "Physiological, Diurnal and Stress-Related Variability of Cadmium-Metallothionein Gene Expression in Land Snails" *PLoS One* **11**:e0150442 (2016). doi: 10.1371/journal.pone.0150442
- [115] S.X. Liu, J.P. Fabisiak, V.A. Tyurin, G.G. Borisenko, B.R. Pitt, J.S. Lazo, V.E. Kagan, "Reconstitution of apo-superoxide dismutase by nitric oxide-induced copper transfer from metallothioneins" *Chem. Res. Toxicol.* **13**, 922-931 (2000). doi: 10.1021/tx0000623
- [116] M. Valko, C.J. Rhodes, J. Moncol, M. Izakovic, M. Mazur "Free radicals, metals and antioxidants in oxidative stress-induced cancer" *Chem. Biol. Interact.* **160**, 1-40 (2006). doi: 10.1016/j.cbi.2005.12.009
- [117] A. Formigari, P. Irato, A. Santon, "Zinc, antioxidant systems and metallothionein in metal mediated-apoptosis: biochemical and cytochemical aspects" *Comp. Biochem. Physiol. C. Toxicol. Pharmacol.* **146**, 443-459 (2007). doi: 10.1016/j.cbpc.2007.07.010
- [118] J.R. Prohaska, A.A. Gybina, "Intracellular copper transport in mammals" *J. Nutr.* **134**, 1003-1006 (2004). doi: 10.1093/jn/134.5.1003
- [119] Y.J. Kang, "Metallothionein redox cycle and function" *Exp. Biol. Med. (Maywood)* **231**, 1459-1467 (2006). doi: 10.1177/153537020623100903
- [120] A. Viarengo, B. Burlando, N. Ceratto, I. Panfoli, "Antioxidant role of metallothioneins: a comparative overview" *Cell. Mol. Biol. (Noisy-le-grand)* **46**, 407-417 (2000).
- [121] A.R. Quesada, R.W. Byrnes, S.O. Krezoski, D.H. Petering, "Direct reaction of H<sub>2</sub>O<sub>2</sub> with sulfhydryl groups in HL-60 cells: zinc-metallothionein and other sites" *Arch. Biochem. Biophys.* **334**, 241-250 (1996). doi: 10.1006/abbi.1996.0452
- [122] A.O. Udom, F.O. Brady, "Reactivation in vitro of zinc-requiring apo-enzymes by rat liver zinc-thionein" *Biochem. J.* **187**, 329-335 (1980). doi: 10.1042/bj1870329

- [123] M. Beltramini, K. Lerch, "Copper transfer between *Neurospora* copper metallothionein and type 3 copper apoproteins" *FEBS Lett.* **142**, 219-222 (1982). doi: 10.1016/0014-5793(82)80138-5
- [124] M. Brouwer, P. Whaling, D.W. Engel, "Copper-Metallothioneins in the American Lobster, *Homarus americanus*: Potential role as Cu(I) donors to apohemocyanin" *Environ. Hlth. Persp.* **65**, 93-100 (1986). doi: 10.1289/ehp.866593
- [125] D.R. Winge, L.T. Jensen, C. Srinivasan, "Metal-ion regulation of gene expression in yeast" *Curr. Opin. Chem. Biol.* **2**, 216-221 (1998). doi: 10.1016/s1367-5931(98)80063-x
- [126] M. Si, J. Lang, "The roles of metallothioneins in carcinogenesis" *J. Hematol. Oncol.* **11**:107 (2018). doi: 10.1186/s13045-018-0645-x
- [127] Y.Q. Pan, M. Niu, S.M. Liu, Y.X. Bao, K. Yang, X.B. Ma, L. He, Y.X. Li, J.X. Cao, X. Zhang, Y. Du, "Effect of MT2A on apoptosis and proliferation in HL60 cells" *Int. J. Med. Sci.* **18**, 2910-2919 (2021). doi: 10.7150/ijms.57821
- [128] P.S. Rao, M. Jaggi, D.J. Smith, G.P. Hemstreet, K.C. Balaji, "Metallothionein 2A interacts with the kinase domain of PKCmu in prostate cancer" *Biochem. Biophys. Res. Commun.* **310**, 1032-1038 (2003). doi: 10.1016/j.bbrc.2003.09.118
- [129] M. Dutsch-Wicherek, J. Sikora, R. Tomaszewska, "The possible biological role of metallothionein in apoptosis" *Front. Biosci.* **13**, 4029-4038 (2008). doi: 10.2741/2991
- [130] D. Liu, M. Wang, T. Tian, X.J. Wang, H.F. Kang, T.B. Jin, S.Q. Zhang, H.T. Guan, P.T. Yang, K. Liu, X.H. Liu, P. Xu, Y. Zheng, Z.J. Dai, "Genetic polymorphisms (rs10636 and rs28366003) in metallothionein 2A increase breast cancer risk in Chinese Han population" *Aging (Albany NY)*. **9**, 547-555 (2017). doi: 10.18632/aging.101177
- [131] Y. Zheng, L. Jiang, Y. Hu, C. Xiao, N. Xu, J. Zhou, X. Zhou, "Metallothionein 1H (MT1H) functions as a tumor suppressor in hepatocellular carcinoma through regulating Wnt/ $\beta$ -catenin signaling pathway" *BMC Cancer*. **17**: 161 (2017). doi: 10.1186/s12885-017-3139-2
- [132] E. Mocchegiani, L. Costarelli, A. Basso, R. Giacconi, F. Piacenza, M. Malavolta, "Metallothioneins, ageing and cellular senescence: a future therapeutic target" *Curr. Pharm. Des.* **19**, 1753-1764 (2013).
- [133] S. Bhandari, C. Melchiorre, K. Dostie, D. Laukens, L. Devisscher, A. Louwrier, A. Thees, M.A. Lynes, "Detection and Manipulation of the Stress Response Protein Metallothionein" *Curr. Protoc. Toxicol.* **71**, 1-28 (2017). doi: 10.1002/cptx.17
- [134] M.A. Lynes, J. Hidalgo, Y. Manso, L. Devisscher, D. Laukens, D.A. Lawrence, "Metallothionein and stress combine to affect multiple organ systems" *Cell Stress Chaperones*. **19**, 605-611 (2014). doi: 10.1007/s12192-014-0501-z
- [135] M. Sato, T. Kawakami, M. Kondoh, M. Takiguchi, Y. Kadota, S. Himeno, S. Suzuki, "Development of high-fat-diet-induced obesity in female metallothionein-null mice" *FASEB J.* **24**, 2375-2384 (2010). doi: 10.1096/fj.09-145466
- [136] M. Sato, T. Kawakami, Y. Kadota, M. Mori, S. Suzuki, "Obesity and metallothionein" *Curr. Pharm. Biotechnol.* **14**, 432-440 (2013). doi: 10.2174/1389201011314040008
- [137] Y. Kadota, Y. Toriuchi, Y. Aki, Y. Mizuno, T. Kawakami, T. Nakaya, M. Sato, S. Suzuki, "Metallothioneins regulate the adipogenic differentiation of 3T3-L1 cells via

- the insulin signaling pathway” *PLoS One*. **12**:e0176070 (2017). doi: 10.1371/journal.pone.0176070
- [138] R.B. Russell, “Classification of Protein Folds” *Molecular Biotechnology* **20**, 17–28 (2002). doi:10.1385/mb:20:1:017
- [139] B. Alberts, A. Johnson, J. Lewis, M. Raff, K. Roberts, P. Walter, in: J.H. Wilson, T. Hunt (Eds), *Molecular Biology of the Cell* (4<sup>th</sup> Ed), Garland Science, New York, 2002.
- [140] R.J. Sommer, “Homology and the hierarchy of biological systems” *Bioessays*. **30**, 653-658 (2008). doi: 10.1002/bies.20776
- [141] P.-A. Binz, J. H. R. Kägi, in: C.D. Klaassen (Ed.) *Metallothionein IV*, Birkhauser verlag, Basel, 1999, pp. 7–13.
- [142] B.A. Fowler, C.E. Hilderbrand, Y. Kojima, M. Webb, “Nomenclature of Metallothionein” *Exp. Suppl.* **52**, 19-22 (1987). doi: 10.1007/978-3-0348-6784-9\_2
- [143] J.H. Kägi, A. Schäffer, “Biochemistry of metallothionein” *Biochemistry*. **27**, 8509-8515 (1988). doi: 10.1021/bi00423a001
- [144] A. Murasugi, C. Wada, Y. Hayashi, “Purification and unique properties in UV and CD spectra of Cd-binding peptide 1 from *Schizosaccharomyces pombe*” *Biochem. Biophys. Res. Commun.* **103**, 1021-1015 (1981). doi: 10.1016/0006-291x(81)90911-6
- [145] A. Murasugi, C. Wada, Y. Hayashi, “Cadmium-binding peptide induced in fission yeast, *Schizosaccharomyces pombe*” *J. Biochem.* **90**, 1561-1564 (1981). doi: 10.1093/oxfordjournals.jbchem.a133627
- [146] N. Kondo, K. Imai, M. Isobe, T. Goto, A. Murasugi, C. Wada-Nakagawa, Y. Hayashi, “Cadystin a and b, major unit peptides comprising cadmium binding peptides induced in a fission yeast separation, revision of structures and synthesis” *Tetrahedron Letters* **25**, 3869-3872 (1984). doi: 10.1016/s0040-4039(01)91190-6
- [147] M. Höckner, K. Stefanon, A. de Vaufleury, F. Monteiro, S. Pérez-Rafael, O. Palacios, M. Capdevila, S. Atrian, R. Dallinger, “Physiological relevance and contribution to metal balance of specific and non-specific Metallothionein isoforms in the garden snail, *Cantareus aspersus*” *Biomaterials* **24**, 1079–1092 (2011). doi: 10.1007/s10534-011-9466-x
- [148] M. Valls, R. Bofill, R. Gonzalez-Duarte, P. Gonzalez-Duarte, M. Capdevila, S. Atrian, “A new insight into metallothionein (MT) classification and evolution. The in vivo and in vitro metal binding features of *Homarus americanus* recombinant MT” *J. Biol. Chem.* **276**, 32835-32843 (2001). doi: 10.1074/jbc.M102151200
- [149] R.D. Schaeffer, V. Daggett, “Protein folds and protein folding” *Protein. Eng. Des. Sel.* **1-2**, 11-9 (2011). <https://doi.org/10.1093/protein/gzq096>
- [150] J. Ejniak, J. Robinson, J. Zhu, H. Försterling, C.F. Shaw, D.H. Petering, “Folding pathway of apo-metallothionein induced by Zn<sup>2+</sup>, Cd<sup>2+</sup> and Co<sup>2+</sup>” *J. Inorg. Biochem.* **88**, 144-152 (2002). [https://doi.org/10.1016/s0162-0134\(01\)00393-2](https://doi.org/10.1016/s0162-0134(01)00393-2)
- [151] S.H. Chen, L. Chen, D.H. Russell, “Metal-induced conformational changes of human metallothionein-2A: a combined theoretical and experimental study of metal-free and partially metalated intermediates” *J. Am. Chem. Soc.* **136**, 9499-508 (2014). <https://doi.org/10.1021/ja5047878>
- [152] C. Ding, R.A. Festa, Y.L. Chen, A. Espart, Ò. Palacios, J. Espín, M. Capdevila, S. Atrian, J. Heitman, D.J. Thiele, “*Cryptococcus neoformans* copper detoxification



- machinery is critical for fungal virulence” *Cell Host Microbe*. **13**, 265-76 (2013). doi: 10.1016/j.chom.2013.02.002
- [153] O. Palacios, A. Espart, J. Espín, C. Ding, D.J. Thiele, S. Atrian, M. Capdevila, “Full characterization of the Cu-, Zn and Cd-binding properties of CnMT1 and CnMT2, two metallothioneins of the pathogenic fungus *Cryptococcus neoformans* acting as virulence factors” *Metallomics* **6**, 279-291 (2014). doi: 10.1039/c3mt00266g
- [154] R. Bofill, M. Capdevila, S. Atrian, “Independent metal-binding features of recombinant metallothioneins convergently draw a step gradation between Zn- and Cu-thioneins” *Metallomics* **1**, 229-234 (2009). doi: 10.1039/b904953c
- [155] M. Capdevila, J. Domènech, A. Pagani, L. Tío, L. Villarreal, S. Atrian, “Zn- and Cd-metallothionein recombinant species from the most diverse phyla may contain sulfide (S<sup>2-</sup>) ligands” *Angew. Chem. Int. Ed. Engl.* **44**, 4618-4622 (2005). doi: 10.1002/anie.200501183
- [156] A. Pagani, L. Villarreal, M. Capdevila, S. Atrian, “The *Saccharomyces cerevisiae* Crs5 Metallothionein metal-binding abilities and its role in the response to zinc overload” *Mol. Microbiol.* **63**, 256-69 (2007). doi: 10.1111/j.1365-2958.2006.05510.x
- [157] M. Niederwanger, S. Calatayud, O. Zerbe, S. Atrian, R. Albalat, M. Capdevila, Ò. Palacios, R. Dallinger “*Biomphalaria glabrata* Metallothionein: Lacking Metal Specificity of the Protein and Missing Gene Upregulation Suggest Metal Sequestration by Exchange Instead of through Selective Binding” *Int. J. Mol. Sci.* **18**:1457 (2017). doi: 10.3390/ijms18071457
- [158] T.K.S. Janssens, D. Roelofs, N.M. Van Straalen “Molecular mechanisms of heavy metal tolerance and evolution in invertebrates” *Insect Sci.* **16**, 3-18 (2009). doi: 10.1111/j.1744-7917.2009.00249.x
- [159] A. Faddeeva-Vakhrusheva, M.F. Derks, S.Y. Anvar, V. Agamennone, W. Suring, S. Smit, N.M. van Straalen, D. Roelofs, “Gene Family Evolution Reflects Adaptation to Soil Environmental Stressors in the Genome of the Collembolan *Orchesella cincta*” *Genome Biol. Evol.* **8**, 2106-2117 (2016). doi: 10.1093/gbe/evw134
- [160] C. Zhang, M. Jansen, L. De Meester, R. Stoks, “Thermal evolution offsets the elevated toxicity of a contaminant under warming: A resurrection study in *Daphnia magna*”. *Evol. Appl.* **11**, 1425-1436 (2018). doi: 10.1111/eva.12637
- [161] I. El Ghazi, B.L. Martin, I.M. Armitage, “New proteins found interacting with brain metallothionein-3 are linked to secretion” *Int. J. Alzheimers Dis.* **2011**, 208634 (2010). doi: 10.4061/2011/208634
- [162] E.A. Ostrakhovitch, P.E. Olsson, S. Jiang, M.G. Cherian, “Interaction of metallothionein with tumor suppressor p53 protein” *FEBS Lett.* **580**, 1235-1238 (2006). doi: 10.1016/j.febslet.2006.01.036
- [163] Z. Jiang, B. Shen, J. Xiang, “Metal-dependent interactions of metallothionein-3  $\beta$ -domain with amyloid- $\beta$  peptide and related physiological implications” *J. Inorg. Biochem.* **196**, 110693 (2019). doi: 10.1016/j.jinorgbio.2019.110693
- [164] P. de Francisco, L.M. Melgar, S. Díaz, A. Martín-González, J.C. Gutiérrez, “The *Tetrahymena* metallothionein gene family: twenty-one new cDNAs, molecular characterization, phylogenetic study and comparative analysis of the gene expression under different abiotic stressors” *BMC Genomics* **17**, 346 (2016). doi: 10.1186/s12864-016-2658-6

- [165] M.J. Jenny, S.L. Payton, D.A. Baltzegar, J.D. Lozier, "Phylogenetic analysis of molluscan metallothioneins: evolutionary insight from *Crassostrea virginica*" *J. Mol. Evol.* **83**, 110–125 (2016). doi: 10.1007/s00239-016-9758-4
- [166] B. Roschitzki, M. Vasák, "Redox labile site in a Zn<sub>4</sub> cluster of Cu<sub>4</sub>Zn<sub>4</sub>-metallothionein-3" *Biochemistry* **42**, 9822–9828 (2003). doi: 10.1021/bi034816z
- [167] C. J. Quaipe, S. D. Findley, J. C. Erickson, G. J. Froelick, E. J. Kelly, B. P. Zambrowicz and R. D. Palmiter, "Induction of a New Metallothionein Isoform (Mt-IV) Occurs During Differentiation of Stratified Squamous Epithelia" *Biochemistry* **33**, 7250–7259 (1994). doi: 10.1021/bi00189a029
- [168] J. Calvo, H. Jung, G. Meloni, "Copper metallothioneins" *IUBMB Life* **69**, 236–245 (2017). doi: 10.1002/iub.1618
- [169] A.C.S. Cabral, J. Jakovleska, A. Deb, J.E. Penner-Hahn, V.L. Pecoraro, E. Freisinger, "Further insights into the metal ion binding abilities and the metalation pathway of a plant metallothionein from *Musa acuminata*" *J. Biol. Inorg. Chem.* **23**, 91–107 (2018). doi: 10.1007/s00775-017-1513-9
- [170] C.A. Blindauer, R. Schmid, "Cytosolic metal handling in plants: determinants for zinc specificity in metal transporters and metallothioneins" *Metallomics.* **2**, 510–529 (2010). doi: 10.1039/c004880a
- [171] A. Moleirinho, J. Carneiro, R. Matthiesen, R. M. Silva, A. Amorim, L. Azevedo, "Gains, Losses and Changes of Function after Gene Duplication: Study of the Metallothionein Family" *PLoS One* **6**, e18487 (2011). doi: 10.1371/journal.pone.0018487
- [172] M. Vasák, D.W. Hasler, "Metallothioneins: new functional and structural insights" *Curr. Opin. Chem. Biol.* **4**, 177–183 (2000). doi: 10.1016/s1367-5931(00)00082-x
- [173] A. Krezel and W. Maret, "Dual Nanomolar and Picomolar Zn(II) Binding Properties of Metallothionein" *J. Am. Chem. Soc.* **129**, 10911–10921 (2007). doi: 10.1021/ja071979s
- [174] W. Maret and A. Krezel, "Cellular zinc and redox buffering capacity of metallothionein/thionein in health and disease" *Mol. Med.* **13**, 371–375 (2007). doi: 10.2119/2007-00036.Maret.
- [175] Y. Uchida, K. Takio, K. Titani, Y. Ihara and M. Tomonaga, "The growth inhibitory factor that is deficient in the Alzheimer's disease brain is a 68 amino acid metallothionein-like protein" *Neuron* **7**, 337–347 (1991). doi: 10.1016/0896-6273(91)90272-2
- [176] E. Artells, O. Palacios, M. Capdevila, S. Atrian, "In vivo-folded metal-metallothionein 3 complexes reveal the Cu-thionein rather than Zn-thionein character of this brain-specific mammalian metallothionein" *FEBS J.* **281**, 1659–1678 (2014). doi: 10.1111/febs.12731
- [177] R. Bogumil, P. Faller, D. L. Pountney and M. Vasák, "Evidence for Cu(I) clusters and Zn(II) clusters in neuronal growth-inhibitory factor isolated from bovine brain" *Eur. J. Biochem.* **238**, 698–705 (1996). doi: 10.1111/j.1432-1033.1996.0698w.x
- [178] M. Vasák, G. Meloni, "Chemistry and biology of mammalian metallothioneins" *J. Biol. Inorg. Chem.* **16**, 1067–1078 (2011). doi: 10.1007/s00775-011-0799-2
- [179] B. Dolderer, H. Echner, A. Beck, H.J. Hartmann, U. Weser, C. Luchinat, C. Del Bianco, "Coordination of three and four Cu(I) to the alpha- and beta-domain of

- vertebrate Zn-metlothionein-1, respectively, induces significant structural changes" *FEBS J.* **274**, 2349-2362 (2007). doi: 10.1111/j.1742-4658.2007.05770.x
- [180] E. Artells, Ò. Palacios, M. Capdevila, S. Atrian, "Mammalian MT1 and MT2 metallothioneins differ in their metal binding abilities" *Metallomics* **5**, 1397-1410 (2013). doi: 10.1039/c3mt00123g
- [181] N. Cols, N. Romero-Isart, R. Bofill, M. Capdevila, P. González-Duarte, R. González-Duarte, S. Atrian, "In vivo copper- and cadmium-binding ability of mammalian metallothionein beta domain" *Protein Eng.* **12**, 265-269 (1999). doi: 10.1093/protein/12.3.265
- [182] R. Bofill, O. Palacios, M. Capdevila, N. Cols, R. González-Duarte, S. Atrian, P. González-Duarte "A new insight into the Ag<sup>+</sup> and Cu<sup>+</sup> binding sites in the metallothionein beta domain" *J. Inorg. Biochem.* **73**, 57-64 (1999). doi: 10.1016/S0162-0134(98)10091-0
- [183] C. Pérez-Zúñiga, À. Leiva-Presa, R.N. Austin, M. Capdevila, Ò. Palacios, "Pb(II) binding to the brain specific mammalian metallothionein isoform MT3 and its isolated  $\alpha$ MT3 and  $\beta$ MT3 domains" *Metallomics* **11**, 349-361 (2019). doi: 10.1039/c8mt00294k
- [184] N. Romero-Isart, N. Cols, M.K. Termansen, J.L. Gelpí, R. González-Duarte, S. Atrian, M. Capdevila, P. González-Duarte, "Replacement of terminal cysteine with histidine in the metallothionein alpha and beta domains maintains its binding capacity" *Eur J Biochem.* **259**, 519-527 (1999). doi: 10.1046/j.1432-1327.1999.00074.x
- [185] Ò. Palacios, E. Jiménez-Martí, M. Niederwanger, S. Gil-Moreno, O. Zerbe, S. Atrian, R. Dallinger, M. Capdevila, "Analysis of Metal-Binding Features of the Wild Type and Two Domain-Truncated Mutant Variants of *Littorina littorea* Metallothionein Reveals Its Cd-Specific Character" *Int. J. Mol. Sci.* **18**:1452 (2017). doi: 10.3390/ijms18071452
- [186] L. Villarreal, L. Tío, M. Capdevila, S. Atrian, "Comparative metal binding and genomic analysis of the avian (chicken) and mammalian metallothionein" *FEBS J.* **273**, 523-535 (2006). doi: 10.1111/j.1742-4658.2005.05086.x
- [187] H. Zhou, K.M. Cadigan, D.J. Thiele, "A copper-regulated transporter required for copper acquisition, pigmentation, and specific stages of development in *Drosophila melanogaster*" *J. Biol. Chem.* **278**, 48210-48218 (2003). doi: 10.1074/jbc.M309820200
- [188] S. Atrian, in: A. Sigel, H. Sigel, R.K.O. Sigel (Eds.) Metal ions in Life Sciences: Metallothioneins and Related Chelators (Vol. 5), RSC Publishing, Cambridge, 2009, 155-181.
- [189] J.A. Marques, S.R. Costa, A.D. Maraschi, C.E.D. Vieira, P.G. Costa, G. de Martinez, C. Martins, H.F. Santos, M.M Souza, J.Z. Sandrini, A. Bianchini "Biochemical response and metals bioaccumulation in planktonic communities from marine areas impacted by the Fundão mine dam rupture (southeast Brazil)" *Sci. Total. Environ.* **2**, 150727 (2021). doi: 10.1016/j.scitotenv.2021.150727
- [190] E. Shahri, M.H. Sayadi, E. Yousefi, M. Savabieasfehiani, "Metal Contamination of Oman Sea Seaweed and Its Associated Public Health Risks" *Biol. Trace. Elem. Res.* (2021) doi: 10.1007/s12011-021-02865-1

- [191] D. Egli, J. Domènech, A. Selvaraj, K. Balamurugan, H. Hua, M. Capdevila, O. Georgiev, W. Schaffner, S. Atrian, “The four members of the *Drosophila* metallothionein family exhibit distinct yet overlapping roles in heavy metal homeostasis and detoxification” *Genes Cells*. **11**, 647-658 (2006). doi: 10.1111/j.1365-2443.2006.00971.x
- [192] M. Valls, R. Bofill, N. Romero-Isart, R. González-Duarte, J. Abián, M. Carrascal, P. González-Duarte, M. Capdevila, S. Atrian, “*Drosophila* MTN: a metazoan copper-thionein related to fungal forms” *FEBS Lett*. **467**, 189-194 (2000). doi: 10.1016/s0014-5793(00)01149-2
- [193] J. Domenech, O. Palacios, L. Villarreal, P. González-Duarte, M. Capdevila, S. Atrian, “MTO: the second member of a *Drosophila* dual copper-thionein system” *FEBS Lett*. **533**, 72-78 (2003). doi: 10.1016/s0014-5793(02)03754-7
- [194] S. Pérez-Rafael, A. Kurz, M. Guirola, M. Capdevila, O. Palacios, S. Atrian, “Is MtnE, the fifth *Drosophila* metallothionein, functionally distinct from the other members of this polymorphic protein family?” *Metallomics* **4**, 342-349 (2012). doi: 10.1039/c2mt00182a
- [195] M. Guirola, Y. Naranjo, M. Capdevila, S. Atrian, “Comparative genomics analysis of metallothioneins in twelve *Drosophila* species” *J. Inorg. Biochem*. **105**, 1050-1059 (2011). doi: 10.1016/j.jinorgbio.2011.05.004
- [196] M. Tomas, J. Domènech, M. Capdevila, R. Bofill, S. Atrian, “The sea urchin metallothionein system: Comparative evaluation of the SpMTA and SpMTB metal-binding preferences” *FEBS Open Bio*. **3**, 89-100 (2013). doi: 10.1016/j.fob.2013.01.005
- [197] M. Guirola, S. Pérez-Rafael, M. Capdevila, O. Palacios, S. Atrian, “Metal dealing at the origin of the Chordata phylum: the metallothionein system and metal overload response in amphioxus” *PLoS One* **7**, e43299 (2012). doi: 10.1371/journal.pone.0043299
- [198] A. Wanninger, T. Wollesen, “The evolution of molluscs” *Biol. Rev. Camb. Philos. Soc*. **94**, 102-115 (2018). doi: 10.1111/brv.12439
- [199] W. Ponder, D.R.R. Lindberg, in: W. Ponder, D.R.R. Lindberg (Eds.), *Phylogeny and Evolution of the Mollusca*, University of California Press, Oakland, 2008.
- [200] G. Maroni, J. Wise, J.E. Young, E. Otto, “Metallothionein gene duplications and metal tolerance in natural populations of *Drosophila melanogaster*” *Genetics* **117**, 739-744 (1987). doi: 10.1093/genetics/117.4.739
- [201] G.M. Adamo, M. Lotti, M.J. Tamas, S. Brocca, “Amplification of the CUP1 gene is associated with evolution of copper tolerance in *Saccharomyces cerevisiae*” *Microbiology* **158**, 2325-2335 (2012). doi: 10.1099/mic.0.058024-0.
- [202] A. Tanguy, D. Moraga, “Cloning and characterization of a gene coding for a novel metallothionein in the Pacific oyster *Crassostrea gigas* (CgMT2): a case of adaptive response to metal induced stress?” *Gene* **273**, 123-130 (2001). doi: 10.1016/s0378-1119(01)00577-7
- [203] V. Pedrini-Martha, S. Koll, M. Dvorak, R. Dallinger, “Cadmium uptake, MT gene activation and structure of large-sized multi-domain metallothioneins in the terrestrial door snail *Alinda biplicata* (Gastropoda, Clausiliidae)” *Int. J. Mol. Sci*. **21**:1631 (2020). doi: 10.3390/ijms21051631

- [204] M.J. Timmermans, J. Ellers, D. Roelofs, N.M. van Straalen “Metallothionein mRNA expression and cadmium tolerance in metal-stressed and reference populations of the springtail *Orchesella cincta*” *Ecotoxicology*. **14**, 727-739 (2005). doi: 10.1007/s10646-005-0020-x
- [205] T.K. Janssens, R. Lopéz, J. Mariën, M.J. Timmermans, K. Montagne-Wajer, N.M. van Straalen, D. Roelofs “Comparative population analysis of metallothionein promoter alleles suggests stress-induced microevolution in the field” *Environ. Sci. Technol.* **42**, 3873-3878 (2008). doi: 10.1021/es702618s
- [206] D. Costa, J. Mariën, T.K. Janssens, C.A. van Gestel, G. Driessen, J.P. Sousa, N.M. van Straalen, D. Roelofs, “Influence of adaptive evolution of cadmium tolerance on neutral and functional genetic variation in *Orchesella cincta*” *Ecotoxicology* **21**, 2078-2087 (2012). doi: 10.1007/s10646-012-0961-9
- [207] L. Tío, L. Villarreal, S. Atrian, M. Capdevila “Functional differentiation in the mammalian metallothionein gene family: metal binding features of mouse MT4 and comparison with its paralog MT1” *J. Biol. Chem.* **279**, 24403-24413 (2004). doi: 10.1074/jbc.M401346200
- [208] P. de Francisco, A. Martín-González, A.P. Turkewitz, J.C. Gutiérrez, “Extreme metal adapted, knockout and knockdown strains reveal a coordinated gene expression among different *Tetrahymena thermophila* metallothionein isoforms” *PLoS One*. **12**:e0189076 (2017). doi: 10.1371/journal.pone.0189076
- [209] L. Vergani, in: A. Sigel, H. Sigel, R.K.O. Sigel (Eds.) *Metal ions in Life Sciences: Metallothioneins and Related Chelators* (Vol. 5), RSC Publishing, Cambridge, 2009, 199-238.
- [210] R. Dallinger, O. Zerbe, C. Baumann, B. Egger, M. Capdevila, Ò. Palacios, R. Albalat, S. Calatayud, P. Ladurner, B.C. Schlick-Steiner, F.M. Steiner, V. Pedrini-Martha, R. Lackner, H. Lindner, M. Dvorak, M. Niederwanger, R. Schnegg, S. Atrian, “Metallomics reveals a persisting impact of cadmium on the evolution of metal-selective snail metallothioneins” *Metallomics* **12**, 702-720 (2020). doi: 10.1039/c9mt00259f
- [211] O. Palacios, S. Pérez-Rafael, A. Pagani, R. Dallinger, S. Atrian, M. Capdevila, “Cognate and noncognate metal ion coordination in metal-specific metallothioneins: the *Helix pomatia* system as a model” *J. Biol. Inorg. Chem.* **19**, 923-935 (2014). doi: 10.1007/s00775-014-1127-4
- [212] L. Schmielau, M. Dvorak, M. Niederwanger, N. Dobieszewski, V. Pedrini-Martha, P. Ladurner, J.R. Pedregal, J.D. Maréchal, R. Dallinger, “Differential response to Cadmium exposure by expression of a two and a three-domain metallothionein isoform in the land winkle *Pomatias elegans*: Valuating the marine heritage of a land snail” *Sci. Total. Environ.* **648**, 561-571 (2019). doi: 10.1016/j.scitotenv.2018.07.426
- [213] C. A. Mebane, in US Department of the Interior & US Geological Survey, Scientific Investigations Report 2006-5245, Reston, Virginia, v. 1.2., 2010, p. 130.
- [214] I.M.L. Somorjai, J. Martí-Solans, M. Diaz-Gracia, H. Nishida, K.S. Imai, H. Escrivà, C. Cañestro, R. Albalat “Wnt evolution and function shuffling in liberal and conservative chordate genomes” *Genome Biol.* **19**: 98 (2018). doi: 10.1186/s13059-018-1468-3
- [215] A. Ferrández-Roldán, J. Martí-Solans, C. Cañestro, R. Albalat, “*Oikopleura dioica*: An Emergent Chordate Model to Study the Impact of Gene Loss on the Evolution of

- the Mechanisms of Development” *Results Probl. Cell. Differ.* **68**, 63-105 (2019). doi: 10.1007/978-3-030-23459-1\_4
- [216] N. Franchi, F. Boldrin, L. Ballarin, E. Piccinni, “CiMT-1, an unusual chordate metallothionein gene in *Ciona intestinalis* genome: structure and expression studies” *J. Exp. Zool. A. Ecol. Genet. Physiol.* **315**, 90-100 (2011). doi: 10.1002/jez.653
- [217] W. Liebrich, A.C. Brown, D.P. Botes, “Cadmium-binding proteins from a tunicate, *Pyura stolonifera*” *Comp. Biochem. Physiol. C. Pharmacol. Toxicol. Endocrinol.* **112**, 35-42 (1995). doi: 10.1016/0742-8413(95)00071-2
- [218] C. Ding, R.A. Festa, T.-S. Sun, Z. Y. Wang “Iron and copper as virulence modulators in human fungal pathogens” *Mol Microbiol* **93**, 10-23 (2014). doi: 10.1111/mmi.12653
- [219] D. Wilson, F. Citiulo, B. Hube “Zinc exploitation by pathogenic fungi” *PLoS Pathog* **8**: e1003034 (2012). doi: 10.1371/journal.ppat.1003034
- [220] E. Ladomersky, M.J. Petris “Copper tolerance and virulence in bacteria” *Metallomics* **7**, 957-964 (2015). doi: 10.1039/c4mt00327f
- [221] A. Espart, S. Gil-Moreno, Ò. Palacios, M. Capdevila, S. Atrian “Understanding the 7-Cys module amplification of *C. neoformans* metallothioneins: how high capacity Cu-binding polypeptides are built to neutralize host nutritional immunity” *Mol. Microbiol.* **98**, 977-92 (2015). doi: 10.1111/mmi.13171
- [222] P. Iturbe-Espinoza, S. Gil-Moreno, W. Lin, S. Calatayud, Ò. Palacios, M. Capdevila, S. Atrian, “The Fungus *Tremella mesenterica* Encodes the Longest Metallothionein Currently Known: Gene, Protein and Metal Binding Characterization” *PLoS One.* **11**, e0148651 (2016). doi: 10.1371/journal.pone.0148651
- [223] K.M. Kocot, A.J. Poustka, I. Stoger, K.M. Halanych, M. SchrodL, “New data from Monoplacophora and a carefully-curated dataset resolve molluscan relationships” *Sci. Rep.* **10**:101 (2020). doi: 10.1038/s41598-019-56728-w
- [224] F.D. Passos, P.V.F. Corrêa, C. Todt, “A new species of *Falcidens* (Mollusca, Aplacophora, Caudofoveata) from the southeastern Brazilian coast: external anatomy, distribution, and comparison with *Falcidens caudatus* (Heath, 1918) from the USA” *Mar. Biodiv.* **48**, 1135-1146 (2018). doi: 10.1007/s12526-016-0559-1
- [225] J.H. Kägi, M. Vasák, K. Lerch, D.E. Gilg, P. Hunziker, W.R. Bernhard, M. Good, “Structure of mammalian metallothionein” *Environ. Health. Perspect.* **54**, 93-103 (1984). doi: 10.1289/ehp.54-1568188
- [226] Q. Q. Yang, X. P. Yu, “A new species of apple snail in the genus *Pomacea* (Gastropoda: Caenogastropoda: Ampullariidae)” *Zool. Stud.* **58**, 1-7 (2019). doi: 10.6620/ZS.2019.58-13.
- [227] M. Halwart, “The golden apple snail *Pomacea canaliculata* in Asian rice farming systems: present impact and future threat, Internat” *J. Pest. Man.* **40**, 199-206 (1994). doi: 10.1080/09670879409371882
- [228] G. Gorsky, R. Fenaux, in: *The Biology of Pelagic Tunicates*, Q. Bone (Ed.), Oxford University Press, Oxford, 1998.
- [229] B. H. Robison, K. R. Reisenbichler, R. E. Sherlock, “Giant larvacean houses: rapid carbon transport to the deep sea floor”, *Science* **308**, 1609-1611 (2005).
- [230] L. Berná, G. D'Onofrio, F. Alvarez-Valin “Peculiar patterns of amino acid substitution and conservation in the fast evolving tunicate *Oikopleura dioica*” *Mol. Phylogenet. Evol.* **62**, 708-717 (2012). doi: 10.1016/j.ympev.2011.11.013

- [231] L. Berná, F. Alvarez-Valin, “Evolutionary genomics of fast evolving tunicates” *Genome Biol. Evol.* **6**, 1724-1738 (2014). doi: 10.1093/gbe/evu122.
- [232] R.B. Edvardsen, H.C. Seo, M.F. Jensen, A. Mialon, J. Mikhaleva, M. Bjordal, J. Cartry, R. Reinhardt, J. Weissenbach, P. Wincker, D. Chourrout, “Remodelling of the homeobox gene complement in the tunicate *Oikopleura dioica*” *Curr. Biol.* **15**:R12-3 (2005). doi: 10.1016/j.cub.2004.12.010
- [233] F. Denoeud, S. Henriët, S. Mungpakdee, J.M. Aury, C. Da Silva, H. Brinkmann, J. Mikhaleva, L.C. Olsen, C. Jubin, C. Cañestro, J.M. Bouquet, G. Danks, J. Poulain, C. Campsteijn, M. Adamski, I. Cross, F. Yadetie, M. Muffato, A. Louis, S. Butcher, G. Tsagkogeorga, A. Konrad, S. Singh, M.F. Jensen, E. Huynh Cong, H. Eikeseth-Otteraa, B. Noel, V. Anthouard, B.M. Porcel, R. Kachouri-Lafond, A. Nishino, M. Ugolini, P. Chourrout, H. Nishida, R. Aasland, S. Huzurbazar, E. Westhof, F. Delsuc, H. Lehrach, R. Reinhardt, J. Weissenbach, S.W. Roy, F. Artiguenave, J.H. Postlethwait, J.R. Manak, E.M. Thompson, O. Jaillon, L. Du Pasquier, P. Boudinot, D.A. Liberles, J.N. Volff, H. Philippe, B. Lenhard, H. Roest Crollius, P. Wincker, D. Chourrout, “Plasticity of animal genome architecture unmasked by rapid evolution of a pelagic tunicate” *Science*. **330**, 1381-5 (2010). doi: 10.1126/science.1194167
- [234] F. Delsuc, H. Philippe, G. Tsagkogeorga, P. Simion, M.K. Tilak, X. Turon, S. Lopez-Legentil, J. Piette, P. Lemaire, E.J.P. Douzery, “A phylogenomic framework and timescale for comparative studies of tunicates” *BMC Biol.* **16**:39 (2018). doi: 10.1186/s12915-018-0499-2
- [235] M. A. Kabir, M. A. Hussain, Z. Ahmad “*Candida albicans*: A Model Organism for Studying Fungal Pathogens” *ISRN microbiology* **2012**: 538694 (2012). doi: 10.5402/2012/538694
- [236] B.L. Vallee, D.S. Auld, “Zinc coordination, function, and structure of zinc enzymes and other proteins” *Biochemistry* **29**, 5647-5659 (1990). doi: 10.1021/bi00476a001
- [237] M. Chabicoovsky, H. Niederstaetter, R. Thaler, E. Hödl, W. Parson, W. Rossmanith, R. Dallinger, “Localisation and quantification of Cd- and Cu-specific metallothionein isoform mRNA in cells and organs of the terrestrial gastropod *Helix pomatia*” *Toxicol. Appl. Pharmacol.* **190**, 25-36 (2003). doi: 10.1016/s0041-008x(03)00148-0
- [238] I.G. Dance, “The structural chemistry of metal thiolate complexes” *Polyhedron* **5**, 1037-1104 (1986). doi: 10.1016/S0277-5387(00)84307-7
- [239] J.A. Loo, “Electrospray ionization mass spectrometry: a technology for studying noncovalent macromolecular complexes” *Int. J. of Mass Spectrometry* **200**, 175-186 (2000).
- [240] D. Fabris, J. Zaia, Y. Hathout and C. Fenselau, “Retention of thiol protons in two classes of protein zinc ion coordination centers” *J. Am. Chem. Soc.* **118**, 12242-12243 (1996).
- [241] Q. Lu, S. Li, F. Shao, “Sweet Talk: Protein Glycosylation in Bacterial Interaction With the Host” *Trends Microbiol.* **23**, 630-641 (2015). doi: 10.1016/j.tim.2015.07.003.
- [242] A. Natarajan, T. Jaroentomeechai, M. Li, C.J. Glasscock, M.P. DeLisa “Metabolic engineering of glycoprotein biosynthesis in bacteria” *Emerging Topics in Life Sciences* **2**, 419-432 (2018). doi: 10.1042/ETLS20180004

- [243] M.F. Mescher, J.L. Strominger, "Purification and characterization of a prokaryotic glucoprotein from the cell envelope of *Halobacterium salinarium*" *J. Biol. Chem.* **251**, 2005-2014 (1976).
- [244] J. Eichler, "Extreme sweetness: protein glycosylation in Archaea" *Nat. Rev. Microbiol.* **11**, 151-156 (2013). doi: 10.1038/nrmicro2957
- [245] U.B. Sleytr, "Heterologous reattachment of regular arrays of glycoproteins on bacterial surfaces" *Nature* **257**, 400-402 (1975).
- [246] H. Nothaft, C.M. Szymanski, "Protein glycosylation in bacteria: sweeter than ever" *Nat. Rev. Microbiol.* **8**, 765-778 (2010). doi: 10.1038/nrmicro2383
- [247] S.A. Longwell, D.H. Dube, "Deciphering the bacterial glycode: recent advances in bacterial glycoproteomics" *Curr. Opin. Chem. Biol.* **17**, 41-48 (2013). doi:10.1016/j.cbpa.2012.12.006
- [248] K.-J. Choi, S. Grass, S. Paek, J.W. St. Geme III, H.-J. Yeo "The Actinobacillus pleuropneumoniae HMW1C-Like Glycosyltransferase Mediates N-Linked Glycosylation of the *Haemophilus influenzae* HMW1 Adhesin" *PLoS ONE* **5**: e15888 (2010). doi:10.1371/journal.pone.0015888
- [249] C.M. Szymanski, R. Yao, C.P. Ewing, T.J. Trust, P. Guerry, "Evidence for a system of general protein glycosylation in *Campylobacter jejuni*" *Mol. Microbiol.* **32**, 1022-1030 (1999). doi: 10.1046/j.1365-2958.1999.01415.x
- [250] O. Gornik, G. Lauc, "Enzyme linked lectin assay (ELLA) for direct analysis of transferrin sialylation in serum samples" *Clin. Biochem.* **40**, 718-723 (2007). doi: 10.1016/j.clinbiochem.2007.01.010
- [251] S. Pérez-Rafael, S. Atrian, M. Capdevila, O. Palacios, "Differential ESI-MS behaviour of highly similar metallothioneins" *Talanta* **83**, 1057-1061 (2011). doi: 10.1016/j.talanta.2010.10.060
- [252] M. Zhou, H. Wu, "Glycosylation and biogenesis of a family of serine-rich bacterial adhesins" *Microbiology* **155**, 317-327 (2009). doi: 10.1099/mic.0.025221-0
- [253] Y. Chen, R. Seepersaud, B.A. Bensing, P.M. Sullam, T.A. Rapoport, "Mechanism of a cytosolic O-glycosyltransferase essential for the synthesis of a bacterial adhesion protein" *Proc. Natl Acad. Sci. U.S.A.* **113**, E1190-E1199 (2016). doi: 10.1073/pnas.1600494113
- [254] H. Nothaft, C.M. Szymanski, "Bacterial protein N-glycosylation: new perspectives and applications" *J. Biol. Chem.* **288**, 6912-6920 (2013) doi: 10.1074/jbc.R112.417857
- [255] J.A. Iwashkiw, N.F. Vozza, R.L. Kinsella, M.F. Feldman, "Pour some sugar on it: the expanding world of bacterial protein O-linked glycosylation" *Mol. Microbiol.* **89**, 14-28 (2013). doi: 10.1111/mmi.12265
- [256] C. Shipman, "Trypsin: A. Mammalian Tissues" in: *Tissue Culture*. Kruse, P. and Patterson, M. (Ed.), Academic Press (1973). doi: 10.1016/B978-0-12-427150-0.50008-5
- [257] S.A. Carr, M.J. Huddleston, M.F. Bean, "Selective identification and differentiation of N- and O-linked oligosaccharides in glycoproteins by liquid chromatography-mass spectrometry" *Protein Sci.* **2**, 183-196 (1993). doi:10.1002/pro.5560020207
- [258] C. Breton, L. Snajdrová, C. Jeanneau, J. Koca, A. Imberty, "Structures and mechanisms of glycosyltransferases" *Glycobiology* **16**, 29R-37R (2006). doi: 10.1093/glycob/cwj016



- [259] L.L. Lairson, B. Henrissat, G.J. Davies, S.G. Withers, "Glycosyltransferases: structures, functions, and mechanisms" *Annu. Rev. Biochem.* **77**, 521-555 (2008). doi: 10.1146/annurev.biochem.76.061005.092322
- [260] J.B. Thoden, F.J. Ruzicka, P.A. Frey, I. Rayment, H.M. Holden, "Structural analysis of the H166G site-directed mutant of galactose-1-phosphate uridylyltransferase complexed with either UDP-glucose or UDP-galactose: detailed description of the nucleotide sugar binding site" *Biochemistry* **36**, 1212-1222 (1997). doi: 10.1021/bi9626517
- [261] L. A. Finney, T. V. O'Halloran, "Transition metal speciation in the cell: insights from the chemistry of metal ion receptors" *Science* **300**, 931-936 (2003).
- [262] A. Krezel, W. Maret, "The Functions of Metamorphic Metallothioneins in Zinc and Copper Metabolism" *Int. J. Mol. Sci.* **18**, 1237 (2017). doi: 10.3390/ijms18061237.
- [263] J.H.R. Kägi, Y. Kojima "Nomenclature of metallothionein: a proposal" *Exp. Suppl.* **34**, 141-142 (1979).
- [264] S. Fogel, J.W. Welch "Tandem gene amplification mediates copper resistance in yeast" *Proc. Natl. Acad. Sci. U.S.A.* **79**, 5342-5346 (1982). doi: 10.1073/pnas.79.17.5342
- [265] X. Hou, B.T. Jones, in: R.A. Meyers (Ed.), *Encyclopaedia of Analytical Chemistry*, John Wiley & Sons Ltd, Chichester, 2000, 9468-9485.
- [266] D.A. Skoog, J. F. Holler, S.R. Crouch, in: *Principles of Instrumental Analysis* (6th ed.), Thomson Brooks/Cole., Belmont, 2007, 169-173
- [267] B.M. Bulheller, A. Rodger, J.D. Hirst. "Circular and linear dichroism of proteins" *Phys. Chem. Chem. Phys.* **9**, 2020-2035 (2007).
- [268] N. Berova, G.A. Ellestad, N. Harada, "Characterization by circular dichroism" *Comprehensive Natural Products II* **9**, 91-146 (2010). doi: 10.1016/B978-008045382-8.00188-X
- [269] S. Kelly, N. Price. "The application of circular dichroism to studies of protein folding and unfolding", *BBA* **1338**, 161-185 (1997). doi: 10.1016/s0167-4838(96)00190-2
- [270] R. Aebersold, M. Mann, "Mass spectrometry-based proteomics" *Nature* **422**, 198-207 (2003). doi: 10.1038/nature01511
- [271] Y. Shen, N. Tolic, C. Masselon, L. Pasa-Tolic, D.G. Camp, K.K. Hixson, R. Zhao, G.A. Anderson, R.D. Smith, *Anal. Chem.* **76**, 144 (2004).
- [272] R. Chen, X.N. Jiang, D.G. Sun, G.H. Han, F.J. Wang, M. Ye, L. Wang, H. Zou "Glycoproteomics analysis of human liver tissue by combination of multiple enzyme digestion and hydrazide chemistry" *J. Proteome Res.* **8**, 651-661 (2009). doi: 10.1021/pr8008012
- [273] K.R. Rebecchi, E.P. Go, L. Xu, C.L. Woodin, M. Mure, H. Desaire, "A general protease digestion procedure for optimal protein sequence coverage and post-translational modifications analysis of recombinant glycoproteins: application to the characterization of human lysyl oxidase-like 2 glycosylation" *Anal. Chem.* **83**, 8484-8491 (2011). doi: 10.1021/ac2017037
- [274] P.M. Drake, B. Schilling, R.K. Niles, M. Braten, E. Johansen, H. Liu, M. Lerch, D.J. Sorensen, B. Li, S. Allen, S.C. Hall, H.E. Witkowska, F.E. Regnier, B.W. Gibson, S.J. Fisher, "A lectin affinity workflow targeting glycosite-specific, cancer-related

- 
- carbohydrate structures in trypsin-digested human plasma” *Anal. Biochem.* **408**, 71-85 (2011). doi: 10.1016/j.ab.2010.08.010
- [275] R. Wang, D.A. Sens, S. Garrett, S. Somji, M.A. Sens, X. Lu, “The resistance of metallothionein to proteolytic digestion: an LC-MS/MS analysis” *Electrophoresis* **28**, 2942-2952 (2007). doi: 10.1002/elps.200600835
- [276] Trypsin Digestion Protocols, OMEGA, <https://www.promega.es/resources/guides/protein-analysis/peptide-analysis/trypsin-digestion-protocols-92e8d80c-64fe-43d7-80b0-3cf3eef61921> (reviewed on 01/07/2021)
- [277] G.J. Kubas, B. Monzyk, A.L. Crumbliss, “Tetrakis(Acetonitrile)Copper(I) Hexafluorophosphate” *Inorg. Synth.* **19**, 90-92 (1979). doi: 10.1002/9780470132500.ch18



# 7.ANNEX

---



# 7. Annex

## 7.1. Data sheets of the parameters measured from the recombinant productions

### 7.1.1. *Arion vulgaris* MT2

**Primary structure:**

GSMSEGRGCNGTCNSNPCQCEDGCQCGDACSCAQNTCKCTNDGCKCGNECTATGSC  
KCGTSCGCN

**M.W.:** 6400.06 (Average)

6395.12 (Monoisotopic)

**num. Cys:** 18

**num. His:** 0

**num. Met:** 1

**Special aa:**

	ICP (ppm)		[Protein] (x10 <sup>-4</sup> M)	Metal-to-protein stoichiometry		
	type	[S]		Zn/MT	Cu/MT	Cd/MT
Zn- AvuMT2	conv.	87	1.43	5.4	--	--
	acid	65.1	1.07	7.2	--	--
Cd- AvuMT2	conv.	--	0.80	--	--	4.0
	acid	49	0.17	--	--	14.4
Cu- AvuMT2 N. A. (peak 1)	conv	<4	<0.07	--	>12.0	--
Cu- AvuMT2 N. A. (peak 2)	conv	31	0.51	--	14.5	--
Cu- HroMT2 L. A.	conv.	5.4	0.09	--	17.8	--

\* N.A. = Normal aeration; L. A. = Low aeration

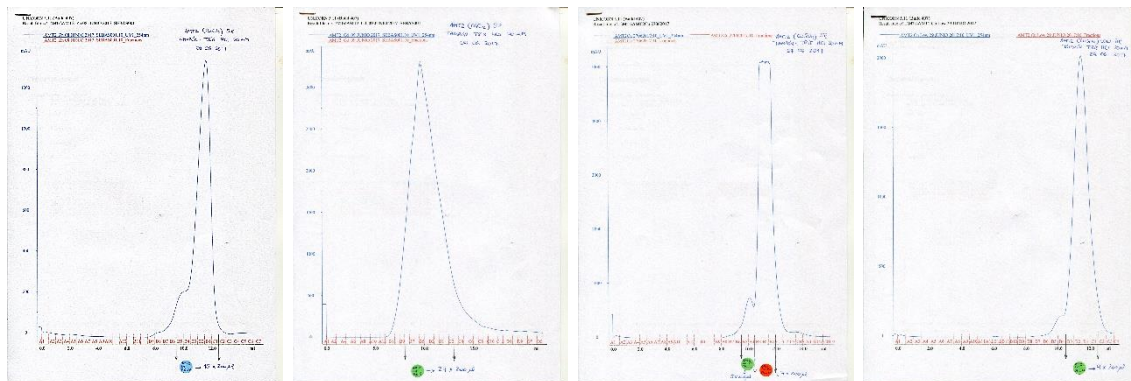


**Figure 7.1.1.1.** From left to right, HPLC spectra corresponding to the production of *Arion vulgaris* MT2 in Zn(II)-, Cd(II)-, and Cu(II)-enriched media (under normal and low oxygenation conditions) of the cultures.

7.1.2. *Pomacea bridgesii* MT1**Primary structure:**

GSMSSSEAHAAHHHGECAKECKKSKASCCEACTEECKKTPCNCGDKCKCSDGCKCQSC  
SAPCKCDGTCQCGKGCTGADSCCKDRKCCK

M.W.: 9235.51 (Average)

9228.58 (Monoisotopic)

num. Cys: 22

num. His: 4

num. Met: 1

Special aa:

	ICP (ppm)		[Protein] (x10 <sup>-4</sup> M)	Metal-to-protein stoichiometry		
	type	[S]		Zn/MT	Cu/MT	Cd/MT
Zn-PbrMT1	conv.	95	1.29	7.4	--	--
	acid	--	--	--	--	--
Cd- PbrMT1	conv.	104	1.41	--	--	5.3
	acid	35	0.48	--	--	8.6
Cu- PbrMT1 (peak 1) N. A.	conv.	9.5	0.13	2.3	13.4	--
Cu- PbrMT1 (peak 2) N. A.	conv.	15	0.2	2.0	12.4	--
Cu- PbrMT1 L. A.	conv.	--	--	--	--	--

\* N.A. = Normal aeration; L. A. = Low aeration

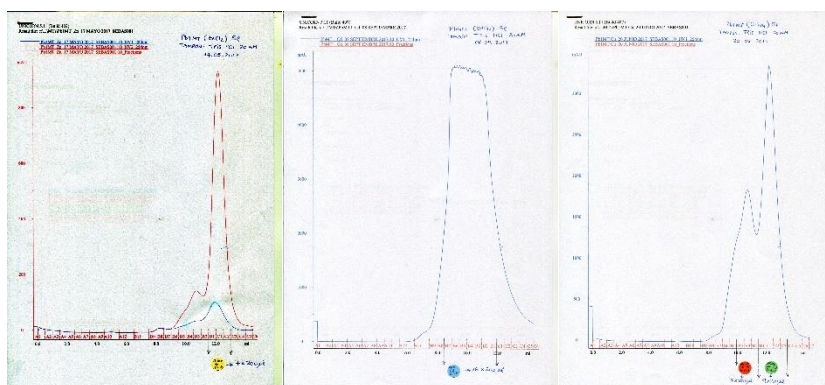


**Figure 7.1.2.1.** From left to right, HPLC spectra corresponding to the production of *Pomacea bridgesii* MT1 in Zn(II)-, Cd(II)-, and Cu(II)-enriched media (under normal oxygenation conditions) of the cultures.

7.1.3. *Pomacea bridgesii* MT2**Primary structure:**

GSMSSANPICTAECEKVPCNCGDKCGCADGCECQTCKRDACTAECRKTPCNCGDKCG  
CGDGCKCQTCKRDACTAECCKKTPCNCGDSC

M.W.: 8975.23 (Average)

8968.39 (Monoisotopic)

num. Cys: 23

num. His: 0

num. Met: 1

Special aa:

	ICP (ppm)		[Protein] (x10 <sup>-4</sup> M)	Metal-to-protein stoichiometry		
	type	[S]		Zn/MT	Cu/MT	Cd/MT
Zn-PbrMT2 (peak 1)	conv.	31	0.40	5.7	--	--
	acid	13	0.17	7.6	--	--
Zn-PbrMT2 (peak 2)	conv.	117	1.52	6.4	--	--
	acid	60	0.78	7.1	--	--
Cd- PbrMT2	conv.	80	1.04	--	--	6.9
	acid	38.6	0.50	--	--	11.0
Cu- PbrMT2 (peak 1) N. A.	conv.	14.2	0.19	--	15.6	--
Cu- PbrMT2 (peak 2) N. A.	conv.	22.4	0.29	--	16.4	--
Cu- PbrMT2 L. A.	conv.	--	--	--	--	--

\* N.A. = Normal aeration; L. A. = Low aeration

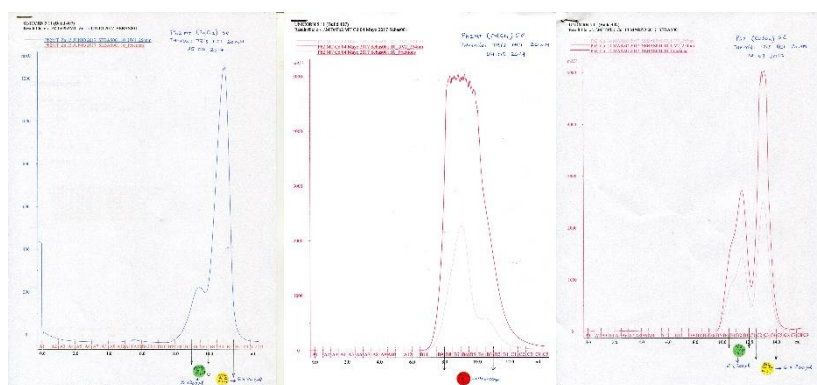


**Figure 7.1.3.1.** From left to right, HPLC spectra corresponding to the production of *Pomacea bridgesii* MT2 in Zn(II)-, Cd(II)-, and Cu(II)-enriched media (under normal oxygenation conditions) of the cultures.



7.1.4. *Arion vulgaris* MT1**Primary structure:**

GSMMSGKACTGACKSEPCQCGNNCQCGGDCDCSQCKTCKCTNEGCKCGQNCTGQAT  
CSCEKSCSCK

**M.W.:** 6556.41 (Average)

6551.35 (Monoisotopic)

**num. Cys:** 18

**num. His:** 0

**num. Met:** 1

**Special aa:**

	ICP (ppm)		[Protein] (x10 <sup>-4</sup> M)	Metal-to-protein stoichiometry		
	type	[S]		Zn/MT	Cu/MT	Cd/MT
Zn-AvuMT1	conv.	42	0.69	6.0	--	--
	acid	41.9	0.69	7.2	--	--
Cd- AvuMT1	conv.	16	0.26	--	--	6.8
Cu- AvuMT1 (peak 1) N. A.	conv.	13	0.21	0.9	11.8	--
Cu- AvuMT1 (peak 2) N. A.	conv.	29	0.48	0.9	10.9	--
Cu- AvuMT1 L. A.	conv.	--	--	--	--	--

\* N.A. = Normal aeration; L. A. = Low aeration

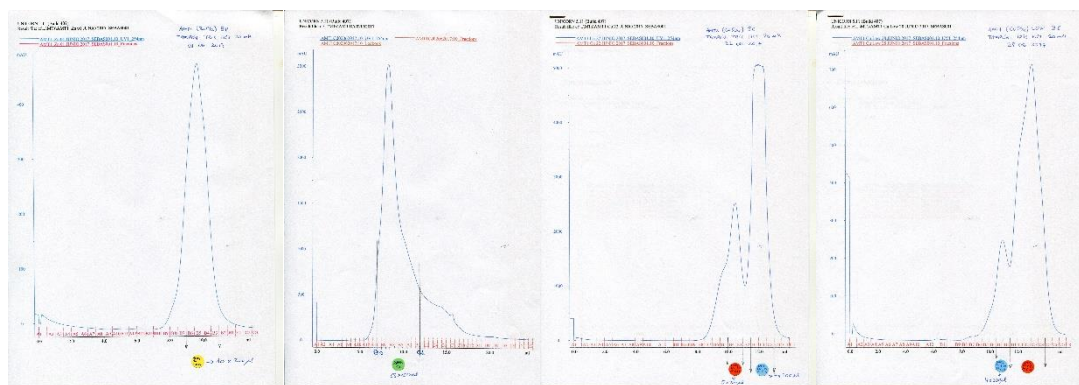


**Figure 7.1.4.1.** From left to right, HPLC spectra corresponding to the production of *Arion vulgaris* MT1 in Zn(II)-, Cd(II)-, and Cu(II)-enriched media (under normal and low oxygenation conditions) of the cultures.

7.1.5. *Nerita peloronta* MT1**Primary structure:**

GSMSDPKGASCTTECKDPCACGTNCKGSDCTCSSCKKSSCKCAADSCACGKGCTG  
PSTCKCDSGCSCR

M.W.: 6863.82 (Average)

6858.49 (Monoisotopic)

num. Cys: 19

num. His: 0

num. Met: 1

Special aa:

	ICP (ppm)		[Protein] (x10 <sup>-4</sup> M)	Metal-to-protein stoichiometry		
	type	[S]		Zn/MT	Cu/MT	Cd/MT
Zn-NpeMT1	conv.	134	2.09	5.9	--	--
Cd- NpeMT1	conv.	62	0.97	--	--	5.5
Cu- NpeMT1 (peak 1) N. A.	conv.	44	0.69	1.5	7.3	--
Cu- NpeMT1 (peak 2) N. A.	conv.	61	0.95	1.9	7.1	--
Cu- NpeMT1 L. A.	conv.	--	--	--	--	--

\* N.A. = Normal aeration; L. A. = Low aeration

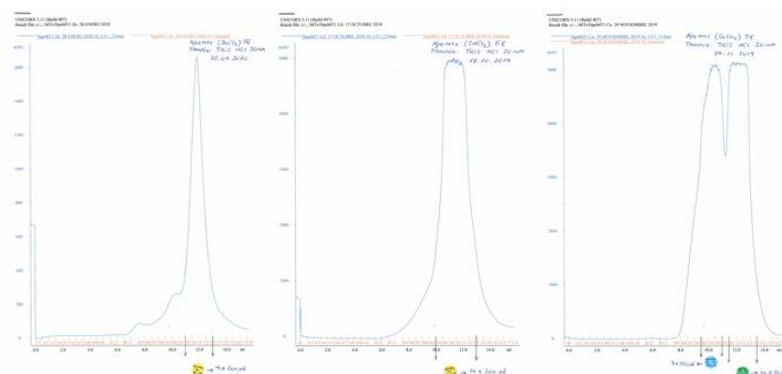


**Figure 7.1.5.1.** From left to right, HPLC spectra corresponding to the production of *Nerita peloronta* MT1 in Zn(II)-, Cd(II)-, and Cu(II)-enriched media (under normal aeration conditions) of the cultures.

7.1.6. *Falciidens caudatus* MT1 and  $\delta$  domain**Primary structure:**

GSMSDVKPCNCADSCNCCCKDGACAGKKCECKVKCCQSGDCGCCQDKCKCAGTCN  
 CGKGCTGPGDCTCDSGCSCCK

**M.W.:** 6863.82 (Average)

6858.49 (Monoisotopic)

**num. Cys:** 23

**num. His:** 0

**num. Met:** 1

**Special aa:**

	ICP (ppm)		[Protein] ( $\times 10^{-4}$ M)	Metal-to-protein stoichiometry		
	type	[S]		Zn/MT	Cu/MT	Cd/MT
Zn-FcaMT1	conv.	197	2.56	6.9	--	--
Cd-FcaMT1	conv.	85	1.10	--	--	6.4
Cu-FcaMT1 (peak 1) N. A.	conv.	24	0.31	2.5	9.0	--
Cu-FcaMT1 (peak 2) N. A.	conv.	38	0.49	2.5	8.3	--
Cu-FcaMT1 L. A.	conv.	--	--	--	--	--

\* N.A. = Normal aeration; L. A. = Low aeration

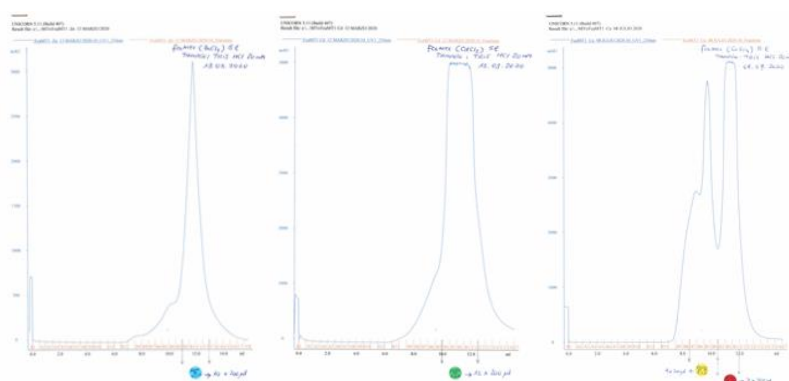


**Figure 7.1.6.1.** From left to right, HPLC spectra corresponding to the production of *Falciidens caudatus* MT1 in Zn(II)-, Cd(II)-, and Cu(II)-enriched media (under normal aeration conditions) of the cultures.

*δ* domain of *Falcidens caudatus* MT1**Primary structure:**

GMSDVKPCNCADSCNCCCKDGACAGKKCECKVKCCQSGDCGCCQDK

M.W.: 4821.59 (Average)

4817.76 (Monoisotopic)

num. Cys: 14

num. His: 0

num. Met: 1

Special aa:

	ICP (ppm)		[Protein] (x10 <sup>-4</sup> M)	Metal-to-protein stoichiometry		
	type	[S]		Zn/MT	Cu/MT	Cd/MT
Zn-δFcaMT1	conv.	87	1.81	4.5	--	--
Cd- δFcaMT1	conv.	100	2.08	--	--	2.7
Cu- δFcaMT1 (peak 1) N. A.	conv.	18	0.37	--	6.3	--
Cu- δFcaMT1 (peak 2) N. A.	conv.	40	0.46	0.6	6.8	--
Cu- δFcaMT1 L. A.	conv.	--	--	--	--	--

\* N.A. = Normal aeration; L. A. = Low aeration

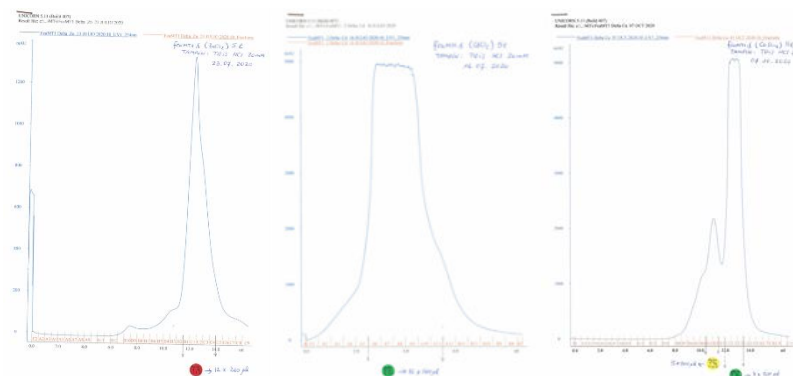


**Figure 7.1.6.2.** From left to right, HPLC spectra corresponding to the production of the *δ* domain *Falcidens caudatus* MT1 in Zn(II)-, Cd(II)-, and Cu(II)-enriched media (under normal aeration conditions) of the cultures.

7.1.7. *Candida albicans* MT1**Primary structure:**

GSMSKFEVNYASGCSCGADCKCASETECKCASKK

M.W.: 3627.14 (Average)

3624.52 (Monoisotopic)

num. Cys: 6

num. His: 0

num. Met: 1

Special aa: F and Y

	ICP (ppm)		[Protein] (x10 <sup>-4</sup> M)	Metal-to-protein stoichiometry		
	type	[S]		Zn/MT	Cu/MT	Cd/MT
Zn- CaCUP1	conv.	46	2.05	2.2	--	--
Cd- CaCUP1	conv.	36	1.60	--	--	2.8
	acid	18	0.80	--	--	3.7
Cu- CaCUP1 N. A.	conv.	<4	<1.78	--	>6.5	--
Cu- CaCUP1 L. A.	conv.	<4	<1.78	--	>4.9	--

\* N.A. = Normal aeration; L. A. = Low aeration

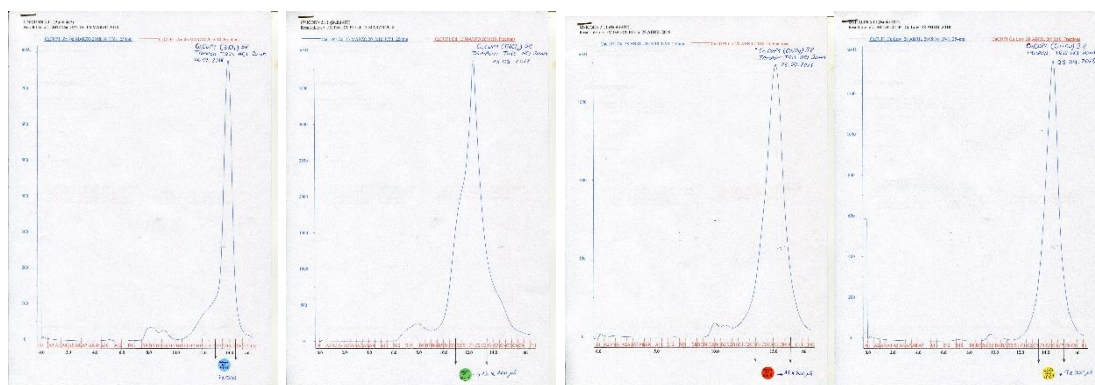


**Figure 7.1.7.1.** From left to right, HPLC spectra corresponding to the production of *Candida albicans* MT1 (CaCUP1) in Zn(II)-, Cd(II)-, and Cu(II)-enriched media (under normal and low aeration conditions) of the cultures.

7.1.8. *Lottia gigantea* MT1**Primary structure:**

GSMSEKPSCCIAEYECCKTKLCCDTGPADCKPGNKPDCAPGKLOCKCPGTCACGV  
GCTGVDNCKCGAGCSCFN

M.W.: 7648.90 (Average)

7643.00 (Monoisotopic)

num. Cys: 19

num. His: 0

num. Met: 1

Special aa: F and Y

	ICP (ppm)		[Protein] (x10 <sup>-4</sup> M)	Metal-to-protein stoichiometry		
	type	[S]		Zn/MT	Cu/MT	Cd/MT
Zn-LgiMT1 (peak 1)	conv.	31	0.48	6.6	--	--
Zn-LgiMT1 (peak 2)	conv.	46	0.72	6.0	--	--
Cd- LgiMT1	conv.	81	1.26	--	--	7.3
Cu- LgiMT1 N. A. (peak 1)	conv.	11	0.17	--	12.9	--
Cu- LgiMT1 N. A. (peak 2)	conv.	10	0.16	--	15.1	--
Cu- LgiMT1 N. A. (peak 3)	conv.	20	0.31	--	12.1	--
Cu- LgiMT1 L. A.	conv.	<4	<0.06	--	>5.0	--

\* N.A. = Normal aeration; L. A. = Low aeration

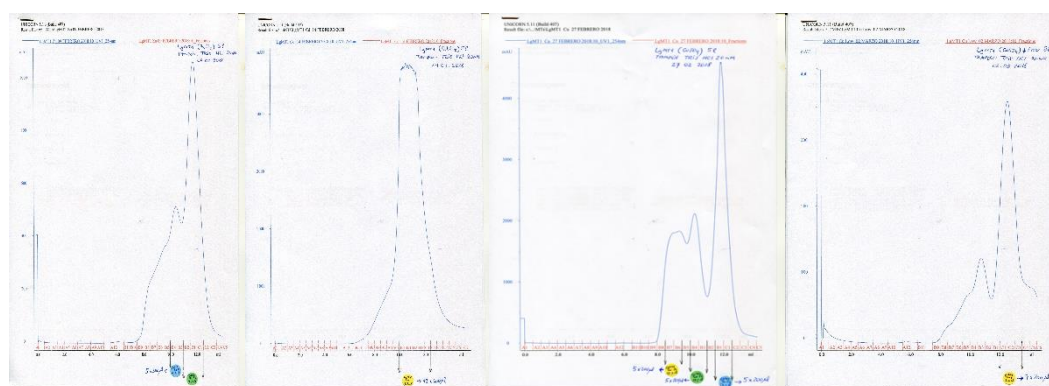


**Figure 7.1.8.1.** From left to right, HPLC spectra corresponding to the production of *Lottia gigantea* MT1 in Zn(II)-, Cd(II)-, and Cu(II)-enriched media (under normal and low aeration conditions) of the cultures.

7.1.9. *Lottia gigantea* MT2 and  $\gamma$  domain**Primary structure:**

GSMSEKASCCIAEYECCKTKSCCDTGPADCCCKPGNKPDCCAPGKLQCKCSGTCACGV  
 GCTGVDNCKCGAGCSCFN

M.W.: 7586.74 (Average)

7580.91 (Monoisotopic)

num. Cys: 19

num. His: 0

num. Met: 1

Special aa: F and Y

	ICP (ppm)		[Protein] (x10 <sup>-4</sup> M)	Metal-to-protein stoichiometry		
	type	[S]		Zn/MT	Cu/MT	Cd/MT
Zn-LgiMT2	conv.	54	0.84	8.0	--	--
Cd- LgiMT2	conv.	67	1.04	--	--	7.7
Cu- LgiMT2 N. A. (peak 1)	conv.	6.5	0.10	--	15.5	--
Cu- LgiMT2 N. A. (peak 2)	conv.	9.9	0.15	--	14.3	--
Cu- LgiMT2 L. A.	conv.	--	--	--	--	--

\* N.A. = Normal aeration; L. A. = Low aeration

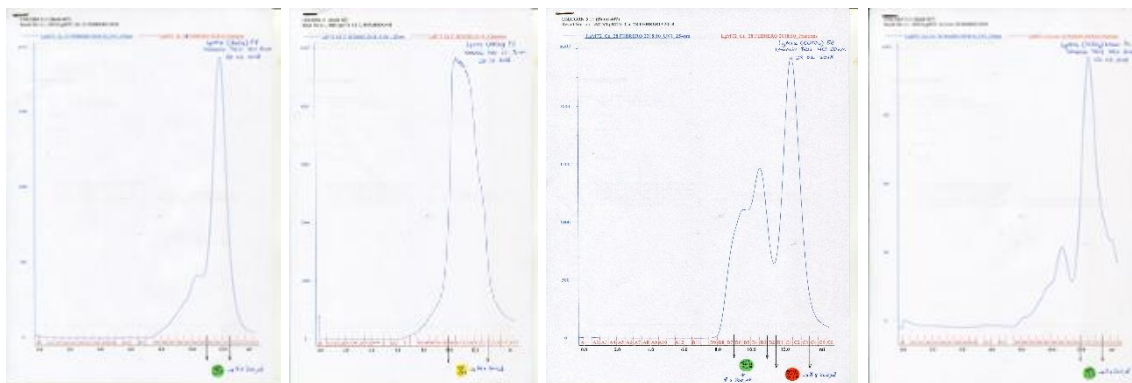


**Figure 7.1.9.1.** From left to right, HPLC spectra corresponding to the production of *Lottia gigantea* MT2 in Zn(II)-, Cd(II)-, and Cu(II)-enriched media (under normal and low aeration conditions) of the cultures.

*γ* domain of *Lottia gigantea* MT2**Primary structure:**

GSMSEKASCCIAEYECCKTKSCCDTGPADCCKPGNKPDCCAPGKLQ

M.W.: 4852.57 (Average)

4848.96 (Monoisotopic)

num. Cys: 10

num. His: 0

num. Met: 1

Special aa: Y

	ICP (ppm)		[Protein] (x10 <sup>-4</sup> M)	Metal-to-protein stoichiometry		
	type	[S]		Zn/MT	Cu/MT	Cd/MT
Zn- $\gamma$ LgiMT2	conv.	97	2.75	2.6	--	--
Cd- $\gamma$ LgiMT2	conv.	45	1.28	--	--	3.7
Cu- $\gamma$ LgiMT2 N. A. (peak 1)	conv.	13	0.40	--	9.8	--
Cu- $\gamma$ LgiMT2 N. A. (peak 2)	conv.	20	0.57	--	7.2	--
Cu- $\gamma$ LgiMT2 L. A.	conv.	--	--	--	--	--

\* N.A. = Normal aeration; L. A. = Low aeration

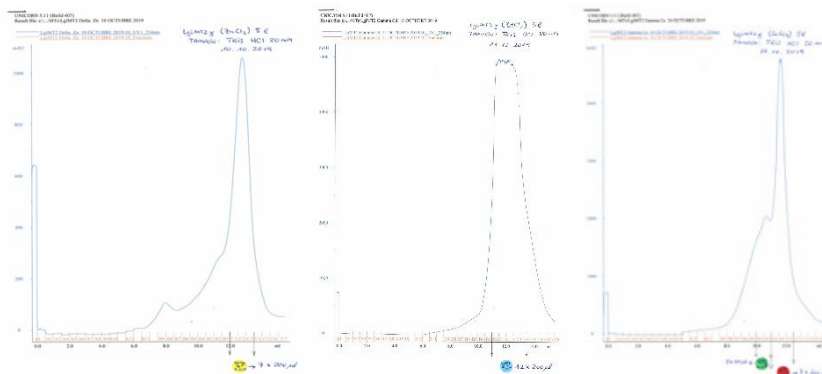


**Figure 7.1.9.2.** From left to right, HPLC spectra corresponding to the production of the  $\gamma$  domain of *Lottia gigantea* MT2 in Zn(II)-, Cd(II)-, and Cu(II)-enriched media (under normal aeration conditions) of the cultures.



7.1.10. *Nautilus pompilius* MT1 and  $\alpha$  domain**Primary structure:**

GSMSDRDCIRCIRTGNCICSDACKGDNCRCGDACKCQKNCSCPSRVTKCSGSCGCGA  
GCTGADSCHCANTCSCK

M.W.: 7472.52 (Average)

7466.72 (Monoisotopic)

num. Cys: 21

num. His: 1

num. Met: 1

Special aa:

	ICP (ppm)		[Protein] ( $\times 10^{-4}$ M)	Metal-to-protein stoichiometry		
	type	[S]		Zn/MT	Cu/MT	Cd/MT
Zn-NpoMT1	conv.	92	1.30	6.5	--	--
Cd- NpoMT1	conv.	77	1.09	--	--	6.6
Cu- NpoMT1 N. A.	conv.	<4	<0.06	--	>14.2	--
Cu- NpoMT1 L. A.	conv.	--	--	--	--	--

\* N.A. = Normal aeration; L. A. = Low aeration

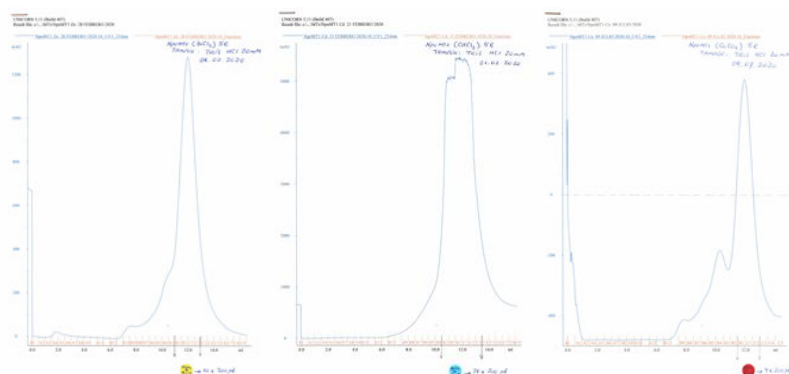


**Figure 7.1.10.1.** From left to right, HPLC spectra corresponding to the production of *Nautilus pompilius* MT1 in Zn(II)-, Cd(II)-, and Cu(II)-enriched media (under normal aeration conditions) of the cultures.

*α* domain of *Nautilus pompilius* MT1**Primary structure:**

GSMSDRDCIRTGNCICSDACKGDNCRCGDACKCQKNCSCPSCRVT

M.W.: 4872.57 (Average)

4868.88 (Monoisotopic)

num. Cys: 12

num. His: 0

num. Met: 1

Special aa:

	ICP (ppm)		[Protein] (x10 <sup>-4</sup> M)	Metal-to-protein stoichiometry		
	type	[S]		Zn/MT	Cu/MT	Cd/MT
Zn-αNpoMT1	conv.	115	2.75	3.2	--	--
Cd- αNpoMT1	conv.	73	1.75	--	--	3.4
Cu-αNpoMT1 N. A. (peak 1)	conv.	--	--	--	--	--
Cu-αNpoMT1 N. A. (peak 2)	conv	5.9	0.14	--	13.3	--
Cu- αNpoMT1 L. A.	conv.	--	--	--	--	--

\* N.A. = Normal aeration; L. A. = Low aeration

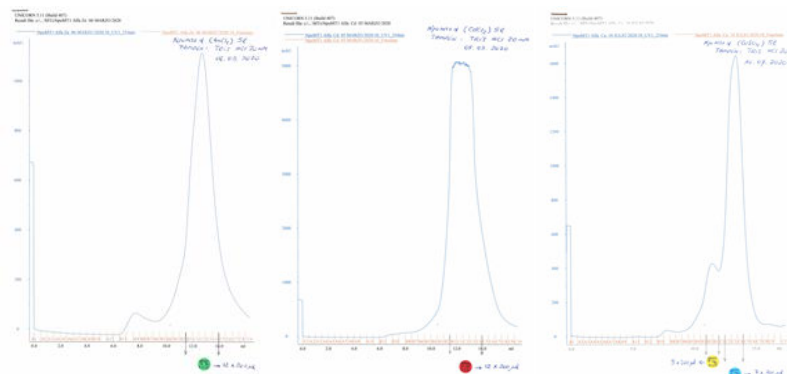


**Figure 7.1.10.2.** From left to right, HPLC spectra corresponding to the production of *α* domain of *Nautilus pompilius* MT1 in Zn(II)-, Cd(II)-, and Cu(II)-enriched media (under normal aeration conditions) of the cultures.

7.1.11. *Nerita peloronta* MT2 and  $\beta$  domain**Primary structure:**

GSMNPNGKPGCTEDCKAAQCQCGTNCRCRDCPCNDCHKATCKCSGSCACGEGCSGP  
 QTCKCEDDCSCH

**M.W.:** 7075.93 (Average)

7070.55 (Monoisotopic)

**num. Cys:** 18

**num. His:** 2

**num. Met:** 1

**Special aa:**

	ICP (ppm)		[Protein] ( $\times 10^{-4}$ M)	Metal-to-protein stoichiometry		
	type	[S]		Zn/MT	Cu/MT	Cd/MT
Zn-NpeMT2	conv.	17	2.86	5.9	--	--
Cd- NpeMT2	conv.	86	1.41	--	--	5.5
Cu- NpeMT2 N. A. (peak 1)	conv.	16	0.26	--	11.4	--
Cu- NpeMT2 N. A. (peak 2)	conv	16	0.26	--	12.0	--
Cu- NpeMT2 L. A.	conv.	--	--	--	--	--

\* N.A. = Normal aeration; L. A. = Low aeration

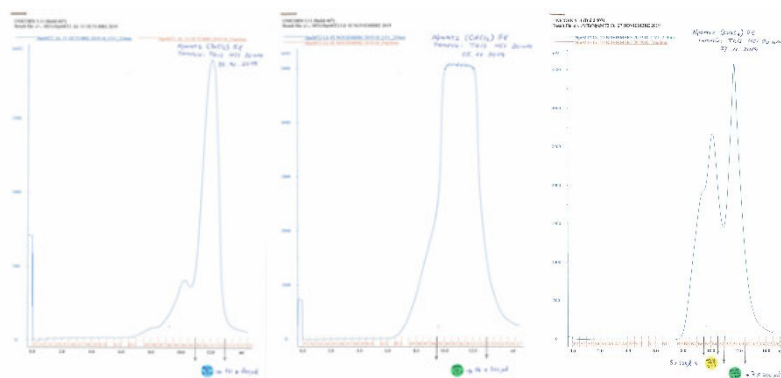


**Figure 7.1.11.1.** From left to right, HPLC spectra corresponding to the production of *Nerita peloronta* MT2 in Zn(II)-, Cd(II)-, and Cu(II)-enriched media (under normal aeration conditions) of the cultures.

*β* domain of *Nerita peloronta* MT2**Primary structure:**

GSMPNPKGPGCTEDCKAAQCQCGTNCRCRDCPCNDCHKAT

M.W.: 4291.83 (Average)

4288.66 (Monoisotopic)

num. Cys: 9

num. His: 1

num. Met: 1

Special aa:

	ICP (ppm)		[Protein] (x10 <sup>-4</sup> M)	Metal-to-protein stoichiometry		
	type	[S]		Zn/MT	Cu/MT	Cd/MT
Zn-βNpeMT2	conv.	120	3.74	2.7	--	--
Cd- βNpeMT2	conv.	120	3.74	--	--	1.6
Cu- βNpeMT2 N. A. (peak 1)	conv.	19	0.59	--	5.3	--
Cu- βNpeMT2 N. A. (peak 2)	conv.	19	0.59	--	5.6	--
Cu- βNpeMT2 L. A.	conv.	--	--	--	--	--

\* N.A. = Normal aeration; L. A. = Low aeration

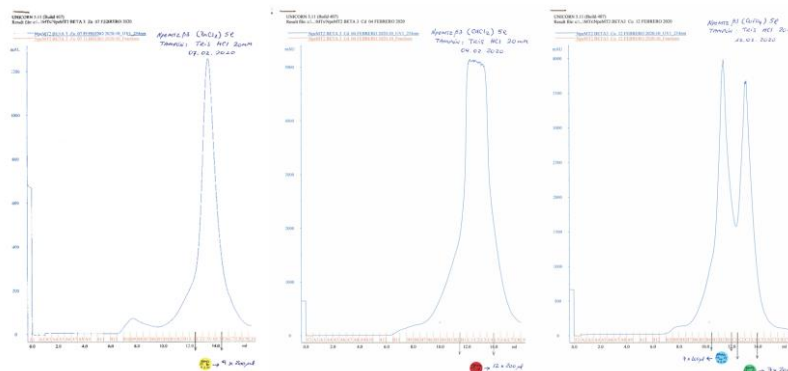


**Figure 7.1.11.2.** From left to right, HPLC spectra corresponding to the production of *β* domain of *Nerita peloronta* MT2 in Zn(II)-, Cd(II)-, and Cu(II)-enriched media (under normal aeration conditions) of the cultures.

7.1.12. *Oikopleura dioica* MT1**Primary structure:**

GSMDPVCSFRCCEENCAGCVDCPAGCDPCKCTLEVCKKVCEGCKDCPPGCEPCKCEKC  
STKKCKSNCCPTSTAE

**M.W.:** 7789.10 (Average)

7783.05 (Monoisotopic)

**num. Cys:** 20

**num. His:** 0

**num. Met:** 1

**Special aa:** F

	ICP (ppm)		[Protein] (x10 <sup>-4</sup> M)	Metal-to-protein stoichiometry		
	type	[S]		Zn/MT	Cu/MT	Cd/MT
Zn-OdiMT1 (peak 1)	conv.	8	0.12	6.4	--	--
Zn-OdiMT1 (peak 2)	conv.	76	1.13	6.2	--	--
Cd- OdiMT1	conv.	23	0.34	--	--	9.7
Cu- OdiMT1 N. A. (peak 1)	conv.	<4	<0.06	--	>10.3	--
Cu- OdiMT1 N. A. (peak 2)	conv	8.3	0.12	--	15.3	--
Cu- OdiMT1 L. A.	conv.	--	--	--	--	--

\* N.A. = Normal aeration; L. A. = Low aeration

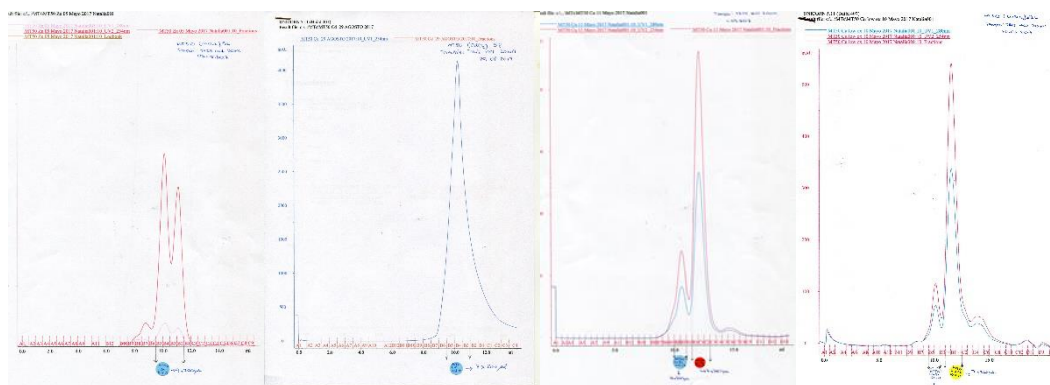


**Figure 7.1.12.1.** From left to right, HPLC spectra corresponding to the production of *Oikopleura dioica* MT1 in Zn(II)-, Cd(II)-, and Cu(II)-enriched media (under normal and low aeration conditions) of the cultures.

7.1.13. *Oikopleura dioica* MT2**Primary structure:**

GSMEVKRPNNCCPAKCLGCKGCPPGCEPCICNMDTCKNICNKCKECPKNEFGCDPCKC  
 PKCSKLGCTCDCCHKKCCVTDGCKTCTPPGCEPCKCSMNACKKVCKQCKNCRKSES  
 GCDPCECSKALKGCKDCCKPKDTCCEASCEGCKNCPGCEPCKCTLNCCMKICDDCK  
 DCPKSENGCDPCNCRKCSRKGNCDCPPSDDCKASCEGCINCPPGCDPCECSMDECK  
 KICKKCNCRKGESGCDPCECRKCSRNGCDCCKPKDSCCEASCEGCTDCPQGCKPCK  
 CTMNSCMKTCDKCKDCPKSASGCDPCECLKSRKGCEDCCPQKNDCEAFCQGCKN  
 CPPGCNPKCTLNFCIKICNECKDCPKSDIGCDPCNVCVKSAGCKDCCKPKKCC

M.W.: 42860.48 (Average)

42826.29 (Monoisotopic)

num. Cys: 123

num. His: 1

num. Met: 7

Special aa: 3F

	ICP (ppm)		[Protein] (x10 <sup>-4</sup> M)	Metal-to-protein stoichiometry		
	type	[S]		Zn/MT	Cu/MT	Cd/MT
Zn-OdiMT2	conv.	LOD	LOD	LOD	--	--
Cd-OdiMT2 (production 1)	conv.	64	0.15	--	--	55.3
Cd-OdiMT2 (production 2)	conv.	50	0.12	--	--	47.8
Cd-OdiMT2 (production 3)	conv.	68	0.17	--	--	40.4
Cu-OdiMT2 N. A.	conv.	LOD	LOD	--	LOD	--
Cu-OdiMT2 L. A.	conv.	--	--	--	--	--

\* N.A. = Normal aeration; L. A. = Low aeration

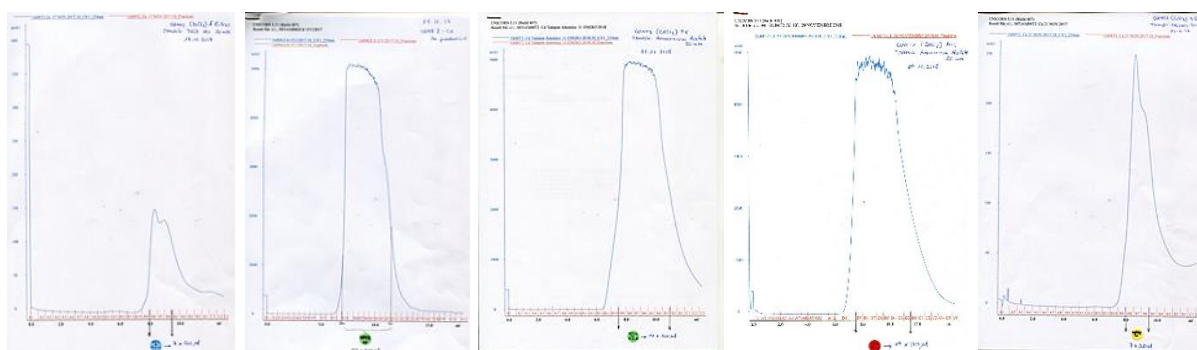


**Figure 7.1.13.1.** From left to right, HPLC spectra corresponding to the production of *Oikopleura dioica* MT2 in Zn(II)-, Cd(II)-, and Cu(II)-enriched media (under normal aeration conditions) of the cultures.

7.1.14. *Ciona robusta* MT1**Primary structure:**

GSMDPCNCAETGVCNCVDCSNCSSCNCDPKICNCAKACCPK

M.W.: 4195.83 (Average)

4192.49 (Monoisotopic)

num. Cys: 12

num. His: 0

num. Met: 1

Special aa:

	ICP (ppm)		[Protein] (x10 <sup>-4</sup> M)	Metal-to-protein stoichiometry		
	type	[S]		Zn/MT	Cu/MT	Cd/MT
Zn- CroMT1	conv.	10	0.24	5.7	--	--
Cd- CroMT1	conv.	19	0.46	--	--	4.9
Cu- CroMT1 N. A.	conv.	13	0.31	--	10.6	--
Cu- CroMT1 L. A.	conv.	<4	<0.09	--	>3.8	--

\* N.A. = Normal aeration; L. A. = Low aeration

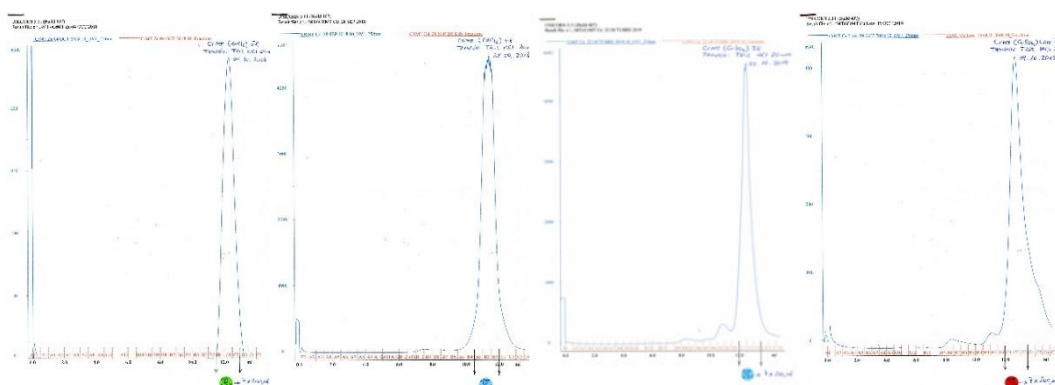


**Figure 7.1.14.1.** From left to right, HPLC spectra corresponding to the production of *Ciona robusta* MT1 in Zn(II)-, Cd(II)-, and Cu(II)-enriched media (under normal and low aeration conditions) of the cultures.

7.1.15. *Halocynthia roretzi* MT1**Primary structure:**

GSMDPCKCSETGVCRNCNDCTNCSKCKCDPALCNCRKGSKQCCGK

M.W.: 4669.45 (Average)

4665.85 (Monoisotopic)

num. Cys: 12

num. His: 0

num. Met: 1

Special aa:

	ICP (ppm)		[Protein] (x10 <sup>-4</sup> M)	Metal-to-protein stoichiometry		
	type	[S]		Zn/MT	Cu/MT	Cd/MT
Zn- HroMT1	conv.	133	3.19	3.9	--	--
Cd- HroMT1	conv.	35	0.85	--	--	4.2
Cu- HroMT1 N. A.	conv	4.3	0.10	--	11.8	--
Cu- HroMT1 L. A.	conv.	<4	<0.10	--	>5.7	--

\* N.A. = Normal aeration; L. A. = Low aeration

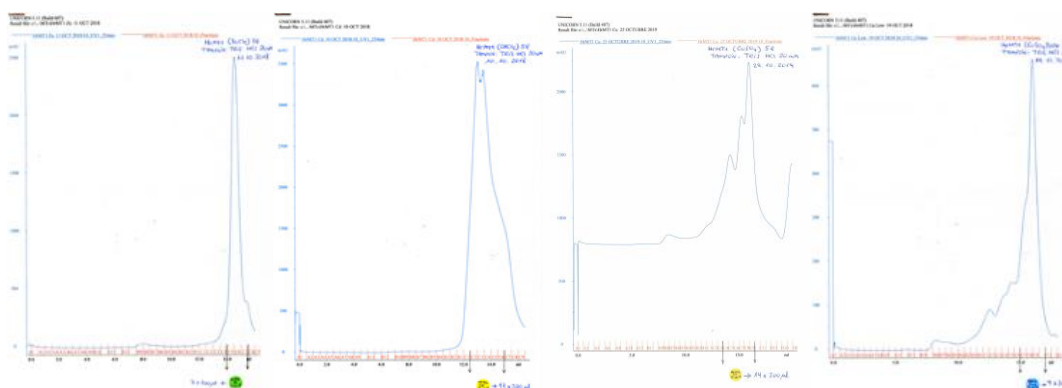


**Figure 7.1.15.1.** From left to right, HPLC spectra corresponding to the production of *Halocynthia roretzi* MT1 in Zn(II)-, Cd(II)-, and Cu(II)-enriched media (under normal and low aeration conditions) of the cultures.



7.1.16. *Halocynthia roretzi* MT2**Primary structure:**

GSMDPCKCSETGVCRCDNCKDCSNCKCDPTLCKCKKESKECCGK

**M.W.:** 4772.57 (Average)

4768.89 (Monoisotopic)

**num. Cys:** 12**num. His:** 0**num. Met:** 1**Special aa:**

	ICP (ppm)		[Protein] (x10 <sup>-4</sup> M)	Metal-to-protein stoichiometry		
	type	[S]		Zn/MT	Cu/MT	Cd/MT
Zn- HroMT2	conv.	108	2.81	3.5	--	--
Cd- HroMT2	conv.	50	1.20	--	--	4.0
Cu- HroMT2 N. A.	conv.	5.2	0.13	--	8.5	--
Cu- HroMT2 L. A.	conv.	<4	<0.10	--	>7.9	--

\* N.A. = Normal aeration; L. A. = Low aeration

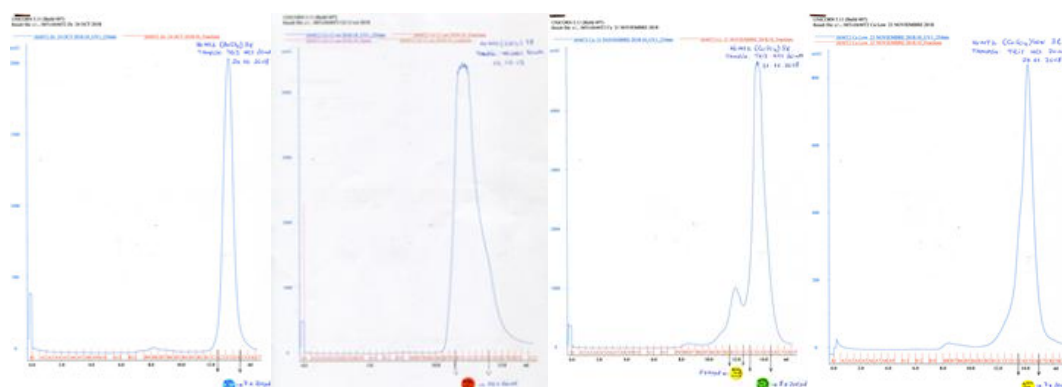


**Figure 7.1.16.1.** From left to right, HPLC spectra corresponding to the production of *Halocynthia roretzi* MT2 in Zn(II)-, Cd(II)-, and Cu(II)-enriched media (under normal and low aeration conditions) of the cultures.

7.1.17. *Botryllus schlosseri* MT1**Primary structure:**

GSMNPCDCKNTGDCQCAGCGDCSGCNCDPALCKCSTSAKTCCAPSCNCKETGKCQC  
 ETCADCSKCNCDPNLCKCTSAKKSCCSADAAGPCNCKETGQCLCSNCSDCSNCNCDP  
 SLCKCASAEEKACCAGPCNCKVTGKCLCVNCVDCTTCNCDPNLCKCTSAKKSCCFEA  
 VGPCNCKETGHCLCSNCSDCSSCNCNPSLCKCASLEKACCSGPCNCKETGHCLCSNCS  
 CSSCNCPSLCKCASLEKACCSGPCNCKVTGVCHCANCVDCTNCNCDPAKCGCSSDK  
 GCCSASAAPCNCKETGNCRCDTCSDCSNCNCGLACKCSAANKGCCYAPCICRTSGKC  
 QCMNCTDCSCDQITCGCPMVKVR

M.W.: 37410.07 (Average)

37380.85 (Monoisotopic)

num. Cys: 105

num. His: 3

num. Met: 3

Special aa: F and Y

	ICP (ppm)		[Protein] (x10 <sup>-4</sup> M)	Metal-to-protein stoichiometry		
	type	[S]		Zn/MT	Cu/MT	Cd/MT
Zn- BscMT1	conv.	60	0.18	34.4	--	--
Cd- BscMT1	conv.	12	0.04	--	--	48.8
Cu- BscMT1 N. A. (peak 1)	conv.	4.3	0.01	--	41.8	--
Cu- BscMT1 N. A. (peak 2)	conv.	<4	<0.01	--	>35.4	--
Cu- BscMT1 L. A.	conv.	LOD	LOD	--	LOD	--

\* N.A. = Normal aeration; L. A. = Low aeration

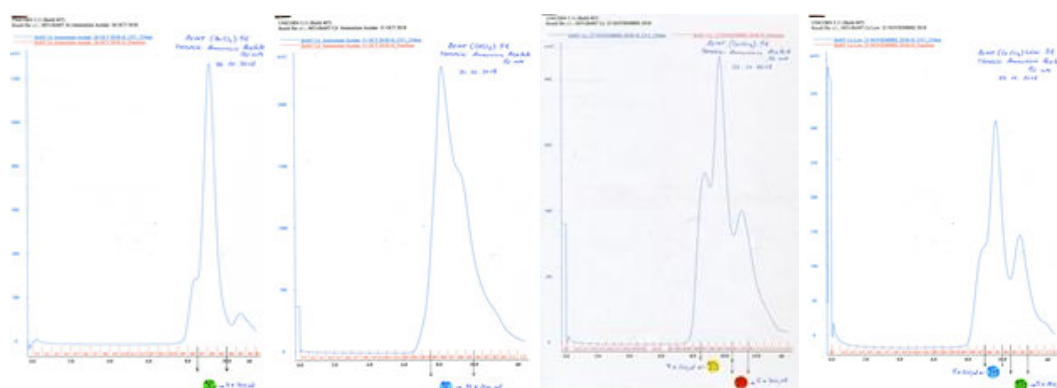


**Figure 7.1.17.1.** From left to right, HPLC spectra corresponding to the production of *Botryllus schlosseri* MT1 in Zn(II)-, Cd(II)-, and Cu(II)-enriched media (under normal and low aeration conditions) of the cultures.

7.1.18. *Salpa thompsoni* MT1**Primary structure:**

GSMDPCNCNTSDMCHCDSCKDCSKCNCARKTCKCSTKGCCSPK

M.W.: 4588.31 (Average)

4584.69 (Monoisotopic)

num. Cys: 12

num. His: 1

num. Met: 2

Special aa:

	ICP (ppm)		[Protein] (x10 <sup>-4</sup> M)	Metal-to-protein stoichiometry		
	type	[S]		Zn/MT	Cu/MT	Cd/MT
Zn- SthMT1	conv.	17	0.38	4.0	--	--
Cd- SthMT1	conv.	30	0.67	--	--	4.3
Cu- SthMT1 N. A.	conv.	<4	<0.09	--	>3.5	--
Cu- SthMT1 L. A.	conv.	--	--	--	--	--

\* N.A. = Normal aeration; L. A. = Low aeration

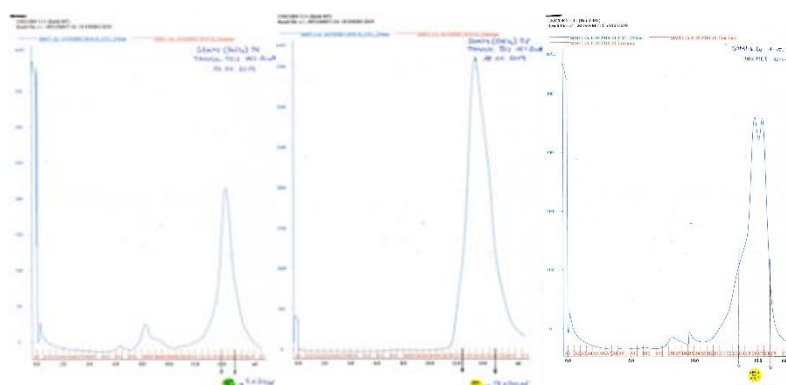


**Figure 7.1.18.1.** From left to right, HPLC spectra corresponding to the production of *Salpa thompsoni* MT1 in Zn(II)-, Cd(II)-, and Cu(II)-enriched media (under normal aeration conditions) of the cultures.

7.1.19. *Salpa thompsoni* MT2**Primary structure:**

GSMDPCNCKVTGACHCDQCTDCGKCSNPANCKCSKPCCPK

M.W.: 4244.95 (Average)

4241.57 (Monoisotopic)

num. Cys: 12

num. His: 1

num. Met: 1

Special aa:

	ICP (ppm)		[Protein] (x10 <sup>-4</sup> M)	Metal-to-protein stoichiometry		
	type	[S]		Zn/MT	Cu/MT	Cd/MT
Zn- SthMT2	conv.	46	1.01	4.3	--	--
Cd- SthMT2	conv.	27	0.65	--	--	4.5
Cu- SthMT2 N. A.	conv.	LOD	LOD	--	LOD	--
Cu- SthMT2 L. A.	conv.	--	--	--	--	--

\* N.A. = Normal aeration; L. A. = Low aeration

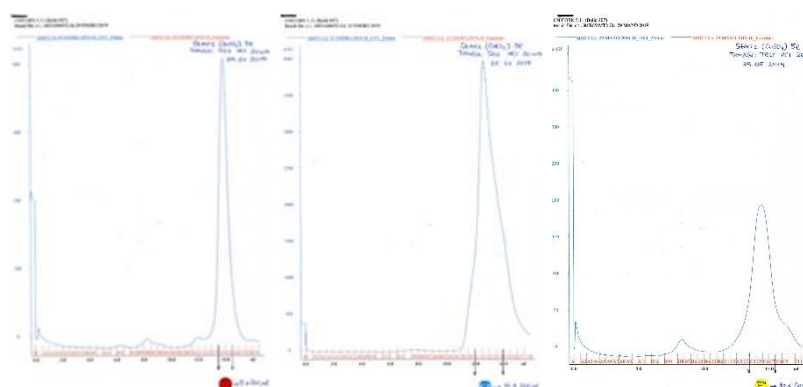


**Figure 7.1.19.1.** From left to right, HPLC spectra corresponding to the production of *Salpa thompsoni* MT2 in Zn(II)-, Cd(II)-, and Cu(II)-enriched media (under normal aeration conditions) of the cultures.

7.1.20. *Salpa thompsoni* MT3**Primary structure:**

GSMDPCNCQDTQSCYCNSTDCSKCACAKTTCKCSAKGCCSPI

M.W.: 4454.10 (Average)

4450.62 (Monoisotopic)

num. Cys: 12

num. His: 0

num. Met: 1

Special aa: Y

	ICP (ppm)		[Protein] (x10 <sup>-4</sup> M)	Metal-to-protein stoichiometry		
	type	[S]		Zn/MT	Cu/MT	Cd/MT
Zn- SthMT3	conv.	28	0.67	4.1	--	--
Cd- SthMT3	conv.	<4	<0.01	--	--	>6.5
Cu- SthMT3 N. A.	conv.	<4	<0.01	--	>4.0	--
Cu- SthMT3 L. A.	conv.	--	--	--	--	--

\* N.A. = Normal aeration; L. A. = Low aeration

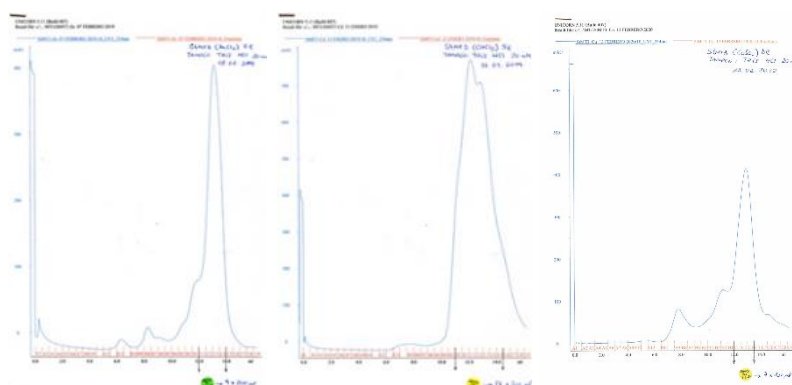


**Figure 7.1.20.1.** From left to right, HPLC spectra corresponding to the production of *Salpa thompsoni* MT3 in Zn(II)-, Cd(II)-, and Cu(II)-enriched media (under normal aeration conditions) of the cultures.

7.1.21. *Salpa thompsoni* MT4**Primary structure:**

GSMDPCNCNTSVMCHCDTCESESNCAKQTCKSSTKRCCSPQ

M.W.: 4599.16 (Average)

4595.69 (Monoisotopic)

num. Cys: 10

num. His: 1

num. Met: 2

Special aa:

	ICP (ppm)		[Protein] (x10 <sup>-4</sup> M)	Metal-to-protein stoichiometry		
	type	[S]		Zn/MT	Cu/MT	Cd/MT
Zn- SthMT4	conv.	26	0.68	3.2	--	--
Cd- SthMT4	conv.	5	0.13	--	--	5.6
Cu- SthMT4 N. A.	conv	LOD	LOD	--	LOD	--
Cu- SthMT4 L. A.	conv.	--	--	--	--	--

\* N.A. = Normal aeration; L. A. = Low aeration

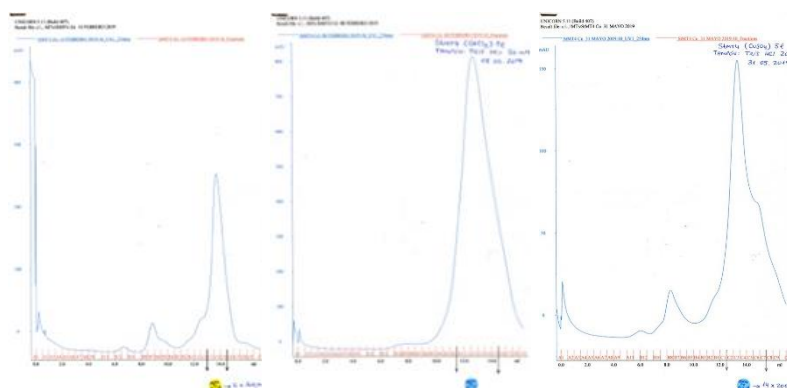
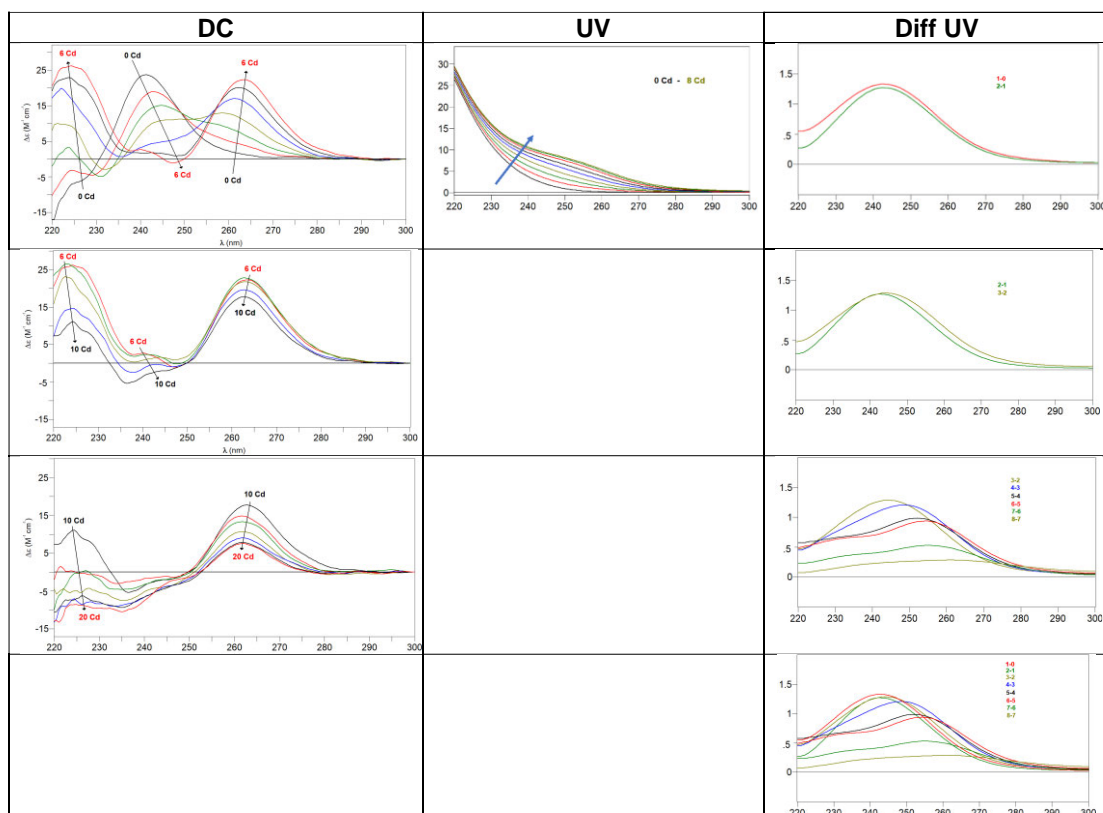


**Figure 7.1.21.1.** From left to right, HPLC spectra corresponding to the production of *Salpa thompsoni* MT4 in Zn(II)-, Cd(II)-, and Cu(II)-enriched media (under normal aeration conditions) of the cultures.

## 7.2. Experimental characterisation of the studied MTs

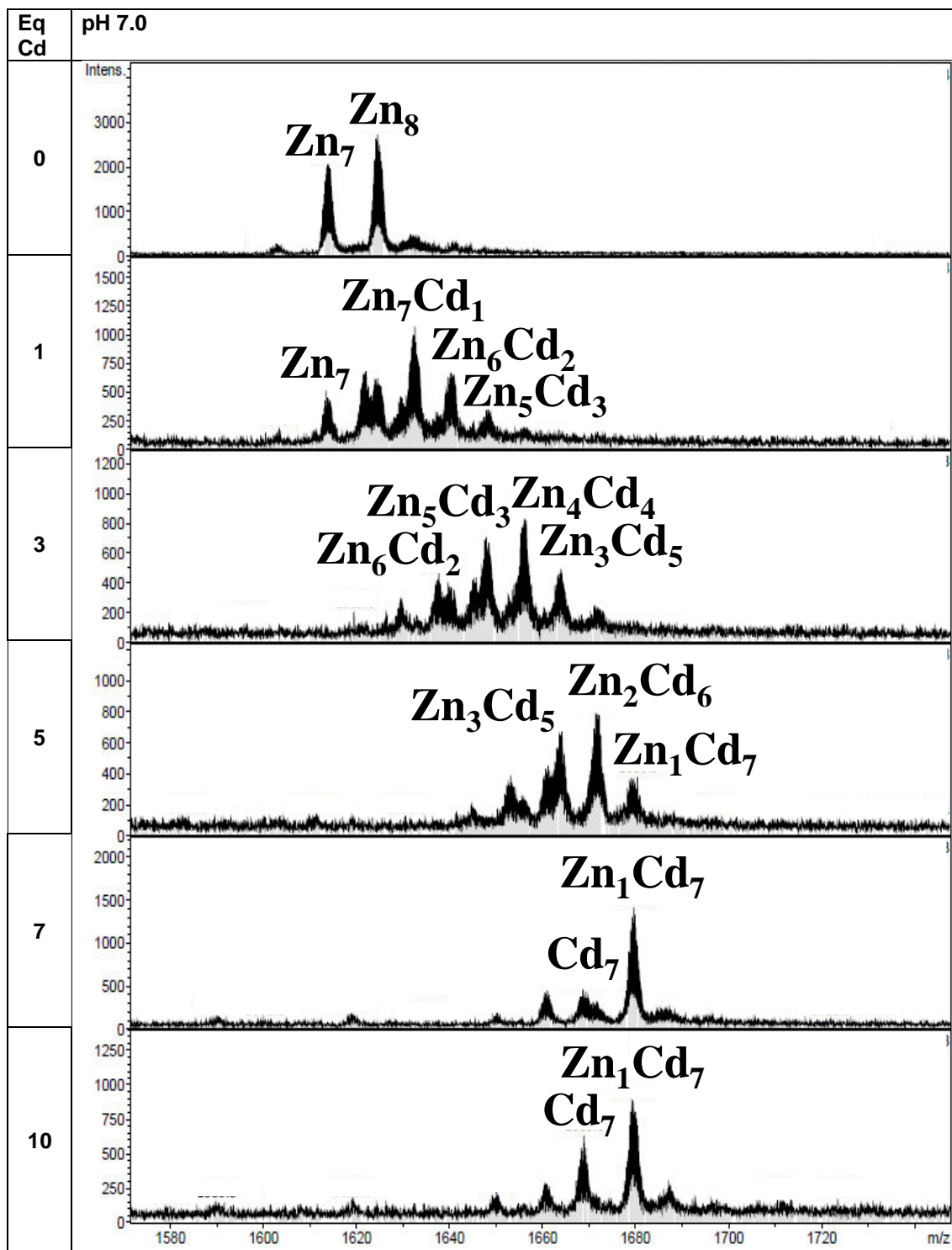
### 7.2.1. Non-specific metallothioneins

#### Sheet 7.2.1.1. Zn/Cd metal exchange experiment of *in vivo* Zn-PbrMT1

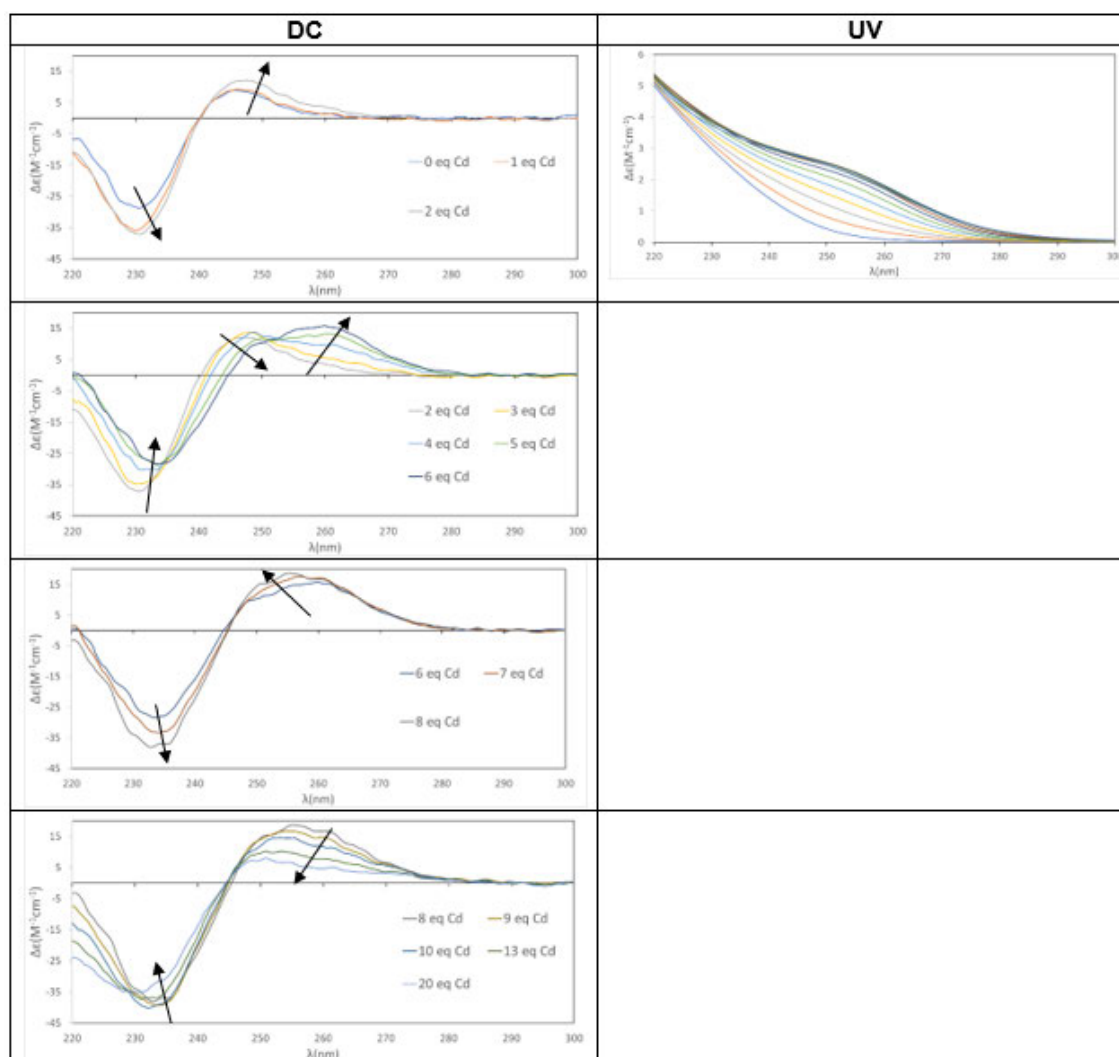


**Figure 7.2.1.1.** CD, UV, and difference UV spectra registered during the Zn/Cd metal exchange experiment of a 6.06  $\mu\text{M}$  solution of Zn-PbrMT1 at pH 7.0 and 25°C.

**Table 7.2.1.1.** Evolution of the Zn/Cd metal exchange experiment of a 6.06  $\mu\text{M}$  solution of Zn-PbrMT1 followed by ESI-MS spectra at pH 7.0.

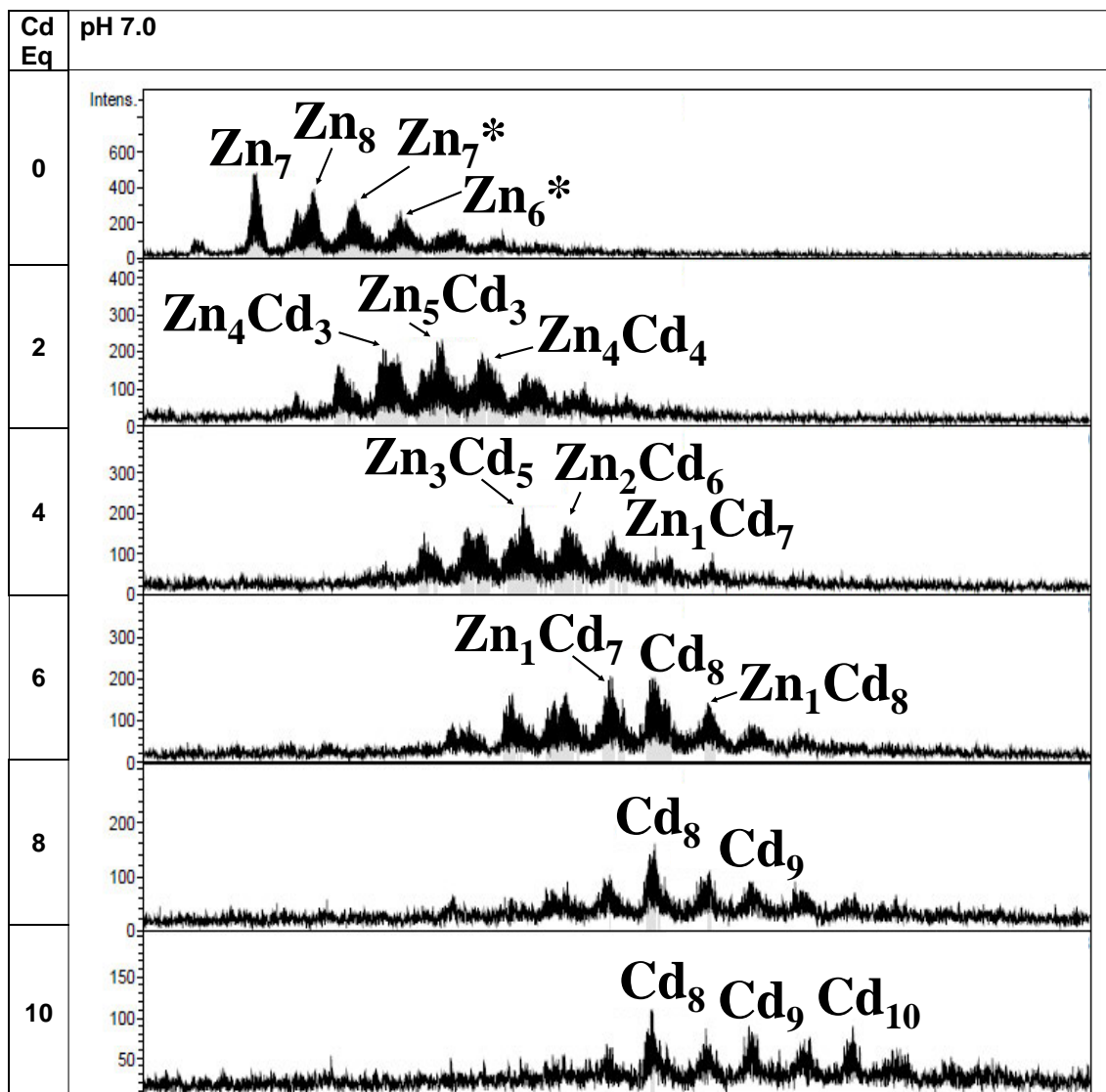


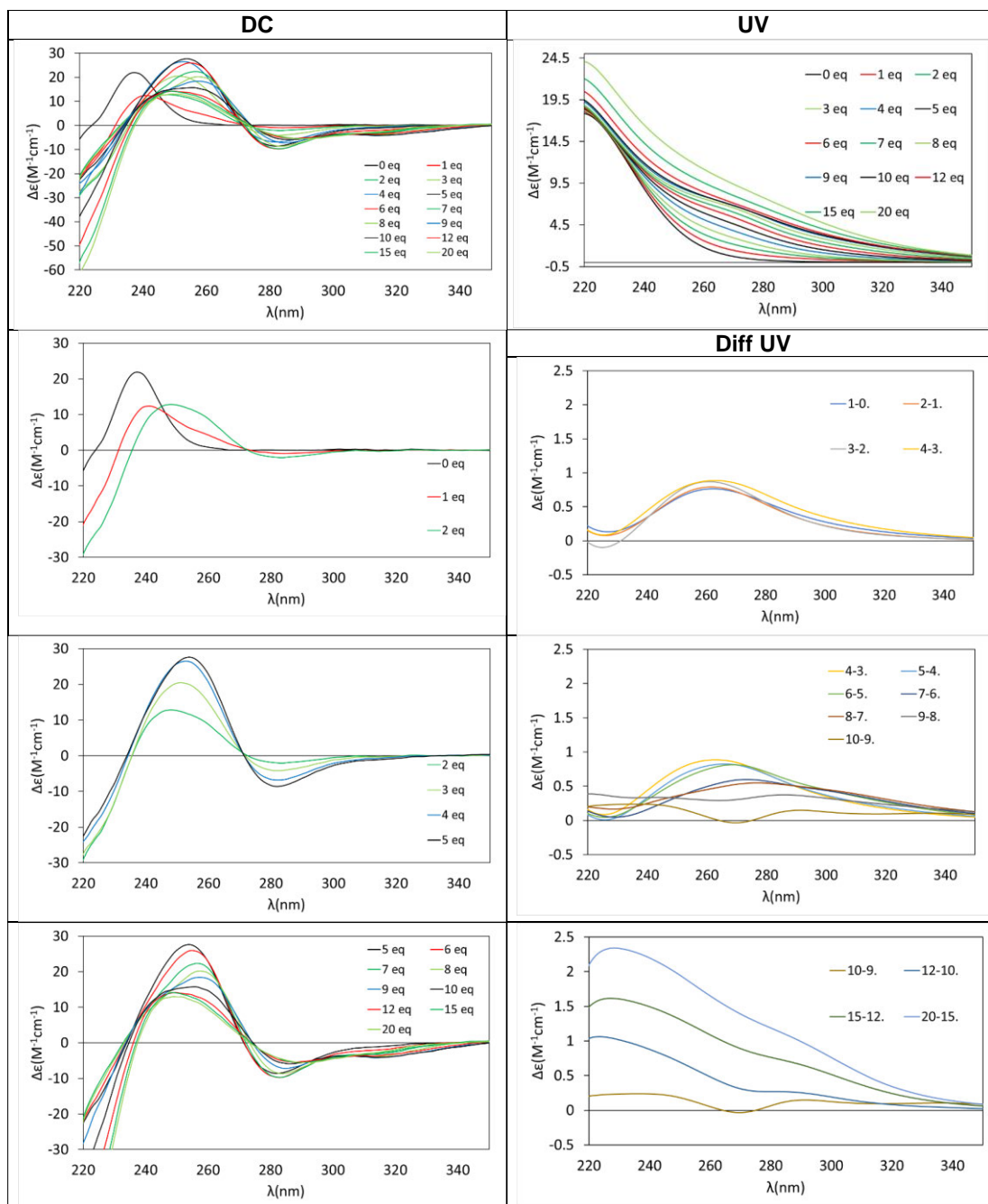


Sheet 7.2.1.2. Zn/Cd metal exchange experiment of *in vivo* Zn-PbrMT2.

**Figure 7.2.1.2.** CD and UV spectra registered during the Zn/Cd metal exchange experiment of a 7.06  $\mu\text{M}$  solution of Zn-PbrMT2 at pH 7.0 and 25°C.

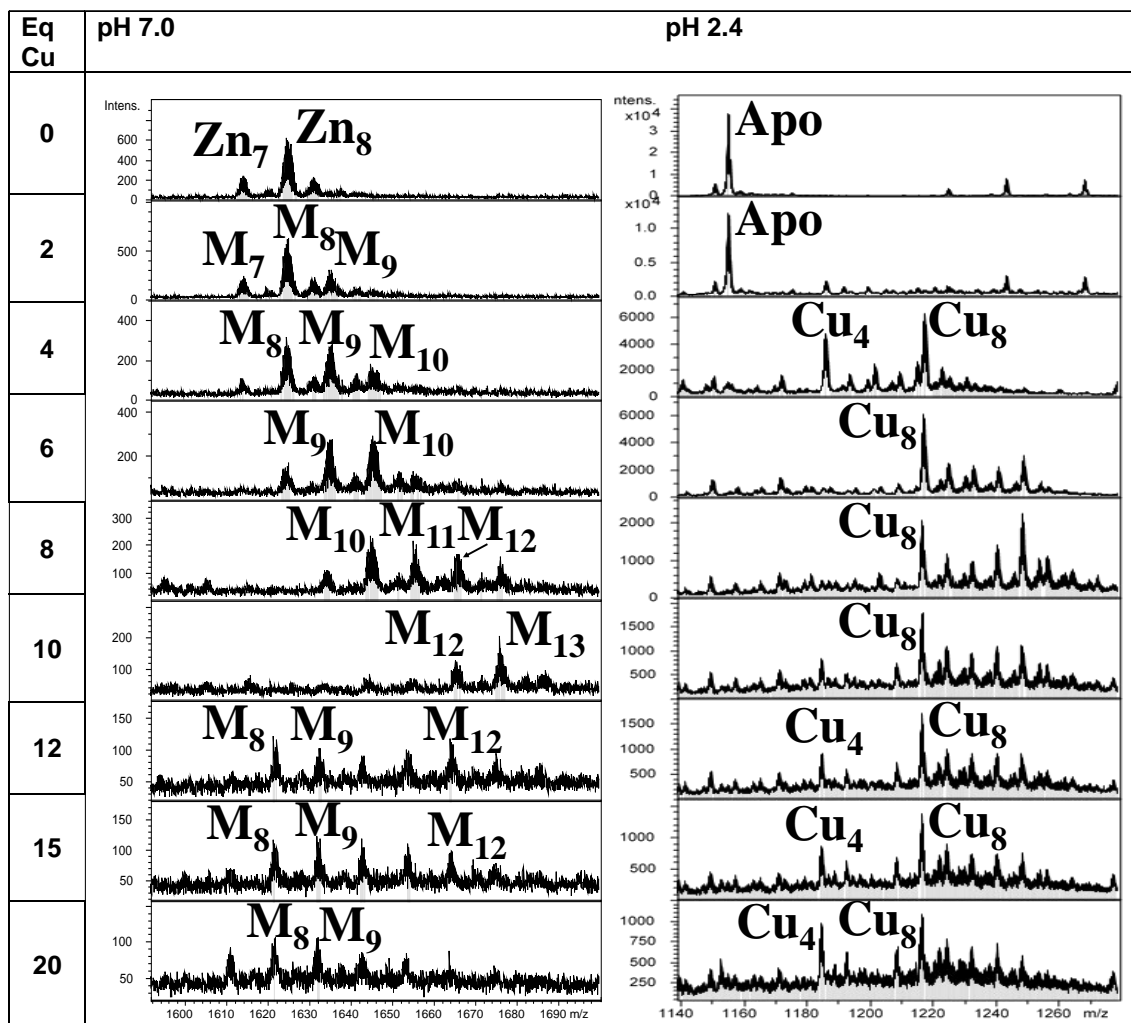
Table 7.2.1.2. Evolution of the Zn/Cd metal exchange experiment of a 7.06  $\mu\text{M}$  solution of Zn-PbrMT2 followed by ESI-MS spectra at pH 7.0.

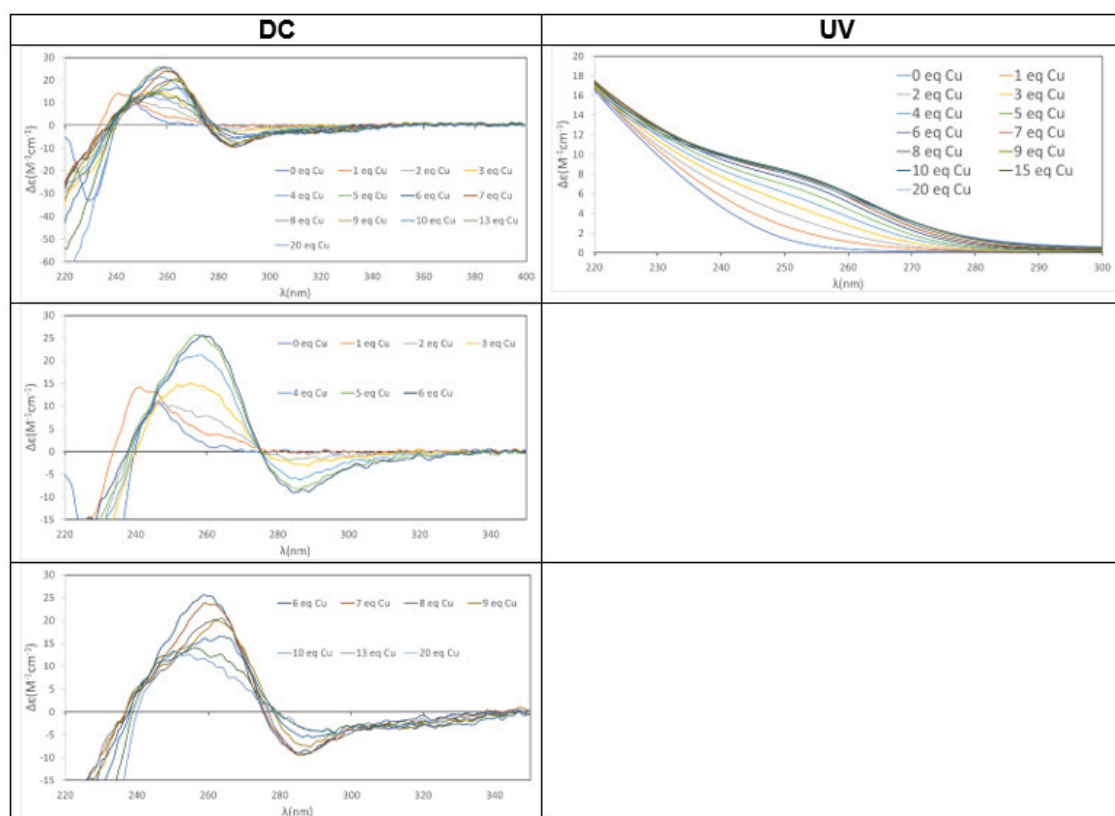


Sheet 7.2.1.3. Zn/Cu metal exchange experiment of *in vivo* Zn-PbrMT1

**Figure 7.2.1.3.** CD, UV, and UV difference spectra registered during the Zn/Cu metal exchange experiment of a 11  $\mu\text{M}$  solution of Zn-PbrMT1 at pH 7.0 and 25°C.

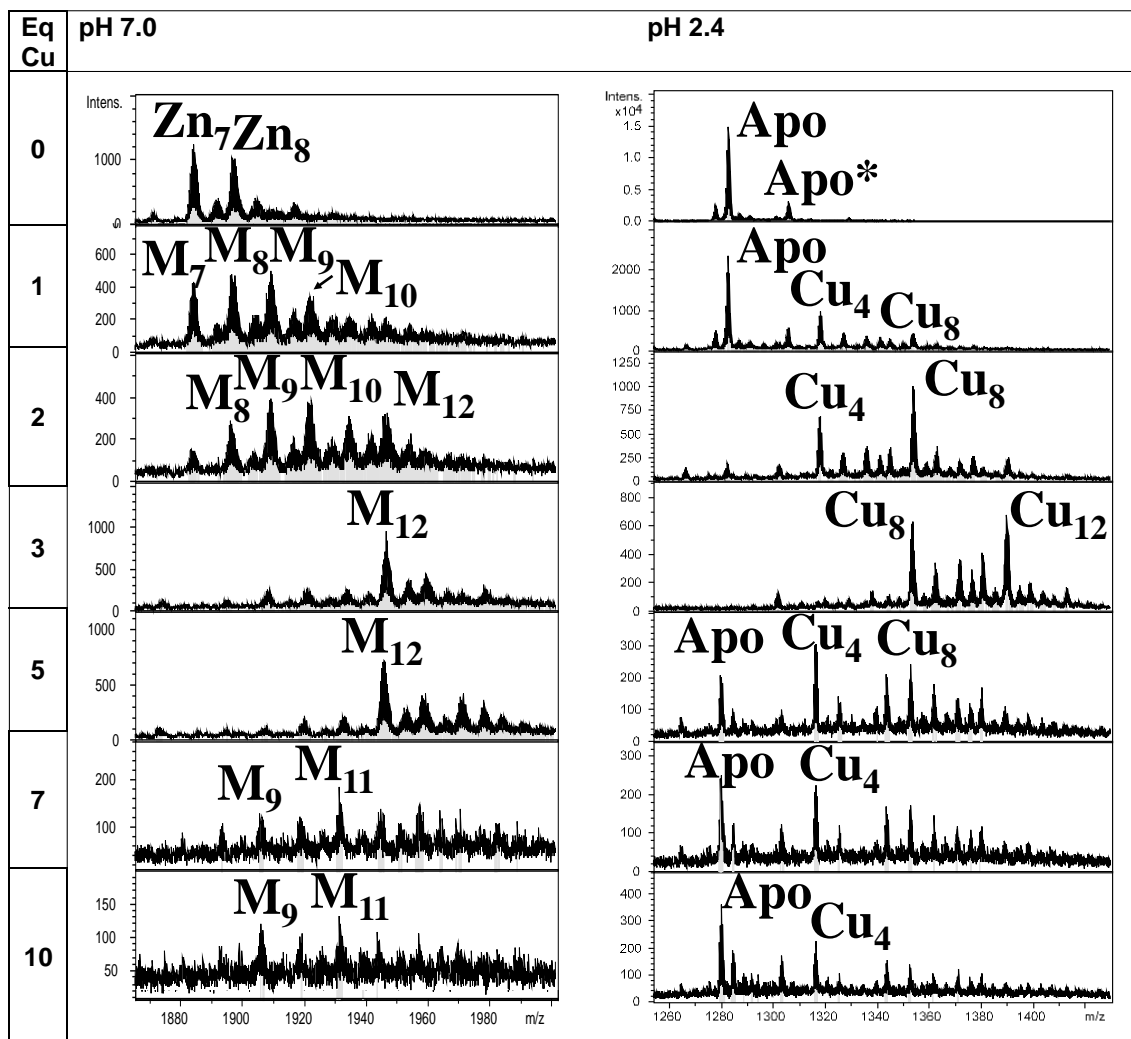
Table 7.2.1.3. Evolution of the Zn/Cu metal exchange experiment of a 11  $\mu\text{M}$  solution of Zn-PbrMT1 followed by ESI-MS spectra at pH 7.0 and pH 2.4.



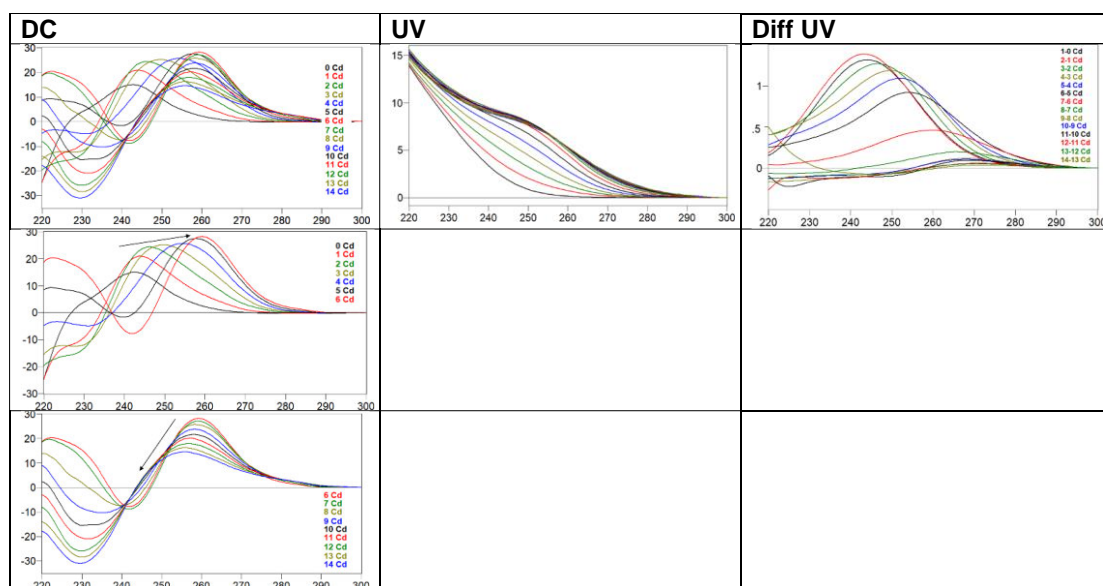
Sheet 7.2.1.4. Zn/Cu metal exchange experiment of *in vivo* Zn-PbrMT2

**Figure 7.2.1.4.** CD and UV spectra registered during the Zn/Cu metal exchange experiment of a 7.06  $\mu M$  solution of Zn-PbrMT2 at pH 7.0 and 25°C.

**Table 7.2.1.4.** Evolution of the Zn/Cu metal exchange experiment of a 7.06  $\mu\text{M}$  solution of Zn-PbrMT2 followed by ESI-MS spectra at pH 7.0 and pH 2.4.

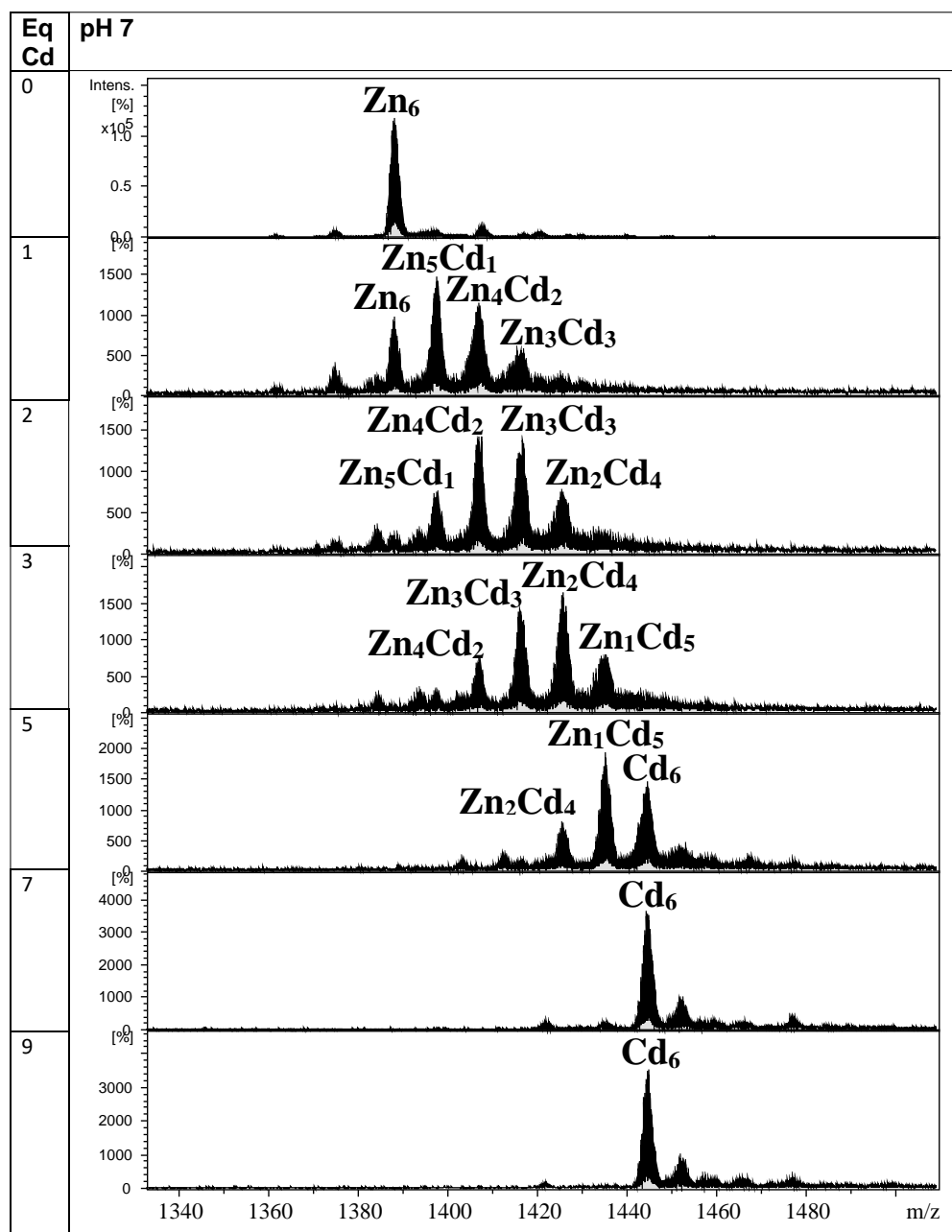


## 7.2.2. Characterisation of Zn-thioneins

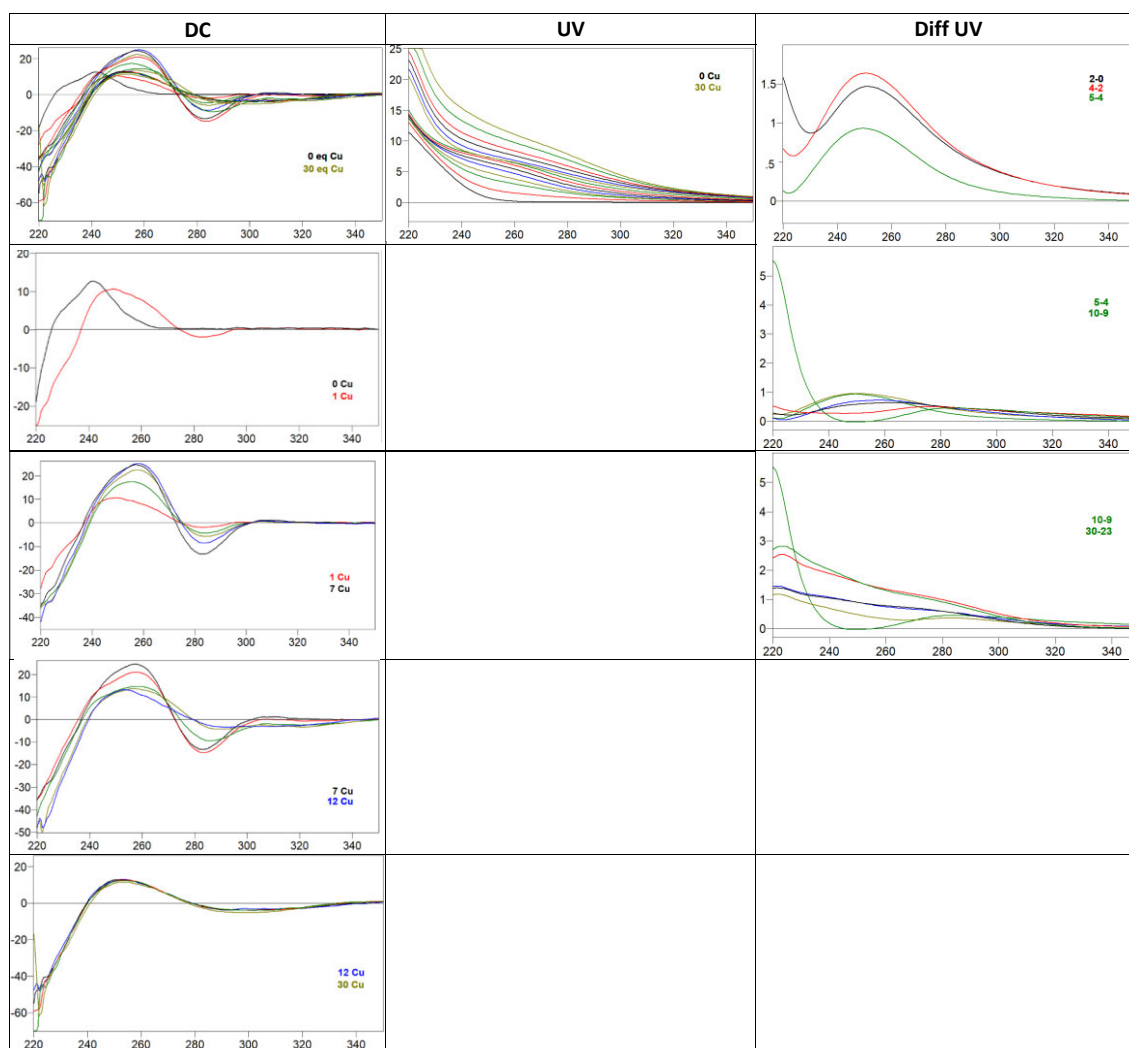
Sheet 7.2.2.1. Zn/Cd metal exchange experiment of *in vivo* Zn<sub>6</sub>-AvuMT1

**Figure 7.2.2.1.** CD, UV and difference UV spectra registered during the Zn/Cd metal exchange experiment of a 9.32  $\mu\text{M}$  solution of Zn<sub>6</sub>-AvuMT1 at pH 7.0 and 25°C.

**Table 7.2.2.1.** Evolution of the Zn/Cd metal exchange experiment of Zn-AvuMT1 followed by ESI-MS spectra at pH 7.0.

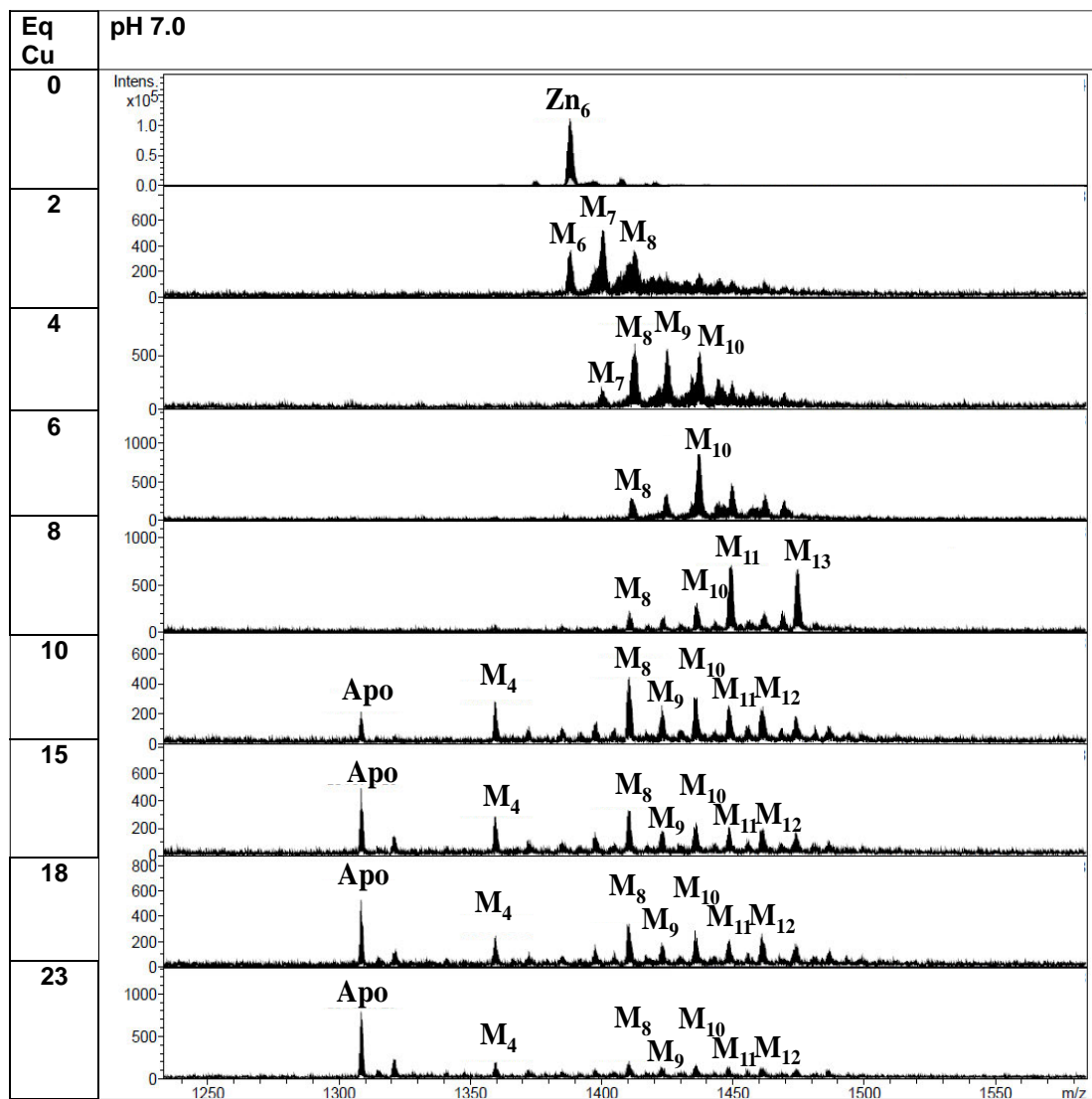




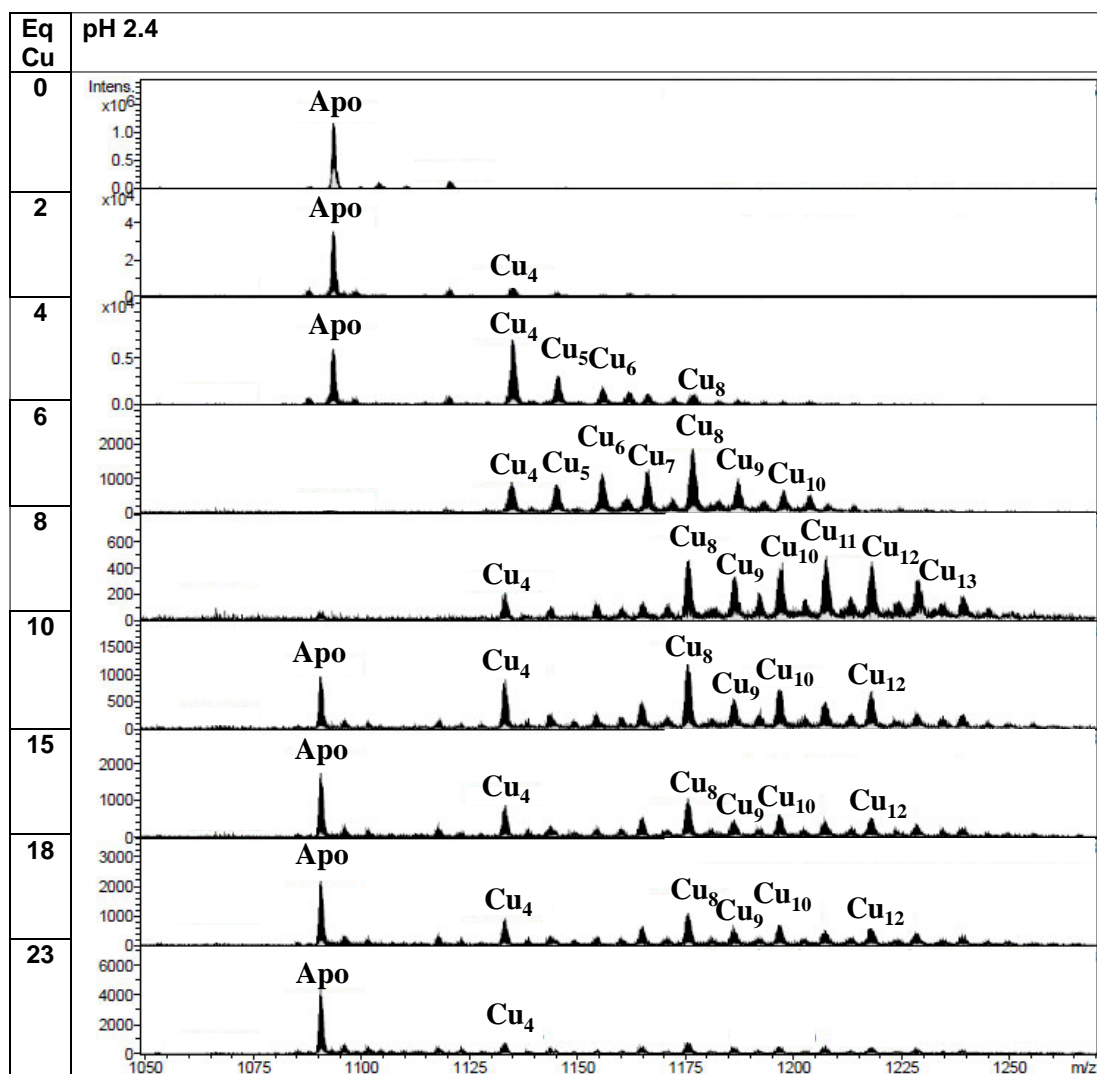
Sheet 7.2.2.2. Zn/Cu metal exchange experiment of *in vivo* Zn<sub>6</sub>-AvuMT1

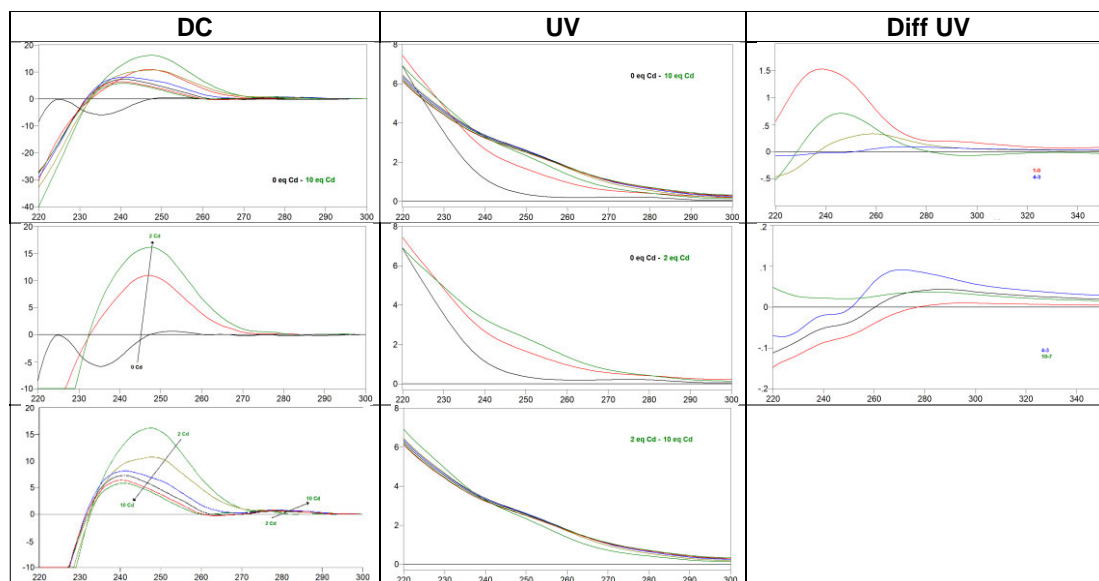
**Figure 7.2.2.2.** CD, UV and difference UV spectra registered during the Zn/Cu metal exchange experiment of a 9.20  $\mu\text{M}$  solution of Zn<sub>6</sub>-AvuMT1 at pH 7.0 and 25°C.

**Table 7.2.2.2.** Evolution of the Zn/Cu metal exchange experiment of Zn-AvuMT1 followed by ESI-MS spectra at pH 7.0.

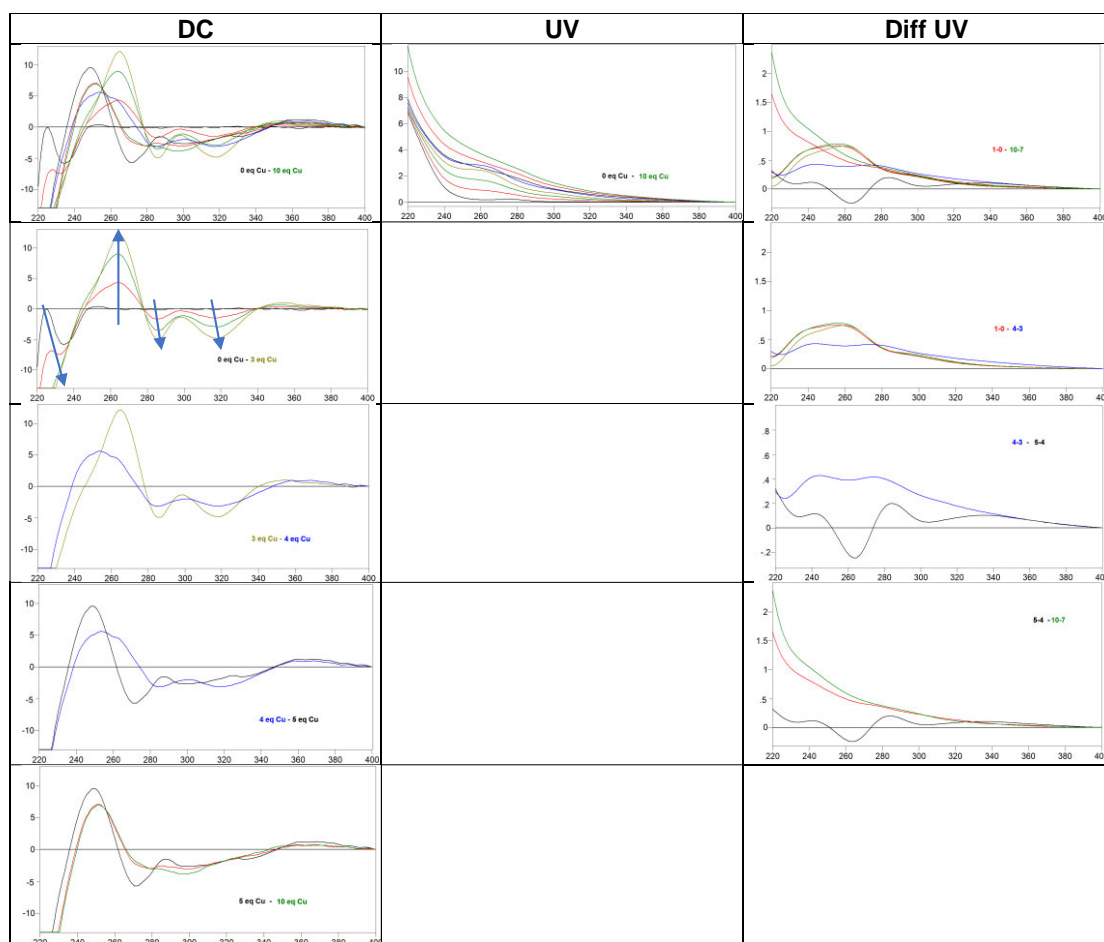


**Table 7.2.2.3.** Evolution of the Zn/Cu metal exchange experiment of Zn-AvuMT1 followed by ESI-MS spectra at pH 2.4.



Sheet 7.2.2.3. Zn/Cd metal exchange experiment of *in vivo* Zn<sub>2</sub>-CaCUP1

**Figure 7.2.2.3.** CD, UV and difference UV spectra registered during the Zn/Cd metal exchange experiment of a 17.2  $\mu\text{M}$  solution of Zn<sub>2</sub>-CaCUP1 at pH 7.0 and 25°C.

Sheet 7.2.2.4. Zn/Cu metal exchange experiment of *in vivo* Zn<sub>2</sub>-CaCUP1

**Figure 7.2.2.4.** CD, UV and difference UV spectra registered during the Zn/Cu metal exchange experiment of a 17.2  $\mu\text{M}$  solution of Zn<sub>2</sub>-CaCUP1 at pH 7.0 and 25°C.

**Table 7.2.2.4.** Evolution of the Zn/Cu metal exchange experiment of Zn-CaCUP1 followed by ESI-MS spectra at pH 7.0.

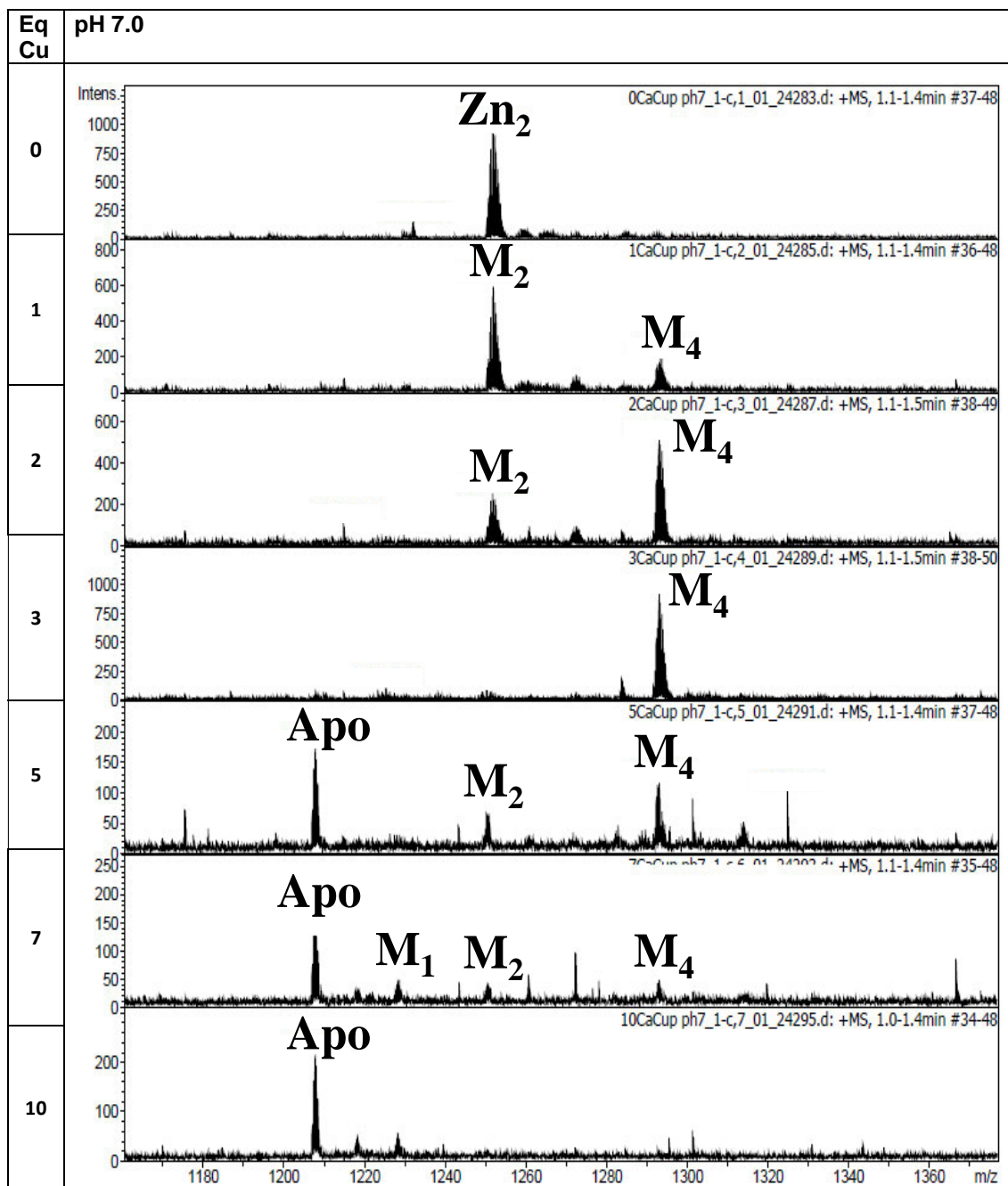
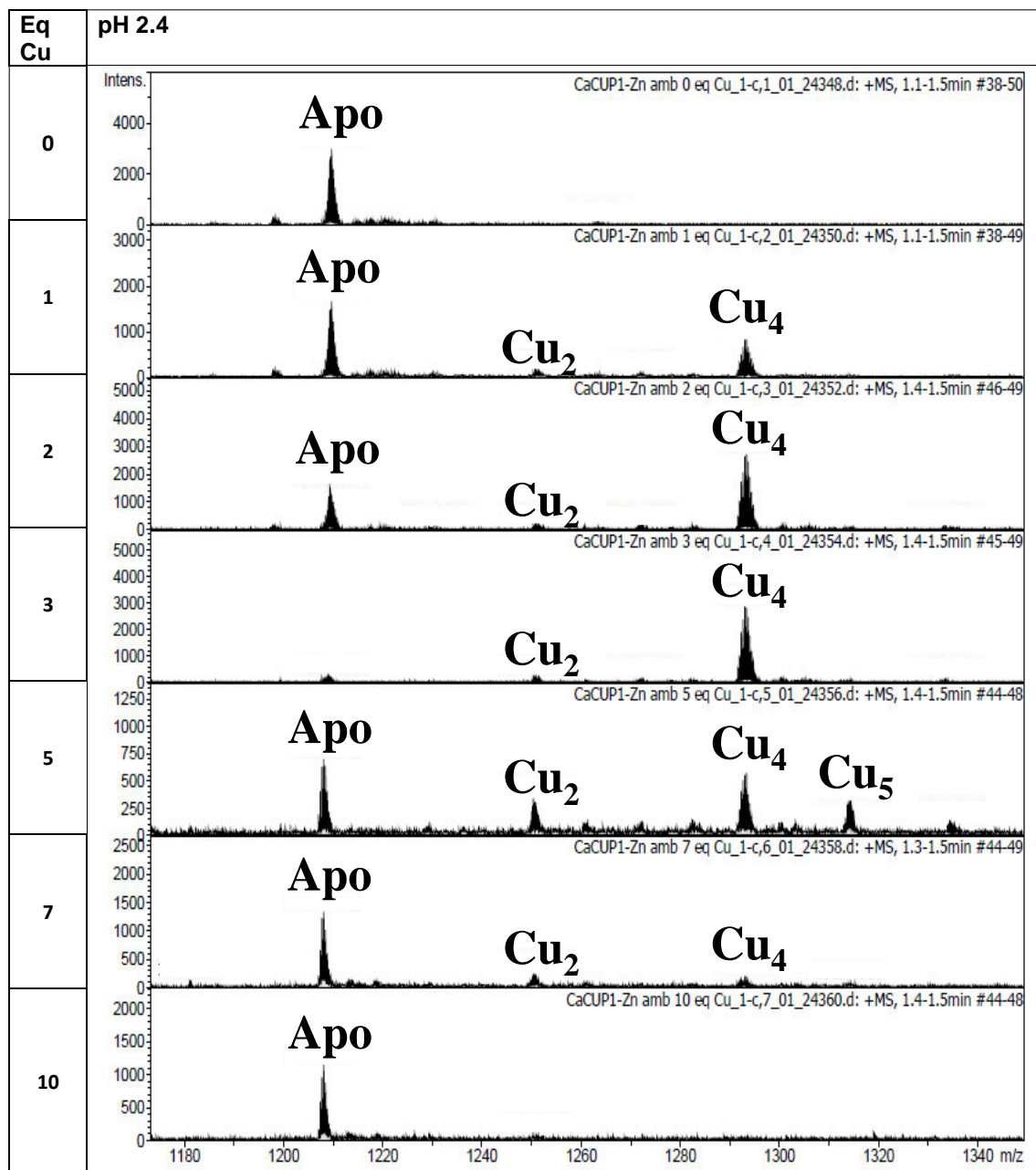


**Table 7.2.2.5.** Evolution of the Zn/Cu metal exchange experiment of Zn-CaCUP1 followed by ESI-MS spectra at pH 2.4.



## 7.2.3. Characterisation of Cd-thioneins

## Sheet 7.2.3.1. Characterisation of OdiMT1 fragments

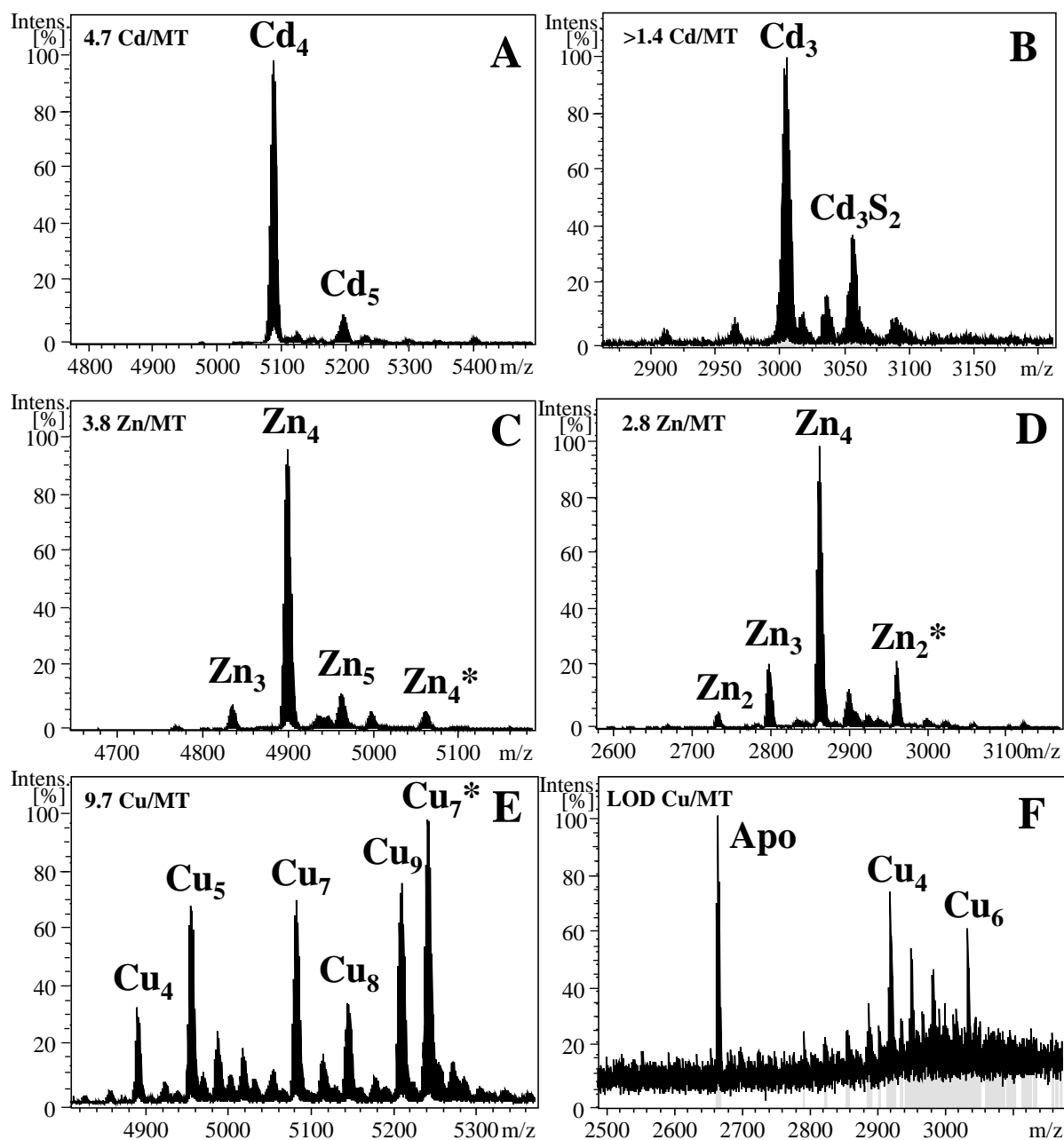


**Figure 7.2.3.1.** ESI-MS spectra measured at pH 7.0 of 12C fragment of OdiMT1 (A, C, E) and t12C fragment (B, D, F) of the Cd(II)- (A and B), Zn(II)- (C and D) and Cu(II)-enriched (E and F) MT productions. On the top left of each panel, it is showed the stoichiometry found by ICP-OES of each production. (LOD= lower than limit of detection)



## Sheet 7.2.3.2. Characterisation of CroMT1, HroMT1, HroMT2, BscMT1 and BscMT1R4

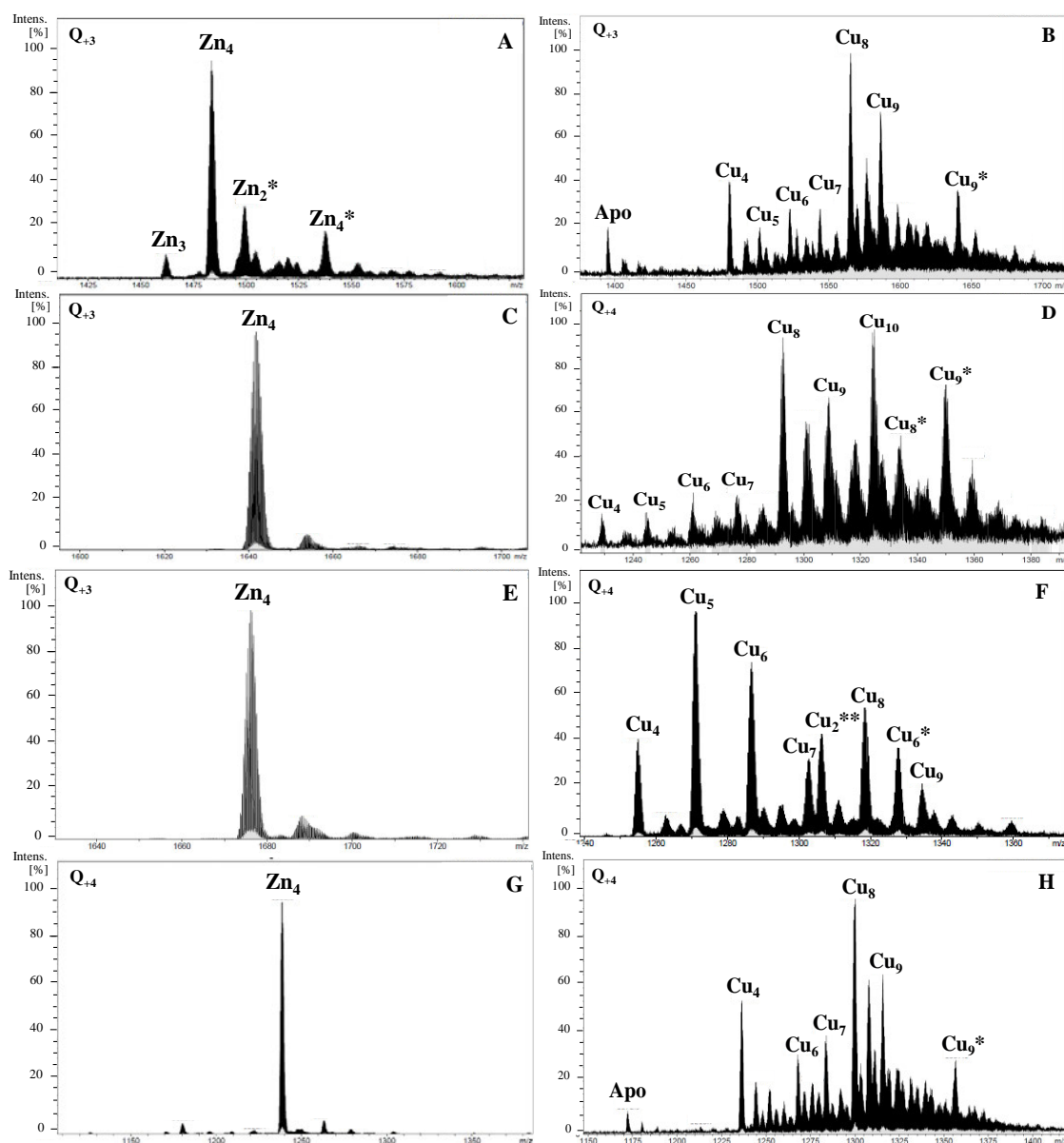


**Figure 7.2.3.2.** ESI-MS spectra measured at pH 7.0 of (A) CroMT1, (C) HroMT1, (E) HroMT2 and (G) BscMT1R4 Zn-productions and (B) CroMT1, (D) HroMT1, (F) HroMT2 and (H) BscMT1R4. Charge state of the spectra are pointed on the top left of the panels.



## **7.3. Published and submitted Articles**

**Article 1:**

**Metal binding functions of metallothioneins in the slug *Arion vulgaris* differ from metal-specific isoforms of terrestrial snails**

**DOI: [10.1039/c8mt00215k](https://doi.org/10.1039/c8mt00215k)**

**Article 2:**

**Metallothioneins of the urochordate *Oikopleura dioica* have Cys-rich tandem repeats, large size and cadmium-binding preference**

**DOI: [10.1039/c8mt00177d](https://doi.org/10.1039/c8mt00177d)**

**Article 3:**

**Two Unconventional Metallothioneins in the Apple Snail *Pomacea bridgesii* Have Lost Their Metal Specificity during Adaptation to Freshwater Habitats**

**DOI: [10.3390/ijms22010095](https://doi.org/10.3390/ijms22010095)**

**Article 4:**

**Modularity in Protein Evolution: Modular Organization and De Novo Domain Evolution in Mollusk Metallothioneins**

**DOI: [10.1093/molbev/msaa230](https://doi.org/10.1093/molbev/msaa230)**

**Article 5:**

**Modular Evolution and Population Variability of *Oikopleura dioica*  
Metallothioneins**

**DOI: [10.3389/fcell.2021.702688](https://doi.org/10.3389/fcell.2021.702688)**



**Article 6:**

**Tunicates Illuminate the Enigmatic Evolution of Chordate Metallothioneins by Gene Gains and Losses, Independent Modular Expansions, and Functional Convergences**

**DOI: [10.1093/molbev/msab184](https://doi.org/10.1093/molbev/msab184)**

**Article 7:**

**Metal-Specificity Divergence between Metallothioneins of *Nerita peloronta* (Neritimorpha, Gastropoda) Sets the Starting Point for a Novel Chemical MT Classification Proposal**

**DOI: [10.3390/ijms222313114](https://doi.org/10.3390/ijms222313114)**

**Manuscript 1:**

**Glycosylated Metallothioneins. Metals as Switchers and Modulators of Glycosylation**